THE UNIVERSITY OF
SYDNEY

Protein with Tau-like repeats (PTL-1) modulates the oxidative stress response, neuronal ageing and lifespan

Yee Lian Chew

A thesis submitted in fulfilment of the requirements for the degree of Doctor of Philosophy

School of Molecular Bioscience

Faculty of Science

University of Sydney

December, 2014

I declare that the research presented here is my own original work unless otherwise specified.

None of this material has been previously used for the purpose of obtaining any other degree.

Yee Lian Chew

Abstract

Protein with Tau-like repeats (PTL-1) is the sole Tau /MAP2/MAP4 homolog in *Caenorhabditis elegans*. Dysregulation of Tau is a pathological hallmark of neurodegenerative diseases such as Alzheimer's disease. Therefore, reducing Tau levels has been suggested as a therapeutic strategy.

We used PTL-1 to model the biological functions of a Tau-like protein without the complication of functional redundancy. Firstly, our data indicate that PTL-1 in the nervous system mediates the oxidative stress response in a pathway that may involve the *C. elegans* homolog of the Nrf2 transcription factor, SKN-1. In addition, we found that *ptl-1* mutant animals are short-lived, and that lifespan modulation by PTL-1 may occur via similar processes to those mediated by SKN-1. We also observed that the short-lived phenotype of *ptl-1* mutants can be rescued by transgenic re-expression of PTL-1 but not human Tau. Secondly, we show that PTL-1 maintains the structural integrity of neurons with increasing age. This phenotype observed in *ptl-1* mutant animals could again be rescued by PTL-1 re-expression but not by human Tau. Thirdly, our data also indicate that the regulation of neuronal ageing by PTL-1 is cell-autonomous. We expressed PTL-1 in touch neurons and showed rescue of the neuronal ageing phenotype of *ptl-1* mutant animals in these neurons but not in another neuronal subset. Knockdown of PTL-1 specifically in touch neurons also resulted in premature neuronal ageing in these neurons but not in a distinct subset of neurons, further supporting the conclusion that PTL-1 functions in a cell-autonomous manner. Interestingly, we showed that expression of PTL-1 in touch neurons alone was unable to rescue the shortened lifespan observed in null mutants, indicating that premature neuronal ageing in touch neurons and organismal ageing can be decoupled.

Our data show that PTL-1 in *C. elegans* is a useful model to investigate the physiological functions of a Tau-like protein. Overall, our findings that PTL-1 is involved in the stress response, neuronal ageing and lifespan modulation suggest that some of the effects of Tau pathology may result from the loss of physiological Tau functions and not solely from a toxic gain-of-function due to an accumulation of Tau.

Publications arising from this work

Research articles

Chew YL, Fan X, Gotz J, Nicholas HR. 2014. Regulation of age-related structural integrity in neurons by protein with Tau-like repeats (PTL-1) is cell autonomous. Sci. Rep. **4**.

Chew YL, Fan X, Gotz J, Nicholas HR. 2013. PTL-1 regulates neuronal integrity and lifespan in *C. elegans*. J Cell Sci. **126:**2079-2091.

Chew YL, Gotz J, Nicholas HR. 2014. Neuronal protein with tau-like repeats (PTL-1) regulates intestinal SKN-1 nuclear accumulation in response to oxidative stress. Aging cell (**online**)

Sections of the above articles were adapted for use in Chapters 3—6 of this thesis.

Review articles

Chew YL, Fan X, Gotz J, Nicholas HR. 2013. Aging in the nervous system of *Caenorhabditis elegans*. Commun. Integr. Biol. **6:**e25288.

Gotz J, Xia D, Leinenga G, **Chew YL**, Nicholas H. 2013. What Renders TAU Toxic. Front. Neurol. **4:**72.

Sections of the above review articles were adapted for use in Chapter 1 of this thesis..

Conference presentations

Protein with Tau-like repeats (PTL-1) regulates neuronal integrity and lifespan in

Caenorhabditis elegans. **Chew YL**, Fan X, Gotz J, Nicholas HR.

- **2012/2014** Genetics Society of Australasia conference, Melbourne/Sydney, Australia
- **2013** 19th International *C. elegans* meeting, Los Angeles, CA, USA
- **2012/2013** Alzheimer's and Parkinson's Disease symposium, Sydney/Brisbane, Australia
- **2012** Society for Neuroscience meeting, New Orleans, LA, USA

Acknowledgements

Thank you to everyone who walked with me on this PhD journey. It was honestly the most challenging and yet amazing experience of my life and I have learnt so much.

Thank you to my supervisor, Dr Hannah Nicholas, for truly being an inspiration. You will always be the person with whom I compare all other scientists.

Thank you to my second supervisor, Prof. Jürgen Götz, for your support and encouragement. Your dedication to your work and to your team is incredible.

Thank you to Anna "Banana" Reid and Slavica "Srećan rođendan" Berber, for being the best PhD buddies in the world. It would have been infinitely harder without your support. Thank you also to Hong, Matt, Mal, Callum, Irene and Priya for strictly enforcing the morning and afternoon tea schedules. Thank you especially to Irene for all your hard work on the PTL-1 project. It would not have come this far without you.

Lastly, thank you to my squishy and thank you to my family. Without you it is all meaningless.

Table of Contents

List of figures

Abbreviations

AD	Alzheimer's disease
bp	Base pairs
cDNA	Complementary DNA
DAPI	4',6-diamidino-2-phenylindole
DIC	Differential Interference Contrast
DNA	Deoxyribonucleic acid
Ex	Extrachromosomal array
GABA	Gamma-aminobutyric acid
GFP	Green Fluorescent Protein
IIS	Insulin-like/IGF-1 signalling
IPTG	Isopropyl β-D-1-thiogalactopyranoside
Is	Integrated array
MAP	Microtubule-associated protein
MAPK	Mitogen-activated protein kinase
MBR	Microtubule-binding repeat
mRNA	Messenger RNA
mRFP	Monomeric red fluorescent protein
PHP	Pseudo hyperphosphorylated
RNA	Ribonucleic acid
S.E.M.	Standard Error of Mean
SV	Synaptic vesicle
Tg	Transgenic
TRN	Touch receptor neuron
UV/TMP	Ultraviolet trimethylpsoralen

C. elegans gene names are italicised and in lowercase letters e.g., *ptl-1,* while protein names are abbreviated with all capital letters e.g., PTL-1.

Chapter 1:
Introduction

1.1 Alzheimer's disease is the most common cause of dementia in the elderly

Dementia is characterised by a progressive loss of cognitive function and is a common feature of neurodegenerative disorders. Alzheimer's disease (AD) is the most common neurodegenerative disease leading to dementia in Western communities, with an estimated 35.6 million people worldwide suffering from this disease (WHO, 2012). Age is the most significant risk factor for developing dementia, which, given the ageing global population, means that this condition is rapidly rising in prevalence. Despite limited data from developing countries, it is estimated that the worldwide incidence of this disease will increase dramatically in the near future. Some estimates indicate that disease incidence will double by 2030 and triple by 2050 (Blennow et al., 2006).

There are two major histopathological hallmarks that are detectable in the brains of people suffering from AD: plaques formed from aggregated β-amyloid (Aβ), and neurofibrillary tangles (NFTs) composed primarily of hyperphosphorylated and aggregated Tau (Riddle et al., 1981). A simplified model for Aβ processing is as follows. Briefly, Aβ cleavage products, including the pathology-associated $A\beta_{1-42}$ peptide, are generated from processing of the amyloid precursor protein (APP) via an amyloidogenic pathway involving sequential cleavage by β-secretase 1 (BACE-1) and γ-secretase complexes. An alternative non-amyloidogenic pathway requires processing by α-secretase and γ-secretase. Both pathways generate soluble ectodomains and an identical intracellular C-terminal fragment (APP intracellular domain, AICD), but only the amyloidogenic pathway generates Aβ products (reviewed in (O'Brien and Wong, 2011, Thinakaran and Koo, 2008)). Mutations in presenilin-1 and -2, which are components of the γ-secretase complex, are associated with an increased risk of early-onset, familial AD, possibly by

favouring the generation of more toxic forms of Aβ (Shen and Kelleher, 2007). In addition, genetic variants of *APOE4* (*apolipoprotein E4)* have been associated with late-onset, sporadic AD (Avramopoulos, 2009, Singh et al., 2006). APOE has many roles in brain physiology, including binding Aβ, and some theories on the role of the APOE4 variant in AD imply that it may be involved in the clearance of toxic Aβ (Kim et al., 2009, Tokuda et al., 2000, Tiraboschi et al., 2004).

Phosphorylated Tau is the major component of NFTs found not only in AD, but in other conditions collectively known as Tauopathies, which includes another dementia, Frontotemporal dementia with Parkinsonism associated with chromosome 17 (FTDP-17) (Lee and Leugers, 2012, Iqbal et al., 2010, Ittner and Gotz, 2011, Gotz et al., 2013, Ittner et al., 2011). No mutations in *MAPT*, the gene that encodes Tau, have thus far been associated with AD. However, mutations in this gene cause several Tauopathies including FTDP-17 (Wade-Martins, 2012). The presence of both Aβ plaques and Tau tangles in AD suggests that both proteins play a pathological role in the disease, although the exact interplay between these factors is still unclear (Lee et al., 2001b, Iqbal et al., 2010, Ittner and Gotz, 2011). Despite this lack of clarity, the importance of Tau in Aβ-dependent neurodegenerative disease is demonstrated by observations that knocking out Tau dramatically reduces Aβ pathology both in *in vitro* and *in vivo* models (Rapoport et al., 2002, Roberson et al., 2007, Ittner et al., 2010). Furthermore, methylene blue, which has been presented as a therapeutic agent for AD, is a chemical that inhibits the aggregation of proteins that adopt a β-sheet conformation, such as Tau (Guzman-Martinez et al., 2013). Improved cognition in AD rodent models treated with methylene blue has been linked to

decreased levels of soluble Tau (O'Leary et al., 2010), suggesting that reducing Tau levels would be favourable for AD patients.

The remainder of this thesis will focus on the role of Tau and Tau-related proteins in neurodegenerative disease and ageing.

1.1.1 Tau in Alzheimer's disease

Tau is a neuronal microtubule-associated protein (MAP) that is predominantly localised to axons (Kosik and Finch, 1987, Weingarten et al., 1975). In mammals, Tau has a role in regulating microtubule assembly, stability, and organisation (Harada et al., 1994, Chen et al., 1992, Cleveland et al., 1977). MAP2, which is expressed in neurons, and MAP4, which is non-neuronal, are other mammalian MAPs that contain similar microtubule-binding domains to Tau. These proteins together comprise the Tau/MAP2/MAP4 family, and *in vivo* studies imply that they display considerable functional redundancy (Dehmelt and Halpain, 2005). In AD and other Tauopathies, it is only partly understood how Tau exerts its toxic effects, whether in fibrillar form (Ittner et al., 2008), or before the formation of tangles due to the loss of some important physiological functions (Gomez-Isla et al., 1997, Lee and Leugers, 2012). Despite the significant advances in understanding Tau functions made using Tau transgenic and knockout models (reviewed in (Ittner et al., 2011, Ke et al., 2012, Gotz and Ittner, 2008, Gotz et al., 2010, Avila et al., 2004, Lee et al., 2001b)), these studies are complicated by the presence of other neuronal MAPs such as MAP2, which may share several physiological roles with Tau. In fact, Tau knockout mice do not display overt defects in neuronal development or function until late stages of adulthood (Harada et al., 1994, Dawson et al., 2001, Tucker et al., 2001).

While most studies on Tau are conducted using the mouse as a model organism, several wild-type and mutant human Tau transgenic models have been established in the nematode *Caenorhabditis elegans* (Kraemer et al., 2003, Miyasaka et al., 2005, Brandt et al., 2009, Fatouros et al., 2012). Kraemer *et al.* expressed wild-type and FTDP-17 mutant human Tau (mutations P301L and V337M) in *C. elegans* to model Tauopathy disorders and found that these Tau transgenic worms were all short-lived and displayed impaired motility, decreased cholinergic transmission and increased GABAergic neuron degeneration compared with non-transgenic worms. Although the expression of both wild-type and mutant human Tau was detrimental to *C. elegans*, transgenic animals expressing mutant Tau were considerably more impaired in the latter three phenotypes compared with transgenic animals expressing wild-type Tau (Kraemer et al., 2003). A forward genetic screen for mutants that ameliorate Tau pathology in these transgenic lines revealed two suppressors of Tau (*sut*) genes, *sut-1* and *sut-2*, which encode a cytoskeletal regulatory protein (Kraemer and Schellenberg, 2007) and a zinc-finger protein (Guthrie et al., 2009), respectively. In a separate study, transgenic *C. elegans* carrying pathology-associated P301L and R406W variants of human Tau displayed a progressive loss of touch sensitivity, which appeared to correlate with the presence of structural abnormalities and aggregated Tau in mechanosensory touch receptor neurons (Miyasaka et al., 2005). Another transgenic line generated by Brandt and colleagues expressed a pseudo-hyperphosphorylated (PHP) Tau in which several serine/threonine residues were mutated to glutamic acid. PHP Tau formed aggregates in transgenic *C. elegans* and led to defects in neuronal development (Brandt et al., 2009). Furthermore, allele ΔK280, a pro-aggregant mutant form of human Tau, was expressed in worms and resulted in defective motility, synaptic transmission and axonal transport

(Fatouros et al., 2012). These investigations demonstrate the usefulness of *C. elegans* as a model for Tauopathies. Given the ease of genetic manipulation of the nematode model, transgenic lines generated could be used to screen for interacting partners of mutated Tau forms, such as the *sut* genes described above, which further illuminate the processes mediating Tau pathology. In fact, some of these models have been used in pharmacological screens to isolate chemical substances that can counteract Tau pathology (McCormick et al., 2013).

1.1.2 Tau and PTL-1

C. elegans has one putative homolog in the Tau/MAP2/MAP4 family of MAPs, called protein with Tau-like repeats-1 (PTL-1) (Goedert et al., 1996, McDermott et al., 1996). PTL-1 contains a high level of sequence homology to Tau/MAP2/MAP4 within the microtubule-binding repeat (MBR) domain in the carboxyl (C)-terminus, and has been shown to regulate microtubule assembly *in vitro* (McDermott et al., 1996, Goedert et al., 1996). Immunohistochemistry and analysis of a *ptl-1* transcriptional reporter line demonstrated that PTL-1 has a neuronal expression pattern in adult worms (Goedert et al., 1996, Gordon et al., 2008). Henceforth PTL-1 will be referred to as the Tau/MAP2 homolog since these are the neuronal MAPs in mammals (Dehmelt and Halpain, 2005). PTL-1 has also been shown to have neuronal functions in worms, as it has been implicated in the regulation of microtubule-based motility in several neurons (Tien et al., 2011) and for the optimal functioning of touch receptor neurons in the response to gentle touch (Gordon et al., 2008). Therefore, *C. elegans* is a convenient *in vivo* model in which to study the physiological roles of a Tau/MAP2-like protein without having to consider compensatory effects produced by other closely-related MAPs.

Amino acid sequence alignment of the longest isoforms of human Tau and mouse Tau together with PTL-1a, the longest isoform in *C. elegans*, indicates a high level of sequence conservation in the C-terminal region of these proteins (**Figure 1.1**). As noted above, the C-terminus contains the MBRs, of which there are four in human and mouse Tau and putatively five in *C. elegans* PTL-1 (Goedert et al., 1996). Although human and mouse Tau show some similarity in the N-terminus, known as the projection domain, there is limited sequence identity. In the N-terminus, *C. elegans* PTL-1 contains a large proline-rich region containing 29 glutamic acid-proline dipeptide repeats, which is not present in the projection domain of human or mouse Tau, although a proline-rich region exists in both mammalian forms immediately upstream of the MBR domain (Buee et al., 2000). The N-terminus in mammalian Tau has been shown to be important for interactions with proteins other than microtubules, such as the kinase Fyn (Ittner et al., 2010, Kanaan et al., 2012). Targeting of Fyn by Tau to the dendritic compartment facilitates Fyn-dependent phosphorylation of the NMDA receptor, which results in excitotoxicity, an important component of Aβ pathology (Ittner et al., 2010).

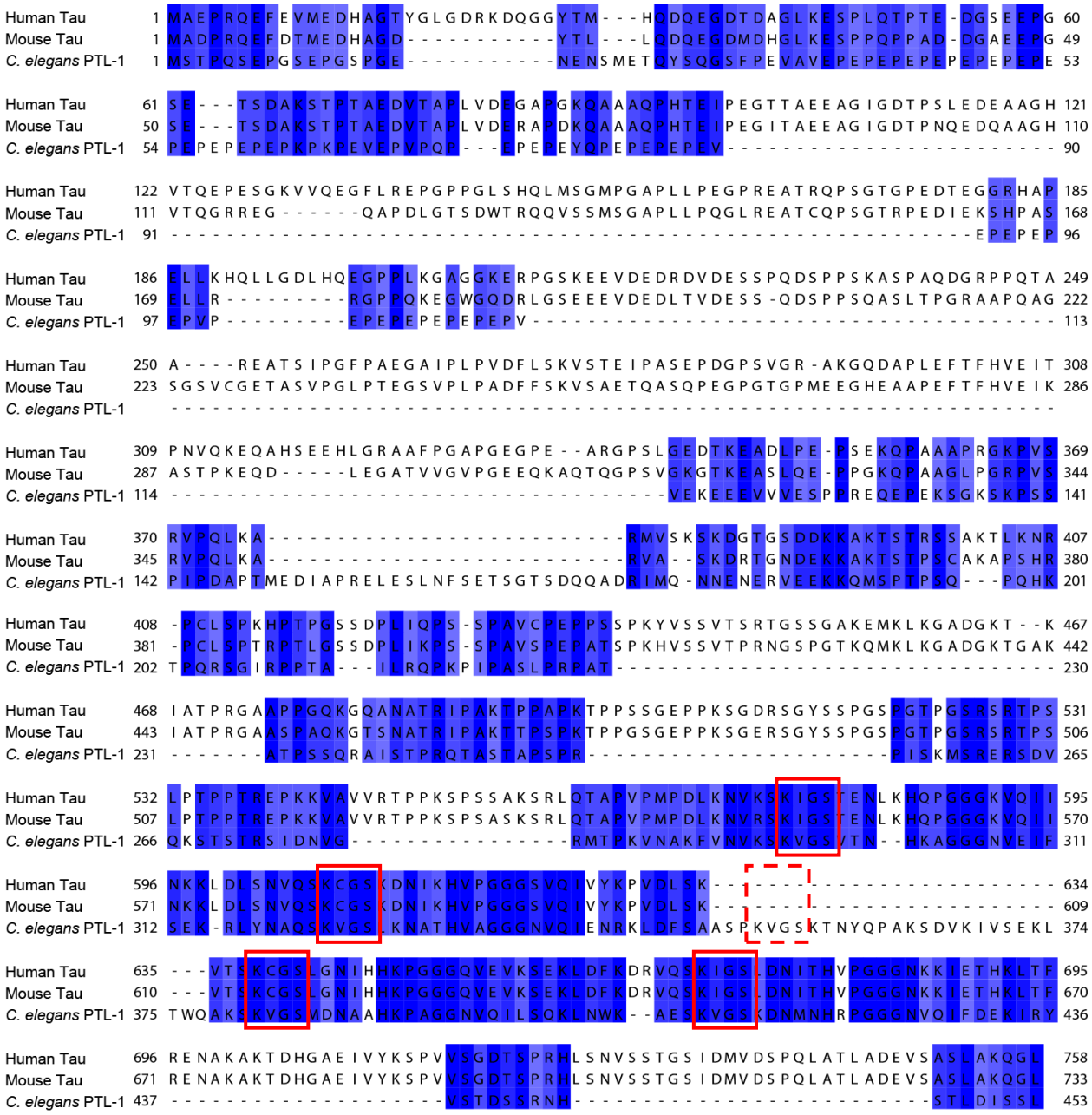

Figure 1.1: Alignment of human Tau, murine Tau and *C. elegans* PTL-1. Alignment was generated using the T-Coffee program (Di Tommaso et al., 2011) using the longest isoform for all organisms, which is P10636.5 for human Tau, P10637.3 for mouse Tau and F42G9.9a for PTL-1. The gradient of blue highlighting indicates the level of similarity between all three sequences – the darker blue highlighting indicates higher sequence similarity whereas lighter blue indicates lower sequence similarity. Dashed lines indicate the absence of identity/similarity. The red boxes indicate the conserved MBRs. The dashed red box indicates a unique MBR for PTL-1.

1.1.3 C. elegans *as a model organism to study ageing*

Ageing is one of the most significant risk factors for the development of neurodegenerative disease. However, the cellular and molecular changes that occur with ageing are not fully understood. *C. elegans* is a useful model in which to study ageing owing, in particular, to its relatively short lifespan and life cycle (**Figure 1.2**). Like in humans, ageing in worms is accompanied by physiological changes including progressive loss of mobility (Herndon et al., 2002, Huang et al., 2004), sarcopenia and deterioration of other tissues (Garigan et al., 2002, Herndon et al., 2002), and a decline in immune function (Youngman et al., 2011). Human physiological ageing (as differentiated from pathological ageing) is additionally associated with subtle physical changes in the brain, such as neuronal restructuring, synaptic loss, and altered calcium homeostasis (Yankner et al., 2008, Hedden and Gabrieli, 2004, Khachaturian, 1994), and these changes have been linked to a progressive impairment of cognitive function (Yankner et al., 2008, Bishop et al., 2010). In light of these observations, it was somewhat surprising that initial studies did not detect any structural decline in the *C. elegans* nervous system with age (Herndon et al., 2002). Recently, however, close examination of neuronal morphology in the nematode has revealed pronounced ageing phenotypes such as aberrant outgrowths and beading along neuron processes, and age-associated synaptic deterioration has also been detected (Tank et al., 2011, Toth et al., 2012, Pan et al., 2011). The nematode model system therefore presents an opportunity to explore the mechanisms by which neuronal ageing is regulated. In this model, it is also possible to dissect the relationship between neuronal ageing and ageing of the whole organism, by examining for example whether accelerated neuronal ageing has repercussions for the entire organism.

Such explorations are greatly facilitated by the simplicity of the *C. elegans* nervous system, which consists of only 302 neurons. These neurons have been anatomically mapped and develop in a stereotypical manner (Hall and Russell, 1991, White et al., 1986), facilitating the study of age-related structural changes. Furthermore, *C. elegans* is small (1mm length in adults), feeds on *Escherichia coli* bacteria seeded onto agar plates, and maintains its population by self-fertilisation (Brenner, 1974), making the maintenance of large numbers of nematode strains simple and relatively affordable. The worm is also transparent (Brenner, 1974), facilitating the study of detailed anatomical structures by both differential interference contrast and fluorescence microscopy in live animals.

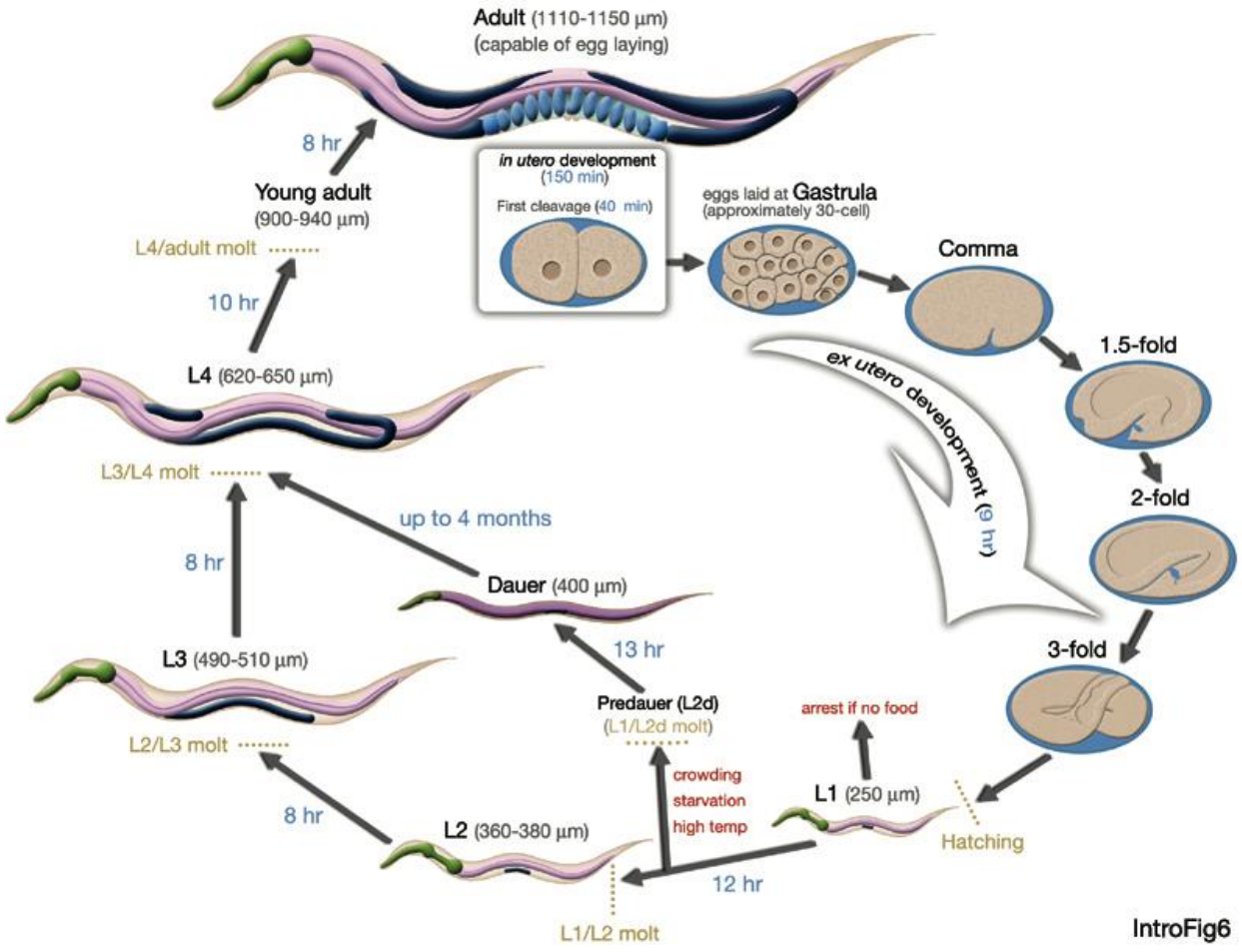

Figure 1.2: The *C. elegans* life cycle (from WormAtlas (Altun and Hall, 2005)). The developmental processes in *C. elegans* are highly stereotyped. The life cycle from egg to egg-laying adult takes 3-7 days depending on the temperature of incubation.

1.1.4 PTL-1 in C. elegans

PTL-1 is expressed predominantly in the nervous system, although expression has also been demonstrated in the embryonic hypodermis and in some adult muscle (Gordon et al., 2008, Goedert et al., 1996). As mentioned above, PTL-1 functions within neurons to regulate touch sensitivity (Gordon et al., 2008) and microtubule-based motility (Tien et al., 2011). *ptl-1* null mutant animals also have fewer viable offspring despite no defects in egg-laying, suggesting that PTL-1 is also involved in essential stages of embryonic development (Gordon et al., 2008). Recently, PTL-1 has been shown to bind to SUP-36 *(SUPpressor 36)*, an S-phase kinase-associated protein (Skp) family member that is involved in pharyngeal development. This association may be required to tether SUP-36 to microtubules (Polley et al., 2014).

1.2 Oxidative stress in Alzheimer's disease

Aside from Aβ plaques and Tau NFTs (Riddle et al., 1981, Ittner and Gotz, 2011), increased oxidative stress has also been observed in the brains of AD patients and in animal AD models (Butterfield et al., 2007, Filipcik et al., 2006, Guglielmotto et al., 2009, Zhao and Zhao, 2013). This indicates that oxidative stress could be either an unrelated by-product of disease, a major or minor driver of pathology, or involved in a feedback loop to amplify AD pathology. Despite this finding, the use of antioxidants in clinical trials for cognitive impairment has produced only marginal or no improvement in patients (Petersen et al., 2005, Yaffe et al., 2004, Kang et al., 2006). Therefore, an improved understanding of the role of oxidative stress in the pathogenesis of AD may be useful for developing alternative avenues of treatment.

1.2.1 Oxidative stress and Tau

Investigations into a pathological link between oxidative stress and Tau have been increasingly developed in several disease models. Mitochondrial dysfunction can result in an imbalance in the release of reactive oxygen species (ROS). Tau transgenic mice display substantial deficits in mitochondria complex I (David et al., 2005), and this is worsened in combination with increased Aβ oligomers (Eckert et al., 2008). Oxidative stress has also been implicated as a causal factor for Tau-induced neurodegeneration in *Drosophila melanogaster* (Dias-Santagata et al., 2007), and for increased Tau phosphorylation and aggregation *in vitro* (Su et al., 2010, Gamblin et al., 2000). These processes have been shown to involve the p38 mitogen-activated protein kinases (MAPKs) that are activated in response to oxidative stress (Zhu et al., 2000, Buee-Scherrer and Goedert, 2002, Goedert et al., 1997). Activated p38 MAPKs have been shown to phosphorylate

Tau (Reynolds et al., 1997), which may contribute to pathological Tau hyperphosphorylation, and also appear to physically associate with filamentous Tau *in vivo* (Zhu et al., 2000).

In addition, activation of an important mediator of the oxidative stress response in mammals, the transcription factor Nrf2/NFE2 (Nuclear factor, erythroid-derived 2), has been recently linked to reduction in the levels of phosphorylated Tau in primary neuron culture via an autophagy adaptor protein NDP52 (Jo et al., 2014). Behavioural improvements in response to methylene blue treatment in an AD mouse model have also been associated with increased expression of Nrf2-regulated genes (Stack et al., 2014). Nrf2 has a cytoprotective effect in several model systems, including mice and *C. elegans*, and this has been linked to increased lifespan in these organisms (Leiser and Miller, 2010, Bishop and Guarente, 2007, Lewis et al., 2010).

1.2.2 SKN-1 is the C. elegans *homolog of the mammalian Nrf-2 family of transcription factors*

SKN-1 is the *C. elegans* homolog of the bZIP (basic region-leucine zipper) Nrf family of transcription factors, which include Jun, c-Fos, and Nrf2 (Bowerman et al., 1992, Amoutzias et al., 2007). In addition to a myriad of roles in cell fate specification in the developing embryo (Bowerman et al., 1992), pathogen resistance (Papp et al., 2012), the unfolded protein response (Glover-Cutter et al., 2013), the starvation response (Paek et al., 2012), longevity (Bishop and Guarente, 2007, Robida-Stubbs et al., 2012, Okuyama et al., 2010, Park et al., 2009, Tullet et al., 2008) and dietary restriction-mediated lifespan extension (Bishop and Guarente, 2007), SKN-1 has also been shown to regulate a conserved response to oxidative stress (An and Blackwell, 2003, An et al., 2005, Inoue et al., 2005, Kahn et al., 2008, Park et al., 2009, Wang et al., 2010). Interestingly, some of these responses appear to be age-dependent, as old worms fail to induce

the SKN-1-dependent gene *gst-4* (glutathione S-transferase 4) in response to stress (Przybysz et al., 2009), and *skn-1* mutant animals display accelerated immunosenescence, or deterioration of the immune system with age (Papp et al., 2012). There are three isoforms of SKN-1, isoforms a, b, and c, and these appear to be regulated from different promoters at the same genetic locus (Bishop and Guarente, 2007) (**Figure 1.3**). Most investigations have focused on isoforms b and c, largely due to the generation of a SKN-1b/c GFP reporter transgenic line. This has facilitated expression studies of these isoforms, which are found in the intestine (SKN-1c) and the ASI neurons (SKN-1b) (An and Blackwell, 2003). Recently another transgenic line encoding all three SKN-1 isoforms within a large transgene has been generated, and the expression patterns in both transgenic lines appear largely similar (Tullet et al., 2008). Yet another transgenic line specifically examining SKN-1a showed widespread expression in the nervous system and also in non-neuronal tissues, albeit these observations are confounded by the fact that the 7.3 kb promoter region in this transgene includes an upstream gene *bec-1,* which is known to be expressed in many tissues (Staab et al., 2014). Importantly, SKN-1b/c re-expression fully compensates for the loss of all three isoforms in dietary-restriction mediated longevity (Bishop and Guarente, 2007), as well as in mutant strains lacking isoforms a and c with regards to the oxidative stress response (An and Blackwell, 2003). Interestingly, the *zu135* allele of *skn-1* that lacks all three isoforms has a wild-type lifespan, but the *zu67* allele lacking SKN-1a/c is short-lived (Bishop and Guarente, 2007). The position of these alleles within the genomic locus is shown in **Figure 1.3**.

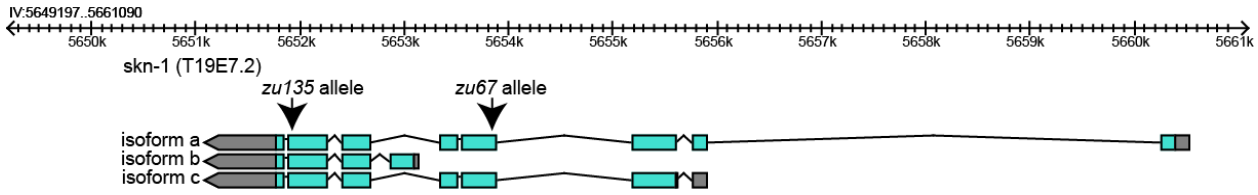

Figure 1.3: The *skn-1*(T19E7.2) locus on *C. elegans* chromosome IV. There are three SKN-1 isoforms confirmed by cDNA: isoforms a, b and c. Two missense alleles discussed in this thesis are *zu135*, which affects all three isoforms, and *zu67*, which affects *skn-1a/c* (http://www.wormbase.org/), indicated by arrows.

The best characterised function of SKN-1 is as a transcription factor that localises to the nucleus to induce the transcription of stress-responsive genes (An and Blackwell, 2003). The SKN-1c isoform in the intestine is normally diffuse in the cytoplasm, but is rapidly localised to the nucleus during stress conditions. The nuclear re-localisation of intestinal SKN-1 in response to stress directly requires phosphorylation by p38 MAPK (Inoue et al., 2005), and is negatively regulated by glycogen synthase kinase-3β (An et al., 2005). In contrast, the SKN-1b isoform in the ASI neurons in the head is constitutively present in the nucleus, and this does not alter when the animal is stressed (An and Blackwell, 2003, Bishop and Guarente, 2007). Expression changes in SKN-1a in response to stress have not yet been examined.

The insulin/IGF-1 signalling (IIS) pathway has also been implicated in the regulation of SKN-1 activity (Tullet et al., 2008). In the context of ageing, the IIS pathway is one of the most well understood regulators of longevity and stress tolerance. When activated by ligand binding, the DAF-2 insulin receptor signals to downstream kinases to phosphorylate the FOXO transcription factor DAF-16, resulting in its exclusion from the nucleus and preventing the subsequent induction of genes involved in longevity and the stress response (Larsen et al., 1995, Kenyon et al., 1993, Ogg et al., 1997). Reduction-of-function mutations in DAF-2 result in a dramatic

extension of lifespan (Kenyon et al., 1993). Mutations in DAF-16 result in premature ageing, and the lifespan extension observed in *daf-2* mutants is dependent on DAF-16 (Kenyon et al., 1993, Ogg et al., 1997, Larsen et al., 1995). It was previously demonstrated that DAF-2 influences SKN-1 re-localisation to intestinal nuclei in response to stress (Tullet et al., 2008), and that SKN-1-mediated modulation of lifespan involves DAF-2 and the downstream effector DAF-16, although the evidence thus far is not entirely consistent (Bishop and Guarente, 2007, Tullet et al., 2008, Wang et al., 2010, Robida-Stubbs et al., 2012). A simplified schematic for lifespan regulation via DAF-2, DAF-16, and SKN-1 is shown in **Figure 1.4**. For example, the *skn-1(zu67)* mutation affecting isoforms a and c does not affect the long-lived phenotype of *daf-2(e1370)* mutant strains, suggesting that SKN-1 is upstream of DAF-2 (Inoue et al., 2005, Tullet et al., 2008). In contrast, knockdown of *skn-1* a/c suppressed longevity in a *daf-2(e1368)* mutant (Tullet et al., 2008). It is important to note that phenotypic differences exist between these *daf-2* mutant strains: *daf-2(e1370)* animals are long-lived and stress resistant but also display a number of abnormalities such as the formation of dauer larvae at 20—25 °C under normal conditions (wild-type animals usually form dauers in stress conditions); whilst *daf-2(e1368)* animals are long-lived, albeit less so than *e1370* animals, but otherwise appear essentially normal (Gems et al., 1998). Therefore, although the regulation of longevity by SKN-1 involves the IIS pathway, the exact mechanism of this regulation has not yet been clarified.

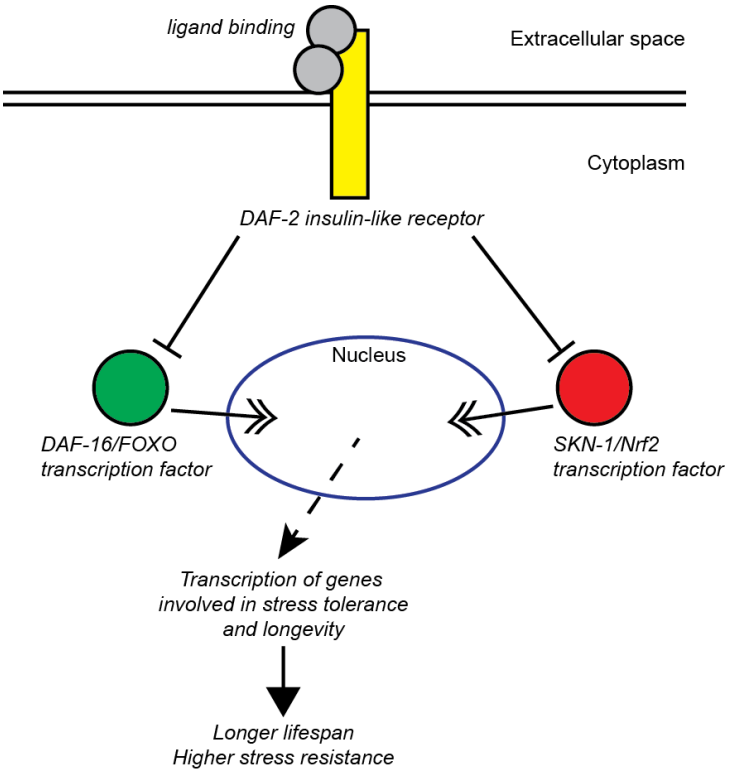

Figure 1.4: Schematic of the IIS pathway in *C. elegans*, showing the involvement of DAF-2, DAF-16, and SKN-1. Briefly, ligand binding to the DAF-2 insulin-like receptor results in the activation of negative regulators of both DAF-16/FOXO and SKN-1/Nrf2 transcription factors, thus preventing the translocation of these factors to the nucleus to induce expression of genes involved in stress tolerance and lifespan extension. In the absence of ligand binding or in *daf-2* reduction-of-function mutants, the negative regulation of DAF-16 and/or SKN-1 is removed and these transcription factors are able to move into the nucleus to regulate transcription.

1.3 Neuronal ageing in C. elegans

1.3.1 Cellular features of neuronal ageing in C. elegans

Although ageing has been described as the most significant risk factor for neurodegenerative disease, the factors that influence the development of dementia are unclear. Furthermore, the complexity of the mammalian nervous system provides a significant challenge to the study of neuronal ageing in mammals. Given the short lifespan of *C. elegans* and the ease of observation using microscopy, the nematode system is a convenient model by which to identify factors that contribute to neuronal ageing. To date, among the 302 neurons of *C. elegans*, age-associated changes have been identified in the mechanosensory touch receptor neurons, in the axons of cholinergic neurons in the ventral nerve cord (VNC), in the axons of GABAergic motor neurons in the ventral and dorsal nerve cord, and in the nerve ring. **Figure 1.5** shows the nervous system visualised using *gfp* reporter lines, and **Figure 1.6** shows age-associated structural changes in touch neurons and GABAergic neurons**.** For clarity, all neurons in *C. elegans* are described using the conventional unique three-letter identifiers. For example, the six touch neurons are the two ALM (Anterior Lateral Microtubule) cells, the AVM (Anterior Ventral Microtubule), the two PLMs (Posterior Lateral Microtubule), and the PVM (Posterior Ventral Microtubule) (Altun and Hall, 2005). Age-associated changes in the nervous system include branching from the cell body and axon, as well as blebbing and beading along the axon (Pan et al., 2011, Tank et al., 2011, Toth et al., 2012). Representative images of these structures are shown in (**Figure 1.7**). In neurons displaying such structures, nuclear DAPI staining appears intact even in severe cases, suggesting that these aged neurons are not undergoing apoptosis or necrosis (Pan et al., 2011).

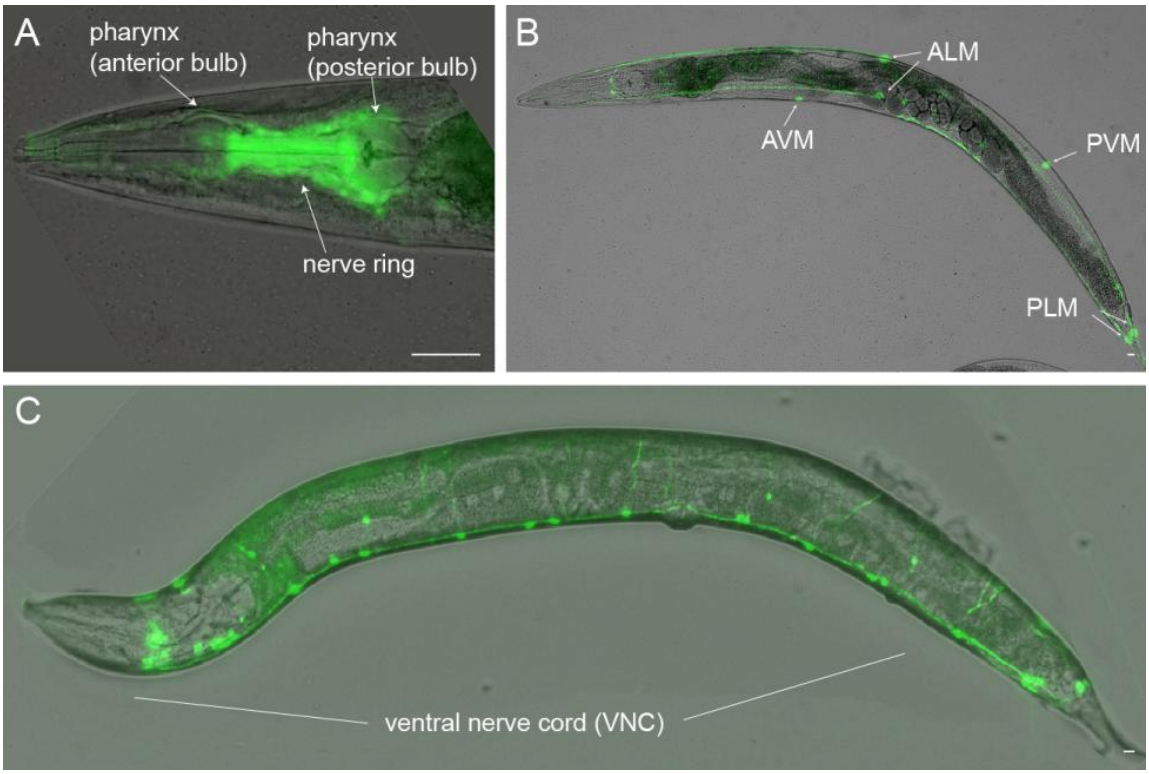

Figure 1.5: Fluorescence reporter lines enable the visualisation of neurons in *C. elegans*. A) Nerve ring (green), positioned between the anterior and terminal bulbs of the pharynx, indicated in the phase image. The P*ptl-1::gfp (sIs11686)* reporter line is shown (McKay et al., 2003). **B)** Touch receptor neurons, showing the cell bodies of the AVM, ALMs, PVM and PLMs. The P*mec-4::gfp (zdIs5)* reporter line is shown (Clark and Chiu, 2003). **C)** Ventral nerve cord GABAergic motor neurons. The P*unc-47::gfp (oxIs12)* reporter line is shown (McIntire et al., 1997). The images are taken from the current study and not from the referenced articles, which indicate the source of the transgenic lines used. Anterior is left. Scale, 10 µm.

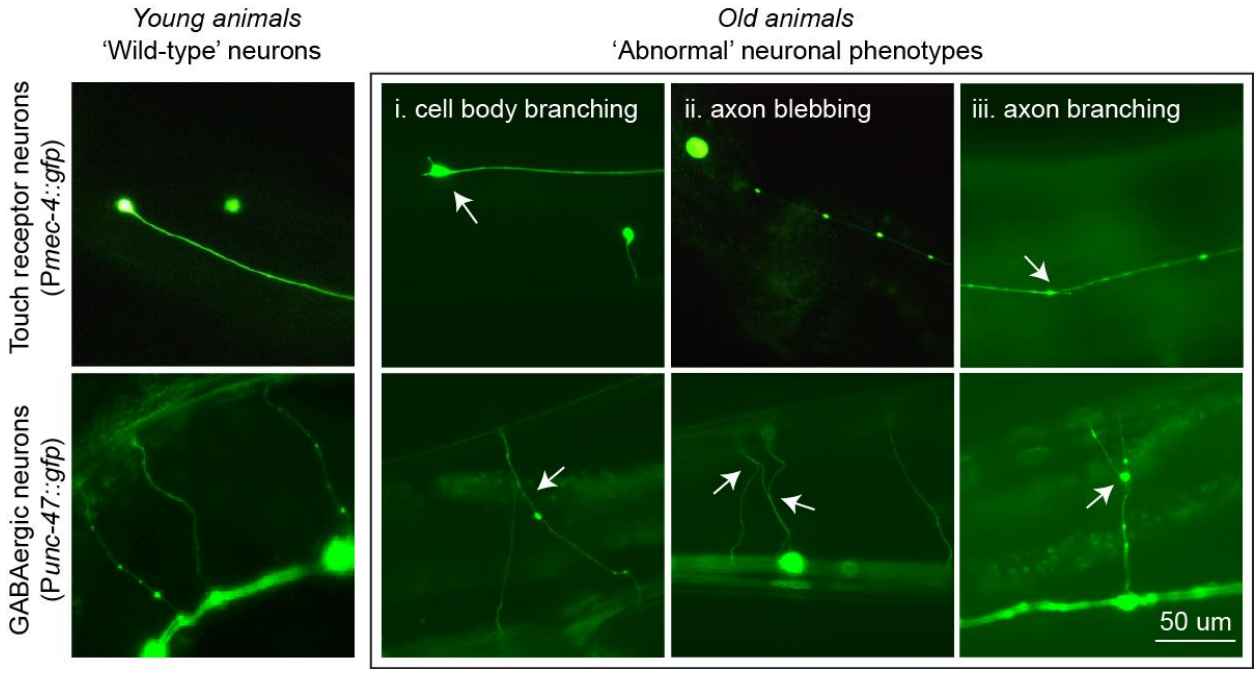

Figure 1.6: Neuronal ageing phenotypes observed in *C. elegans* touch receptor neurons and GABAergic neurons. (Top) Touch receptor neurons are visualised using the P*mec-4::gfp (zdIs5)* reporter. Young adult animals have a long, straight and unbranched axon with a round cell body in the ALM neuron. Older animals accumulate structural abnormalities such as (i) cell body branching, (ii) axon blebbing, and (iii) axon branching. (Bottom) Ventral nerve cord GABAergic neurons are visualised using the P*unc-47::gfp (oxIs12)* reporter. Young adult animals have unbranched commissures that extend dorsally from the ventral cord. Older animals display branching from these commissures.

Blebs are defined as triangular-shaped protrusions from the processes (Pan et al., 2011). When several of these blebs form along the process, this can distort the structure of the axon, such that the axon adopts a wavy appearance (Pan et al., 2011) (**Figure 1.7B**). These wavy processes have been quantified in touch neurons and found to increase in frequency with age (Toth et al., 2012). In old animals, branches or even axon splitting can sometimes be observed at the sites of these blebs (Pan et al., 2011). Neither branches nor blebs co-localise with late endosome or lysosome markers (Pan et al., 2011), or with synaptic protein markers (Toth et al., 2012).

Beading, or bubble-like lesions, refers to focal enlargements that occur along the length of the axonal process (Pan et al., 2011, Toth et al., 2012). These beads were observed in touch neurons, and have dark, fluorescence-free regions in the centre of the structure (Pan et al., 2011, Toth et al., 2012) (**Figure 1.7C**).

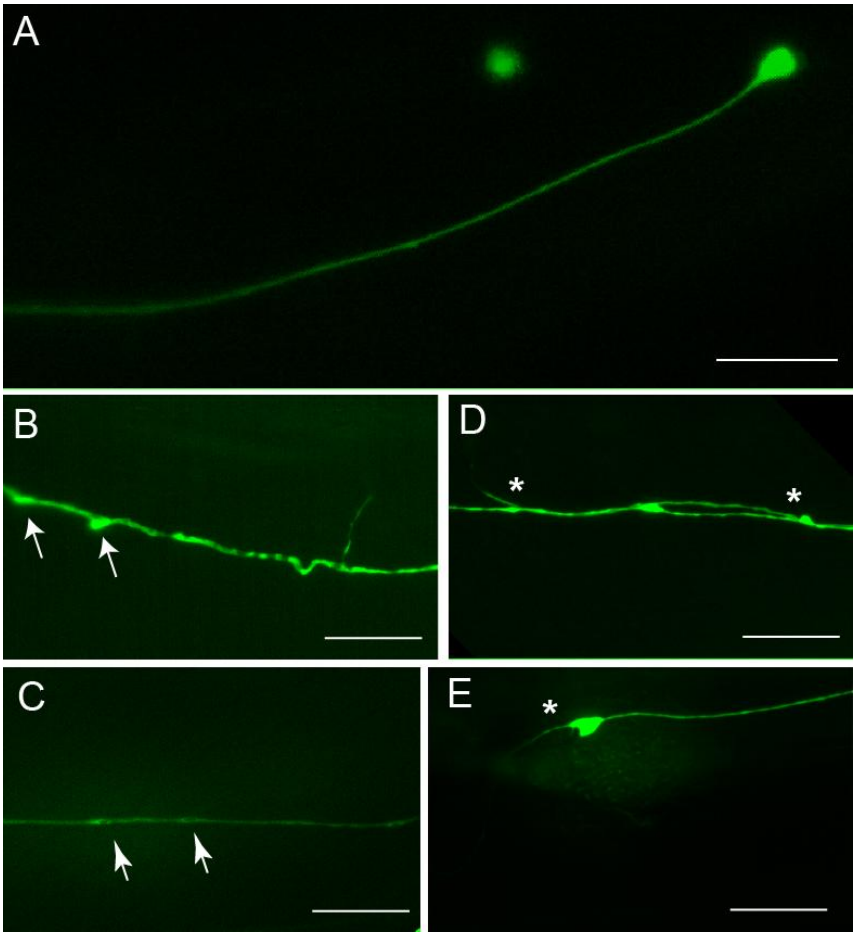

Figure 1.7: Touch receptor neurons develop abnormal structures in the cell body and axon in a progressive, age-dependent manner. Here, touch neurons are visualised using the P*mec-4::gfp* reporter line. **A)** A 'normal' touch receptor neuron (ALM). The cell body of AVM is out of focus. **(B-E)** Age-associated abnormal structures in ALM touch neurons. **B)** Blebs (arrows) form along the process, creating a wavy appearance along the axon. **C)** Beading (arrowheads) along the axon. **D)** Branching (asterisks) along the axon. Some branches appear to develop from blebs. **E)** Branching from the cell body. Scale, 10 µm.

Branching refers to novel extensions emanating from the neuronal cell body or along the axonal process. Branches have been visualized using several distinct fluorescent neuronal reporter transgenes (Pan et al., 2011, Tank et al., 2011, Toth et al., 2012) (**Figure 1.7D,E**) and were also observed by immunostaining with an anti-acetylated α-tubulin antibody, revealing that the outgrowths contain acetylated microtubules (Pan et al., 2011). The branching process is dynamic, since protrusions have been observed to form and retract, and secondary branches may extend from existing branches (Pan et al., 2011, Toth et al., 2012). Interestingly, a small but significant correlation was observed between the presence of extra branches in touch neurons and decreased mobility and sensitivity to gentle touch (Tank et al., 2011).

Complementing the work performed using transgenic strains expressing fluorescence reporter transgenes, examination of touch neurons in non-transgenic wild-type animals by electron microscopy (EM) also revealed these morphological changes. This indicates that the observed structures are not simply an artefact associated with fluorescence transgenes (Toth et al., 2012). In addition, EM studies revealed that some novel outgrowths developing from touch neuron processes co-localise with mitochondria at the branch points (Toth et al., 2012). These observations were confirmed by assays showing co-localisation of these branch points with mitochondria-specific GFP in touch neurons (Toth et al., 2012). It is unclear if mitochondria accumulate due to cytoskeletal changes at these points, or if the presence of mitochondria induces branching at these sites.

Another age-related effect found in the worm neurons is synaptic deterioration, such as a reduction in synaptic vesicles and size of the presynaptic terminal (Toth et al., 2012). Synaptic

integrity is a well-established parameter of neuronal ageing in mammals (BertoniFreddari et al., 1996, Matsumoto, 1998, Geinisman et al., 1986), and loss of synaptic integrity correlates well with memory and behavioural regression (Geinisman et al., 1995). Similarly, reduction in synaptic integrity is associated with impaired locomotion in aged *C. elegans* (Toth et al., 2012). Using EM studies, the number of synaptic vesicles in the nerve ring could be quantified, revealing that old adult worms have significantly fewer synaptic vesicles compared with young adult animals (Toth et al., 2012).

Notably, different types of neurons showed differential susceptibility to age-related changes. For example, touch receptor neurons accumulate aberrant branching with age, whereas two of the nerve ring interneurons and some dopaminergic neurons appear to remain intact (Toth et al., 2012). Moreover, different subsets of touch neurons also display differential severity of morphological defects, and even vary in the type of defects that can be observed (Toth et al., 2012, Pan et al., 2011). It is intriguing that this kind of ageing heterogeneity exists even between neurons of the same type.

1.3.2 Genetic aspects of neuronal ageing in C. elegans

In addition to the cellular characteristics of neuronal ageing in *C. elegans* that are reminiscent of age-associated neuronal changes in higher organisms, several conserved regulators of ageing have also been identified (Apfeld and Kenyon, 1998, Kenyon et al., 1993, Gaglia et al., 2012, Youngman et al., 2011, Alper et al., 2010).

1.3.2.1 The IIS pathway

In addition to its roles in whole organism lifespan as detailed above, the IIS pathway in *C. elegans* has been found to be involved in nervous system ageing. *daf-2* reduction-of-function mutants display delayed neuronal branching in touch receptor and cholinergic neurons (Pan et al., 2011, Tank et al., 2011, Toth et al., 2012). Furthermore, *daf-16* appears to be required for the *daf-2*-mediated delay in appearance of neuronal defects, since *daf-16;daf-2* double mutants display wild-type levels of branching in touch neurons (Tank et al., 2011). Interestingly, Toth and colleagues reported that the branching phenotypes observed in *daf-2* and *daf-16* mutant strains have subtle differences compared with those observed in aged wild-type animals. For example, ALM branching is rare (close to 0% incidence) in aged wild-type worms, but occurs at a ~10% frequency in *daf-2* mutant animals of the same stage (Toth et al., 2012). This suggests that the profile of neuronal ageing phenotypes is different between wild-type animals and IIS mutants, although the reasons for this have not yet been explored.

Like DAF-16, the heat shock factor (HSF)-1 transcription factor is repressed by insulin signalling. HSF-1 functions with DAF-16 to regulate proteostasis and chaperone expression when active in response to heat stress (Garigan et al., 2002). Reduction of HSF-1 activity results in a shortened lifespan (Morley and Morimoto, 2004) as well as a significantly higher frequency of touch neuron defects compared with wild-type (Toth et al., 2012, Pan et al., 2011). Furthermore, *hsf-1;daf-16* double mutants do not show enhancement of the accelerated onset of phenotypes observed in single mutants, suggesting that these transcription factors may largely act within the same pathway to regulate neuronal ageing (Pan et al., 2011). Similarly, knockdown of HSF-1 by RNAi does not affect the lifespan of *daf-16* mutants (Morley and Morimoto, 2004).

1.3.2.2 Mechanosensory signal transduction

Mechanosensory-defective (or *mec*) mutants are defective in their response to gentle touch. Interestingly, some of these mutants also show lifespan phenotypes. Mutations in mechanosensory channel components MEC-2, MEC-4, MEC-6, MEC-10 and extracellular matrix (ECM) proteins MEC-5 and MEC-9 result in a shortened lifespan, whereas mutations in ECM protein MEC-1 and α-tubulin MEC-12 do not (Pan et al., 2011). However, these mutants all display a high frequency of neuronal defects at earlier ages compared with wild-type (Pan et al., 2011). Pan and colleagues suggest that defects in nerve attachment in certain *mec-1* mutants may be responsible for the accelerated onset of defects observed in touch neurons. This is supported by the finding that animals carrying mutations in *him-4* and *fbl-1*, which encode ECM proteins hemicentin (Vogel and Hedgecock, 2001) and fibulin (Kubota et al., 2012), are defective in nerve attachment and also display a high frequency of touch neuron defects at a young age (Pan et al., 2011).

Some reports suggest that the ability of touch neurons to function correctly is correlated with healthy neuronal ageing. Tank and colleagues found that animals that display high levels of branching in touch neurons are also generally less touch sensitive (Tank et al., 2011), although a similar experiment led by others did not find any significant correlation (Toth et al., 2012). In addition, a gain-of-function mutation in the neuronal SLO-1 hyperpolarising ion channel results in touch insensitivity. *slo-1* mutant animals also display an accelerated onset of touch neuron defects (Pan et al., 2011). The involvement of synaptic activity in neuronal ageing is not limited to touch neurons, as mutations in *unc-13*, *unc-18* and *dgk-1* that impact synaptic transmission in

the ventral and dorsal nerve cord also result in higher levels of beading in axons at young stages (Pan et al., 2011).

1.3.2.3 MAPK signalling pathway

MAPK signalling pathways regulate many processes including cell proliferation, differentiation, survival, and apoptosis. The neuronal c-Jun N-terminal kinase (*jnk-1*) is a positive modulator of DAF-16 and is involved in regulating longevity. Over-expression of *jnk-1* extends lifespan in *C. elegans*, whereas loss of *jnk-1* shortens lifespan (Oh et al., 2005). Loss of *jnk-1* also results in a higher frequency of branching in both touch receptor and GABAergic neurons (Tank et al., 2011). JKK-1 and MEK-1 are stress-responsive kinases upstream of JNK-1 that both show strong similarity to the mammalian MAP kinase kinase MKK-7 (Villanueva et al., 2001). Loss of *mek-1* did not affect branching frequency, but loss of *jkk-1* resulted in the acceleration of the branching phenotype (Tank et al., 2011). This suggests that a pathway involving JNK-1 and JKK-1, but not MEK-1, regulates neuronal ageing in *C. elegans*.

Interestingly, the loss of genes strictly required for axon regeneration following laser axotomy, namely *dlk-1, mkk-4* and *pmk-3* (Hammarlund et al., 2009), does not affect the frequency of branching in touch neurons (Tank et al., 2011). This indicates that pathways involved in axon regeneration and age-related branching are distinct. Other *C. elegans* MAPK genes are also differentially involved in neuronal ageing. MLK-1 is thought to activate the p38 homolog PMK-1, and loss of this protein results in accelerated branching in touch neurons. However, loss of NSY-1, orthologous to the human apoptosis signal-regulating kinases (ASKs) (Wes and

Bargmann, 2001), or SEK-1, a MAP kinase kinase able to activate both PMK-1 and JNK-1 (Tanaka-Hino et al., 2002), did not affect neuronal ageing (Tank et al., 2011).

1.3.2.4 Longevity and ageing effectors

The capacity of other factors that regulate lifespan independently of IIS signalling to influence neuronal ageing has also been explored. For instance, the *eat-2* mutant has impaired pharyngeal pumping that prevents feeding, and therefore displays a DAF-16-independent lifespan extension that is attributed to caloric restriction (Raizen et al., 1995). Caloric restriction has been well-studied in many systems and is one of the strongest environmental contributors to longevity (Fontana et al., 2010). Unlike *daf-2* mutants, *eat-2* mutants did not show a delayed onset of neuronal defects (Pan et al., 2011, Tank et al., 2011).

lmn-1 encodes a conserved nuclear lamin protein in *C. elegans*. Mutations in lamin genes in humans are associated with an ageing disorder known as Hutchinson-Gilford Progeria Syndrome (HGPS) (Prokocimer et al., 2013), and in *C. elegans* result in a shortened lifespan (Haithcock et al., 2005). Transcript levels of *lmn-1* are also reduced in adult worms compared with embryos (D'Angelo et al., 2009). Interestingly, mutations in *lmn-1* also result in a higher frequency of touch neuron defects in young adulthood (Pan et al., 2011).

Respiration can also affect ageing. Modest inhibition of respiration leads to an extension of lifespan in both invertebrates (Copeland et al., 2009, Kayser et al., 2004) and vertebrates (Lapointe and Hekimi, 2008, Dell'agnello et al., 2007), whereas severe impairments shorten lifespan (Rea et al., 2007). *clk-1* encodes a ubiquinone biosynthetic enzyme, and mutations in

this gene result in reduced respiration and lifespan extension (Kayser et al., 2004). *clk-1* mutants also show delayed touch neuron branching (Tank et al., 2011). In contrast, *mev-1* respiratory chain mutants are short-lived (Ishii et al., 1990) and display an accelerated onset of branching (Tank et al., 2011). These data suggest that factors that affect respiration rates also affect neuronal health.

The genetic factors that have been shown to modulate neuronal ageing as detailed above are summarised in **Figure 1.8**.

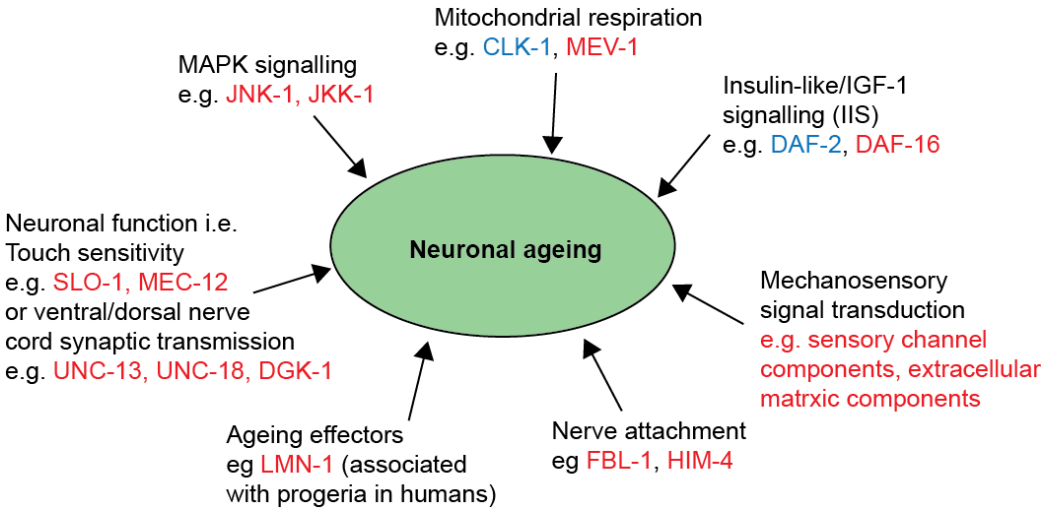

Figure 1.8: Summary of genetic regulators of neuronal ageing in *C. elegans*. For details and citations, see text. Proteins of which loss/reduction-of-function have been shown to result in accelerated neuronal ageing are indicated in red, whereas proteins of which loss/reduction-of-function result in delayed neuronal ageing are indicated in blue.

1.3.3 Do regulators of neuronal ageing act cell autonomously?

These reports indicate that many molecular players regulate neuronal ageing in *C. elegans*. Although many of these genes are expressed in neurons, some, including *daf-2* and *daf-16*, are also expressed in other tissues (Kimura et al., 2011). Despite this potential complexity, Tank and

colleagues found that neuronal re-expression of DAF-16 in *daf-16;daf-2* double mutants was sufficient to rescue the delayed onset of neuronal defects observed in *daf-2* single mutants, identifying neurons as the cellular focus of DAF-16-mediated control of neuronal ageing (Tank et al., 2011). The converse experiment, using RNAi to knock down *daf-16* solely in non-neuronal cells in a *daf-2* mutant, resulted in a restoration to wild-type lifespan, but did not affect the delay in neuronal branching that is observed in *daf-2* mutants (Tank et al., 2011). In contrast, others showed that re-expression of DAF-16 in all neurons or in body wall muscles in a *daf-16* single mutant was not sufficient to rescue the onset of neuronal defects (Pan et al., 2011). It is possible that these contrasting observations could be due to differences in scoring parameters. In addition, Tank *et al.*, observed that knock down of *daf-2* in non-neuronal cells resulted in wild-type levels of branching in touch neurons despite these animals displaying an extended lifespan (Tank et al., 2011). Together these observations suggest that *daf-2* and *daf-16* are able to regulate neuronal ageing in a cell-autonomous manner. In addition, these findings indicate that, at least in the case of the IIS pathway, regulation of neuronal ageing and whole organism lifespan can be decoupled from one another.

As previously mentioned, the IIS-regulated transcription factor HSF-1 was also reported to regulate neuronal ageing (Pan et al., 2011, Toth et al., 2012). Interestingly, re-expression of HSF-1 solely in touch neurons was able to completely rescue this phenotype (Toth et al., 2012), indicating that, like DAF-16, HSF-1 can also act cell-autonomously to regulate neuronal ageing.

1.4 Thesis overview

There is strong interest in the roles of Tau in neuronal ageing and pathology, and significant advancement has been made in this field despite the challenges involved with functional redundancy in rodent models. In *C. elegans*, the Tau homolog PTL-1 was first characterised almost two decades ago, but until now only a limited understanding of its functions within neurons and in the context of ageing has been gained. We have investigated the functions of PTL-1 within the stress response, neuronal ageing, and longevity in *C. elegans*. Results of these investigations are detailed in four chapters. The first chapter is a brief description of the *ptl-1* mutant strains used in this study. The second chapter explores the role of PTL-1 in the stress response and longevity, and its relationship with the transcription factor SKN-1 that is involved in the induction of detoxification enzymes. The third chapter describes the functions of PTL-1 in neuronal ageing in two distinct subsets of neurons and demonstrates that the levels of PTL-1 are critical in regulating both tissue ageing and lifespan. In the fourth chapter, investigations on the role of PTL-1 in ageing are extended by investigating whether the maintenance of structural integrity by PTL-1 is cell autonomous, and also by exploring the role of PTL-1 within the touch neurons in regulating longevity.

Chapter 2:
Materials and methods

2.1 Materials

2.1.1 Chemicals and reagents

- 6x Loading Dye Solution (Fermentas, Glen Burnie, MD, Australia)
- Acetic acid, glacial (Ajax Laboratory Chemicals, Taren Point, NSW, Australia)
- Agar bacteriological (In Vitro, Noble Park North, VIC, Australia)
- Agarose (DNA grade) (Progen Industries, Darra, QLD, Australia)
- Ampicillin sodium salt (Amresco, Solon, USA)
- Bacto peptone (Amyl Media, Dandenong, VIC, Australia)
- Calcium chloride (Riedel-de Haën, Seelze, Germany)
- Carbenicillin (AG Scientific, San Diego, CA, USA)
- Cholesterol (Sigma Chemical Company, Castle Hill, NSW, Australia)
- Copper (II) Sulfate Pentahydrate (Ajax Laboratory Chemicals)
- DAKO pen (Dako, North Sydney, NSW, Australia)
- DAPI fluorescent mounting medium (Dako)
- Deoxynucleotide triphosphates (dNTPs) (Bioline, Alexandria, NSW, Australia)
- Di-potassium hydrogen orthophosphate (Ajax Laboratory Chemicals)
- Disodium ethylenediamine tetraacetate (Ajax Laboratory Chemicals)
- Di-sodium hydrogen orthophosphate (Ajax Laboratory Chemicals)
- Ethidium bromide (Roche Molecular Biochemicals)
- Ethylene glycol tetraacetic acid (EGTA) (Amresco)
- Ethylenediaminetetraacetic acid (EDTA) (Ajax Laboratory Chemicals)
- Generuler™ DNA ladder mix (Progen Industries)
- Glucose (Ajax Laboratory Chemicals)
- Glycerol (Sigma Chemical Company, Castle Hill, NSW, Australia)
- Hydrogen peroxide (H_2O_2) 30 % (w/v) (Sigma Chemical Company, NSW, Australia)
- Iron(II) sulfate (Sigma Chemical Company, Castle Hill, NSW, Australia)
- Isopropanol (BDH Chemicals, Port Fairy, VIC, Australia)
- Isopropyl β-D-1-thiogalactopyranoside (IPTG) (Biochemicals, Gymea, NSW, Australia)
- Magnesium chloride (Biolab Scientific)
- Magnesium sulfate heptahydrate (BDH Chemicals, Port Fairy, VIC, Australia)
- Methanol (Sigma-Aldrich)
- Mounting media (Dako)
- Neomycin, G418 (Sigma-Aldrich)
- Normal goat serum (Life Technologies-Invitrogen)
- Nystatin (Sigma-Aldrich)
- Paraformaldehyde (Sigma Chemical Company, Castle Hill, NSW, Australia)
- Paraquat dichloride hydrate (Sigma Chemical Company, Castle Hill, NSW, Australia)
- Poly-L-lysine (Sigma-Aldrich)
- Potassium acetate (Crown Technology Inc., Indianapolis, IN, USA)

- Potassium chloride (BDH Chemicals)
- Potassium dihydrogen orthophosphate (BDH Chemicals)
- Potassium phosphate (Ajax Laboratory Chemicals)
- Puromycin dihydrochloride (Sigma-Aldrich)
- Sodium acetate (Ajax Laboratory Chemicals)
- Sodium azide (Sigma Chemical Company, Castle Hill, NSW, Australia)
- Sodium chloride (Ajax Laboratory Chemicals)
- Sodium dodecyl sulfate (lauryl sulfate sodium salt) (SDS) (Sigma Chemical Company)
- Sodium hydroxide (Ajax Laboratory Chemicals)
- Sodium hypochlorite 12.5% w/v solution (Nuplex Industries, Seven Hills, Australia)
- Levamisole hydrochloride (Sigma Chemical Company, Castle Hill, NSW, Australia)
- Tris-hydroxymethyl-methylamine (Tris) (Ajax Laboratory Chemicals)
- Triton X (Amresco)
- Tween 20 (Amresco)
- Yeast extract (In Vitro, Noble Park North, VIC, Australia)
- Zinc sulfate (Sigma Chemical Company, Castle Hill, NSW, Australia)

2.1.2 Antibodies

- Anti V5-HRP, generating by crosslinking an Anti-V5 antibody (R960-25; mouse monoclonal IgG2) with horseradish peroxidase (HRP) using glutaraldehyde (Life Technologies)
- Monoclonal Anti-Acetylated Tubulin antibody produced in mouse, clone 6-11B-1 (Sigma-Aldrich; #T7451)
- Alexa Fluor 555 goat anti-rabbit IgG (Invitrogen, # A-21428)
- Alexa Fluor 488 F(ab')2 Fragment of Goat Anti-Mouse IgG (H+L) Antibody (Invitrogen #A-11017)

2.1.3 Enzymes

- Phusion® High-Fidelity DNA Polymerase (New England Biolabs, #M0530S)
- *Taq* DNA Polymerase with Standard *Taq* Buffer (New England Biolabs, #M0273S)
- T4 DNA ligase (New England Biolabs)
- Gateway® BP Clonase® II enzyme (Life Technologies- Invitrogen)
- Gateway® LR Clonase® II enzyme (Life Technologies- Invitrogen)
- Gateway® LR Clonase® II Plus enzyme (Life Technologies- Invitrogen)
- Proteinase K (Boehringer Ingelheim Pty. Ltd., North Ryde, NSW, Australia)

2.1.4 Kits and commercial reagents

- S.N.A.P.™ UV-Free Gel Purification Kit (Life Technologies)
- QIAquick PCR Purification Kit (Qiagen)
- JETSTAR 2.0 Plasmid Midiprep kit (Astral Scientific)

2.1.5 Equipment

- Microscopes: Nikon stereo microscope, Olympus BX51 Microscope, Olympus
- Biolistic transformation of *C. elegans:* PDS-1000/He™ System from BioRad

2.1.6 External procedures

- Sequencing of DNA was performed by Macrogen (Seoul, Korea)
- Oligonucleotide primers for PCR were generated by Sigma-Aldrich and Integrated DNA Technologies.

2.1.7 Bacterial strains

- OP50 *E. coli*
- HB101 *E. coli* [F- mcrB mrr hsdS20(rB- mB-) recA13 leuB6 ara-14 proA2 lacY1 galK2 xyl-5 mtl-1 rpsL20(SmR) glnV44 λ-]
- HT115 *E. coli* [F-, mcrA, mcrB, IN(rrnD-rrnE)1, rnc14::Tn10(DE3 lysogen: lavUV5 promoter -T7 polymerase].
- DH5alpha *E. coli* [F- endA1 glnV44 thi-1 recA1 relA1 gyrA96 deoR nupG Φ80d*lacZ*ΔM15Δ(*lacZYA-argF*)U169, hsdR17(rK- mK+), λ–]
- One Shot® TOP10 Chemically Competent *E. coli* (Life Technologies- Invitrogen) [FmcrAΔ(mrr-hsdRMS-mcrBC) φ80lacZΔM15 ΔlacX74 nupG recA1 araD139 Δ(araleu)7697 galE15 galK16 rpsL(StrR) endA1 λ-]
- Alpha-select silver efficiency Chemically Competent *E. coli* (Bioline) [F- *deo*R *end*A1 *rec*A1 *rel*A1 *gyr*A96 *hsd*R17(rk-, mk+) *sup*E44 *thi*-1 *pho*A Δ(*lac*ZYA-argF)U169 Φ80*lac*ZΔM15 λ-]

2.1.8 Nematode strains

2.1.8.1 Strains received from the Caenorhabditis Genetics Centre (CGC)

Strain name	Genotype	Source
N2	Wild-type, strain Bristol	CGC
RB809	*ptl-1(ok621)* III; not outcrossed	CGC
FX00543	*ptl-1(tm543)* III; not outcrossed	National Bioresource Project, Japan
CZ10175	*zdIs5*[P*mec-4*::*gfp* + *lin-15*(+)] I	CGC
EG1285	*oxIs12*[*Punc-47*::*gfp* + *lin-15*(+)] X	CGC
MT464	*unc-5(e53)* IV; *dpy-11(e224)* V; *lon-2(e678)* X	CGC
LD1	*ldIs7 [skn-1B/C::GFP + pRF4(rol-6(su1006))]*	CGC
LD1171	*ldIs3 [*P*gcs-1::GFP + pRF4(rol-6(su1006))]*	CGC
CB450	*unc-13(e450) I*	CGC
CB928	*unc-31(e928) IV*	CGC
TU3403	*ccIs4251 [*P*myo-3::GFP(NLS)::LacZ* + P*myo-3::GFP* + *dpy-20(+)]. uIs71 [pCFJ90(*P*myo-2::mCherry)* + P*mec-18::sid-1]; sid-1(qt2)* V	CGC
TJ356	*zIs356 [*P*daf-16::daf-16a/b::GFP + rol-6]* IV	CGC
EU1	*skn-1(zu67) IV/ nT1 [unc-?(n754) let-?] (IV;V)*	CGC
TU3401	*ccIs4251 [*P*myo-3::GFP(NLS)::LacZ* + P*myo-3::GFP* + *dpy-20(+)]. uIs71 [pCFJ90(*P*myo-2::mCherry) + mec-18p::sid-1] ; sid-1(qt2)* V	CGC
SJ4005	*zcIs4[*P*hsp-4::gfp]*	CGC

2.1.8.2 Strains generated in this project

Strain name	Genotype
APD004	*ptl-1(ok621)* III; outcrossed 6x to wild-type
APD009	*ptl-1(ok621)* III; *oxIs12*[*Punc-47*::*gfp* + *lin-15*(+)] X
APD010	*ptl-1(ok621) III; zdIs5*[P*mec-4*::*gfp* + *lin-15*(+)] I
APD011	*ptl-1(ok621)* III; *bus-17(e2800)* X.
APD015	*ptl-1(tm543)* III
APD016	*zdIs5* I; *ptl-1(tm543)* III
APD017	*oxIs12* X*; ptl-1(tm543)* III
APD018	*apdIs4*[P*ptl-1:hTau40:ptl-1* 3′ UTR; P*myo-2::mCherry*; P*rpl-28::PuroR::rpl-16_outron::NeoR::let-858*_3′ UTR]
APD021	*apdIs5*[P*ptl-1:ptl-1::v5:ptl-1* 3′ UTR; P*myo-2::mCherry*; P*rpl-28::PuroR::rpl-16_outron::NeoR::let-858*_3′ UTR]
APD025	*apdIs4*; outcrossed 6x to wild-type
APD026	*apdIs5*; outcrossed 6x to wild-type
APD030	*apdIs4*; *zdIs5* I; *ptl-1(ok621)* III

Strain name	Genotype
APD031	*apdIs4*; *zdIs5* I
APD032	*apdIs4*; *oxIs12* X; *ptl-1(ok621)* III
APD033	*apdIs4*; *oxIs12* X
APD034	*apdIs4*; *ptl-1(ok621)* III
APD035	*apdIs5*; *zdIs5* I; *ptl-1(ok621)* III)
APD036	*apdIs5*; *zdIs5* I
APD037	*apdIs5*; *oxIs12* X; *ptl-1(ok621)* III
APD038	*apdIs5*; *oxIs12* X
APD039	*apdIs5*; *ptl-1(ok621)* III
APD050	*zdIs5* I; *uIs71*
APD055	*ptl-1(ok621)* III;*ldIs7*
APD059	*ptl-1(ok621); zIs356* IV
APD062	*ptl-1(ok621)* III;*daf-2(e1370)* III
APD069	*ptl-1(tm543)* III;*ldIs7*
APD066	*oxIs12;* P*mec-18::sid-1;* P*myo-2::mCherry; sid-1(qt2)*
APD070	*apdIs9[*P*mec-7:ptl-1::v5:PTL-1 3′UTR]*; outcrossed 6x to wild-type
APD074	*apdIs9[*P*mec-7:ptl-1::v5:PTL-1 3′UTR]; ptl-1(ok621) III; oxIs12*
APD075	*apdIs9[*P*mec-7:ptl-1::v5:PTL-1 3′UTR]; ptl-1(ok621) III; zdIs5*
APD076	*apdIs9[*P*mec-7:ptl-1::v5:PTL-1 3′UTR]; ptl-1(ok621) III*
APD077	*apdIs5; ldIs7*
APD078	*apdIs5; ldIs7; ptl-1(ok621)* III
APD081	*apdIs9[*P*mec-7:ptl-1::v5:PTL-1 3′UTR]; oxIs12*
APD082	*apdIs9[*P*mec-7:ptl-1::v5:PTL-1 3′UTR]; zdIs5*
APD083	*daf-2(e1370)* III; *ldIs7*
APD084	*daf-2(e1370)* III; *ldIs7; ptl-1(ok621)* III
APD088	*apdIs10*[P*aex-3:ptl-1::v5:ptl-1* 3′ UTR; P*myo-2::mCherry*; P*rpl-28::PuroR::rpl-16_outron::NeoR::let-858*_3′ UTR]
APD089	*apdIs4*; *ldIs7*
APD090	*apdIs4*; *ldIs7; ptl-1(ok621)* III
APD091	*ldIs3*; *ptl-1(ok621)* III
APD092	*ldIs3*; *ptl-1(tm543)* III
APD093	*apdIs5*; *ldIs3*
APD094	*apdIs5*; *ldIs7; ptl-1(ok621)* III
APD096	*apdIs10*; outcrossed 6x to wild-type
APD097	*apdIs10; zdIs5* I
APD098	*apdIs10; zdIs5* I; *ptl-1(ok621)* III
APD099	*apdIs10; oxIs12* X
APD100	*apdIs10; oxIs12* X; *ptl-1(ok621)* III
APD101	*apdIs10*; *ldIs7*
APD102	*apdIs10*; *ldIs7; ptl-1(ok621)* III
APD103	*apdIs10*; *ldIs3*

Strain name	Genotype
APD104	*apdIs10*; *ldIs3; ptl-1(ok621)* III
APD105	*apdIs10*; *ptl-1(ok621)* III
APD113	*jsIs682*[P*rab-3::GFP::RAB-3*; pJM23]*;lin-15B(n765)* X; *vdEx263*[P*mec-4::mCherry + odr-1::dsRed*]. ***vdEx263* was a kind gift from Nick Valmas and Massimo Hilliard (Queensland Brain Institute, University of Queensland)**
APD114	*jsIs682;lin-15B(n765)* X; *vdEx263*; *ptl-1(ok621)*
APD118	*unc-13(e450)* I*; ldIs7*
APD120	*unc-31(e928)* IV*; ldIs7*
APD121	*unc-13(e450)* I; *ldIs3*
APD122	*unc-31(e928)* IV; *ldIs3*
APD123	*apdEx10*[P*ptl-1:ptl-1::gfp:ptl-1* 3′ UTR; P*rpl-28::PuroR::rpl-16_outron::NeoR::let-858*_3′ UTR]
APD125	*unc-13(e450)* I*; ldIs7; ptl-1(ok621)* III
APD126	*unc-31(e928)* X*; ldIs7; ptl-1(ok621)* III
APD127	*ptl-1(ok621)* III*; skn-1(zu67) IV/nT1[unc-?(n754) let-?]*(IV;V)
APD128	*apdEx10*; *sid-1(pk3321)*; *uIs69*
APD130	*apdEx10; sid-1(qt2); uIs71*
APD136	*apdEx13;* outcrossed 6x to wild-type
APD138	*apdEx13; ldIs7*
APD139	*apdEx13; ldIs7; ptl-1(ok621)* III
APD140	*apdEx13; ldIs3*
APD141	*apdEx13; ldIs3; ptl-1(ok621)* III

2.1.9 Integrated and extrachromosomal arrays

Array name	Plasmid used	Genotype
apdIs4	pY007	*apdIs4*[P*ptl-1:hTau40:ptl-1* 3′ UTR; P*myo-2::mCherry*; P*rpl-28::PuroR::rpl-16_outron::NeoR::let-858*_3′ UTR]
apdIs5	pY005	*apdIs5*[P*ptl-1:ptl-1::v5:ptl-1* 3′ UTR; P*myo-2::gfp*; P*rpl-28::PuroR::rpl-16_outron::NeoR::let-858*_3′ UTR]
apdIs9	pY009	*apdIs9*[P*mec-7:ptl-1::v5:ptl-1* 3′ UTR; P*myo-2::mCherry*; P*rpl-28::PuroR::rpl-16_outron::NeoR::let-858*_3′ UTR]
apdIs10	pY011	*apdIs10*[P*aex-3:ptl-1::v5:ptl-1* 3′ UTR; P*myo-2::mCherry*; P*rpl-28::PuroR::rpl-16_outron::NeoR::let-858*_3′ UTR]
apdEx10	pY013	*apdEx10*[P*ptl-1:ptl-1::gfp:ptl-1* 3′ UTR; P*rpl-28::PuroR::rpl-16_outron::NeoR::let-858*_3′ UTR]
apdEx13	pY015	*apdEx13*[P*gpa-4:ptl-1::v5:ptl-1* 3′ UTR; P*myo-2::mCherry;* P*rpl-28::PuroR::rpl-16_outron::NeoR::let-858*_3′ UTR]

2.1.10 Plasmid list

Plasmid	Composition	Vector	Insert	Generated by

name				
pY001	P*ptl-1* L4L1R	pDONRP4P1R	P*ptl-1* (from gDNA)	YL Chew
pY002	*ptl-1*::v5 L1L2	pDONR221	*ptl-1::*v5 (from cDNA)	YL Chew
pY003	*ptl-1* 3′UTR L2RL3	pDONRP2RP3	*ptl-1* 3′UTR (from gDNA)	YL Chew
pY004	v5::*ptl-1* L1L2	pDONR221	v5::*ptl-1* (from cDNA)	YL Chew
pY005	P*ptl-1*: *ptl-1*::v5: *ptl-1* 3′UTR in pBCN41	pBCN41	Multisite LR of pY001, PY002, pY003	YL Chew
pY006	P*mec-7* L4L1R	pDONRP4P1R	P*mec-7* (from gDNA)	YL Chew
pY007	P*ptl-1*: *hTau40*: *ptl-1* 3′UTR in pBCN40	pBCN40	Multisite LR of pY001, *hTau40* (LI), pY003	YL Chew
pY008	P*ptl-1*: v5::*ptl-1*: *ptl-1* 3′UTR in pBCN40	pBCN40	Multisite LR of pY001, PY004, pY003	YL Chew
pY009	P*mec-7*: v5::*ptl-1*: *ptl-1* 3′UTR in pBCN40	pBCN40	Multisite LR of pY006, pY002, pY003	YL Chew
pY010	P*mec-7*: v5::*ptl-1*: *ptl-1* 3′UTR in pBCN40	pBCN40	Multisite LR of pY006, PY004, pY003	YL Chew
pY011	P*aex-3* L4L1R	pDONRP4P1R	P*aex-3*(from gDNA)	YL Chew
pY012	*ptl-1::gfp* in pPD95.75	pPD95.75	*ptl-1* (from cDNA) cloned HindIII/SmaI into pPD95.75	X Fan
pY013	P*ptl-1*:*ptl-1gfp*:*unc-54* 3′ UTR in pBCN41	pBCN41	*ptl-1::gfp* from pY012 cloned ClaI/ApaI into pY005	X Fan
pY014	P*gpa-4* L4L1R	pSBlim-7	P*gpa-4* (from gDNA) cloned SphI/AgeI into pSBlim-7	YL Chew
pY015	P*gpa-4*: *ptl-1*::v5: *ptl-1* 3′UTR in pBCN40	pBCN40	Multisite LR of pY014, pY002, pY003	YL Chew

Where cDNA is complementary DNA and gDNA is genomic DNA from *C. elegans*.

2.1.11 Primers used for cloning (all sequences are written 5′ to 3′)

To amplify PTL-1::V5 cDNA with attB1 and attB2 sites

Forward:

GGGGACAAGTTTGTACAAAAAAGCAGGCTCAATGTCAACCCCTCAATCAGAG

*Reverse***:**

TCACGTAGAATCGAGACCGAGGAGAGGGTTAGGGATAGGCTTACCCGCCGCGCGAT

TGAATATAAAATCAGG

To amplify V5::PTL-1 cDNA with attB1 and attB2 sites

Forward:

ATGGGTAAGCCTATCCCTAACCCTCTCCTCGGTCTCGATTCTACGGCGGCGTCAACC

CCTCAATCAGAG

Reverse:

GGGGACCACTTTGTACAAGAAAGCTGGGTTCAGCGATTGAATATAAAATCAGGAG

To clone the PTL-1 cDNA into pPD95.75 using HindIII and SmaI restriction sites

*Forward***:** TTTTAAGCTTTTGGTCCGTTGTCAGTCGAG

Reverse: TTTTCCCGGGGGAGACCGAGGAGAGGGTTAG

To amplify the *ptl-1* promoter with attB4 and attB1r sites

Forward: GGGGACAACTTTGTATAGAAAAGTTGCATTCCGCATGGTTGGAAAGAG

Reverse:

GGGGACTGCTTTTTTGTACAAACTTGATTTTTCCTGAAAAATTGAAATTGGGAG

To clone the *gpa-4* promoter into pSBlim-7 (entry clone with attL4 and attL1r sites) using SphI and AgeI restriction sites

Forward: AATTGCATGCGCTGATTTGCCGTTTGTCG

Reverse: CTTATTCATTTTGTGAACACTTTTCAACAACCGGT

To amplify the *aex-3* promoter with attB4 and attB1r sites

Forward: GGGGCAACTTTGTATAGAAAAGTTGGCTTCCACAAAAACTGCCGC

Reverse: GGGGCTGCTTTTTTGTACAAACTTGTTTTTATTAGGATAGGTACATTGG

To amplify the *mec-7* promoter with attB4 and attB1r sites

Forward: GGGGCAACTTTGTATAGAAAAGTTGTAGTAATCTAGAAATGTAAACC

Reverse: GGGGCTGCTTTTTTGTACAAACTTGGTTGCTTGAAATTTGGACCC

To amplify the *ptl-1* 3′UTR with attB4 and attB1r sites

Forward:

GGGGACAGCTTTCTTGTACAAAGTGGGATAACAATCGCTGATGTATACCGCGC

Reverse:

GGGGACAACTTTGTATAATAAAGTTGACACTTTTAATTACCACTTTATTGAAGAG

2.2 Methods

2.2.1 Nematode maintenance

C. elegans strains were cultured on Nematode Growth Medium [NGM: 2 % (w/v) agar, 50 mM NaCl, 0.25 % (w/v) peptone, 1 mM $CaCl_2$, 5 µg/ml cholesterol, 25 mM KH_2PO_4 and 1 mM $MgSO_4$ in H_2O] plates seeded with the *Escherichia coli* strain OP50, unless otherwise specified. Hermaphrodite animals were used for all experiments. The wild-type strain used for all experiments is N2 (Bristol), obtained from the CGC. These were cultured at 15–25 ºC depending on the desired growth rate.

For maintenance in liquid culture: liquid medium consisted of S-Basal [0.1 M NaCl, 50 mM potassium phosphate pH 6.0, 5 µg/ml cholesterol in H_2O] that was supplemented with 10 mM potassium citrate pH 6.0, 1% (v/v) trace metals solution [5 mM Na_2EDTA (1.86 g), 2.5 mM $FeSO_4$, 1 mM $MnCl_2$, 1 mM $ZnSO_4$, 0.1 mM $CuSO_4$], 3 mM CaCl, and 3 mM $MgSO_4$ to make S-Medium. Up to 300,000 young adult animals could be cultured in 50 mL of S-Medium supplemented with HB101 bacteria used to feed the worms. To prevent microbial contamination, streptomycin (50 µg/mL) and nystatin (300 U/mL) were added to the culture medium.

In the case where animals were contaminated with bacterial or fungal contamination, gravid hermaphrodites were placed into 20 µl of bleaching solution (1.7 M NaOH, 2.1% v/v NaOCl) on an OP50-seeded NGM plate. Surviving eggs were maintained on plates or in liquid as described.

2.2.2 Synchronisation of animals

Large synchronous populations were obtained by washing a few thousand gravid hermaphrodites in bleaching solution. Bleaching solution ruptures adult hermaphrodites but the eggs that are released survive and are recovered in M9 buffer [22 mM KH_2PO_4, 50 mM Na_2HPO_4, 86 mM

NaCl, 1 mM $MgSO_4$] in the absence of bacterial food. Eggs were left in M9 buffer for at least 8 hours to allow them to hatch and arrest at the first larval stage (L1). Larvae were then distributed on to OP50-seeded NGM plates allowing them to grow synchronously. Alternatively, young adult animals were plated onto an OP50-seeded NGM plate and allowed to lay eggs for up to 4 hours at the desired temperature. The parent was then removed and the eggs allowed to hatch.

2.2.3 Genotyping by PCR

For determination of the strain genotype, individual worms were picked into a lysis solution [50 mM KCl, 10 mM Tris pH8.3, 2.5 mM $MgCl_2$, 0.45 % NP-40, 0.45 % Tween-20, 0.01 % gelatine and 0.5 mg/ml Proteinase K (Promega)] in a 0.2 mL tube and frozen at -80 °C for at least 10 minutes. These were then placed at 65 °C for 60 minutes followed by incubating at 95 °C for 15 minutes in a thermocycler. The entire lysed sample was then used as a template for PCR using the standard Taq polymerase and buffer system [20 mM Tris-HCl, 10 mM $(NH_4)_2SO_4$, 10 mM KCl, 2 mM $MgSO_4$, 0.1% Triton® X-100 pH 8.8 @ 25°C] from New England Biolabs. Primers were used at a final concentration of 0.2 µM for all reactions. PCR conditions for the *ptl-1* mutant alleles are detailed below:

***ptl-1(ok621)* genotyping:**

Primers used are **PTL-1 FF2** (CGAACCTGAACCGGAACCAG), **PTL-1 IR2** (GAGATGGCGCTGTTGAAGCAG) and **PTL-1 FR2** (GCCACTTCGCTGGAAATTACC).

Cycling conditions for the PCR: 94°C 2 min, then 94°C 20 sec, 65°C 20 sec, 72°C 45 sec (33 cycles in total of steps 2 to 4), then 72° C 5 min.

Expected size for: wild-type allele: 751 bp; *ok621* allele: 461 bp.

***ptl-1(tm543)* genotyping:**

Primers used are **PTL-1 FR2** (GCCACTTCGCTGGAAATTACC), **PTL1tm543 FF** (GTTCTGTCCGTCTTATTGTATCC). Cycling conditions for the PCR: 94°C 2 min, then 94°C 20 sec, 65°C 20 sec, 72°C 45 sec (33 cycles in total of steps 2 to 4), then 72° C 5 min.

Expected size for: wild-type allele: 1170 bp; *tm543* allele: 382 bp.

2.2.4 Generation of strains by crossing

For outcrossing, all strains were mated with N2 males for six generations.

For crosses with strains containing fluorescent reporters, progeny of the cross were genotyped for the desired mutant allele by PCR and screened by microscopy (both under the dissecting and upright microscope) to return both components to homozygosity. An exception is the P*gcs-1:gfp* (*ldIs3)* fluorescence reporter, which has a low signal under normal (unstressed) conditions. These were genotyped by PCR for the P*gcs-1::gfp* transgene using primers **Pgcs-1for** (GGACTACGGTAGGAGTTCTG) and **gfp_rev** (CGGGCATGGCACTCTTG). Animals that contained the transgene produced a band at 586 bp. In addition, for the GFP::RAB-3 *(jsIs821 III)* transgene that is on the same chromosome as *ptl-1*, recombinant animals that contained both the GFP::RAB-3 transgene and a *ptl-1(ok621)* mutation were generated by allowing heterozygous progeny of a cross between *ptl-1(ok621)* males and GFP::RAB-3 hermaphrodites to generate self progeny. At a low frequency (~3-4 per 100), these self progeny undergo recombination on one chromosome in between these genetic components. Recombinant progeny were isolated after screening for both components.

For crosses with strains containing mutant alleles, progeny of the cross were allowed to self and the parent genotyped by PCR for the allele in question. For the *daf-2(e1370) III* allele, which is a single base change, animals were genotyped by dauer assay, as *daf-2* mutant animals but not wild-type or *ptl-1(ok621)* animals would form dauers constitutively when moved to 25 °C (Riddle et al., 1981, Vowels and Thomas, 1992). As both *daf-2* and *ptl-1* genes are located on chromosome III, it was necessary to isolate recombinant animals to return both *daf-2(e1370)* and *ptl-1(ok621)* alleles to homozygosity. 5 recombinant lines were isolated and three were assayed for the same phenotype (SKN-1::GFP re-localisation to intestinal nuclei in response to stress, see section **2.2.9**). As all three lines produced the same phenotype (**Appendix 1**), we proceeded to use one line (APD084) for subsequent experiments.

Another more complicated cross involved the *skn-1(zu67) IV* mutation, which is also a single base change. As *skn-1(zu67)* animals are maternal lethal (Bowerman et al., 1992), i.e. they produce dead eggs and no live progeny, the mutation is balanced with a *nT1[unc-?(n754) let-?] (IV;V)* chromosomal translocation. In summary, animals that are homozygous for the *nT1* balancer (*nT1/nT1*) are dead, animals that are heterozygous (*skn-1(zu67)/nT1*) are alive but move in an uncoordinated manner (due to the presence of the *unc* allele in *nT1*), and animals that are homozygous for the *skn-1* allele and do not contain the *nT1* balancer (*skn-1(zu67)/skn-1(zu67)*) are alive and display wild-type movement but produce dead eggs. To generate *skn-1(zu67);ptl-1(ok621)* double mutant animals, *ptl-1(ok621)* males were mated with *skn-1(zu67)/nT1* hermaphrodites and wild-type moving progeny containing the *ptl-1(ok621)* allele were then crossed with progeny displaying uncoordinated movement and also containing *ptl-1(ok621)*. A detailed schematic for this cross is shown in **Figure 2.1.**

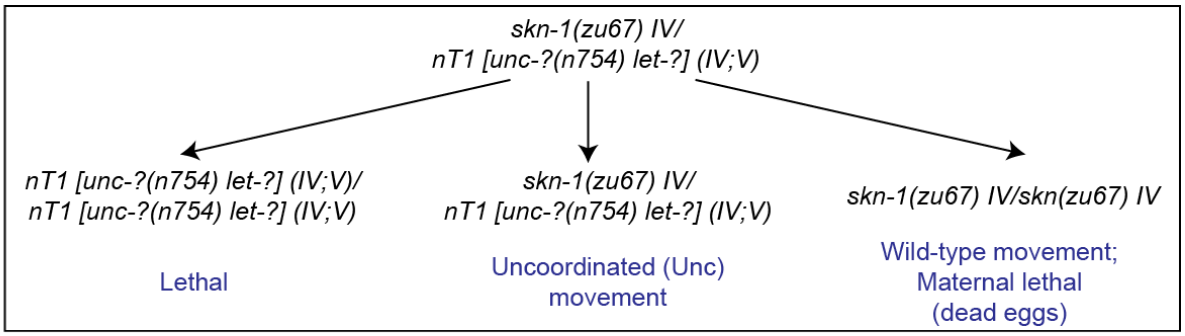

1) *ptl-1(ok621) III/ptl-1(ok621)III* ♂ X *skn-1(zu67) IV/ nT1 [unc-?(n754) let-?] (IV;V)* ♀

ptl-1(ok621) III/+ ; *skn-1(zu67) IV/+* ♂ ♀ (wild-type movement)

OR

ptl-1(ok621)III/+ ; *nT1 [unc-?(n754) let-?] (IV;V)/+* ♂ ♀ (uncoordinated)

2) *ptl-1(ok621) III/+; skn-1(zu67) IV/+* ♂ X *ptl-1(ok621)III/+; nT1 [unc-?(n754) let-?] (IV;V)/+* ♀

ptl-1(ok621) III/ptl-1(ok621) III		*skn-1(zu67) IV/+*	(wild-type movement)
OR	;	OR	
ptl-1(ok621) III/+		*skn-1(zu67) IV/nT1 [unc-?(n754) let-?] (IV;V)*	(uncoordinated)
OR		OR	
+/+		+/+	(wild-type movement)

Pick uncoordinated movement worms to self.
Genotype parent for *ptl-1(ok621)* and select *ptl-1(ok621)/ptl-1(ok621)* animals.

Maintain *skn-1(zu67)/nT1 [unc-?(n754) let-?]* by picking uncoordinated worms to self.
Assays were conducted using wild-type moving *skn-1(zu67)/skn(zu67)* first generation progeny of *skn-1(zu67)/nT1 [unc-?(n754) let-?]* parents

Figure 2.1: Schematic for the generation of *skn-1(zu67); ptl-1(ok621)* double mutant animals. Details of strain construction are provided in the text. For all assays using *skn-1(zu67)*, first generation *skn-1(zu67)/skn-1(zu67)* progeny of *skn-1(zu67)/nT1[unc-?(n754) let-?]* parents with or without the *ptl-1(ok621)* allele were picked based on a wild-type movement phenotype. The phrase "to self" indicates that animals were allowed to self-fertilise.

The presence of single base changes was verified by sequencing (Macrogen, Korea).

2.2.5 Generation of plasmid constructs

Cloning was performed using the Gateway (Invitrogen, Life Technologies) system according to the manufacturer's instructions or by conventional restriction enzyme digest where appropriate. Dual antibiotic selection plasmids pBCN40 and pBCN41, encoding visual markers *Pmyo-2*::*mCherry* and P*myo-2*::*gfp*, respectively, were generously provided by Drs J. Semple and B. Lehner (EMBL Centre for Genomic Regulation Systems Biology Unit, Barcelona). The hTau40 entry clone (in pENTR-SD-D-Topo) was kindly provided by Dr L. Ittner (Brain and Mind Research Institute, University of Sydney). Detailed information regarding templates and primers used can be found in sections **2.1.10** and **2.1.11** The Multisite LR reaction (Invitrogen) was used to combine entry clones into destination vector pBCN40 or pBCN41.

2.2.6 Generation of transgenic lines

Transgenic worms for rescue experiments were generated by biolistic transformation using the PDS-1000/He™ particle delivery system (BioRad) according to the manufacturer's instructions. Wild-type worms were bombarded with 7 µg of linearised plasmid DNA using previously established methods (Praitis et al., 2001). Selection post-bombardment was undertaken using the dual antibiotic selection protocol (Semple et al., 2012) (**Figure 2.2**).

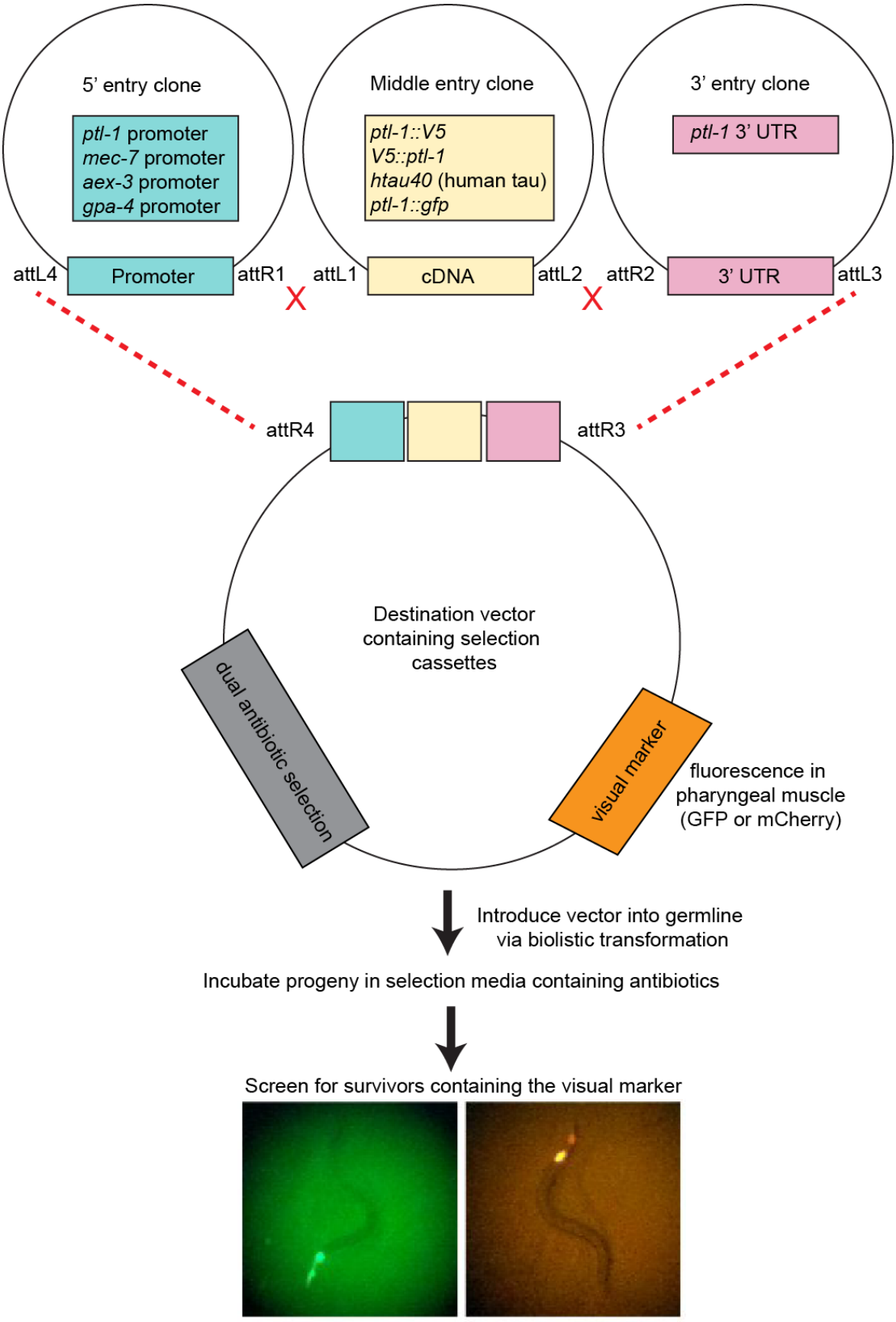
5' entry clone
ptl-1 promoter
mec-7 promoter
aex-3 promoter
gpa-4 promoter
Middle entry clone
ptl-1::V5
V5::ptl-1
htau40 (human tau)
ptl-1::gfp
3' entry clone
ptl-1 3' UTR
attL4
Promoter
attR1
attL1
cDNA
attL2
attR2
3' UTR
attL3
attR4
attR3
Destination vector containing selection cassettes
dual antibiotic selection
visual marker
fluorescence in pharyngeal muscle (GFP or mCherry)
Introduce vector into germline via biolistic transformation
Incubate progeny in selection media containing antibiotics
Screen for survivors containing the visual marker

Figure 2.2: Generation of transgenic *C. elegans*. Using the Gateway recombination cloning system (Life Technologies), 5′ entry clones containing the promoter sequence, middle entry clones containing the gene coding sequence, and 3′ entry clones containing the 3′ UTR were generated following a BP reaction. These were combined in a second (LR) recombination reaction to generate destination vectors that also contained a dual antibiotic selection marker and a fluorescence visual marker to facilitate selection of transformed animals. These constructs were introduced into wild-type animals by biolistic transformation. The progeny of these bombarded worms were isolated and incubated in antibiotic selection media for 3-4 days. Surviving animals were screened for the presence of the visual marker (P*myo-2::gfp* or P*myo-2::mCherry*) and transgenic lines were subsequently isolated.

Integrated lines or extrachromosomal lines were selected using the visual marker P*myo-2::mCherry* or P*myo-2::gfp*. Transgenic lines were all outcrossed six times to wild-type before assays were conducted.

2.2.7 Imaging of fluorescing transgenic lines

Animals were prepared for microscopy by anesthetising them in 0.1–0.2% levamisole (Sigma) in M9 buffer on small pads made of 3–4% agarose (Progen) in M9 buffer.

2.2.8 Touch sensitivity assay:

Animals were synchronised by hypochlorite treatment and cultured at 25 °C, with one day-old adults used for all assays. Touch assays were performed according to established methods (Chalfie and Sulston, 1981). A positive response was determined as acceleration of the animal away from touch. The number of positive responses was then expressed as a percentage of total touches (ten) for each animal. This positive score was combined for all animals of the same genotype and strains compared using a One-way ANOVA, Bonferroni post-test (GraphPad Prism 6, GraphPad Software Inc.). Assays were conducted blind to the genotype of the worms.

2.2.9 SKN-1::GFP, Pgcs-1::gfp and DAF-16::GFP localisation experiments

For SKN-1::GFP experiments: animals were cultured at 20 °C and larval stage 2 (L2) worms used for analysis in all experiments. To observe GFP re-localisation under stress conditions, animals were incubated with 50 mM sodium azide (Sigma) in M9 buffer (azide treated), or M9 alone (untreated) for 10 minutes with gentle agitation at room temperature. SKN-1::GFP localisation experiments were conducted using the *ldIs7* strain (integrated SKN-1 B/C::GFP), where expression was reported to be the highest in the L2 stage (An and Blackwell, 2003). Initially, SKN-1::GFP intestinal nuclear localisation was scored as positive if GFP was observed in any of the intestinal nuclei. We later refined our scoring scheme for all other SKN-1::GFP assays such that SKN-1::GFP nuclear localisation was scored as "high" if GFP was seen in all intestinal nuclei, "medium" if GFP was observed only in anterior or posterior nuclei, or "low" if GFP was not observed in any intestinal nuclei, essentially as in (Tullet et al., 2008). Untreated animals for all experiments showed no response. For *daf-2(e1370)* mutant strains, animals were incubated at either 15 or 20 °C and SKN-1::GFP assays conducted using the refined scoring scheme as above.

DAF-16::GFP localisation assays were conducted using the *zIs356* transgene (integrated DAF-16::GFP). For DAF-16::GFP localisation experiments, day 1 adult animals incubated with 50 mM sodium azide (azide treated) or M9 buffer (untreated) for 10 minutes with gentle agitation at room temperature were scored as positive if GFP was observed in any of the intestinal nuclei.

For P*gcs-1::gfp* experiments, day 1 adult animals were treated in 50 mM sodium azide (azide treated) or M9 buffer (untreated) for 10 minutes and scored as "high" if GFP was clearly seen in the intestine, "medium" if GFP was seen in both anterior and posterior ends of the animal, or "low" if GFP was observed only around the pharynx, as in (Wang et al., 2010). Untreated

animals for all experiments showed no response or a very low basal response in all genotypes tested.

In all experiments, samples were imaged using a BX51 Microscope (Olympus) and micrographs captured using AnalySIS software (Olympus). Experiments were conducted blind to the genotype of the strains.

2.2.10 Quantification of fluorescence intensity

Fluorescence images were captured on a BX51 Microscope (Olympus) using AnalySIS software (Olympus). ImageJ (Schneider et al., 2012) was used to analyse images. The integrated density in the selected regions, which normalises the fluorescence intensity to the area of the selected region, was quantified and corrected by subtracting the mean fluorescence of the background. This corrected total fluorescence was then used for statistical analysis (one-way ANOVA, GraphPad Prism, GraphPad Software Inc.).

2.2.11 Lifespan assay

Age-matched animals synchronised by egg-laying were cultured on plates at 25 °C and the number of surviving animals recorded every day until death. 100-120 day 1 adults per strain were plated at the start of each assay. Animals that were lost or displayed internal hatching or bursting were censored. To separate adult worms from their progeny, adult worms were moved to new NGM plates every second day until the assay was completed. Survival curves were generated using GraphPad Prism 6 (GraphPad Software Inc.). For several strains, lifespan assays were conducted twice independently and these are highlighted in the text.

2.2.12 Neuron imaging assay:

Age-matched animals synchronised by egg-laying were cultured on plates at 20 or 25 °C. Starting animals were day one adults in all cases. For longitudinal assays where individual animals were monitored every day during their lifetimes, these animals were individually mounted into 0.2% levamisole (Sigma) on 3% agarose pads prepared on standard microscope slides. These animals were rescued by picking them onto a drop of M9 buffer, and recovered well if incubated in levamisole for under two minutes. For transverse assays where populations of animals were monitored every second day for 15 days, surviving adult worms on a plate were mounted as described, but were not recovered post-imaging. To separate adult worms from their progeny, adult worms were moved to new NGM plates every second day until the assay was completed. Assays were conducted blind to the genotype of the worms. To score the incidence of aberrant neuronal structures in touch receptor neurons, worms were scored as positive if the neuron displayed branching or blebbing at the cell body or axon. For some experiments, cell body branching and axon branching/blebbing were scored separately. For scoring in GABAergic neurons, worms were scored as positive if at least one of the observed commissures displayed branching. For all transverse assays, the proportion of animals scored as positive was expressed then as a percentage of the sample size observed at that time point. A schematic for each of the neuronal imaging experiments is shown in **Figure 2.3**.

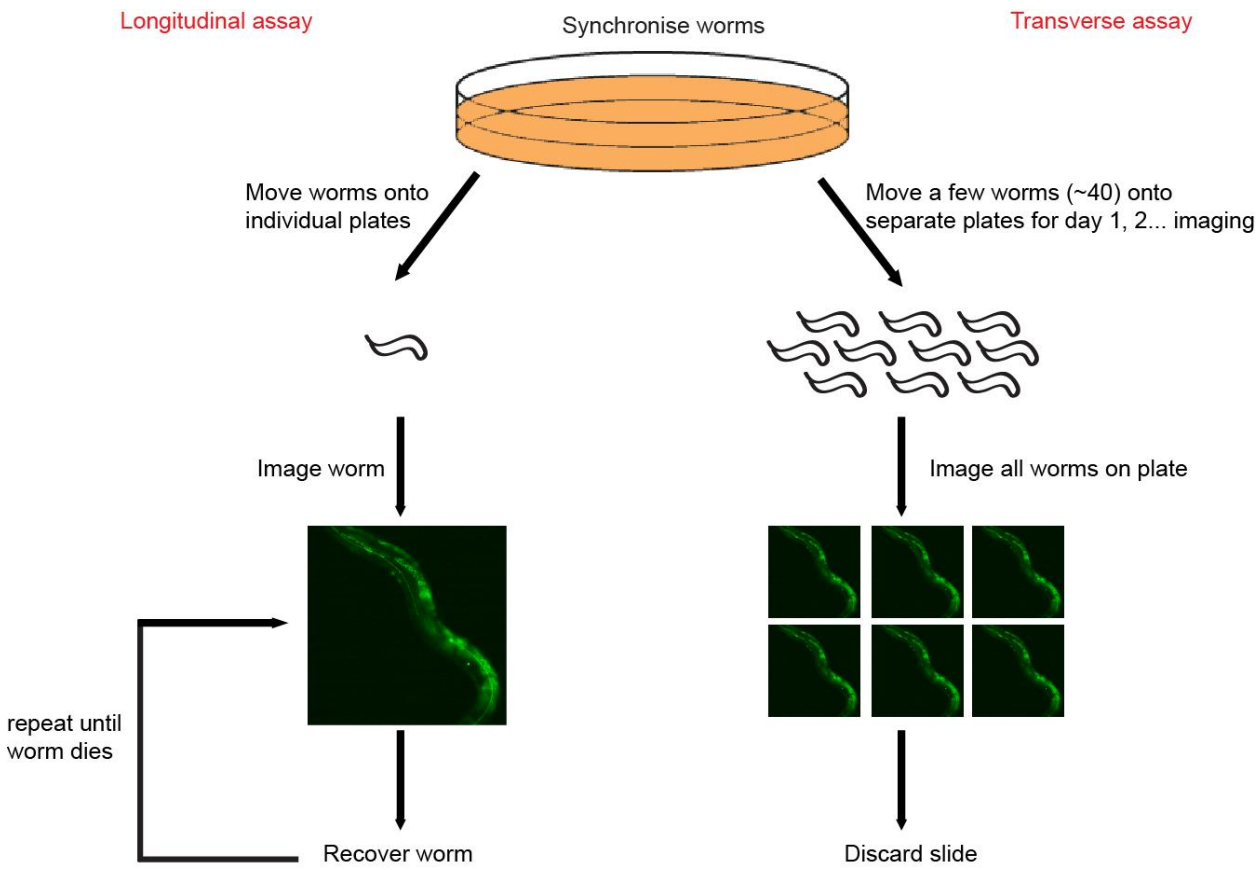

Figure 2.3: Schematic for two imaging experiments to investigate neuronal ageing. Longitudinal (individual) and transverse (population-based) experiments were conducted to visualise neurons with age. For longitudinal experiments, one plate held a single animal that was imaged, recovered after imaging, and this process repeated for the same worm every day until death. In this method, five worms per genotype were assayed per biological replicate. For transverse experiments, many worms (~40 per genotype per replicate) are moved to one plate per time point, for example day 1, 5, 7, and 9 of adulthood. At each time point, all the worms on that plate are imaged and the population subsequently discarded.

2.2.13 RNA interference experiments

For touch neuron-specific RNA interference (RNAi) experiments using strains APD050 and APD066 and control strains CZ10175 (*zdIs5*) and EG1285 (*oxIs12*): Experiments were conducted at 20 °C. *sid-1(qt2)* animals expressing SID-1 in touch neurons only (P*mec-18::sid-1*

transgene) from parent strain TU3403 (Calixto et al., 2010) were synchronised by hypochlorite bleaching and L1 worms plated onto 25 µg/mL carbenicillin plates seeded with RNAi bacteria. The bacterial strain is *E. coli* HT115, which contains the T7 RNA polymerase gene under the control of lac operon regulatory elements. HT115 RNAi feeding bacteria were transformed with the pL4440 empty vector (EV), or pL4440 containing *ptl-1* or *unc-22* DNA from the *C. elegans* RNAi library generated by the Ahringer laboratory (Fraser et al., 2000). 3 mM isopropyl β-D-1-thiogalactopyranoside (IPTG) was used to induce T7 RNA polymerase expression in HT115 bacterial cultures. The pL4440 plasmid contains two T7 promoter regions flanking the gene-specific cDNA such that induction of T7 RNA polymerase will result in RNA being transcribed in both directions, forming dsRNA. *unc-22* knockdown was used as a control for the experiment; knockdown of *unc-22* in muscle results in paralysis/twitching (Fire et al., 1991), so animals that have the *sid-1(qt2)* mutation are no longer susceptible to RNAi knockdown in muscle and will not be paralysed, whereas animals that are wild-type for *sid-1* will be paralysed. CZ10175 and EG1285 strains, which are wild-type at the *sid-1* locus and also contained the relevant *gfp* transgenes (*zdIs5* or *oxIs12*), were used as negative controls. After one generation fed on RNAi bacteria, animals were imaged at day 1, 3, 5 and 7 of adulthood to visualise touch receptor neurons or GABAergic neurons. To maintain knockdown, animals were transferred to new RNAi plates on days 2, 4 and 6 of the experiment. Scoring was conducted in the same manner as for other neuronal imaging assays. Imaging was conducted blind to the identity of the RNAi clones. To test knockdown of *ptl-1* in touch neurons by feeding RNAi, PTL-1::GFP animals with the touch neuron-specific SID-1 transgene (strain APD130) were treated as described above by feeding either EV or *ptl-1* RNAi bacteria and imaged after two generations of RNAi treatment to determine if GFP levels were decreased in touch neurons after *ptl-1* but not EV RNAi treatment.

RNAi knockdown confirmation was conducted via knockdown of PTL-1::GFP animals instead of quantitative PCR of *ptl-1* transcripts as we aimed to show not only that knockdown of PTL-1 was occurring, but also that it was taking place in particular neurons.

For pan-neuronal knockdown experiments using strain APD128: Animals were treated for two generations with RNAi bacteria on NGM-carbenicillin-IPTG plates essentially as described above. In the pan-neuronal RNAi strain derived from parent strain TU3401, *sid-1(pk3321)* animals contained a P*unc-119::sid-1* transgene that expressed SID-1 in all neurons (Calixto et al., 2010) and a PTL-1::GFP transgene. Knockdown of PTL-1::GFP in these transgenic lines by *ptl-1* RNAi feeding was determined by scoring the brightness of the fluorescence signal in the nerve ring of *ptl-1* RNAi-treated animals and EV RNAi-treated animals as detailed in section **2.2.10**. Fluorescence intensity was measured using ImageJ software and compared using GraphPad Prism 6 (GraphPad Software Inc.).

2.2.14 Stress assays and pharmacological assays

For oxidative stress assays using H_2O_2, animals were incubated at 1 or 10 mM hydrogen peroxide for 1-2 hours in M9 buffer at room temperature. Untreated animals were incubated period in M9 buffer. Animals were scored for survival 2-3 hours after treatment. For oxidative stress assays using paraquat, animals were incubated with paraquat (100 mM) or were untreated (M9 buffer) for 3 or 5 hours in M9 buffer at room temperature. Survival was scored 24 hours post-recovery. For acute heat shock assays using an incubator, animals were heat-shocked at 37.5 °C for 2 hours or kept at 25 °C for 2 hours (control) and survival scored 48 hours later. For acute heat shock assays using a water bath, animals were heat-shocked using the same conditions as

above and survival scored 24 hours later. For all stress experiments, at least 100 day one adult animals synchronised by hypochlorite treatment were assayed. Scoring was conducted blind to the genotype of the worms.

Pharmacological assays were performed on unseeded plates spread with levamisole (Sigma) at a final concentration of 1 mM. Animals to be assayed were synchronised by egg-laying at 20 °C. Animals were picked onto drug plates and scored at room temperature for paralysis (defined as no response to tapping with a platinum wire) at 15-minute intervals for 90 minutes. Scoring was conducted blind to the genotype of the worms.

2.2.15 Immunofluorescence

One day-old adults synchronised by egg-laying or hypochlorite treatment and cultured at room temperature were used for all experiments. Animals were permeabilised using the freeze-crack protocol as previously described (Crittenden and Kimble, 1999). Samples were immediately fixed in ice-cold 4% paraformaldehyde at 4 °C for >12 hours. The primary antibody used was mouse monoclonal anti-V5 (R960-25, Life Technologies) [1:200] or mouse monoclonal anti-acetyl alpha-tubulin (T7451, Sigma) [1:200]. The secondary antibody used was goat anti-mouse Alexa Fluor-568 or Alexa Fluor -488 (Sigma) [1:500]. All antibody dilutions were made in 30% (v/v) normal goat serum (Life Technologies). Samples were mounted onto microscope slides using VectaShield mounting medium (Vector Labs) containing 4′,6-diamidino-2-phenylindole (DAPI) where applicable. Samples were imaged using a BX51 Microscope (Olympus). Micrographs were captured using AnalySIS software (Olympus).

2.2.16 Immunoblot

Samples for immunoblot were prepared by washing worms off plates in M9 buffer, followed by repeated washes in M9 and a final wash in distilled water. Samples resuspended in Laemmli buffer underwent three freeze-thaw cycles in liquid nitrogen before boiling for 5 minutes at 95 °C, and were immediately loaded onto 10% acrylamide gels. Primary antibodies used are mouse monoclonal Tau-13 antibody (Abcam) [1:5000] that binds human Tau, mouse monoclonal anti-V5 antibody conjugated to HRP (R961-25, Life Technologies) [1:2000], and mouse monoclonal anti-acetyl alpha-tubulin (T7451, Sigma) [1:2000]. The secondary antibody used was goat anti-mouse conjugated to horseradish peroxidase (NA931, GE Healthcare) [1:10000]. Blots were developed with Immobilon Western chemiluminescent substrate (Millipore) on film.

2.2.17 Statistical analysis:

The α-level is 0.05 for all analyses. Statistical analyses for the major experiments conducted in this work are detailed below:

For SKN-1::GFP and P*gcs-1::gfp* localisation experiments, experiments were conducted three times and the data from all biological replicates averaged and converted to percentages. These were then compared using a one-way ANOVA for the percentage of animals displaying "low" fluorescence (according to the scoring scheme detailed above) in GraphPad Prism 6 (GraphPad Software Inc.). This analysis provides two-tailed p-values.

Survival curves were analysed in GraphPad Prism 6 (GraphPad Software Inc.) to provide two-tailed p-values. Tests used were the log-rank test, which gives equal weight to deaths at all time points, and the Wilcoxon test, which gives more weight to deaths at early time points (Machin et al., 2006). The log-rank test is commonly used for *C. elegans* lifespan data (Apfeld and Kenyon,

1999, Tank et al., 2011, Huang et al., 2004) but we also report p-values from the Wilcoxon test to accommodate the possibility that hazard ratios were not consistent through the assay.

For neuron imaging experiments, we grouped data into categories of "displays branching/blebbing" or "does not display branching/blebbing" and used Pearson's chi-squared test in Microsoft Excel (Microsoft) to determine if the incidence of branching/blebbing in a mutant population at a single time point is different from the 'expected value' of the wild-type strain at the same time point. This analysis provides one-tailed p-values that were used to determine if the incidence of abnormal neuronal structures in a mutant strain at a time point was different from the wild-type strain.

Chapter 3:
Brief description of two *ptl-1* deletion mutants

3.1 Introduction

PTL-1 has been previously shown to be involved in the regulation of microtubule-based transport (Tien et al., 2011), embryogenesis (Gordon et al., 2008), and sensitivity to gentle touch (Gordon et al., 2008). These phenotypes were determined using a *ptl-1(ok621)* null mutant strain. For our investigations into the functions of PTL-1 as a Tau-like protein, we tested several phenotypes using *ptl-1(ok621)* mutant animals, and also elected to assay a previously uncharacterised *ptl-1* allele, referred to as *tm543*. These experiments would then form the basis for further investigation into the roles of PTL-1 in the stress response and ageing. In this chapter, a basic characterisation of this new allele is presented.

3.2 **ptl-1(tm543)** ***and*** **ptl-1(ok621)** ***mutant strains***

PTL-1 in *C. elegans* displays high sequence similarity to mammalian Tau/MAP2/MAP4 in the C-terminal MBR domain. It is encoded on chromosome III by the gene *ptl-1 (F42G9.9),* which is predicted to contain four distinct transcripts (a-d; http://www.wormbase.org) (**Figure 3.1A**). The longest predicted isoform (*F42G9.9a*) is composed of eight coding exons, with exons 5–7 encoding the MBRs (**Figure 3.1B**). Two deletion alleles have been generated for *ptl-1*: the *ok621* mutation generated by the Oklahoma Medical Research Foundation (OMRF) arm of the *C. elegans* Knockout Consortium (WormBase ID: WBVar00091905), and the *tm543* mutation generated by the National Bioresource Project, Japan (WormBase ID: WBVar00249582) (**Figure 3.1B)**. *ptl-1(ok621)* is reported to be a null mutation (Gordon et al., 2008), whereas *ptl-1(tm543)* is a shorter deletion encompassing the exons encoding the MBR region, and may result in a truncated protein that has retained the N-terminal projection domain (**Figure 3.1C**). Both mutant strains were generated using ultraviolet trimethylpsoralen (UV/TMP) treatment.

As a reference for our experiments, we used the sequence of isoform a (F42G9.9a) since this is a confirmed transcript that generates a protein with five MBRs (Gordon et al., 2008, Goedert et al., 1996), whereas the other confirmed isoform of PTL-1 (isoform b) has only four putative MBRs (Goedert et al., 1996, McDermott et al., 1996). That is, in the generation of all transgenic lines used in this study, we used the sequence of the longest isoform of PTL-1.

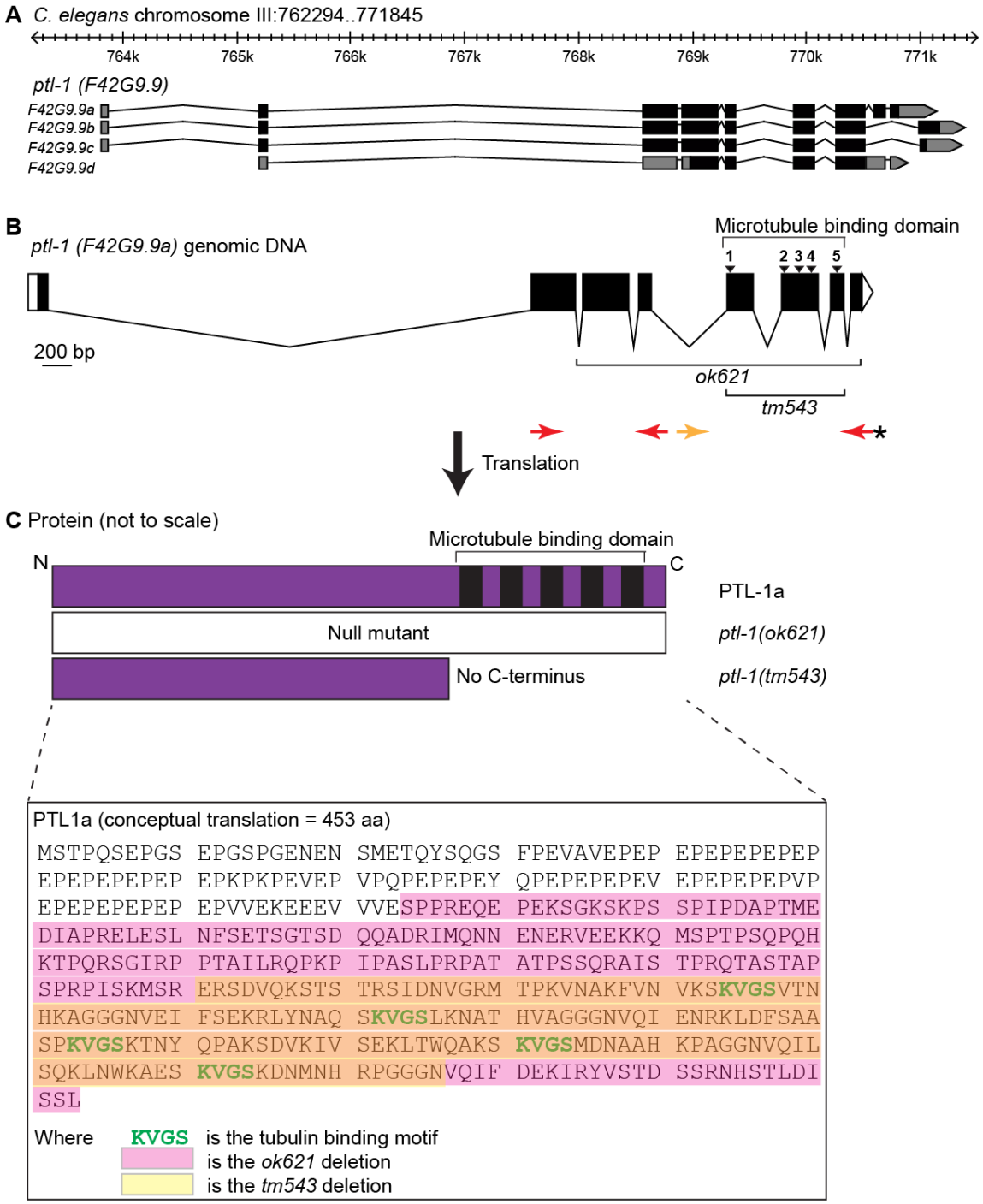

Figure 3.1: Schematic of *ptl-1* (F42G9.9) genomic locus, showing alleles *ok621* and *tm543*, and predicted protein sequence. A) Sequence of *C. elegans* chromosome III indicating predicted *ptl-1* transcripts F42G9.9 isoforms a-d. **B)** Genomic locus of the longest isoform of *ptl-1* (PTL-1a) from transcript F42G9.9a indicating regions comprising the *ok621* and *tm543* deletions. Exons are shown as black boxes, introns as solid lines and untranslated regions at the 5′ and 3′ ends as white boxes. 5′ is on the left. Regions encoding putative microtubule-

binding repeats are marked 1-5 with arrowheads. The coloured arrows below the schematic indicate where genotyping primers bind for *ok621* (red) and *tm543* (orange). The red arrow with an asterisk (*) was used as a reverse primer for genotyping both alleles. **C)** Schematic of the PTL-1 protein highlighting the microtubule-binding domain and predicted protein products of *ptl-1(ok621)* (predicted null mutant) and *ptl-1(tm543)* (microtubule-binding domain-deficient allele). The conceptual translation of the PTL-1a isoform is shown below, indicating the MBRs and the regions deleted by *ok621* and *tm534* mutations.

We attempted to confirm the end points of the *tm543* deletion, but technical difficulties in the sequencing reaction due to the presence of the C-terminal repeat region prevented us from confirming the exact sequence of the deletion (data not shown). However, using primers flanking the putative deleted region, we were able to robustly genotype for *ptl-1(tm543)* mutant animals (**Figure 3.2**).

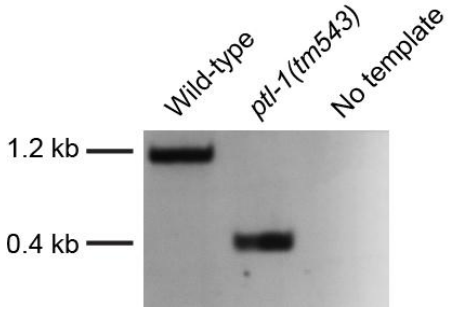

Figure 3.2: Genotyping of *ptl-1(tm543)* using PCR. Primers used were "PTL-1 tm543 FF" and "PTL-1 ok621 FR2", sequences given in the Methods section. The first lane shows the product generated using genomic DNA from a wild-type animal, lane two shows the product from a *ptl-1(tm543)* animal, and lane three shows the absence of contaminating DNA in the no DNA template control. PCR products were run on a 1% agarose gel. The approximate sizes (in kb) of the PCR products are shown on the left.

The FX00543 strain had not previously been outcrossed, and we used our newly established PCR protocol to genotype *ptl-1(tm543)* animals to facilitate outcrossing of this strain six times to wild-type. This outcrossed strain was renamed APD015 and was used for the remainder of the

experiments using the *tm543* allele. At the start of this investigation, FX00543 had only been partially characterised, with mutant animals curated as being homozygous viable and mildly defective in chemotaxis towards sodium chloride (S Mitani, National Bioresource Project, Japan).

3.3 **ptl-1** *mutant alleles display allelic differences in touch sensitivity*

Mammalian MAPs such as Tau and MAP2 are known to execute a range of physiological functions in neurons (Drubin and Kirschner, 1986, Avila et al., 2004, Ittner et al., 2010, Dehmelt and Halpain, 2005). As two alleles of *ptl-1* are now available, we investigated the functions of PTL-1 in *C. elegans* neurons by assaying both *ptl-1(ok621)* and *ptl-1(tm543)* mutant strains. Although PTL-1 is expressed in several neuronal subtypes in adult worms, the highest levels are detected in the touch receptor neurons (Gordon et al., 2008, Goedert et al., 1996), which regulate the response to gentle touch (Chalfie et al., 1985, Chalfie and Sulston, 1981). We first tested whether we could detect touch insensitivity in a positive control strain *mec-12(e1605)* (Fukushige et al., 1999), and indeed we found that this strain was significantly less touch sensitive compared with wild-type (**Figure 3.3A**) Previously published data indicate that *ptl-1(ok621)* mutants are mildly touch insensitive compared with wild-type worms (Gordon et al., 2008). In line with this, we found that *ptl-1(ok621)* worms were less touch sensitive (touch sensitivity = 74±2 %) compared with wild-type (82±2 %) (**Figure 3.3A**). We also tested animals carrying the *ptl-1(tm543)* C-terminal deletion, and observed that there was no difference in touch sensitivity between this mutant (83±2 %) and wild-type (**Figure 3.3B**). These findings suggest that loss of full-length PTL-1, but not the MBR domain alone, results in a small but significant difference in touch response.

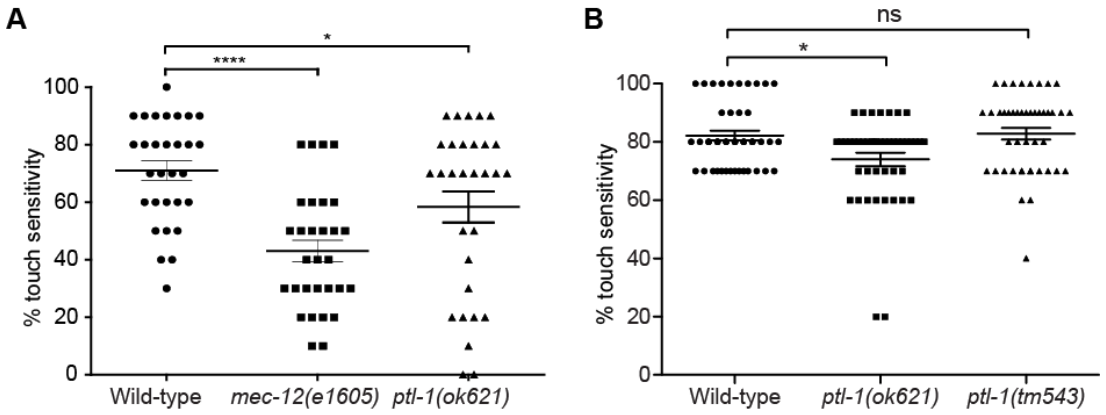

Figure 3.3: *ptl-1(ok621)* and *ptl-1(tm543)* mutant animals display allelic differences in touch sensitivity. Data for sensitivity to gentle touch, shown for **A)** *ptl-1(ok621)* (n = 30 total for two biological replicates) and **B)** *ptl-1(tm543)* mutant animals and wild-type controls (n = 45 total for three biological replicates). Error bars indicate mean ± SEM. One-way ANOVA, Bonferroni post-test, p value is indicated by ns = no significance, * <0.05.

3.4 Discussion

Given the availability of two *ptl-1* deletion alleles, including the previously uncharacterised MBR-deficient *tm543* allele, we now have the opportunity to investigate functions that are attributable to the MBR domain alone. *ptl-1(ok621)* animals do not generate a protein product whereas *ptl-1(tm543)* animals are predicted to produce a truncated protein containing only the N-terminus and lacking the MBRs. The N-terminus of PTL-1 is largely conserved amongst nematodes, is proline-rich, highly acidic, and also contains several serine/threonine-proline motifs that are potential phosphorylation sites (Goedert et al., 1996, Gordon et al., 2008, McDermott et al., 1996). By assaying for touch sensitivity, we have found allelic differences between these strains, where full length PTL-1, but not the MBR domain, is necessary to confer wild-type sensitivity to gentle touch. Using both deletion alleles, we aimed to expand our knowledge on PTL-1 function by testing both alleles in the contexts of stress responsiveness and ageing. The results of these investigations will be reported in the subsequent three results chapters.

Chapter 4:
PTL-1 is involved in the oxidative stress response and longevity regulation

4.1 Section 1: Role of PTL-1 in the oxidative stress response

4.1.1 Introduction

Oxidative stress has been implicated as a major pathological factor in AD and other dementias. Furthermore, markers of Tau pathology such as increased phosphorylation and aggregation have been linked to increased oxidative stress (Su et al., 2010, Gamblin et al., 2000, Dias-Santagata et al., 2007). One proposed mechanism by which oxidative stress influences Tau pathology is via the transcription factor Nrf2, which regulates the detoxification response. Activation of Nrf2 and induction of Nrf2-responsive genes after methylene blue treatment have been correlated with decreased Tau phosphorylation and improved behavioural responses (Stack et al., 2014, Jo et al., 2014). We tested if PTL-1 in neurons could interact with the Nrf2 homolog in *C. elegans*, SKN-1, in the regulation of both the stress response and longevity. Section one of this chapter details the investigation of the role of PTL-1 in the oxidative stress response in *C. elegans*, and section two contains our data on the modulation of lifespan by PTL-1.

4.1.2 ptl-1 *mutant animals are defective in the response to oxidative stress*

Due to the link between oxidative stress and Tau-associated pathology, we investigated if *ptl-1* mutant animals displayed a normal stress response. We tested the survival of *ptl-1* mutant animals after oxidative stress and heat stress. In general, we found that there was high variation in survival in all strains, including wild-type, after stress assays were conducted. However, we were able to resolve a difference in the oxidative stress response between *ptl-1* mutant strains and wild-type controls.

We first tested for the response to oxidative stress using hydrogen peroxide (H_2O_2) and paraquat treatment. After an acute exposure to H_2O_2 or paraquat, we monitored the survival of young

adult *ptl-1(ok621)* null mutant and *ptl-1(tm543)* MBD-lacking mutant animals. With H_2O_2 treatment, over many experimental replicates (7-8), we demonstrated that both *ptl-1* mutant strains showed on average a decreased survival after exposure to 1 or 10 mM H_2O_2 compared with wild-type controls (**Figure 4.1A**). After exposure to 10 mM H_2O_2 for 2 hours, on average 9% of *ptl-1(ok621)* and 15% of *ptl-1(tm543)* animals were alive compared with 45% of wild-type animals (**Figure 4.1A**). However, we could not detect any differences in survival when animals were treated with the redox-active chemical paraquat (**Figure 4.1B**). Although a general trend of decreased survival was observed in *ptl-1* mutant animals exposed to paraquat compared with wild-type controls, these differences were not statistically significant. This could be attributable to the high variation in survival in all strains in response to treatment (**Figure 4.1B**).

We next investigated survival in response to acute heat stress (**Figure 4.1C,D**). Large fluctuations in temperature (~ 5 °C from the desired temperature) were detected when worms were heat shocked at 37.5 °C both in a standing incubator (air) (**Figure 4.1C**) or in a water bath (liquid) (**Figure 4.1D**). These fluctuations in temperature over the two hours of heat stress could contribute to the large variation observed for the survival of all three strains post-treatment. We also did not observe a significant difference between the survivals of both *ptl-1* mutant strains compared to wild-type animals (**Figure 4.1C,D**).

Although there were considerable difficulties in acquiring consistent data for these stress assays, our data using H_2O_2 treatment appeared to indicate a reduction in the capacity of *ptl-1* mutant animals to survive oxidative stress. We next elected to investigate the pathways by which PTL-1 regulates the oxidative stress response.

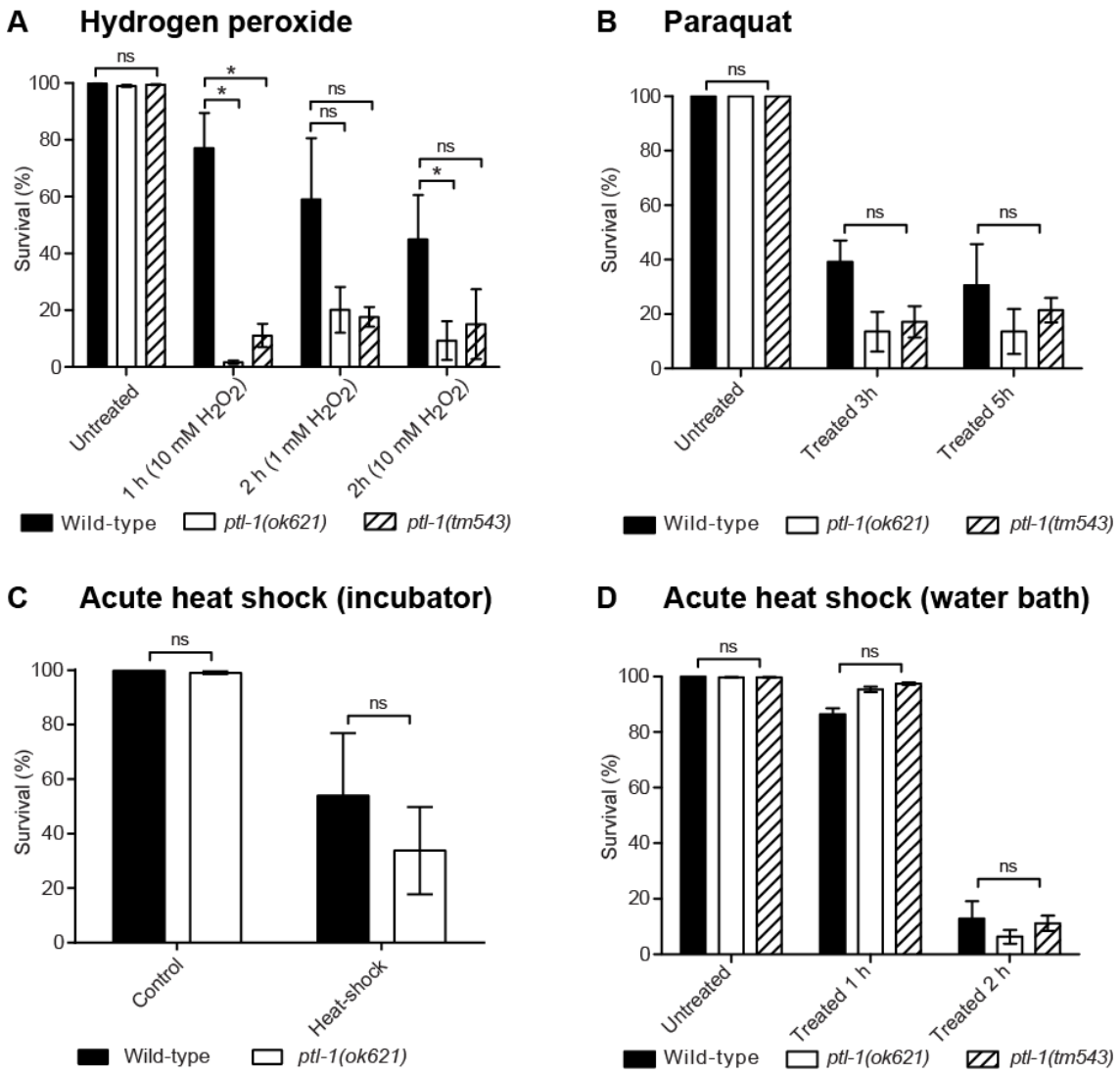

Figure 4.1: PTL-1 regulates the response to oxidative stress. A) *ptl-1* mutants are hypersensitive to hydrogen peroxide stress. Animals were incubated at either 1 mM or 10 mM hydrogen peroxide for 1-2 hours in liquid at room temperature. Untreated animals were incubated for the same time period in M9 buffer. Animals were scored for survival 2-3 hours after treatment. 7-8 replicates were conducted per treatment condition, with at least 100 animals scored per treatment. **B)** Animals were incubated with paraquat (100 mM) or were untreated (M9 buffer) for 3 or 5 hours in liquid at room temperature. Survival was scored 24 hours post-recovery. 2 replicates were conducted per treatment condition, with at least 100 animals scored per treatment. **C)** Acute heat shock assay using an incubator. Animals were heat shocked at 37.5 °C for 2 hours (heat shock) or kept at 25 °C for 2 hours (control) and survival scored 48 hours later. 2 duplicates were conducted, and at least 100 animals scored per treatment condition. **D)** Acute heat shock assay using a water bath. Animals were heat shocked at 37.5 °C for 2 hours (heat shock) or kept at

25 °C for 2 hours (control) and survival scored 24 hours later. 2 replicates were conducted, with at least 100 animals scored per treatment. For all stress experiments, first day adults synchronised by hypochlorite treatment were assayed. Statistical analysis: two-way ANOVA, p value is indicated by ns = not significant, *<0.05.

4.1.3 ptl-1 *mutant animals display a defective SKN-1 re-localisation response to oxidative stress but show no defect for DAF-16*

The role of the transcription factor SKN-1 in modulating the response to oxidative stress has been extensively studied in *C. elegans* (An and Blackwell, 2003, An et al., 2005, Glover-Cutter et al., 2013, Inoue et al., 2005, Kahn et al., 2008, Park et al., 2009, Staab et al., 2014). SKN-1b and SKN-1c are the two most studied isoforms, largely due to the generation of a SKN-1b/c::GFP (*ldIs7*) reporter transgenic line (An and Blackwell, 2003), henceforth referred to as SKN-1::GFP. SKN-1c is present in the intestine and is normally diffuse in the cytoplasm, but in response to stress it rapidly localises to the nucleus (**Figure 4.2Ai,ii**) (An and Blackwell, 2003). SKN-1b is present in the ASI neurons, and appears to be constitutively nuclear (**Figure 4.2Ai,** indicated as white arrows in the head) (An and Blackwell, 2003). Initial investigations found that although the SKN-1::GFP reporter can be observed in intestinal nuclei after treatment with heat stress or paraquat, acute incubation with sodium azide (NaN_3) was shown to be the most effective in inducing nuclear re-localisation of SKN-1::GFP (An and Blackwell, 2003). Furthermore, levels of SKN-1::GFP appeared to be the highest at larval stage two (L2) (An and Blackwell, 2003). Therefore, for all assays described here, SKN-1::GFP re-localisation was examined in L2 animals after treatment with sodium azide.

We investigated whether localisation of SKN-1 was affected by defective PTL-1. We first examined intestinal SKN-1::GFP. In control wild-type and *ptl-1* mutant animals treated with M9

buffer alone (untreated), there was no observable nuclear SKN-1::GFP in the intestine (**Figure 4.2B**). For this reason, we do not display graphs for SKN-1::GFP localisation in untreated animals in subsequent presentations of data, although in all cases untreated controls were conducted alongside azide treatments. Wild-type animals showed a largely consistent response to sodium azide, in which SKN-1::GFP localised to some or all intestinal nuclei in ~60% of animals (**Figure 4.2B**). In contrast, a significantly lower proportion of *ptl-1(ok621)* animals (~20%) displayed nuclear SKN-1::GFP in response to azide stress (**Figure 4.2B**). We next determined if SKN-1::GFP expression in the ASI neurons changed when animals were exposed to sodium azide. In azide-treated animals, we did not detect a change in the constitutively nuclear SKN-1::GFP localisation or fluorescence intensity in the ASI neurons in either wild-type or *ptl-1(ok621)* animals compared with untreated controls (**Figure 4.2Ai**). This is consistent with data from previous research showing that SKN-1::GFP expression in the ASI neurons does not change after exposure to stress (An and Blackwell, 2003).

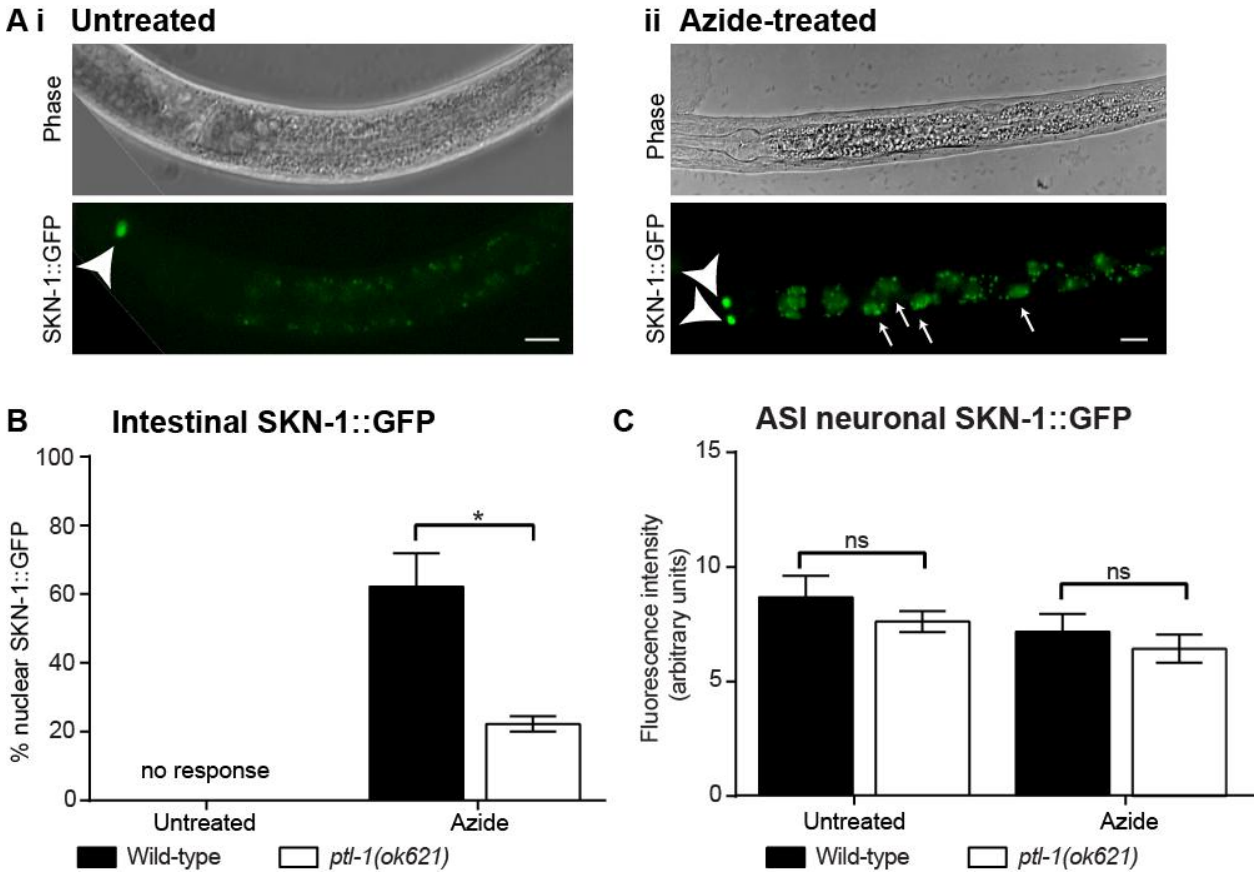

Figure 4.2: PTL-1 regulates the stress-mediated SKN-1 re-localisation to intestinal nuclei. A) The SKN-1B/C::GFP *(ldIs7)* transgenic strain was used. (i) Untreated animals do not show clear nuclear SKN-1::GFP in the intestine. (ii) Intestinal SKN-1 re-localisation to the nucleus in response to sodium azide (50 mM) stress is indicated by white arrows pointing to intestinal nuclei. White arrowheads pointing in the head region indicate nuclear SKN-1 in the ASI neurons, which is unaffected by stress. Scale, 10 µm. **B)** *ptl-1(ok621)* mutant animals are defective in SKN-1::GFP re-localisation to intestinal nuclei in response to azide stress. No nuclear SKN-1::GFP was observed in untreated animals. n=15 per replicate, data shown are averaged from three independent experiments. Statistical analysis: one-way ANOVA, p value is indicated by ns = not significant, *<0.05. **C)** SKN-1::GFP fluorescence in ASI nuclei does not change in intensity in response to azide stress in either wild-type or *ptl-1(ok621)* mutant animals. n=15. Quantification of fluorescence signal was measured in ImageJ. Statistical analysis: one-way ANOVA, p value is indicated by ns = not significant, *<0.05. n=15 per strain per treatment.

The insulin signalling pathway is known to be involved in the regulation of the stress and longevity response (Tullet et al., 2008, Honda and Honda, 1999, Li et al., 2014, Kenyon et al., 1993, Wolkow et al., 2000). Important players in this pathway include the DAF-2 insulin-like receptor (Kenyon et al., 1993) and the downstream effector DAF-16, a FOXO transcription factor (Ogg et al., 1997). Briefly, in response to DAF-2 ligand binding, DAF-16 is phosphorylated by downstream kinases and excluded from the nucleus, preventing DAF-16-mediated expression of longevity and stress responsive signals (Kaletsky and Murphy, 2010). We investigated if DAF-2 signalling via DAF-16 was also affected in *ptl-1* mutant animals. Like SKN-1, DAF-16 in the intestine is normally diffuse in the cytoplasm, and localises to the nucleus in response to various stressors (Lee et al., 2001a) (**Figure 4.3Ai**). Using a DAF-16 translational reporter (*zIs356*), we assayed for intestinal DAF-16 localisation in response to azide treatment. This was performed using a DAF-16::GFP reporter expressed under the control of the *daf-16* promoter. Our data indicate that the localisation of DAF-16::GFP is unaffected by loss of PTL-1 in treated animals (**Figure 4.3Aii**).

We also investigated if PTL-1 was acting within the IIS pathway in its regulation of SKN-1::GFP localisation. Here, we attempted to resolve subtle differences by binning our data into three categories: “high” where GFP was observed in all intestinal nuclei, “medium” where GFP was observed only in the most anterior/posterior nuclei, and “low” where no nuclear GFP was observed (Tullet et al., 2008). Contrary to data previously published by others (Tullet et al., 2008), we were unable to resolve an effect of *daf-2(e1370)* reduction-of-function on SKN-1::GFP re-localisation at either 15 °C or 20 °C (**Figure 4.3Bi,ii**). Tullet *et al.* observed constitutive nuclear SKN-1::GFP in the intestine, i.e. in the absence of stress exposure, in *daf-*

2(e1370) mutant animals at both 15 °C and 20 °C (Tullet et al., 2008). This may be due to the difference in transgenic lines used in the current study compared with the previous investigation - we used a SKN-1::GFP integrated transgenic line that expresses at a much lower level compared with the extra-chromosomal line used in the earlier experiments (Tullet et al., 2008). Importantly, we observed that the addition of a *daf-2(e1370)* mutation did not affect the defective SKN-1::GFP response in *ptl-1(ok621)* mutant animals (**Figure 4.3B**). Therefore, the regulation of intestinal SKN-1 by PTL-1 does not involve the IIS pathway.

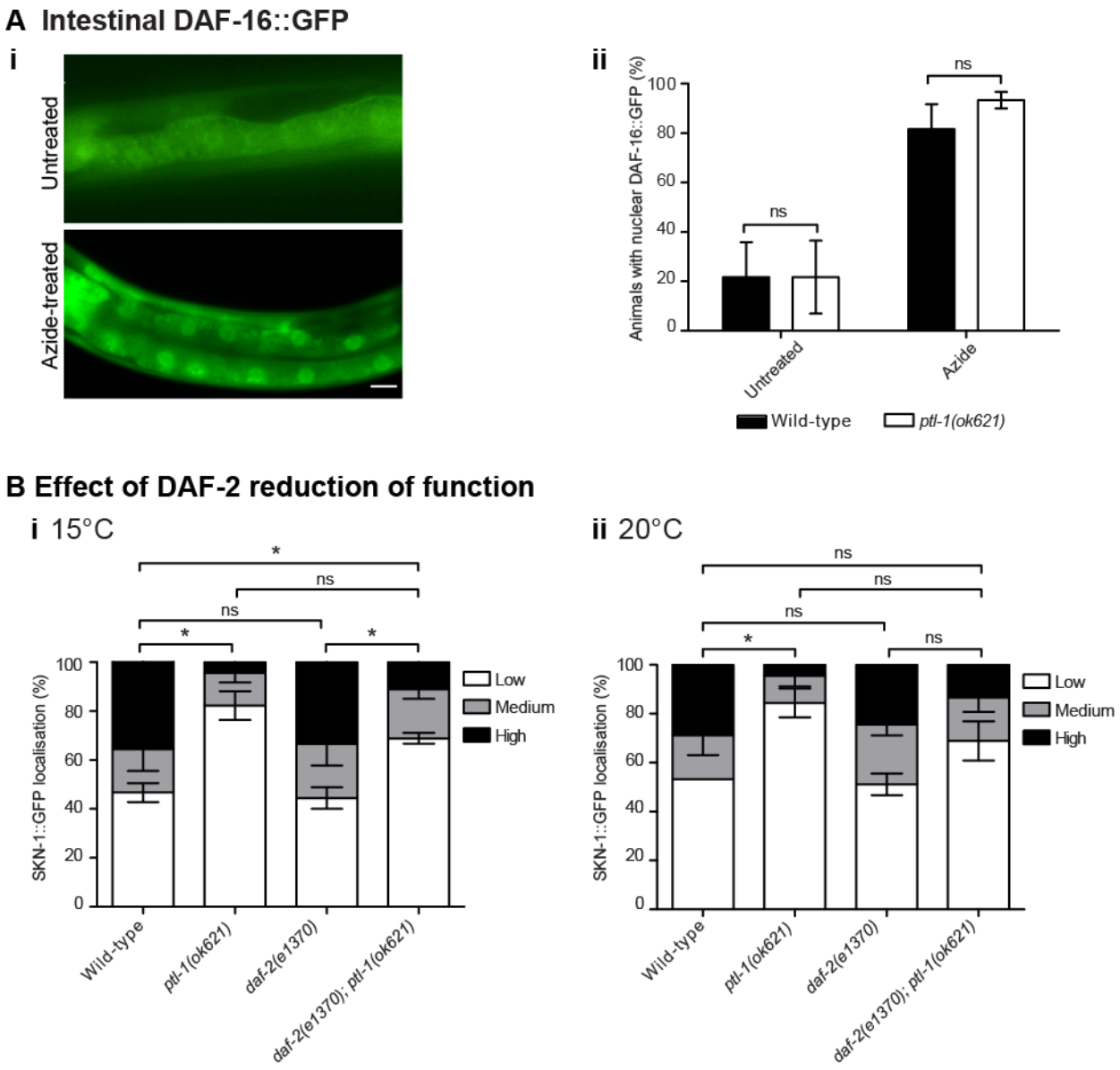

Figure 4.3: PTL-1 does not regulate DAF-16::GFP nuclear localisation, and SKN-1 nuclear re-localisation is not affected by mutations in *daf-2*. A) (i) P*daf-16*::DAF-16::GFP *(zls356)* nuclear re-localisation in (top) an untreated animal (image taken from (Schafer et al., 2006)), and (bottom) in response to azide stress. (ii) *ptl-1(ok621)* mutant animals do not display a defect in DAF-16::GFP nuclear re-localisation in response to 50 mM sodium azide treatment. Untreated animals are incubated in M9 buffer only. Treatment was for 10 minutes at room temperature in liquid. Worms were scored as positive if DAF-16::GFP was localised to at least 1 intestinal nucleus. n=20 per replicate, data shown are averaged from three independent experiments. **B)** *ptl-1* null mutation results in a defect in intestinal SKN-1::GFP nuclear re-localisation in the presence of a *daf-2(e1370)* mutation at (i) 15 °C or (ii) 20 °C.

n=15 per biological replicate. Scoring is as follows: low – no observable intestinal nuclear GFP, medium – GFP in anterior/posterior intestinal nuclei only, high – GFP in all intestinal nuclei (Tullet et al., 2008). Statistical analysis: One-way ANOVA comparing the incidence of 'low' fluorescence. P-values indicated by ns = not significant, *<0.05. For all experiments, averaged data from three independent experiments are shown.

4.1.4 Defective SKN-1 re-localisation in ptl-1 *mutant animals in response to oxidative stress can be rescued by PTL-1 but not human Tau re-expression*

To confirm that the defect observed in intestinal SKN-1::GFP localisation in *ptl-1* mutant worms is attributable to the loss of PTL-1 function, we generated a transgenic line expressing the *ptl-1* cDNA under the control of the *ptl-1* promoter and the *ptl-1* 3′ UTR control element. As no commercial antibody against PTL-1 is available, we tagged PTL-1 at the C-terminus with the short peptide V5 in order to enable detection of PTL-1 expressed from the transgene with a V5-specific antibody. Transgenic worms were generated by biolistic transformation, and an integrated line was obtained after selection using the dual antibiotic method (Semple et al., 2012). We confirmed that our transgene was expressed by immunoblotting (**Figure 4.4A**) and immunofluorescence (**Figure 4.4B**). The migration of the band observed on the immunoblot is consistent with previous experiments that have shown that PTL-1 runs at approximately 75 kDa on an SDS-PAGE gel (Goedert et al., 1996) (**Figure 4.4A**). Furthermore, using a V5-specific antibody for immunofluorescence staining, we detected PTL-1::V5 localising to axons and cell bodies in neurons, including those comprising the nerve ring in the head, as well as in the tail (**Figure 4.4B**). We confirmed expression of the transgene in touch neurons by staining for PTL-1::V5 in transgenic animals crossed with the P*mec-4::gfp* reporter line and observing co-localisation between signals from anti-V5 immunofluorescence and GFP (**Figure 4.4Biii)**. We also generated integrated transgenic lines expressing V5::PTL-1 (N-terminal tag) under the

control of the same regulatory elements, however these were not used in our experiments (**Appendix 2**). We refer to the transgenic line described above as "PTL-1 Tg" followed by "*ptl-1(ok621)*" if it is in the *ptl-1* null mutant background.

As noted, PTL-1 in *C. elegans* and Tau in humans have high sequence similarity in the C-terminal domain that is important for microtubule binding, and also have a similar overall charge distribution (Gordon et al., 2008, McDermott et al., 1996, Goedert et al., 1996). To determine if there is functional conservation between these two proteins, we generated transgenic *C. elegans* strains expressing a cDNA of the longest isoform of human Tau (hTau40, referred to here as hTau). The hTau cDNA was expressed under the control of the *ptl-1* promoter and PTL-1 3′ UTR as described above. hTau transgenic animals were similarly generated by biolistic transformation and an integrated line was isolated. Immunoblotting analysis showed that hTau is expressed in the transgenic line but not in non-transgenic wild-type worms (**Figure 4.4C**). We refer to this transgenic line as "hTau Tg".

To extend our earlier findings (**Figure 4.2**), we determined if two *ptl-1* mutant strains are defective in SKN-1::GFP re-localisation. *ptl-1* null mutant animals (*ok621*), as shown previously, displayed a defect in SKN-1::GFP re-localisation to intestinal nuclei in response to stress (**Figure 4.4D**). In addition, truncated PTL-1 mutant (*tm543*) animals also displayed a similar phenotype (**Figure 4.4D**). This could be rescued by re-expression of PTL-1::V5 in a *ptl-1(ok621)* null mutant (**Figure 4.4D**). We chose to perform our rescue experiments in the *ptl-1(ok621)* background only as this is a null mutation and hence we should avoid any potentially detrimental effects of expressing transgenic PTL-1 together with truncated forms of the protein, as would be

the case with the *ptl-1(tm543)* mutant strain. Our findings indicate that the defect in stress responsive SKN-1 localisation is attributable to loss of PTL-1. In contrast, re-expression of hTau did not rescue this phenotype in a *ptl-1* null mutant (**Figure 4.4E**). This demonstrates that with regards to the regulation of SKN-1 in *C. elegans*, hTau and PTL-1 do not display functional conservation.

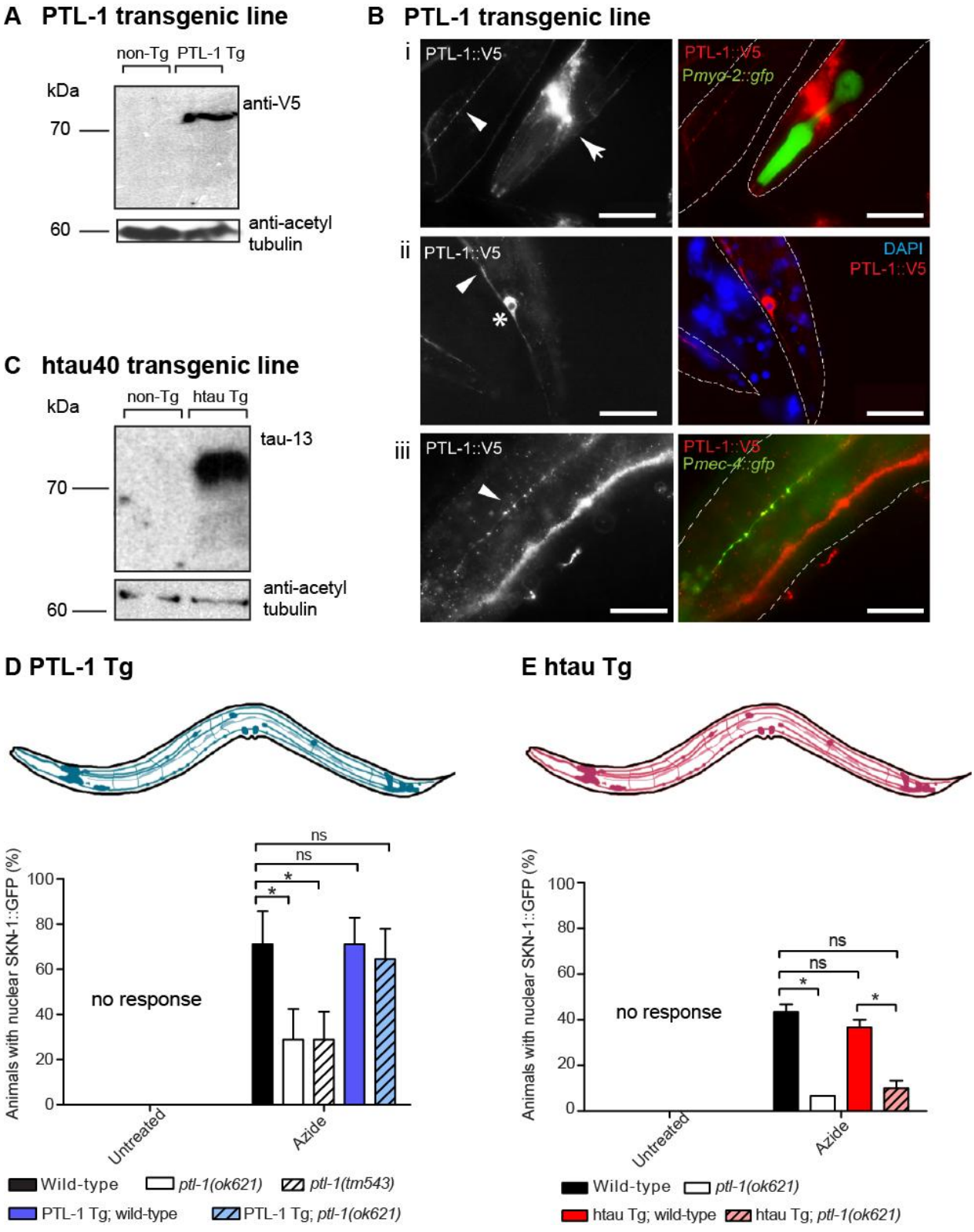

Figure 4.4: Defective SKN-1::GFP re-localisation in response to stress can be rescued by re-expression of PTL-1 but not human Tau. 'PTL-1 Tg' refers to the PTL-1::V5 transgene, 'hTau Tg' refers to the human Tau

transgene. **A)** Immunoblot showing the presence of a band corresponding to PTL-1::V5 expression from the transgene, probed using an anti-V5 antibody. Non-Tg refers to non-transgenic wild-type animals. **B)** (i,ii,iii) Immunofluorescence micrographs showing the expression of the PTL-1::V5 transgene (anti-V5 antibody) in neurons. Grayscale images on the left show the red channel only, the nerve ring is indicated by arrows, axons by arrowheads, and cell bodies by asterisks. In (i), where the pharynx is shown, *gfp* expression can be observed from the P*myo-2*::*gfp* transformation reporter. Co-localisation with a reporter line for touch receptor neurons (P*mec-4::gfp*) is shown in (iii), demonstrating that the transgene is expressed in touch neurons, where PTL-1 was previously shown to be highly expressed (Goedert et al., 1996, Gordon et al., 2008). Dotted lines indicate the outline of the animal as determined by phase-contrast microscopy. Ventral is down. Scale, 50 µm. **C)** Immunoblot showing the presence of a band corresponding to the hTau40 transgene, probed using the Tau-13 antibody. Non-Tg refers to non-transgenic wild-type animals**. D)** Defective SKN-1 re-localisation to the intestinal nucleus in *ptl-1(ok621)* or *ptl-1(tm543)* mutant animals in response to azide stress can be rescued by re-expression of PTL-1 under the regulation of the *ptl-1* promoter. SKN-1 re-localisation was scored as positive if GFP was localised to at least 1 intestinal nucleus. **E)** Human Tau does not rescue the defect in SKN-1 re-localisation seen in *ptl-1* mutant animals. For **D** and **E**, n=15 per biological replicate, showing data averaged from three independent experiments. Statistical analysis: One-way ANOVA. P-values indicated by ns = not significant, *<0.05.

4.1.5 ptl-1 *mutant animals are defective in the induction of a SKN-1::GFP responsive gene*

To complement the SKN-1::GFP experiments, we utilised another reporter transgene, P*gcs-1*::*gfp* (*ldIs3*) (Wang et al., 2010). GCS-1 (γ-glutamylcysteine synthetase) is a phase II detoxification enzyme that is induced at the transcriptional level by SKN-1 in response to oxidative stress (Liao and Yu, 2005). GFP expression from this transgene is low under normal conditions but it becomes highly expressed in the intestine and tail when the animal is exposed to stress conditions (Oliveira et al., 2009, An and Blackwell, 2003) (**Figure 4.5A**). Detection of SKN-1 responsiveness using the P*gcs-1::gfp* reporter transgene has several advantages: firstly it can be undertaken in young adult animals, which are larger and easier to score compared with L2

animals, secondly the P*gcs-1::gfp* signal in induced animals is brighter than the SKN-1::GFP and also facilitates more rapid scoring. These advantages allow for more animals (n=40) to be assayed in each P*gcs-1::gfp* experiment compared with 15 animals in SKN-1::GFP assays. We scored P*gcs-1::gfp* transgene induction as follows: (L) low – faint GFP in head, (M) medium – GFP in head and tail, and (H) high – GFP in head, tail and throughout intestine (Wang et al., 2010) (**Figure 4.5A**).

In untreated animals, a low baseline induction of the transgene was observed in wild-type animals, *ptl-1* mutant strains, and PTL-1 transgene re-expressing animals (**Figure 4.5B**). This was consistent for all strains assayed in this study. For simplicity, we show only data from azide-treated animals for the remainder of this section and P*gcs-1::gfp* data from untreated animals in all subsequent assays can be found in **Appendix 4**. When we assayed animals treated with sodium azide, induction of *Pgcs-1::gfp* was found to be defective in both *ptl-1(ok621)* and *ptl-1(tm543)* mutant strains and this defect could be rescued by re-expression of PTL-1 (**Figure 4.5B**). In addition, we found that induction of another SKN-1 responsive gene, HSP-4 (Glover-Cutter et al., 2013), is defective in *ptl-1(ok621)* mutant animals compared with wild-type (**Appendix 5**). This suggests that *ptl-1* mutant animals are generally defective in the induction of genes regulated by SKN-1 in response to stress.

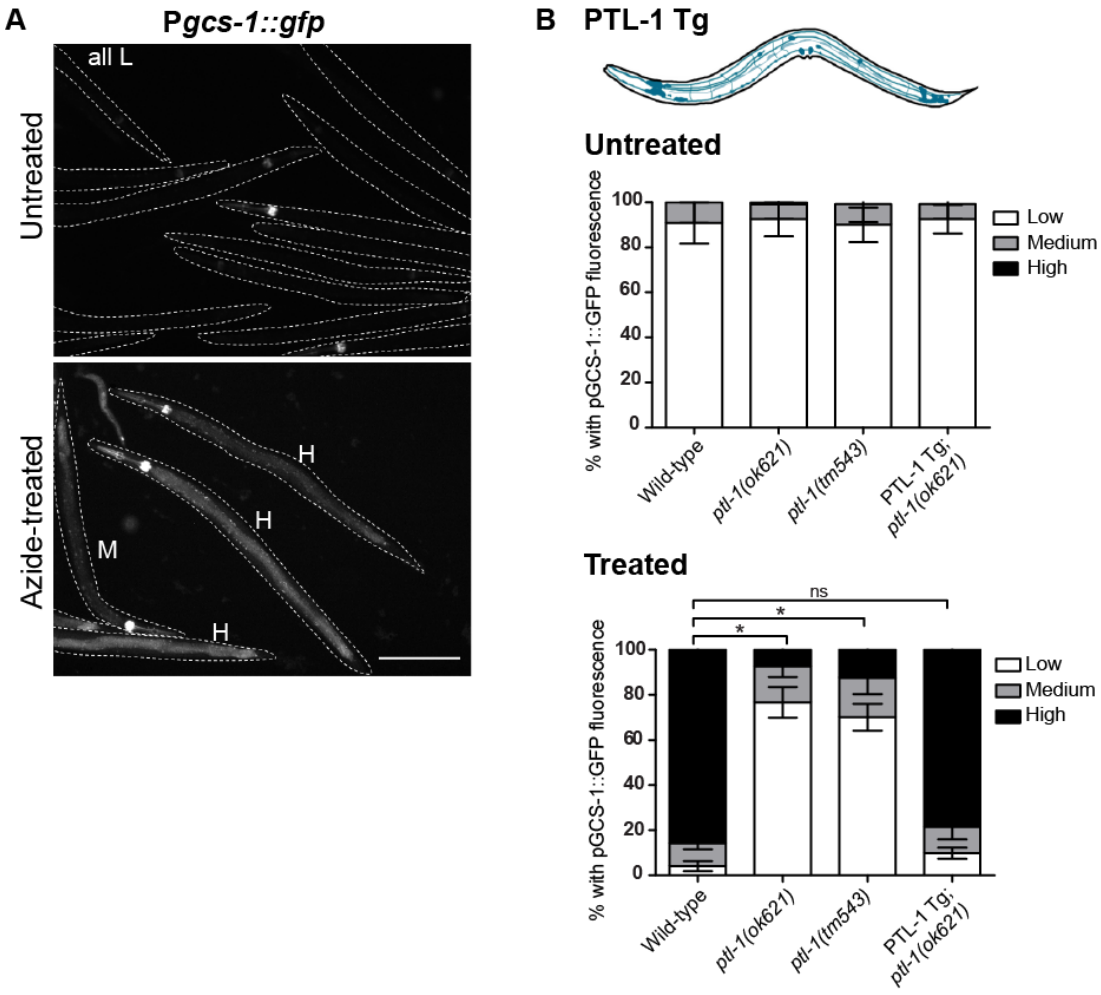

Figure 4.5: *ptl-1* mutants show defective induction of the SKN-1-regulated *gcs-1* promoter. A) 50 mM sodium azide treatment induces GFP expression in P*gcs-1::gfp (ldIs3)* animals. Untreated animals were incubated in M9 buffer only and showed no response (data not shown). Treatment was for 10 minutes at room temperature in liquid. n=15 per biological replicate. **B)** *ptl-1* mutant strains show defective P*gcs-1::gfp* induction in response to 50 mM sodium azide treatment, which can be rescued by re-expression of PTL-1 under the regulation of the *ptl-1* promoter. Untreated animals show a baseline induction of P*gcs-1::gfp*. Scoring was conducted as described in (Wang et al., 2010) for P*gcs-1::gfp* experiments. n=40 per biological replicate. Statistical analysis: One-way ANOVA comparing the incidence of 'low' fluorescence. P-values indicated by ns = not significant, *<0.05. For all experiments, averaged data from three independent experiments is shown.

Given the defects in SKN-1::GFP and P*gcs-1::gfp* re-localisation and induction in response to azide stress observed in *ptl-1* mutant animals at L2 and young adult stages, we aimed to investigate if these defects arise post-development (post-larval stage four/L4), or as a result of a developmental deficiency. To distinguish between these possibilities, we planned to knockdown *ptl-1* by RNAi at L4 stage and determine if similar defects in P*gcs-1::gfp* induction seen in *ptl-1* mutant strains could be observed after knockdown. However, a technical issue we faced was that PTL-1 is predominantly expressed in neurons (Chew et al., 2014a, Gordon et al., 2008), and wild-type neurons that do not express the dsRNA transporter SID-1 are refractory to RNAi (Feinberg and Hunter, 2003, Winston et al., 2002). To test if we could knockdown PTL-1 in neurons, we used a transgenic line where SID-1 was re-expressed in neurons alone (using an *unc-119* promoter) in a *sid-1(pk3321)* null mutant background (referred to as the "pan-neuronal SID-1" line) (Calixto et al., 2010). In order to visualise if *ptl-1* could be knocked down by RNAi, we generated a PTL-1::GFP fusion reporter that contains the coding sequence of PTL-1 fused to GFP at the C-terminus under the regulation of the *ptl-1* promoter and an *unc-54* 3′ UTR. Using this transgenic line, we confirmed the expression pattern in the nervous system (**Figure 4.6**), and we additionally observed PTL-1 expression in non-neuronal tissues, as previously shown in examinations using a transcriptional reporter line expressing GFP from a *ptl-1* promoter (Gordon et al., 2008). We further discuss the relevance of non-neuronal expression of PTL-1 in **Chapter 6** of this thesis.

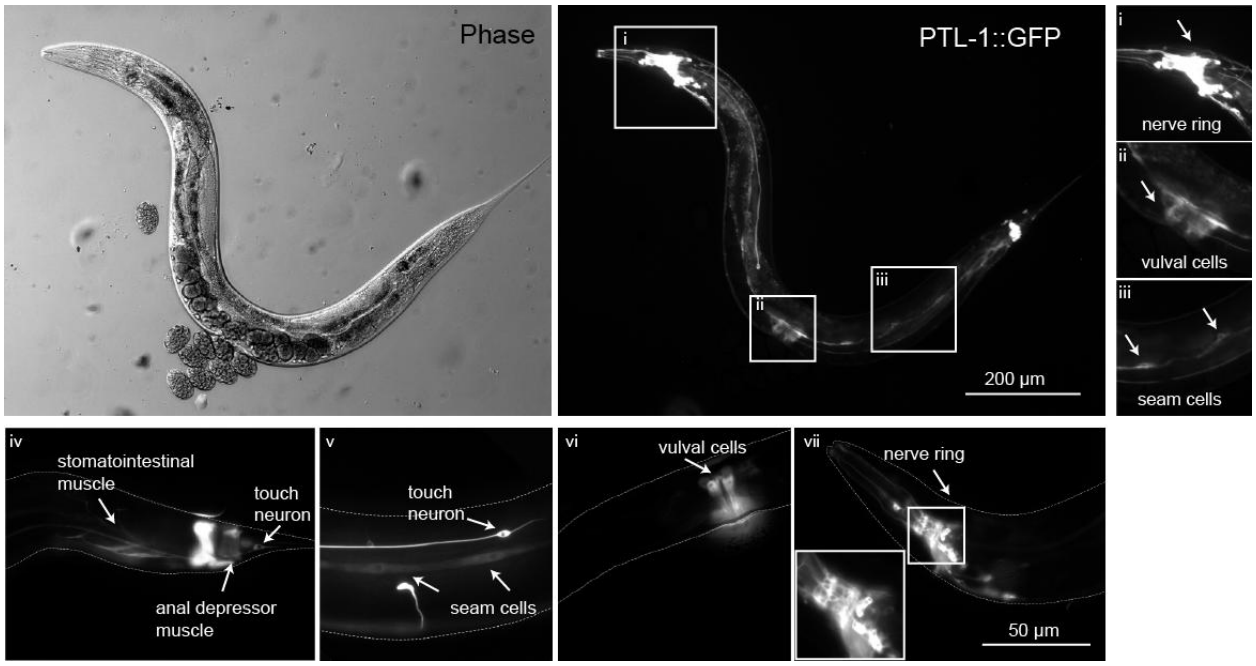

Figure 4.6: PTL-1 is enriched in neurons but is also expressed in non-neuronal tissues. a) PTL-1 expression as shown by a translational GFP fusion is enriched in neurons and is also present in non-neuronal tissues in an adult animal. (i-iii) Micrographs from a single transgenic animal indicating particular anatomical features where PTL-1::GFP is expressed including the nerve ring in the head, cells in the vulva and seam cells. (iv-vii) Micrographs from other transgenic animals indicating PTL-1::GFP expression in muscle, seam cells, vulval cells and neurons. The inset in (vii) is a magnified image of the nerve ring. Anatomical features are highlighted by white arrows.

The PTL-1::GFP fusion protein was expressed in pan-neuronal SID-1 transgenic animals and an RNAi by feeding protocol (Timmons et al., 2001, Timmons and Fire, 1998) used to test if *ptl-1* could be efficiently knocked down at the L4 stage. Bacteria expressing *ptl-1* RNAi feeding constructs or empty vector (EV) RNAi controls were fed to L4 animals and these animals imaged the following day to determine if any knockdown of *ptl-1* was detectable. Interestingly, the fluorescence intensity of PTL-1::GFP decreased in both EV and *ptl-1* RNAi-treated animals with age. However, we did not observe any significant change in PTL-1::GFP signal between *ptl-1* RNAi and EV controls until day 3-4 of adulthood (**Figure 4.7**). Although these data were

collected from few (2-4) animals per treatment per time point, we concluded that we could not use this method to determine if PTL-1-mediated regulation of SKN-1 required PTL-1 during or post-development, as we could not confidently reduce PTL-1 levels at the early stages of adulthood.

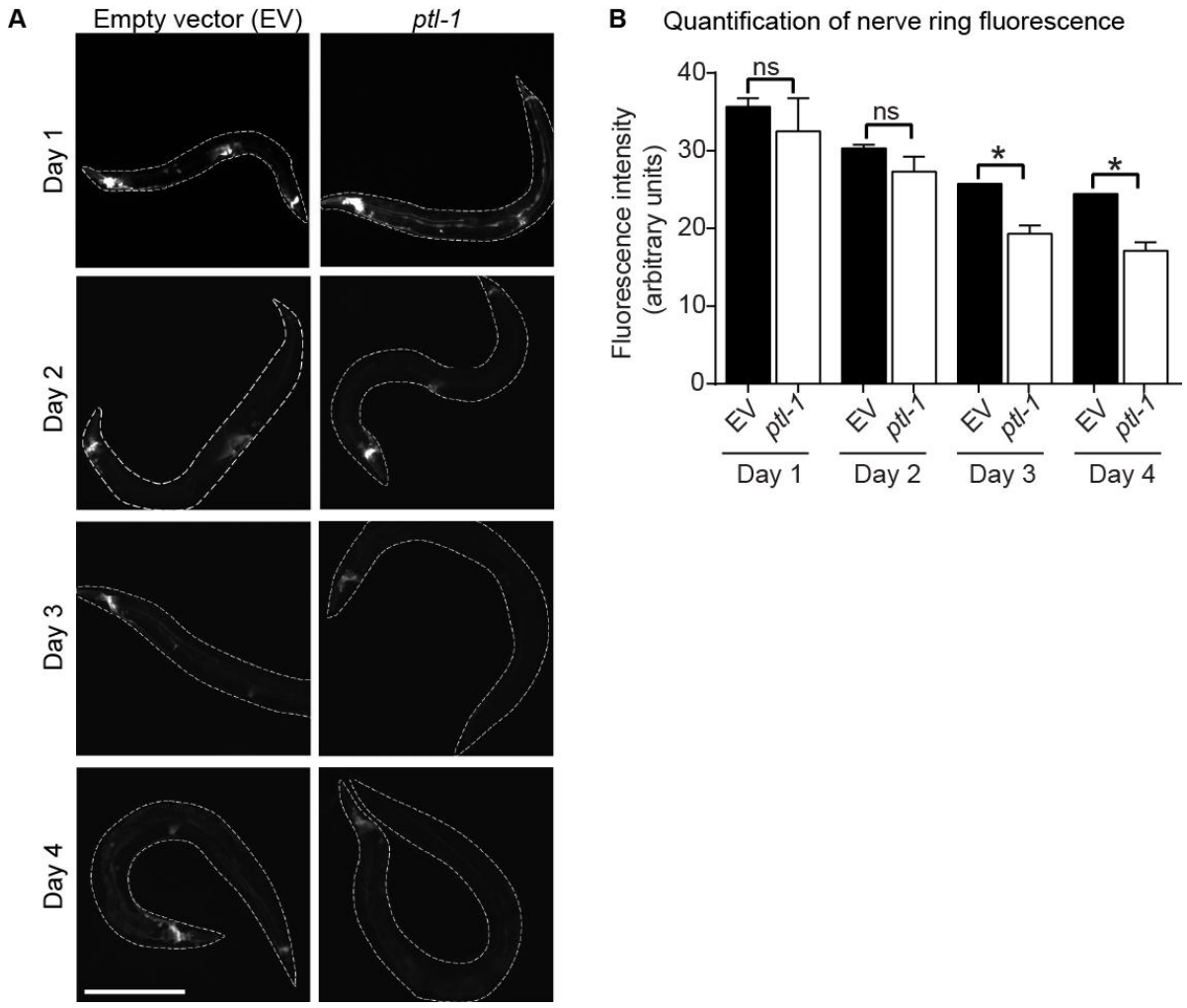

Figure 4.7: Pan-neuronal knockdown of *ptl-1* by RNAi feeding at post-developmental stage. A) PTL-1::GFP animals were picked onto NGM plates seeded with RNAi feeding bacteria (empty vector, EV controls or *ptl-1* RNAi) at L4 stage. Animals were imaged at days 1-4 of adulthood using the same exposure time for imaging. Scale, 200 µm. Images show representative animals from each treatment group. **B)** Quantification of fluorescence signal at

the nerve ring was measured using ImageJ software. n=1-4 animals per treatment per time point. Error bars indicate mean +/- SEM. Statistical analysis: unpaired t-test, p value is indicated by ns = not significant, *<0.05.

4.1.6 PTL-1 re-expression in all neurons but not specifically in ASI neurons rescues SKN-1 re-localisation defects

PTL-1 is expressed in both neuronal and non-neuronal tissue (Chew et al., 2014a, Gordon et al., 2008). Although it is generally accepted that PTL-1 is expressed predominantly in neurons (Goedert et al., 1996, McDermott et al., 1996, Gordon et al., 2008), we aimed to confirm that regulation of SKN-1 in the intestine involved a signal from neuronal PTL-1. To achieve this, we generated a transgenic line expressing PTL-1::V5 under the regulation of an *aex-3* pan-neuronal promoter. We immunostained for V5 expressed from this transgene and observed PTL-1::V5 expressed widely in neurons (**Figure 4.8A**). We found that pan-neuronal expression of PTL-1 rescued the defect in SKN-1::GFP nuclear re-localisation (**Figure 4.8B**) and *Pgcs-1::gfp* induction (**Figure 4.8C**) in *ptl-1* null mutant animals in response to stress. These data demonstrate that PTL-1 acts in the neurons to regulate intestinal SKN-1 and SKN-1-regulated targets.

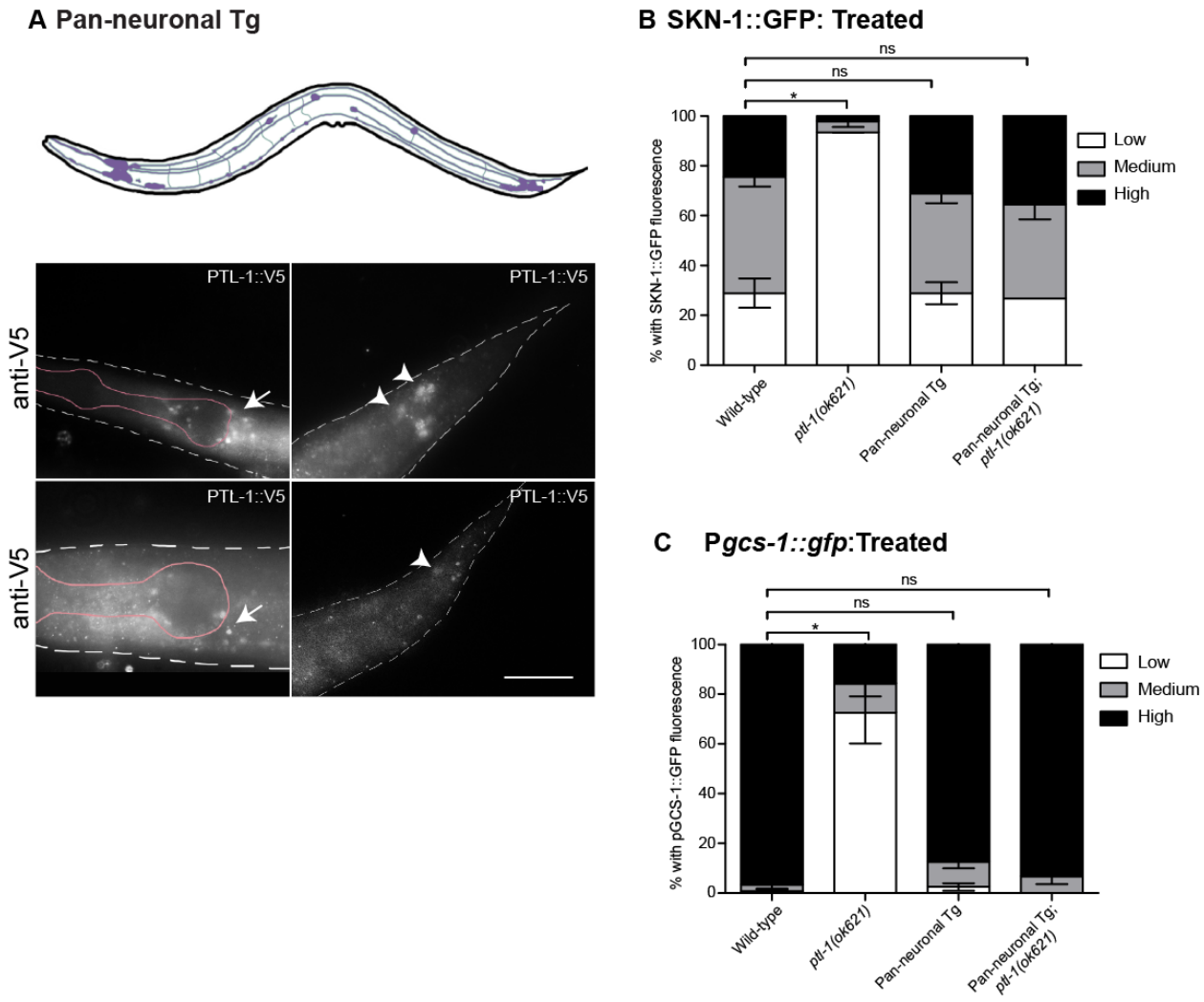

Figure 4.8: PTL-1 in neurons regulates SKN-1 nuclear re-localisation in the intestine. A) Immunohistochemistry for PTL-1::V5 in pan-neuronal (*aex-3* promoter) transgenic line. Left panels show the head, with the white arrow indicating neurons of the nerve ring and the pink outline indicating the approximate position of the pharynx. Right panels show the tail, with the white arrowheads indicating tail neurons. Pan-neuronal re-expression of PTL-1 rescues the defect in **B)** intestinal SKN-1 nuclear re-localisation (n=15 per biological replicate) and **C)** P*gcs-1::gfp* induction (n=40 per biological replicate) in response to 50 mM sodium azide. Untreated animals were incubated in M9 buffer only and showed no response for SKN-1::GFP re-localisation (data not shown). Treatment was for 10 minutes at room temperature in liquid. Scoring was conducted as described in (Tullet et al., 2008) for SKN-1::GFP and as in (Wang et al., 2010) for P*gcs-1::gfp* experiments. Statistical analysis: One-way

ANOVA comparing the incidence of 'low' fluorescence. P-values indicated by ns = not significant, *<0.05. For all experiments, averaged data from three independent experiments are shown.

Given that SKN-1b is expressed in the ASI neurons and that it could co-localise with PTL-1, we aimed to determine if expressing PTL-1 in ASI neurons alone had an effect on intestinal SKN-1 localisation in response to stress. We generated a transgene expressing PTL-1::V5 under the control of the *gpa-4* ASI-specific promoter. Immunostaining for V5 indicated that transgene expression was restricted to few neurons in the head (**Figure 4.9A**), although due to technical difficulties we were unable to resolve unambiguously if these were the ASI neurons. We found that ASI-specific expression of PTL-1 did not rescue the defect in SKN-1::GFP nuclear re-localisation (**Figure 4.9Bi**) and *Pgcs-1::gfp* induction (**Figure 4.9Bii**) in *ptl-1* null mutant animals in response to stress. This indicates that expression of PTL-1 in the ASI neurons alone is not sufficient to modulate SKN-1::GFP re-localisation to the intestinal nuclei.

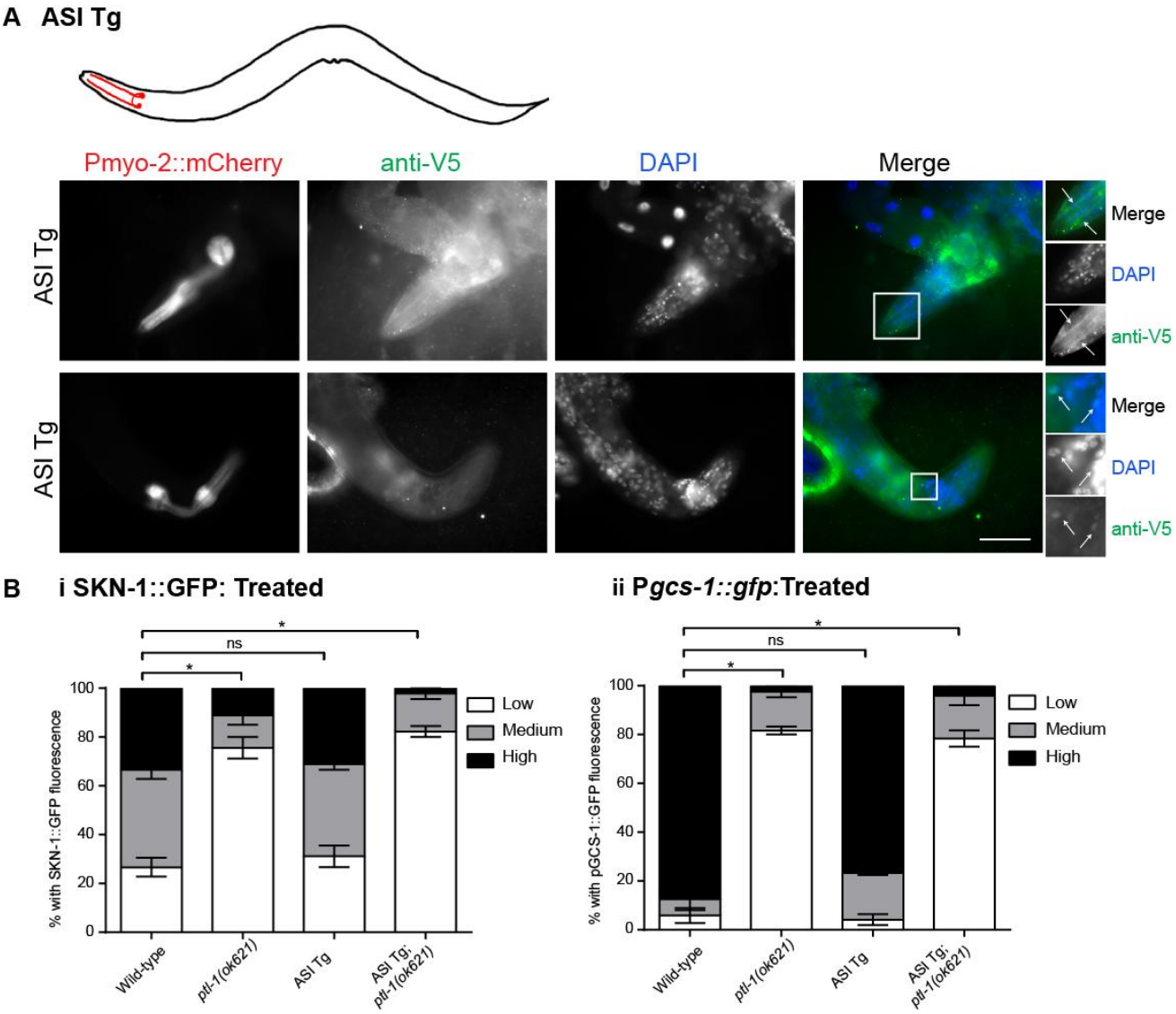

Figure 4.9: ASI-specific PTL-1 re-expression does not rescue SKN-1::GFP re-localisation and P*gcs-1::gfp* induction in *ptl-1(ok621)* mutant animals when exposed to azide stress. A) Immunohistochemistry of transgenic animals carrying an extrachromosomal array of PTL-1::V5 expressed under the control of the *gpa-4* promoter using an anti-V5 monoclonal antibody. Transgenic animals express the P*myo-2::mCherry* marker, which expresses in pharyngeal muscle. Arrows indicate the axon (upper panel) and cell body (lower panel) of head neurons, putatively ASI neurons, where PTL-1:V5 is localised. Rightmost panels are magnified insets indicating staining from DAPI, anti-V5 immunofluorescence and a composite merged image. Signal intensity has been increased in insets for clarity. **B) (**i) Intestinal SKN-1 nuclear re-localisation in animals treated with sodium azide (50mM) for 10 minutes at room temperature in liquid. n=15 per biological replicate. (ii) P*gcs-1::gfp* induction in response to 50 mM sodium

azide. n=40 per biological replicate. Scoring was conducted as described in (Tullet et al., 2008) for SKN-1::GFP and as in (Wang et al., 2010) for P*gcs-1::gfp* experiments. Statistical analysis: One-way ANOVA comparing the incidence of 'low' fluorescence. P-values indicated by ns = not significant, *<0.05. For all experiments, averaged data from three independent experiments is shown.

4.1.7 Synaptic vesicle mutants show defective SKN-1 re-localisation that is dependent on PTL-1

Our observation that neuronal expression of PTL-1 was sufficient to rescue SKN-1::GFP nuclear re-localisation in the intestine (**Figure 4.8**) suggests that part of the response to oxidative stress involves a cross-talk between the neurons and the intestine. One possibility is that loss of or mutations in PTL-1 result in a defect in vesicle transport or exocytosis from the nervous system, and that these vesicles contain the signal required for communication between these tissues. We assayed mutants that are defective in vesicle release to determine if this was the case. UNC-13 regulates conformational changes in the membrane protein syntaxin to mediate exocytosis, and thus *unc-13(e450)* mutants are defective in synaptic vesicle (SV) exocytosis (Richmond et al., 1999, Madison et al., 2005). We found that *unc-13* mutant animals also display a defect in SKN-1::GFP nuclear re-localisation and P*gcs-1::gfp* induction in response to azide stress (**Figure 4.10A**). To determine if PTL-1 is involved in the regulation of stress responsive SKN-1::GFP localisation by SV release mutants, we generated a *unc-13(e450);ptl-1(ok621)* double mutant strain expressing the SKN-1::GFP transgene and assayed for intestinal re-localisation of SKN-1::GFP with azide treatment. We elected to test SKN-1::GFP localisation and not P*gcs-1::gfp* induction for this purpose as we aimed to test for a direct link between SKN-1, PTL-1 and UNC-13. We did not observe a significant difference in SKN-1::GFP localisation phenotypes between azide-treated *unc-13(e450)* and *unc-13(e450);ptl-1(ok621)* animals (**Figure 4.10B**), suggesting that PTL-1 and UNC-13 may act in similar pathways to regulate SKN-1.

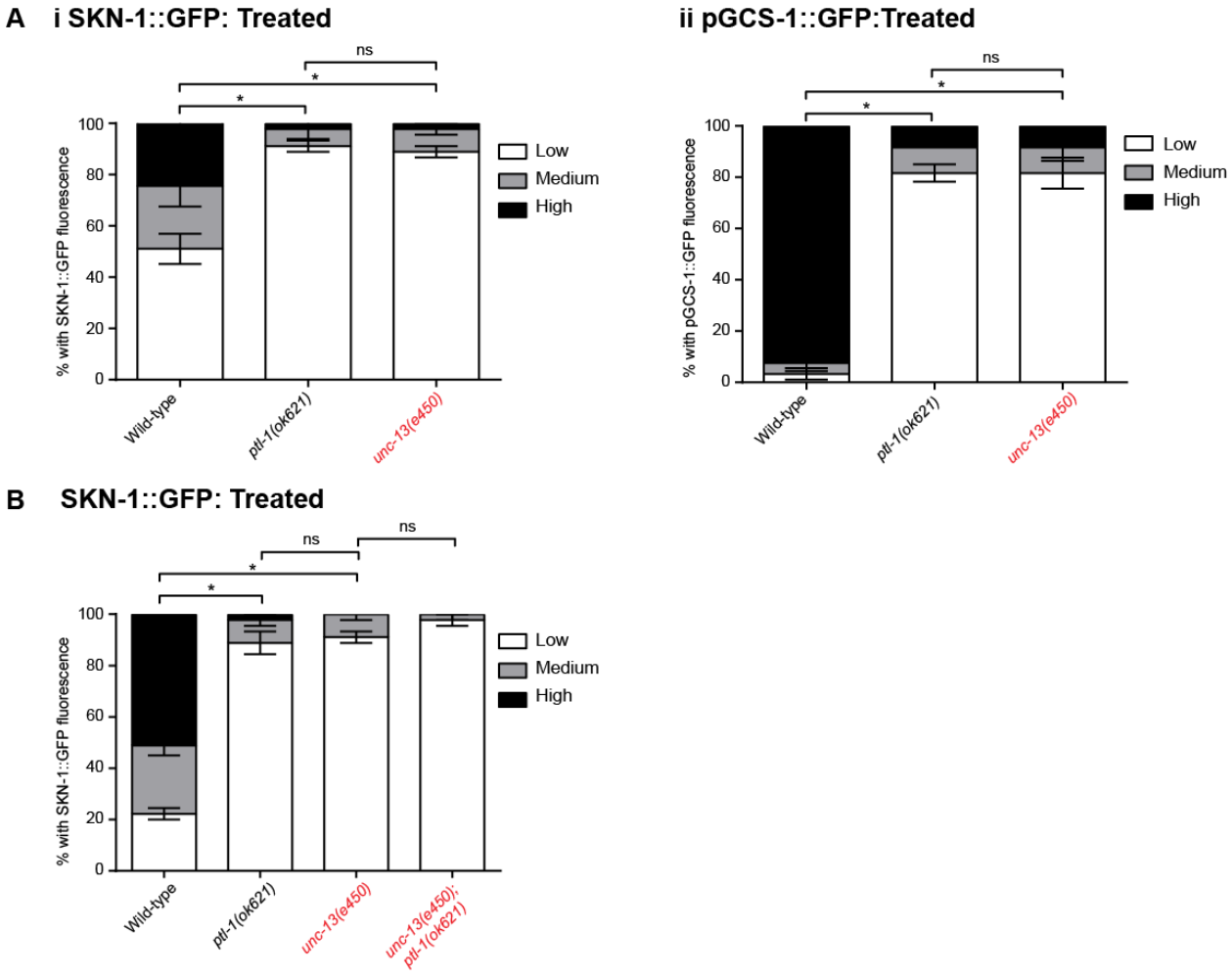

Figure 4.10: SKN-1::GFP re-localisation and P*gcs-1::gfp* induction are defective in *unc-13* mutant animals. **A)** (i) Intestinal SKN-1 nuclear re-localisation in animals treated with sodium azide for 10 minutes at room temperature in liquid. n=15 per biological replicate,. (ii) P*gcs-1::gfp* induction (n=40 per biological replicate) in response to sodium azide. **B)** Intestinal SKN-1 nuclear re-localisation for *unc-13;ptl-1* double mutants treated with sodium azide. Scoring was conducted as described in (Tullet et al., 2008) for SKN-1::GFP and as in (Wang et al., 2010) for P*gcs-1::gfp* experiments. Untreated animals are incubated in M9 buffer only and showed no response. Statistical analysis: One-way ANOVA comparing the incidence of 'low' fluorescence. P-values indicated by ns = not significant, *<0.05. For all experiments, averaged data from three independent experiments is shown.

We next tested if another type of vesicle transport was involved in PTL-1-mediated regulation of SKN-1. UNC-31 is the *C. elegans* homolog of CAPS (calcium-dependent activator protein for secretion) and functions in calcium-regulated dense-core vesicle (DCV) fusion. *unc-31(e928)* mutants are defective in DCV exocytosis (Lin et al., 2010). We found that *unc-31* mutant animals were intermediate between wild-type and *ptl-1(ok621)* mutant animals with regards to SKN-1::GFP nuclear re-localisation or P*gcs-1::gfp* induction in response to azide stress (**Figure 4.11A**). Next, *unc-31(e928);ptl-1(ok621)* double mutant animals were tested for intestinal re-localisation of SKN-1::GFP with azide treatment. As above, we did not test P*gcs-1::gfp* induction after azide treatment in the *unc-31;ptl-1* double mutant strain. Intriguingly, we did not resolve a significant difference between *unc-31(e928)* single mutant and *unc-31(e928);ptl-1(ok621)* double mutant animals (**Figure 4.11B**). Given that UNC-13 and UNC-31 appear to differentially regulate SKN-1, our data implies that through a different pathway from UNC-13, the *unc-31(e928)* mutation suppresses the effect of the *ptl-1(ok621)* mutation on SKN-1 localisation.

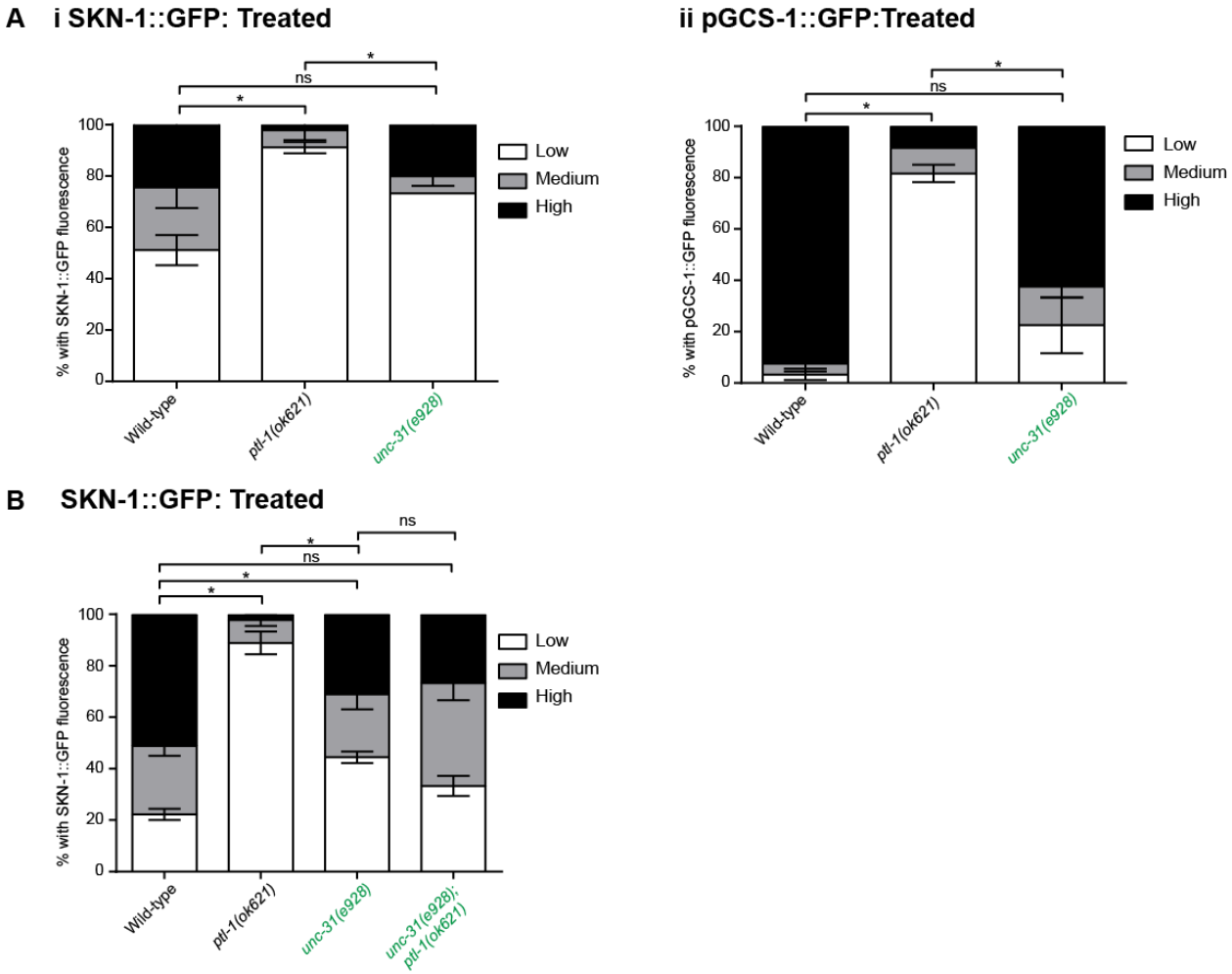

Figure 4.11: SKN-1::GFP re-localisation and P*gcs-1::gfp* induction are not defective in *unc-31* mutants. A) (i) Intestinal SKN-1 nuclear re-localisation in animals treated with sodium azide for 10 minutes at room temperature in liquid. n=15 per biological replicate. (ii) P*gcs-1::gfp* induction in response to sodium azide. n=40 per biological replicate. **B)** Intestinal SKN-1 nuclear re-localisation for *unc-13;ptl-1* double mutants treated with sodium azide. Scoring was conducted as described in (Tullet et al., 2008) for SKN-1::GFP and as in (Wang et al., 2010) for P*gcs-1::gfp* experiments. Untreated animals are incubated in M9 buffer only and showed no response. Statistical analysis: One-way ANOVA comparing the incidence of 'low' fluorescence. P-values indicated by ns = not significant, *<0.05. For all experiments, averaged data from three independent experiments are shown.

Given our observations in the synaptic vesicle release mutant *unc-13(e450)*, we investigated if any differences could be observed in synaptic vesicle transport in *ptl-1(ok621)* mutant animals.

We visualised synaptic vesicles using a GFP::RAB-3 (*jsIs682*) marker in a strain expressing P*mec-4::mCherry (vdEx263*) to highlight touch neurons, and counted the number of GFP::RAB-3 punctae in a defined region of the axon in the ALM touch neuron. RAB-3 is a member of the Ras GTPase family that is involved in the regulation of SV release in neurons and is used as a marker for SVs (Mahoney et al., 2006, Margeta et al., 2009). Interestingly, we observed a small but significant difference between wild-type and *ptl-1(ok621)* animals when we monitored the number of GFP::RAB-3 punctae in this manner (**Figure 4.12A**). We observed that *ptl-1(ok621)* mutant animals had on average a lower number of GFP::RAB-3 punctae compared with wild-type when punctae were counted along 70 µm of the ALM axon, starting from but not including the cell body. Specifically, *ptl-1(ok621)* animals had 11 punctae per 70 µm whereas wild-type animals showed 14 punctae per 70 µm (**Figure 4.12B**). This is in contrast with an earlier investigation that showed no significant difference in the number of SV punctae in *ptl-1(ok621)* mutant animals (Tien et al., 2011), albeit using a different SV reporter (SNB-1::mRFP) and a different scoring protocol. In our investigation, punctae were all counted manually and blind to the genotype of the strains. However, there were difficulties in developing a consistent scoring scheme for counting punctae, as some punctae are large and brighter whereas others are small and have a dimmer GFP signal. A more refined scoring scheme is required for future experimentation, possibly by quantifying fluorescence intensity along the axon using image analysis software and setting a strict definition for regions to be counted as puncta only if they exceed a particular signal threshold.

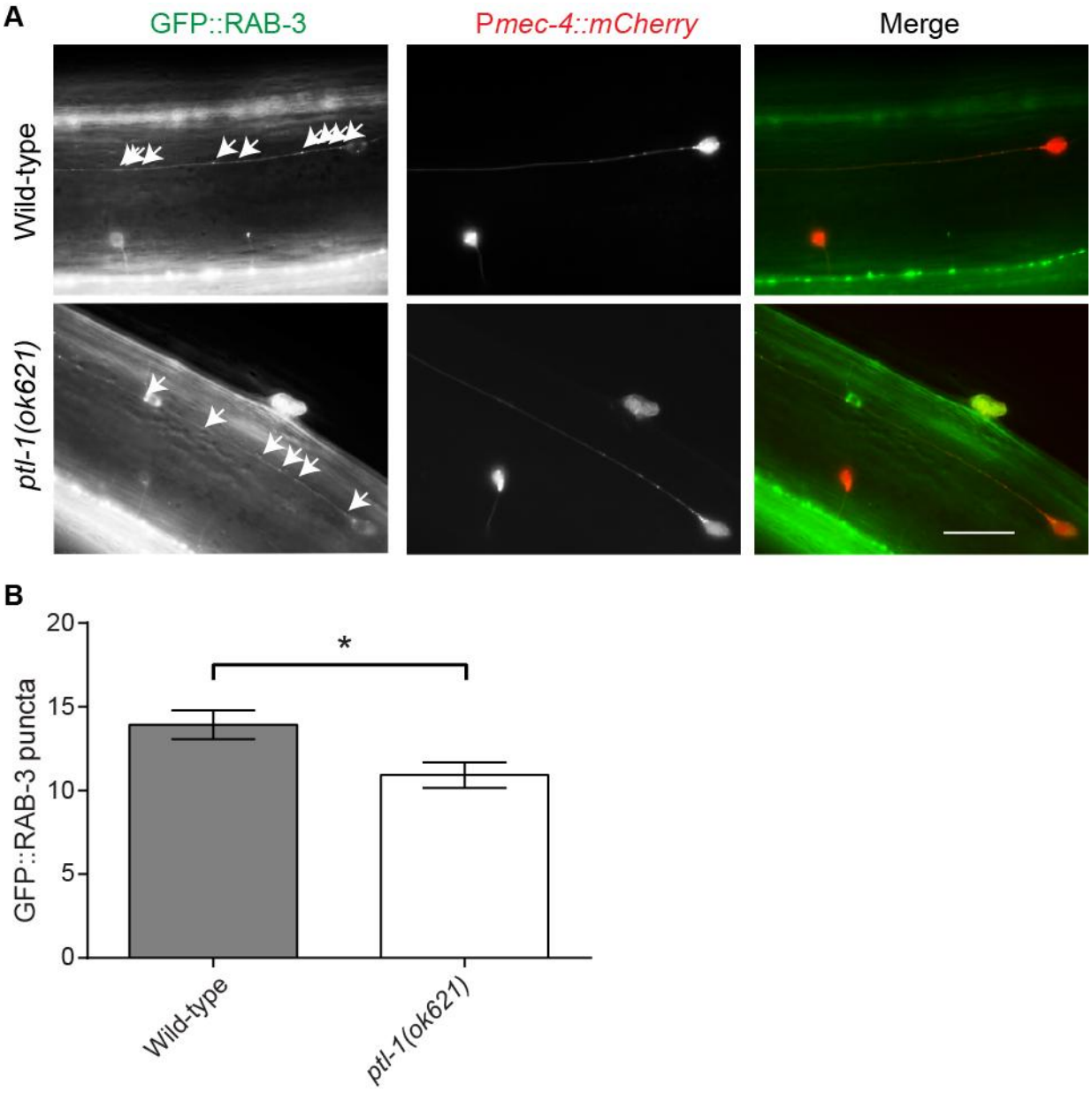

Figure 4.12: *ptl-1(ok621)* mutant animals have fewer synaptic vesicles in ALM neurons compared with wild-type. A) Images indicating the GFP::RAB-3 (*jsIs682*) synaptic vesicle marker co-localising with ALM in wild-type and *ptl-1(ok621)* animals. The ALM neuron was visualised using a P*mec-4::mCherry* (*vdEx263*) touch neuron reporter. Representative images are shown. Arrows indicate GFP::RAB-3 punctae quantified in this experiment. Scale, 10 µm. **B)** The average number of GFP::RAB-3 punctae counted 70 µm along the axon from (but not including) the cell body of ALM in wild-type and *ptl-1(ok621)* animals. The average of three replicates is shown, n =11-12 neurons per replicate. Statistical analysis: unpaired t-test, two-tailed p-value is represented by *<0.05.

4.1.8 Discussion

Chronic oxidative stress has been postulated to contribute towards Tau pathology (Jo et al., 2014, Stack et al., 2014). We have demonstrated that the Tau-like protein PTL-1 is involved in (i) modulating the response to oxidative stress, and (ii) regulating the nuclear re-localisation of intestinal SKN-1 via the nervous system in a process that may require the synaptic vesicle fusion protein UNC-13.

In ASI neurons, SKN-1b is constitutively nuclear-localised (An and Blackwell, 2003). In the intestine, SKN-1c is normally diffuse in the cytoplasm, but localises to the intestinal nucleus in response to stress (An and Blackwell, 2003). This re-localisation process requires p38 mitogen-activated protein kinase (Inoue et al., 2005) and is also negatively regulated by glycogen synthase kinase 3 (GSK-3) (An et al., 2005). Another factor that has been shown to normally inhibit nuclear re-localisation of SKN-1 is the insulin receptor DAF-2, which does this in parallel to inhibition of another transcription factor that regulates stress and longevity, DAF-16 (Tullet et al., 2008). In our hands, we did not see any effect of a *daf-2* reduction-of-function on SKN-1 re-localisation, although we used a transgenic line with considerably lower expression compared with the transgenic line used in (Tullet et al., 2008). We now propose the microtubule-associated protein PTL-1 as an additional factor that is required for the efficient movement of intestinal SKN-1 from the cytoplasm to the nucleus. We also showed that loss of PTL-1 did not affect DAF-16 movement into the intestinal nuclei, which is also normally induced by stress, and DAF-2 reduction-of-function did not alter the effect of *ptl-1* mutation on intestinal SKN-1 re-localisation. This suggests that regulation of SKN-1 by PTL-1 does not involve the insulin-like signalling pathway.

Using pan-neuronal transgenic lines that restrict PTL-1 expression to the nervous system, we have shown that PTL-1 in neurons promotes SKN-1 nuclear re-localisation in the intestine and hence the induction of SKN-1-responsive genes. We also found that expressing PTL-1 in ASI neurons alone, where SKN-1b remains constitutively nuclear, does not rescue the effect of *ptl-1* null mutation on intestinal SKN-1c localisation. This implies that any interaction between PTL-1 and SKN-1b in the ASI neurons does not affect SKN-1c in the intestine.

Regulatory processes that occur between proteins found in different tissues have been demonstrated previously in the insulin-like signalling pathway in *C. elegans*. DAF-16 in the intestine or neurons can signal to DAF-16 in other tissues to modulate lifespan, although the relative effect of intestine-derived signalling is higher than that of neuron-derived signalling (Libina et al., 2003). Reducing DAF-16 activity in all tissues also modulates expression levels of the insulin-like peptide INS-7 in the intestine but not in neurons (Murphy et al., 2007). In addition, the negative regulator WDR-23, which targets SKN-1 for proteasomal degradation, is expressed in several tissues including the neurons and intestine (Choe et al., 2009, Staab et al., 2013). *wdr-23* null mutant animals display severe aldicarb resistance, suggesting that WDR-23 regulates acetylcholine signalling at neuromuscular junctions. However, intestine-specific expression of WDR-23, and hence intestine-specific SKN-1 degradation, is sufficient to rescue aldicarb resistance in *wdr-23* mutant animals (Staab et al., 2013). This implies that SKN-1 activation in the intestine is required to modulate proper functioning of neurons. These investigations reveal that there is substantial cross-talk between the nervous system and the intestine of *C. elegans*, particularly involving factors that regulate longevity or stress tolerance.

By monitoring synaptic vesicle distribution using a synaptobrevin-1 (SNB-1) reporter PTL-1 has previously been shown to regulate kinesin-based transport on microtubules (Tien et al., 2011). We postulated that one mechanism by which PTL-1 in the nervous system regulates SKN-1 in the intestine is via signalling molecules carried by synaptic vesicles released from the nervous system to communicate with other tissues. Using an *unc-13* mutant strain that is defective in synaptic vesicle exocytosis (Richmond et al., 1999), we demonstrated that SKN-1 re-localisation into intestinal nuclei requires UNC-13. Furthermore, *unc-13;ptl-1* double mutant animals were not significantly more defective in regulation the movement of intestinal SKN-1 into the nucleus, suggesting that PTL-1 and UNC-13 act within similar pathways to modulate SKN-1 localisation. However, we acknowledge that a shortcoming with the method used to investigate these interactions is that only on average 10-15% of *ptl-1* mutant animals display nuclear SKN-1::GFP, meaning that there is only a small window to resolve a worsening of this effect. Further experimentation is required to determine if UNC-13 is genuinely involved in the regulation of SKN-1 by PTL-1. Despite this caveat, our data present the first demonstration of the importance of SV exocytosis in the SKN-1 intestinal response. Interestingly, the promoter region of the *unc-13* gene contains SKN-1 binding sites and its expression is also regulated by WDR-23 in neurons (Staab et al., 2014). We also showed that the SV marker GFP::RAB-3 displayed fewer punctae in a designated region of the axon in *ptl-1* mutant animals compared with wild-type controls, providing additional evidence of a defect in SV transport. Taken together, these findings suggest that a feedback loop exists between the nervous system and intestine to regulate neuronal function and the stress response.

4.2 Section 2: PTL-1 in longevity

4.2.1 Introduction

Investigations conducted in many systems suggests that there is a close relationship between the stress response and longevity (Buffenstein et al., 2008, Gemma et al., 2007, Sanz and Stefanatos, 2008). In the previous section, we demonstrated that PTL-1 is involved in regulating the response to oxidative stress via the Nrf2 homolog in *C. elegans*, SKN-1. In mammals, Nrf2 has also been linked to lifespan modulation (Lewis et al., 2010, Bishop and Guarente, 2007, Leiser and Miller, 2010), as has SKN-1 in *C. elegans* (Bishop and Guarente, 2007, An et al., 2005). Here, we investigated if PTL-1 is involved in longevity, and whether it does so within a similar pathway to SKN-1.

4.2.2 ptl-1 *mutant animals are short-lived*

The data described above demonstrate that PTL-1 is involved in the stress response via the SKN-1 transcription factor. For many genes in *C. elegans*, stress responsiveness is correlated with lifespan, such that some mutants that display decreased longevity also have lower tolerance to some stressors (reviewed in (Zhou et al., 2011)). We first investigated if PTL-1 plays a role in modulating longevity. We conducted lifespan experiments on *ptl-1(ok621)* and *ptl-1(tm543)* mutant strains and found that both strains were short-lived compared with wild-type controls (**Figure 4.13A,B**). Analysis of the two survival curves indicates that this difference is statistically significant; however, it appears that lifespan reduction is more severe in the *ptl-1(ok621)* null mutant strain that has a 37% shorter median lifespan compared with wild-type (median lifespan 5 days versus 8 days), whereas the median lifespan in the *ptl-1(tm543)* mutant strain is 10% shorter than wild-type (median lifespan 9 days versus 10 days) (**Figure 4.13**).

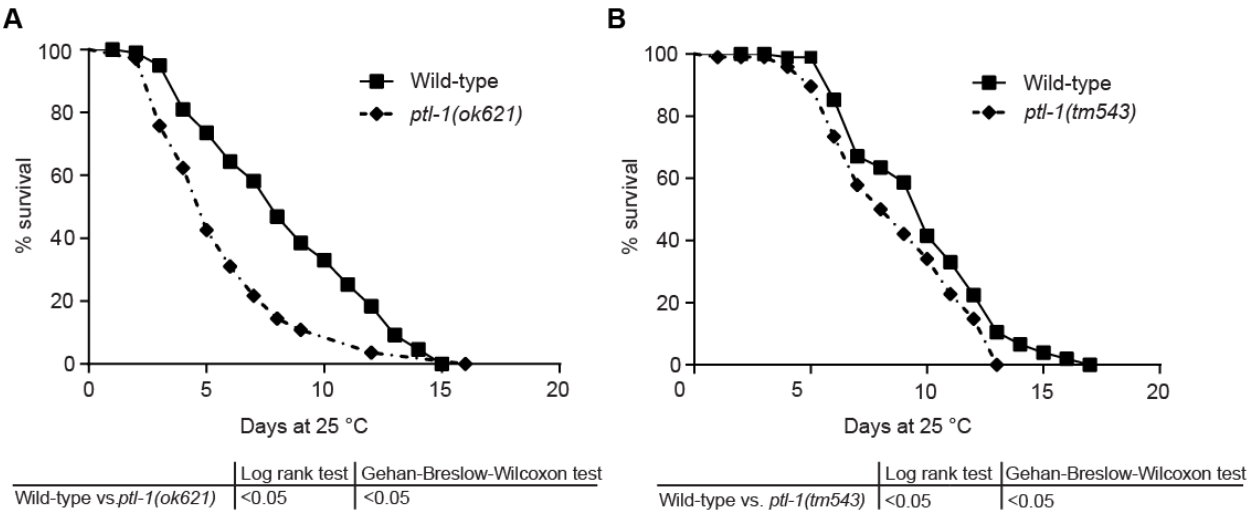

Figure 4.13: *ptl-1* mutant animals are short-lived compared with wild-type. Survival curves for **A)** *ptl-1(ok621)* and **B)** *ptl-1(tm543)* mutant strains compared with wild-type controls. n = 100 at day 0. Results of statistical analysis are indicated by p-values underneath each graph.

4.2.3 Lifespan reduction in ptl-1 *mutant strains can be rescued by re-expression of PTL-1 but not human Tau*

We checked if lifespan reduction observed in *ptl-1* mutants could be rescued by re-expression of PTL-1 to determine if loss of PTL-1 was genuinely responsible for this phenotype. We found that re-expressing PTL-1 in a *ptl-1* null mutant background resulted in a survival curve that was very similar to non-transgenic wild-type worms (median lifespan 8 days for both strains). Therefore, re-expressing PTL-1 in a *ptl-1* null mutant is able to rescue the lifespan reduction observed in *ptl-1(ok621)* animals (median lifespan 7 days) (**Figure 4.14A**). Interestingly, expressing the PTL-1 transgene together with endogenous PTL-1 led to a reduction in lifespan (median lifespan 7 days). This reduction in lifespan for the "PTL-1 Tg; wild-type" strain is

statistically significant according to the Gehan-Breslow-Wilcoxon test for significance. Increasing the number of copies of *ptl-1* thus appears to produce a detrimental effect.

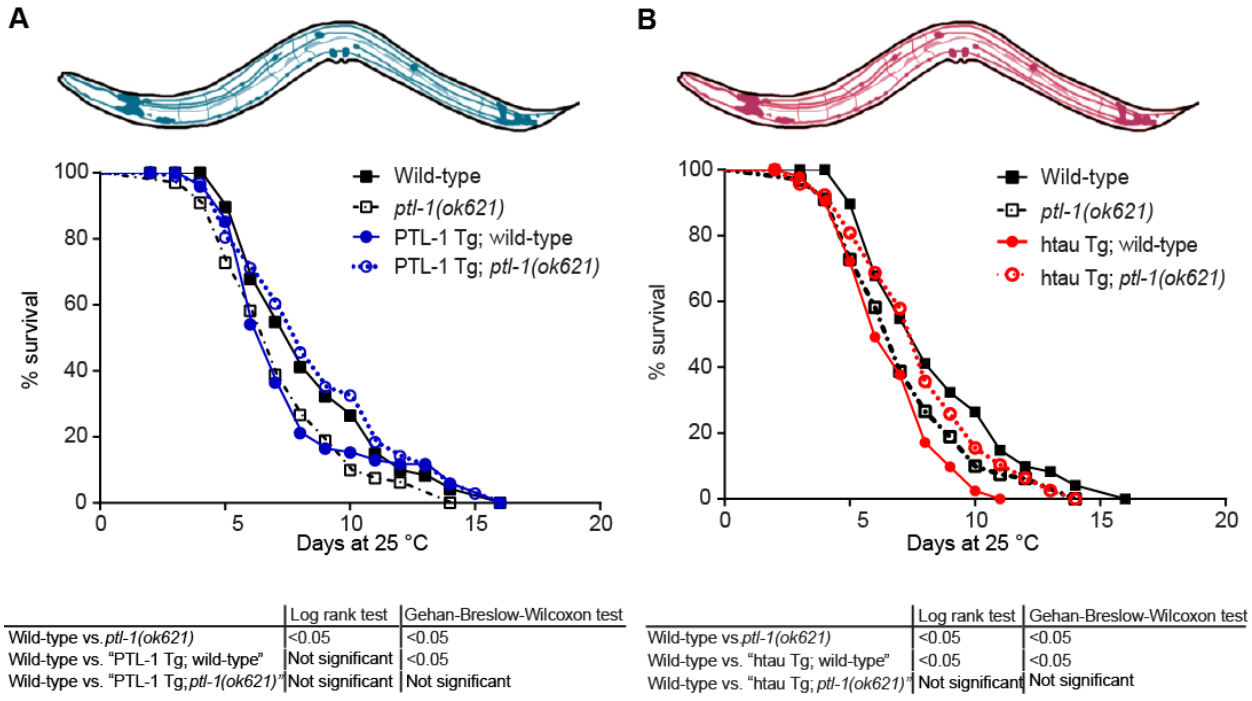

	Log rank test	Gehan-Breslow-Wilcoxon test
Wild-type vs.*ptl-1(ok621)*	<0.05	<0.05
Wild-type vs. "PTL-1 Tg; wild-type"	Not significant	<0.05
Wild-type vs. "PTL-1 Tg;*ptl-1(ok621)*"	Not significant	Not significant

	Log rank test	Gehan-Breslow-Wilcoxon test
Wild-type vs.*ptl-1(ok621)*	<0.05	<0.05
Wild-type vs. "htau Tg; wild-type"	<0.05	<0.05
Wild-type vs. "htau Tg;*ptl-1(ok621)*"	Not significant	Not significant

Figure 4.14: The reduction in lifespan observed in *ptl-1* null mutant animals can be rescued by re-expression of PTL-1 but not human Tau. A) Survival curves for PTL-1 transgenic worms. **B)** Survival curves for human Tau transgenic worms. n=100 for each strain at the start of the assay. Results of statistical analysis are shown in the tables below the graphs.

When we conducted the same experiment on transgenic lines expressing human Tau, we found that the "hTau Tg;wild-type" line showed a significant reduction in lifespan compared with the wild-type control (**Figure 4.14B**). Interestingly, we also observed that the transgenic line expressing hTau in a *ptl-1* null mutant has a lifespan that is intermediate between that of non-transgenic wild-type (median lifespan 8 days) and *ptl-1(ok621)* null mutant (median lifespan 7 days) strains, and is not significantly different from these control strains (**Figure 4.14B**).

Furthermore, "hTau Tg;wild-type" animals have a significantly shorter lifespan (median lifespan 6 days) compared with non-transgenic wild-type worms or with the "hTau Tg; *ptl-1(ok621)*" strain (median lifespan 8 days) (**Figure 4.14B**). While these observations suggests that hTau may compensate in part for the absence of PTL-1 in the regulation of whole organism lifespan, overall our data indicate that hTau expression does not robustly rescue for the loss of PTL-1.

4.2.4 PTL-1 and SKN-1 use similar pathways to regulate longevity

The *skn-1(zu67)* mutation, which affects isoforms SKN-1a and SKN-1c, has been previously demonstrated to confer a short-lived phenotype (An et al., 2005, Bishop and Guarente, 2007). We recapitulated this result with a 13% reduction in median lifespan (median lifespan 7 days for *skn-1* mutant animals versus 8 days in wild-type). We generated a *ptl-1(ok621);skn-1(zu67)* double mutant strain and conducted a lifespan experiment to investigate if SKN-1and PTL-1 act in the same pathway to regulate longevity. Our data indicate that *ptl-1(ok621);skn-1(zu67)* double mutant animals (median lifespan 7 days) were not significantly shorter or longer-lived compared to *skn-1(zu67)* or *ptl-1(ok621)* single mutant animals (median lifespans 7 days), in two independent lifespan experiments (**Figure 4.15, Appendix 3**). This suggests that SKN-1 and PTL-1 may regulate lifespan via similar pathways.

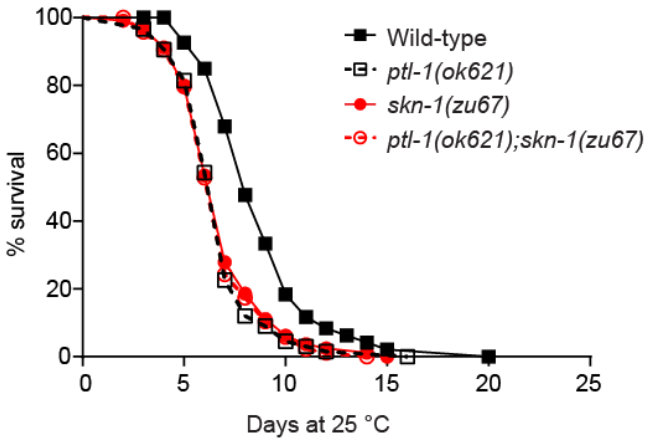

Comparison	Log rank test	Gehan-Breslow-Wilcoxon test
Wild-type vs. *ptl-1(ok621)*	<0.05	<0.05
Wild-type vs. *skn-1(zu67)*	<0.05	<0.05
Wild-type vs. *ptl-1(ok621);skn-1(zu67)*	<0.05	<0.05
skn-1(zu67) vs. *ptl-1(ok621)*	n.s.	n.s.
ptl-1(ok621);skn-1(zu67) vs. *ptl-1(ok621)*	n.s.	n.s.
skn-1(zu67) vs. *ptl-1(ok621);skn-1(zu67)*	n.s.	n.s.

Figure 4.15: *ptl-1(ok621);skn-1(zu67)* double mutant animals are not significantly shorter or longer lived compared to *ptl-1(ok621)* or *skn-1(zu67)* single mutant animals. Survival curves for *skn-1(zu67)* and *ptl-1(ok621)* single mutants together with the *skn-1(zu67);ptl-1(ok621)* double mutant strain. n = 120 at day 0. Results of statistical analysis are indicated by p-values underneath each graph. Lifespan experiments were conducted twice independently and the results of one lifespan experiment are shown. Data from the second lifespan experiment are shown in **Appendix 3**.

4.2.5 Discussion

In the previous section, we showed that PTL-1 is involved in stress tolerance. We expanded our investigation of PTL-1 into its role in the modulation of lifespan. We demonstrate that both null and truncated mutant alleles of PTL-1 are short-lived compared with wild-type. We also found that re-expressing PTL-1 in *ptl-1* null mutant animals using a *Pptl-1::*PTL-1:V5 transgene was sufficient to fully rescue the lifespan defect. In addition, we observed that increasing the number of copies of *ptl-1* by expressing the P*ptl-1::*PTL-1:V5 transgene in a wild-type background also results in a shortening of lifespan. This indicates that a tight regulation of PTL-1 levels is required to maintain wild-type lifespan.

Interestingly, re-expressing human Tau did not rescue the lifespan phenotype observed in *ptl-1* null mutant animals. In fact, expression of human Tau transgene in a wild-type background resulted in a significantly shorter lifespan compared with wild-type controls, which is consistent with previous findings that human Tau expression in *C. elegans* is detrimental (Kraemer et al., 2003). Technical challenges prevented a comparison of expression levels of hTau and PTL-1 in the transgenic lines generated in this study, and it is possible that differences in expression between these transgenes could explain the lack of rescue by hTau. Importantly, our finding that the detrimental effects of expressing human Tau are ameliorated in the absence of endogenous PTL-1 suggests some functional conservation between Tau and PTL-1. Although these proteins do not have high similarity over the entire sequence, the imperfect tandem repeats in the C-terminal microtubule-binding domain that constitute the only region of homology between these proteins show high amino acid identity. Therefore, it is possible that the microtubule-binding functions of these proteins are responsible for their role in lifespan.

The *skn-1(zu67)* allele, which affects SKN-1a and SKN-1c, also results in a shortened lifespan (Bishop and Guarente, 2007). In this report, we have shown that *ptl-1(ok621);skn-1(zu67)* double mutant animals are neither shorter- nor longer-lived compared to single *ptl-1* or *skn-1* mutant animals, and these strains are all short-lived compared with wild-type. This suggests that the regulation of longevity by PTL-1 or SKN-1 may involve similar processes. Curiously, the *skn-1(zu135)* allele that affects all three SKN-1 isoforms does not significantly affect lifespan (Bishop and Guarente, 2007), suggesting that interactions between SKN-1a/c and SKN-1b isoforms regulate longevity. We did not test if a *ptl-1* null mutation would affect the lifespan of *skn-1(zu135)* animals.

Factors that influence the stress response are often also involved in regulating longevity. This observation appears to lend support to the "free radical/oxidative stress" theory of ageing, which suggests that a chronic build-up of free radical metabolites results in tissue damage and senescence (reviewed in (Buffenstein et al., 2008, Gemma et al., 2007, Sanz and Stefanatos, 2008)). Although this theory has since been widely challenged, there is a general agreement that the ability to tolerate oxidative stress is linked to longevity. SKN-1 in *C. elegans*, like its mammalian Nrf2 counterpart, regulates both stress tolerance and ageing, and has also been shown to be involved in mediating a physiological process that is impaired with ageing (Naidoo et al., 2008), the unfolded protein response (UPR) (Glover-Cutter et al., 2013). Given that Tau pathology in AD models has also been linked to oxidative stress, our findings provide an interesting avenue for further investigation into the role of a Tau-like protein in stress tolerance and longevity.

Chapter 5: PTL-1 regulates ageing of the nervous system

5.1 Introduction

In the previous chapter, we demonstrated the involvement of PTL-1 in the stress response and longevity. Given the close relationship between stress tolerance, lifespan and tissue ageing, as well as the involvement of the mammalian homologue Tau in age-related neurodegeneration, we proceeded to investigate if PTL-1 was involved in ageing of the nervous system. We based our experimental approach on recent publications detailing the subtle parameters of cell body branching, axon blebbing or axon branching in touch receptor neurons or ventral nerve cord GABAergic neurons (Tank et al., 2011, Pan et al., 2011, Toth et al., 2012). In addition, we investigated if the phenotypes observed in *ptl-1* mutant animals could be rescued by re-expression of PTL-1 or human Tau.

5.2The **ptl-1(ok621)** *and* **ptl-1(tm543)** *mutant strains show a high frequency of abnormal neuronal structures in touch receptor neurons in early adulthood*

Previous investigations have demonstrated that *C. elegans* adult animals develop structural abnormalities with age in neurons such as the TRNs, which include branching along the cell body or axon, and blebbing along the axon (Tank et al., 2011, Pan et al., 2011, Toth et al., 2012), as detailed in **Chapter 1**. In the first instance, we grouped all these structural defects into a single category and scored animals that displayed any of these defects as positive. We studied the appearance of abnormal neuronal structures in wild-type and *ptl-1(ok621)* null mutant animals by imaging the ALM touch neuron in individual worms until the animals died (longitudinal experiment) (**Figure 5.1**). By assaying 15 worms of each genotype every day over their entire lifespan, we observed a progressive phenotype as previously reported, where wild-type neurons accumulated branching and blebbing structures with age (**Figure 5.1A**).

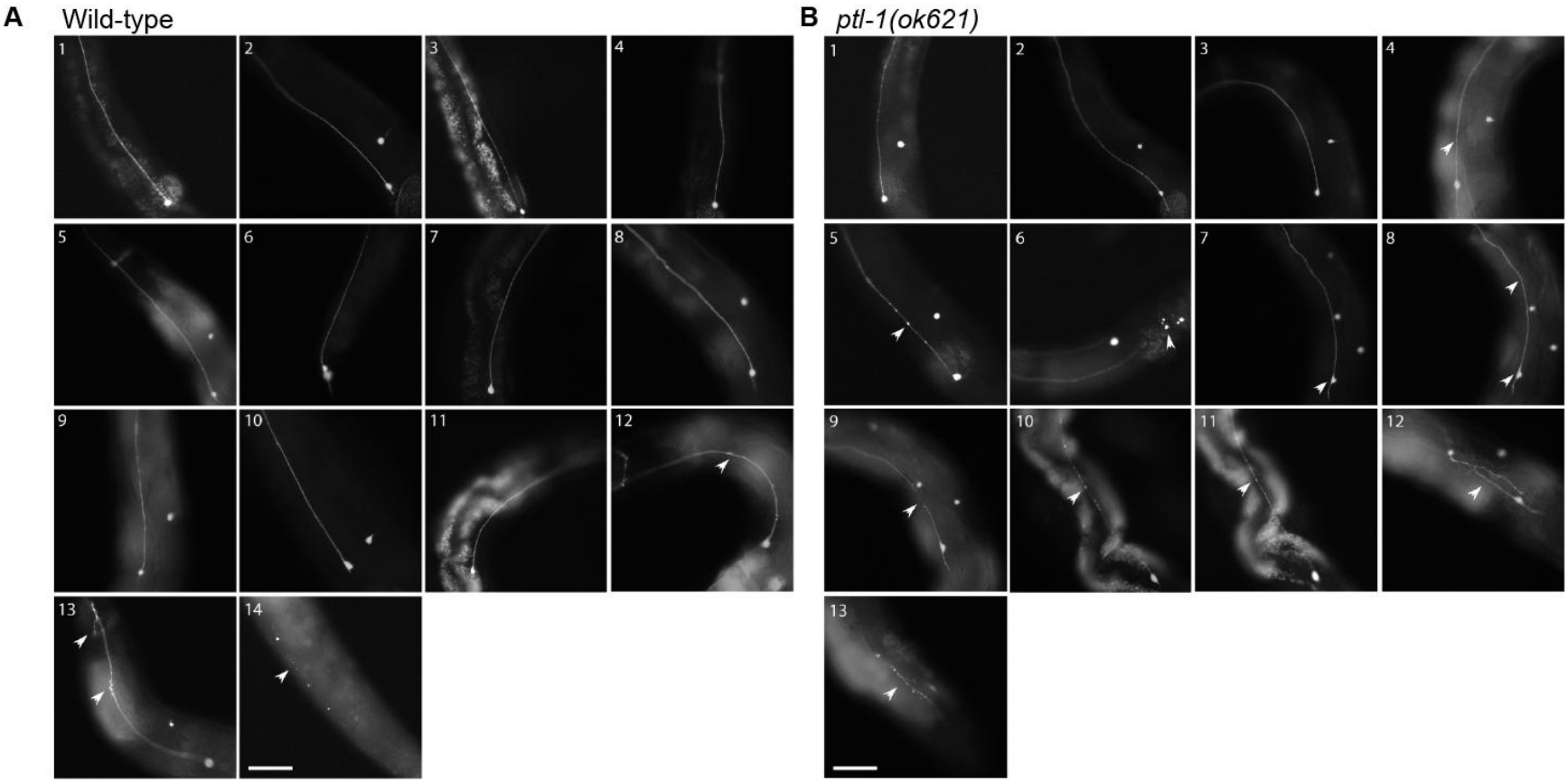

Figure 5.1: Imaging worms every day until death reveals that *ptl-1(ok621)* mutant animals display a higher frequency of abnormal neuronal structures in touch neurons compared with wild-type. Anterior touch receptor neuron imaging assay for individual animals, showing the neuron of a representative **A)** wild-type, and **B)** *ptl-1(ok621)* worm. Neurons were visualised using the P*mec-4*::*gfp (zdIs5)* reporter. Worms were imaged every day until death. Arrowheads indicate the presence of structural defects such as cell body branching, axon blebbing and axon branching. Scale, 50 µm for all panels.

Interestingly, our data indicate that the accumulation of morphological changes is significantly accelerated in the touch receptor neurons in *ptl-1(ok621)* mutants (**Figure 5.1B**, **Figure 5.2**). **Figure 5.2A** highlights the differences between individual wild-type and *ptl-1(ok621)* animals at similar stages of adulthood. At day 7, the anterior touch neuron in a wild-type animal does not appear substantially different to the same neuron at day 1, however, in the *ptl-1(ok621)* mutant animal, the ALM neuron shows axon blebbing at day 5 that was not present at day 1 (indicated by arrowheads). We observed that the proportion of *ptl-1(ok621)* animals with neurons displaying abnormal structures reached 50% on day 4, compared with wild-type animals where this level was reached on day 8 (**Figure 5.2B**).

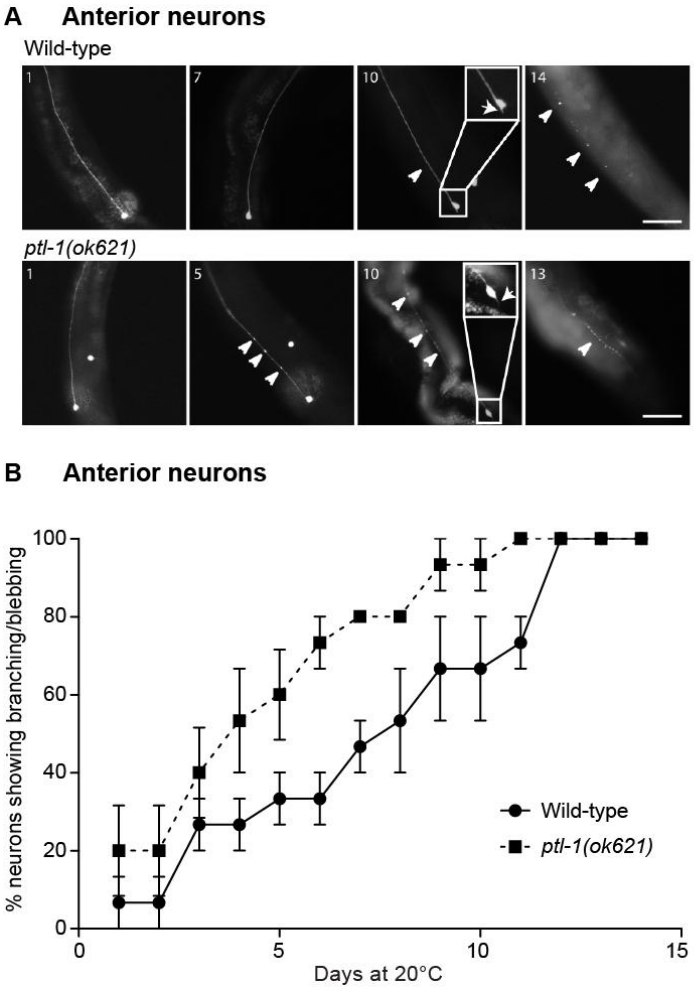

Figure 5.2: The *ptl-1(ok621)* mutant strain displays an accelerated onset of appearance of abnormal neuronal structures in ALM touch neurons. A) A representative animal is shown for each genotype (n =15 total). Neurons were visualised using the P*mec-4*::*gfp (zdIs5)* reporter. Worms were imaged every day until death. Representative time points are shown in this figure (from **Figure 5.1B**), with arrowheads indicating blebbing and arrows indicating branching phenotypes. Insets on day 10 show a close-up of the cell body for the respective animal. (Top) ALM neuron of a wild-type worm. The worm died on day 15. (Bottom) ALM neuron of a *ptl-1(ok621)* mutant worm. The worm died on day 14. Scale, 50 µm for all panels. Percentage of branching/blebbing observed in ALM neurons of the complete data set of wild-type and *ptl-1(ok621)* animals (n =15, or 5 animals in 3 biological replicates) assayed in a longitudinal experiment. Error bars indicate mean ± SEM. A paired t-test was applied to the mean percentage branching/blebbing observed in each strain at each time point (for all replicates) and the average of the entire curve compared; p value is <0.001.

To complement this experiment, we used a transverse approach, observing synchronised populations of wild-type and *ptl-1* mutant animals on alternate days from day 1 to 15 of adulthood (**Figure 5.3**). We included *ptl-1(tm543)* mutant animals in these assays to test if we could detect a neuronal ageing phenotype in this strain. Based on our previous experiments, we refined our scoring model in two ways: firstly, we recorded data for the touch receptor neurons at the anterior and posterior halves of the animal separately, as it became apparent that the posterior touch neurons accumulate branches and blebs at a much faster rate compared with the anterior touch neurons, showing a high incidence of these abnormal structures even in early adulthood (**Appendix 6, Figure 5.3A,B**). Additionally, since PTL-1 has not been detected in one of the three posterior touch neurons (PVM) (Goedert et al., 1996, Gordon et al., 2008), we analysed the morphology of PLM and PVM neurons separately (**Figure 5.3C**). Our second refinement for scoring was that for all strains tested, we separately scored for cell body branching, axon blebbing, and axon branching (**Figure 5.3A-C**).

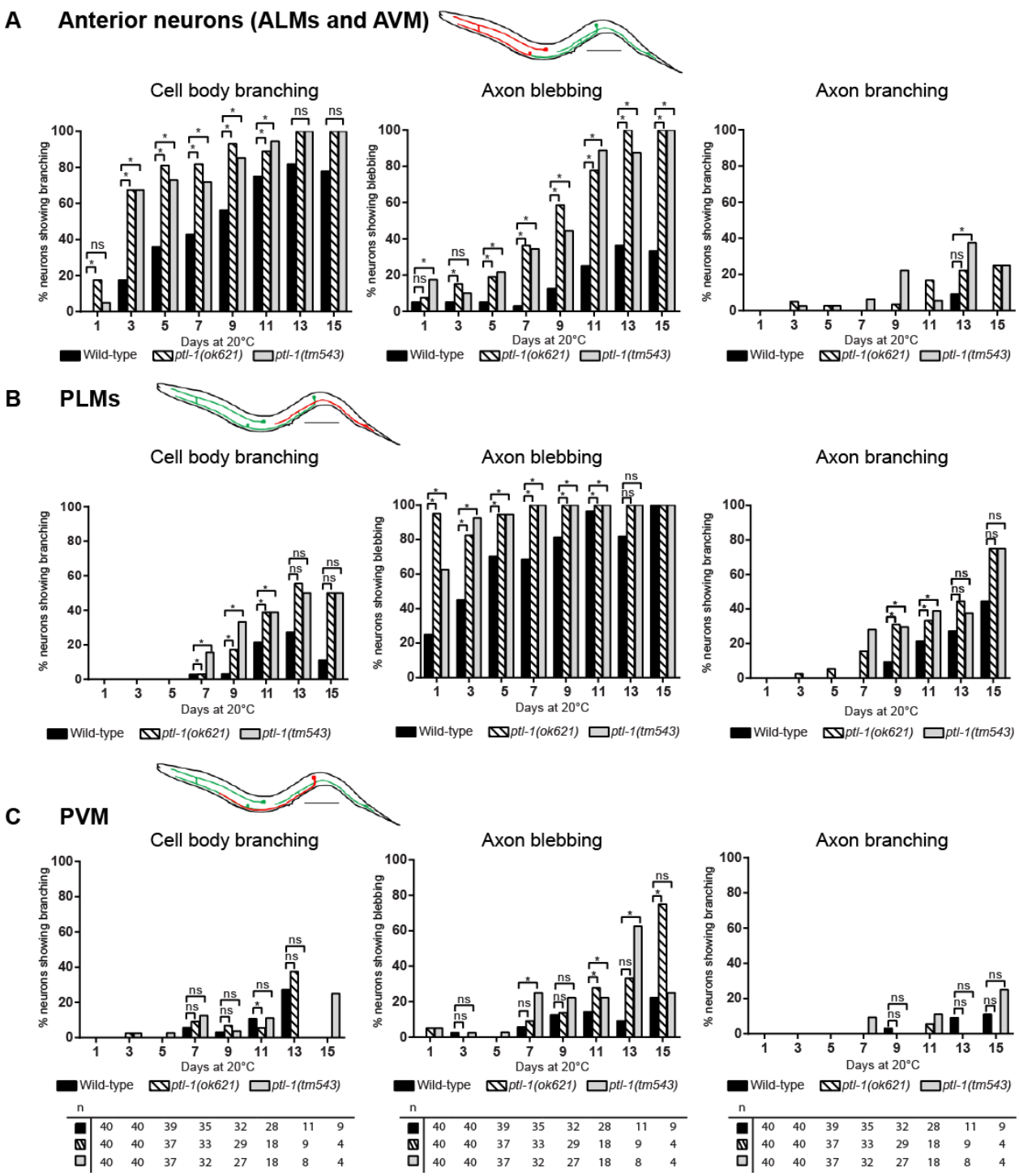

Figure 5.3: The *ptl-1(ok621)* and *ptl-1(tm543)* mutant strains display accelerated onset of appearance of abnormal neuronal structures in touch receptor neurons. Neurons were visualised using the P*mec-4*::*gfp (zdIs5)* reporter. The neuron(s) scored in panels A, B and C are highlighted in red, the remaining touch neurons in green. **A)** Anterior touch neurons, **B)** PLM neurons, and **C)** PVM neurons in wild-type and *ptl-1* mutants scored for cell body

branching, axon axon blebbing, and axon branching. Statistical analysis, χ^2 test for independence, p value indicated by ns = no significance, * <0.05. Sample sizes are indicated below graphs.

Consistent with earlier findings obtained by us and others (Pan et al., 2011, Tank et al., 2011, Toth et al., 2012), we found that wild-type animals accumulated structural abnormalities in neurons with age (**Figure 5.3**). In the anterior neurons of wild-type animals, these structural abnormalities occur in a particular order, with cell body branching occurring first, followed by axon blebbing and axon branching (**Figure 5.3A**). In contrast, in PLMs, a higher incidence of axon blebbing was observed in early adulthood, with cell body and axon branching occurring later in life. There was also a generally higher incidence of axon branching in PLMs compared with anterior neurons (**Figure 5.3B**). The PVMs of wild-type animals did not display a high incidence of any structural abnormalities in early to mid-adulthood (before day 9) (**Figure 5.3C**).

When we scored for cell body branching, axon blebbing and axon branching in *ptl-1* mutant animals in both anterior and posterior touch neurons, we observed a generally similar onset of abnormal structures with age as in wild-type animals (**Figure 5.3**). We also observed a higher incidence of abnormal structures in the *ptl-1(ok621)* null mutant compared with wild-type for anterior touch neurons and PLMs (**Figure 5.3A,B**). In addition, we found similar trends in the MBR-deficient *ptl-1(tm543)* strain. For anterior touch neurons, on day 5 of the assay we observed cell body branching in 81% of *ptl-1(ok621)* and 73% of *ptl-1(tm543)* animals assayed compared with 36% of wild-type controls. At the same time point, blebbing can be seen in 19% of *ptl-1(ok621)* and 22% of *ptl-1(tm543)* animals compared with 5% in wild-type controls, whereas axon branching is observed in 3% of both *ptl-1* mutant strains assayed compared with 0% of wild-type control animals (**Figure 5.3A**). We also observed similar trends in the PLMs,

where *ptl-1* mutant animals displayed a higher incidence of all three phenotypes compared with wild-type (**Figure 5.3B**). In the PVMs, although we observed at some time points a high incidence of structural abnormalities in both *ptl-1* mutant strains (for example, axon blebbing at days 13-15, where n<10), at time points before day 11 of adulthood there were generally no significant differences between *ptl-1* mutant animals and wild-type controls (**Figure 5.3C**). Our results suggest that the *ptl-1(tm543)* mutation could be hypomorphic, such that the protein product in this mutant is able to sustain wild-type levels of touch sensitivity (**Figure 3.3**), but is not sufficient to protect the organism from susceptibility to age-dependent loss of structural integrity.

Taken together, these observations demonstrate that PTL-1 is important in maintaining neuronal morphology in touch receptor neurons, as a complete loss of this protein or expression of a protein lacking the MBR domain results in a higher incidence of abnormal neuronal structures in younger animals. For subsequent assays on neuronal morphology, data are presented only for anterior touch receptor neurons as the percentage of animals showing abnormal structures in these neurons is low at early time points and is less variable compared with the same phenotype in posterior touch receptor neurons (**Appendix 6, Figure 5.3B**), making it easier to monitor changes in neuronal morphology with time.

5.3 The **ptl-1(ok621)** *and* **ptl-1(tm543)** *mutant strains show a high frequency of abnormal neuronal structures in GABAergic neurons in early adulthood*

We next investigated if these effects are specific for selected neuronal populations or whether they reflect a general consequence of perturbing PTL-1 function. To this end, we examined a

second neuronal cell type in which PTL-1 is also expressed (Gordon et al., 2008, McKay et al., 2003). Using a P*unc-47*::*gfp* reporter line, we visualised the 25 GABAergic neurons, which are located mainly in the ventral nerve cord, as well as in the head and the tail (McIntire et al., 1997). These neurons have commissures that project dorsally from the ventral side, and these commissures at times appear branched. Representative images of the branching phenotype in wild-type and *ptl-1(ok621)* animals are shown in **Figure 5.4A**. These branched commissures are observable in wild-type animals in early adulthood, and the incidence of these structures increases in late adulthood (day 13-15) (**Figure 5.4B**). We assayed this phenotype in *ptl-1* mutant animals and observed an accelerated accumulation of branching structures in both *ptl-1(ok621)* and *ptl-1(tm543)* animals compared with wild-type, when each *ptl-1* mutant strain was assayed separately (**Figure 5.4B**), or together (**Figure 5.4C**). In early to mid-adulthood, the GABAergic neurons do not appear to accumulate branching structures at substantially differing rates when comparing *ptl-1(ok621)* and *ptl-1(tm543)* mutant strains (**Figure 5.4C**). In particular at day 5, 68% of *ptl-1(ok621)* and 64% of *ptl-1(tm543)* animals displayed branching phenotypes compared with 41% in wild-type controls (**Figure 5.4C**).

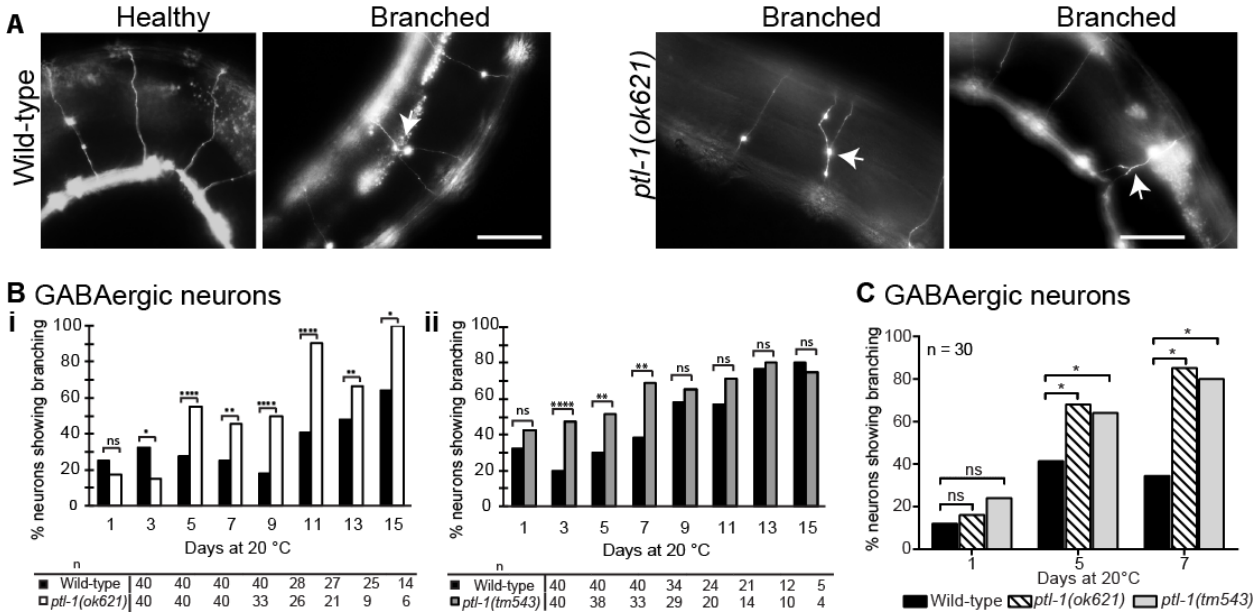

Figure 5.4: The *ptl-1(ok621)* and *ptl-1(tm543)* mutant strains show defects in maintaining neuronal integrity with age in GABAergic neurons. Neurons were visualised using the P*unc-47*::*gfp (oxIs12)* reporter. **A)** A representative image of the phenotype scored in GABAergic neurons, showing healthy neurons and a branched commissure in wild-type, and representative images of branched commissures in *ptl-1(ok621)* worms. Arrows indicate branching. Scale, 50 µm. **B)** The incidence of branching in GABAergic neurons for *ptl-1* mutant strains where each assay was conducted separately for each mutant. **C)** The incidence of branching in GABAergic neurons for *ptl-1* mutant strains where both mutants were assayed in the same experiment.

In conclusion, *ptl-1* mutant strains also display defects in a neuronal subtype other than touch receptor neurons, suggesting that PTL-1 has a broader role in the maintenance of neuronal structural integrity.

5.4 Functional consequences of mutations in ptl-1

We next tested if loss of fully functional PTL-1 could affect the functionality of GABAergic motor neurons. The drug levamisole has been widely used to pharmacologically determine if *C. elegans* strains are defective in motor neuron activity, which requires cholinergic transmission.

Acetylcholine is an excitatory neurotransmitter at neuromuscular junctions (Richmond and Jorgensen, 1999). Once synthesised, acetylcholine is loaded onto synaptic vesicles and is transported into the synaptic cleft. It then binds to and activates acetylcholine receptors that are usually on post-synaptic sites, is enzymatically hydrolysed and the resulting choline then transported back into the pre-synaptic cell to be recycled (reviewed in (Rand, 2007)). A cholinergic agonist, levamisole results in hypercontracted paralysis in wild-type animals, followed by relaxation and death. Resistance to levamisole is therefore associated with defective cholinergic signalling (Lewis et al., 1980). We found that *ptl-1* mutant strains show significantly lower sensitivity to levamisole compared with wild-type controls at early and mid-adulthood, with the *ptl-1(tm543)* strain appearing to have lower sensitivity compared with *ptl-1(ok621)* (**Figure 5.5**). This suggests that *ptl-1* mutant animals are defective in cholinergic transmission. Additionally, if graphs from day 1 to day 7 were compared (**not shown**), we observed a substantial decrease in levamisole sensitivity for both *ptl-1* mutant strains between day 1 and day 7, which correlates with the higher incidence of branching commissures in GABAergic neurons at later time points (**Figure 5.4C**).

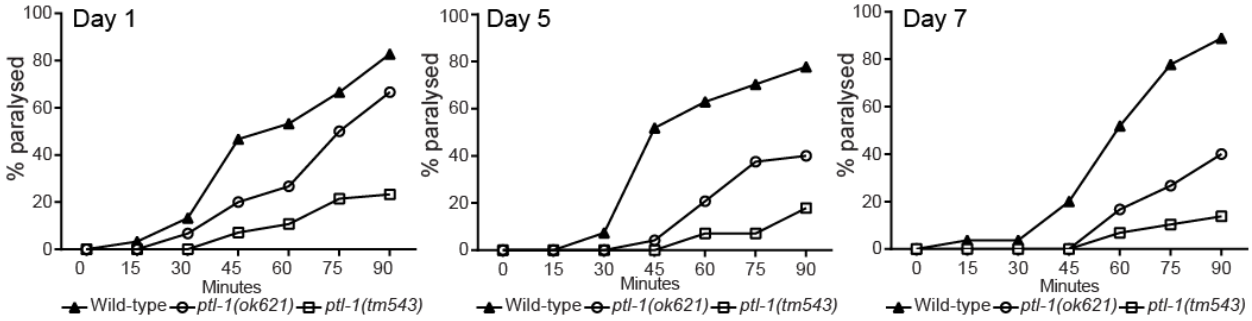

Figure 5.5: The *ptl-1(ok621)* and *ptl-1(tm543)* mutant strains display allelic differences in levamisole sensitivity. Assay for paralysis after levamisole exposure. Worms were scored for paralysis over 90 minutes on drug plates on day 1, 5 and 7 of adulthood (n = 30 per strain, per time point). Statistical analysis, one-way ANOVA; *ptl-*

1(ok621) and *ptl-1(tm543)* mutant strains, but not wild-type controls, show significant decreases in drug sensitivity between day 1 and day 7 (p value <0.05) when all graphs are combined.

The six mechanosensory touch receptor neurons regulate the response of worms to gentle touch (Chalfie and Sulston, 1981). We showed in **Chapter 3** that we could confirm the mild touch insensitive phenotype of *ptl-1(ok621)* animals as previously demonstrated (Gordon et al., 2008), and in addition that *ptl-1(tm543)* animals did not display a resolvable touch insensitive phenotype (**Figure 3.3**) at day one of adulthood. We observed a progressive accumulation of abnormal neuronal structures in the touch neurons with age in *ptl-1* mutants (**Figure 5.3**); however, we could not reliably assay for touch sensitivity in late adulthood, as animals become considerably less motile with age (Huang et al., 2004), making it difficult to score positive responses defined as "movement away from touch" when body movement is poor in aged animals (Chalfie and Sulston, 1981). This prevented us from conducting an analogous experiment in the touch neurons to the levamisole assay described above to monitor GABAergic motor neuron functionality with age. Interestingly, others have described that touch sensitivity appears to decline in day 10 adult wild-type animals, which have relatively high levels of touch neuron branching (Tank et al., 2011).

5.5 Re-expression of PTL-1 but not human Tau rescues defects observed in **ptl-1** *null mutant animals*

To confirm that the neuronal ageing phenotypes found in *ptl-1* mutant worms are attributable to the loss of PTL-1 function, we tested if re-expressing PTL-1 in the *ptl-1(ok621)* mutant strain could rescue these phenotypes. We described the transgenic line where PTL-1::V5 is expressed under the regulation of a *ptl-1* promoter and 3′ UTR in **Chapter 4**, and refer to this as "PTL-1

Tg" followed by "*ptl-1(ok621)*" if it is in the *ptl-1* null mutant background. As in the earlier chapter, we chose to perform our rescue experiments in the *ptl-1(ok621)* background only. We also assayed the touch receptor neurons only and not the GABAergic neurons as abnormal structures in the touch neurons become apparent in early to mid-adulthood (**Figure 5.3**) whereas GABAergic neuron branching tends to increase in incidence only later in life (**Figure 5.4**), meaning that it is easier to resolve differences in touch neuron ageing.

We crossed PTL-1 Tg worms with both the *ptl-1(ok621)* mutant strain and the P*mec-4*::*gfp* reporter line, and assayed for age-related morphological changes in touch receptor neurons as previously described. For simplicity, we pooled all age-related defects (cell body branching, axon blebbing, and axon branching) into a single category and scored worms that displayed any of these phenotypes as positive. We found that re-expressing PTL-1 in *ptl-1(ok621)* animals appeared to delay the accumulation of abnormal neuronal structures to almost wild-type levels (**Figure 5.6A**), such that when these animals were assayed from day 5 onwards, the proportion of animals showing these phenotypes in anterior touch neurons was not significantly different from wild-type. For example, at day 5 of this assay 20% of "PTL-1 Tg; *ptl-1(ok621)*" worms displayed abnormal structures in anterior touch neurons compared with 32% in wild-type. Thus we were able to rescue the accelerated accumulation of abnormal structures in touch neurons of *ptl-1(ok621)* mutants by re-expressing PTL-1 in these animals. Somewhat surprisingly, we also observed that animals expressing the PTL-1 transgene on a wild-type background accumulated branches and blebbing structures with increased frequency compared with non-transgenic wild-type controls (**Figure 5.6B**), and that these levels were comparable with that observed in the strain carrying only the *ptl-1(ok621)* mutation (**Figure 5.6C**). For example, at day 5 of this assay,

55% of "PTL-1 Tg; wild-type" worms displayed abnormal neuronal structures, compared with 32% in wild-type controls (**Figure 5.6B**). It therefore appears that modulation of PTL-1 levels by either a null mutation or increasing the gene copy number (by introducing copy(ies) of a PTL-1 transgene in addition to the endogenous gene locus) negatively affects neuronal integrity.

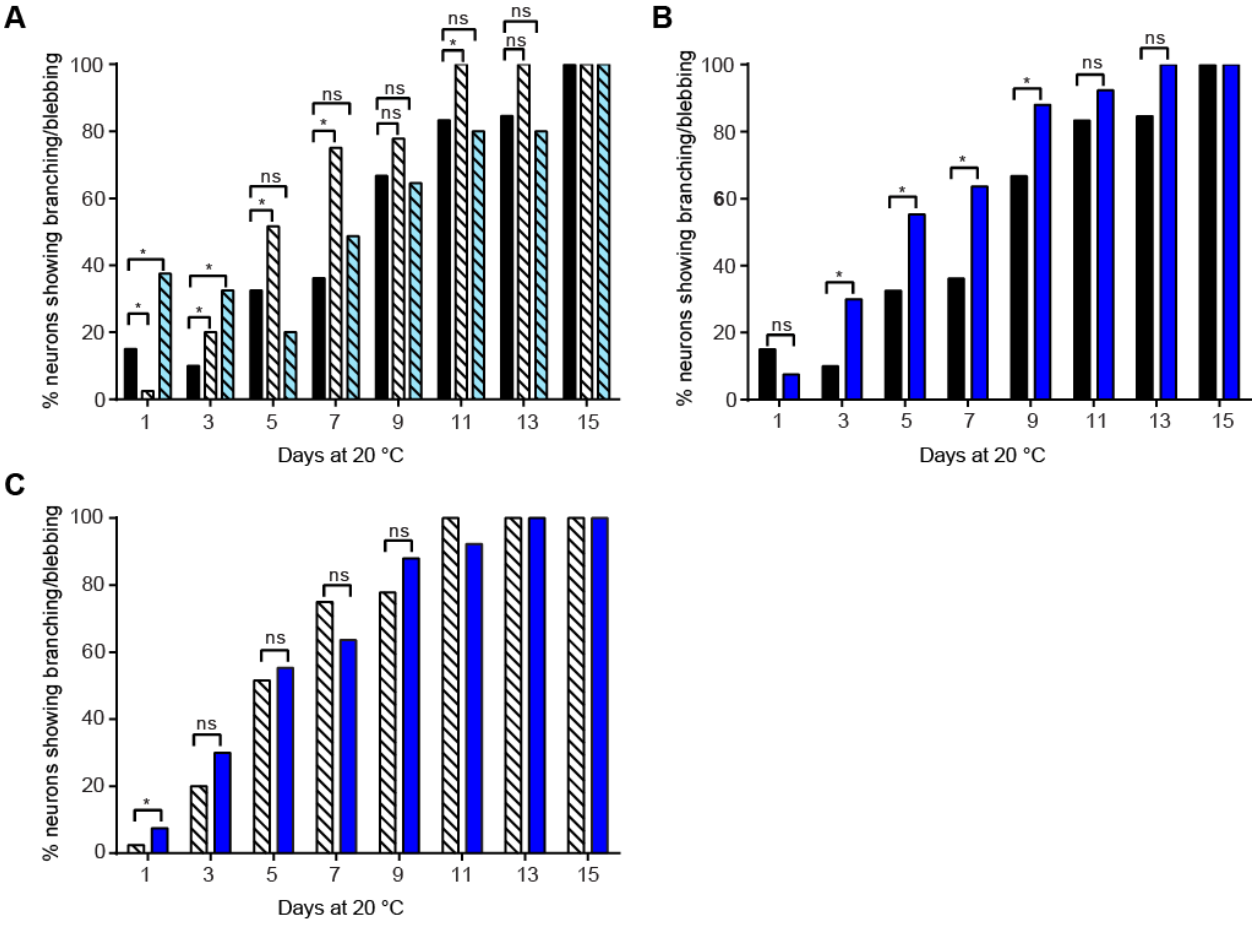

n	D1	D3	D5	D7	D9	D11	D13	D15
Wild-type	40	40	40	36	33	15	13	4
ptl-1 (ok621)	40	40	34	32	27	11	8	2
PTL-1 Tg; *ptl-1 (ok621)*	40	40	40	37	31	20	10	3
PTL-1 Tg; wild-type	40	40	38	33	25	13	8	3

Figure 5.6: Re-expression of PTL-1 rescues age-related abnormal neuron morphology and touch sensitivity in the *ptl-1(ok621)* mutant. 'PTL-1 Tg' refers to the PTL-1::V5 transgene, and the terms 'wild-type' and '*ptl-1(ok621)*' following this refer to the genotype at the genomic *ptl-1* locus, whether wild-type or *ok621* mutant respectively. **A)** Neuron imaging time course of PTL-1 transgenic worms, showing data for anterior touch receptor

neurons visualised using the P*mec-4*::*gfp (zdIs5)* reporter. **A)** shows control strains together with the PTL-1 Tg; *ptl-1(ok621)* rescue strain. **B)** shows the effect of the PTL-1 Tg alone, compared with wild-type controls. **C)** compares the PTL-1 Tg transgenic line with the *ptl-1(ok621)* mutant strain. Sample sizes are indicated below the graphs. The χ^2 test for independence was used to analyse differences between genotypes. p value is indicated by * < 0.05, ns = not significant. For statistical analysis in **C)**, the expected value is that observed for "*ptl-1(ok621)*". For all other graphs the expected value was that observed for wild-type.

Using the human Tau transgenic line detailed in **Chapter 4** (**Figure 4.4**), which expresses the longest isoform of human Tau (hTau40) under the regulation of the *ptl-1* promoter and 3′ UTR, we next investigated whether human Tau would rescue the defects observed in the *ptl-1* null mutant. We refer to this transgenic line as "hTau Tg" followed by "*ptl-1(ok621)*" if it is in the *ptl-1* null mutant background. We found that the frequency of abnormal structures observed in anterior touch receptor neurons in "hTau Tg; *ptl-1(ok621)*" is not significantly different compared with the non-transgenic *ptl-1* null mutant strain on days 3, 5, 7 and 9 of the assay (**Figure 5.7A**), indicating no robust rescue of the neuronal ageing phenotype. Interestingly, we observed that hTau expression in a wild-type background was detrimental to worms in terms of neuronal ageing, where these transgenic animals displayed a higher incidence of branching and blebbing phenotypes in anterior touch receptor neurons compared with non-transgenic wild-type worms at day 3, 5, 7 and 9 of the assay (**Figure 5.7B**). This observation reflects our earlier finding that "hTau Tg; wild-type" animals are short-lived compared with wild-type controls (**Chapter 4**). Our data are also consistent with previous reports indicating that wild-type hTau expression under the control of a pan-neuronal promoter results in defects in motility, cholinergic neuron transmission, and lifespan (Kraemer et al., 2003). It is notable that hTau transgenic lines reported in the study conducted by Kraemer *et al.* were generated by microinjection (Kraemer et

al., 2003), whereas the transgenic lines in our study were generated by biolistic transformation, which we would expect to introduce a lower transgene copy number than by microinjection, and hence a lower expected expression level (Praitis et al., 2001). Therefore it appears that wild-type hTau, even at a low expression level, is detrimental to *C. elegans* when expressed in addition to endogenous PTL-1.

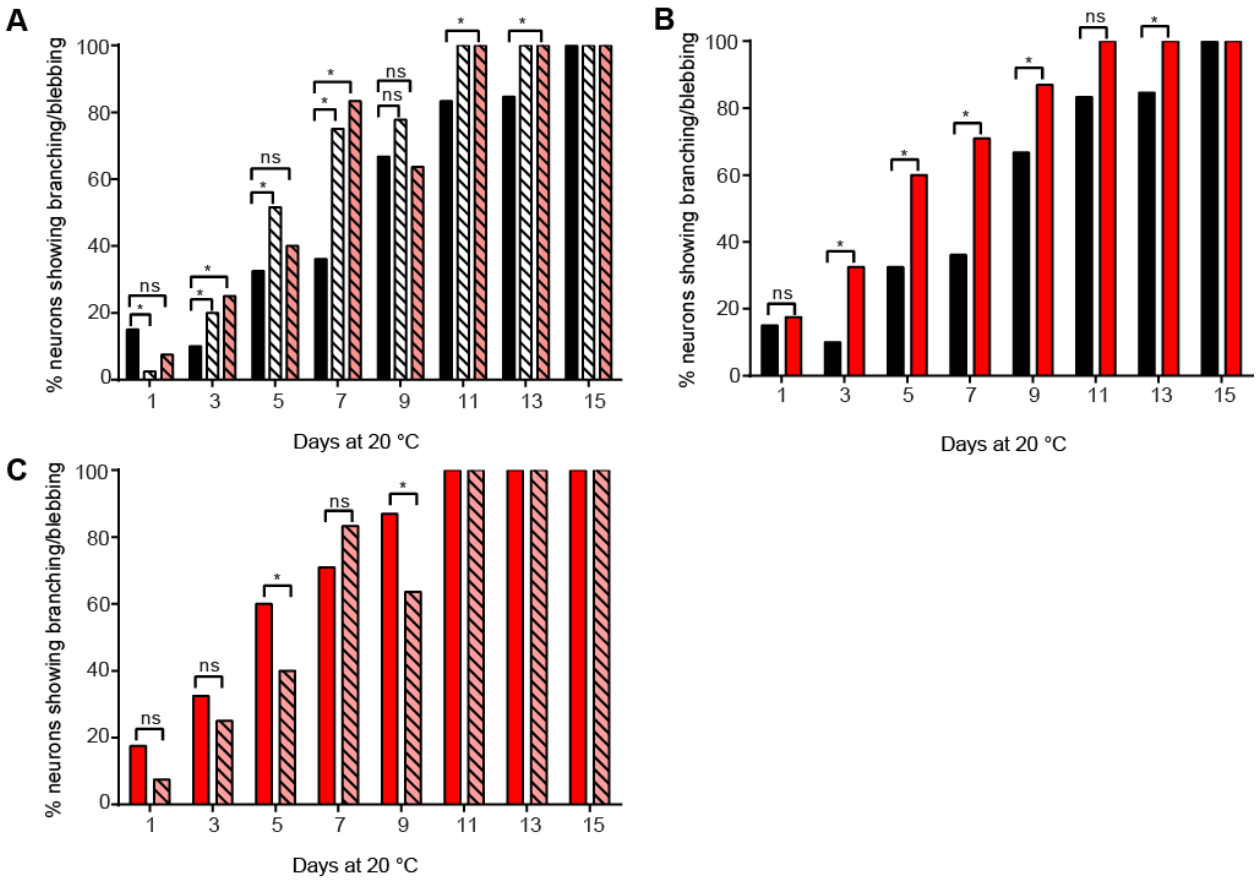

	D1	D3	D5	D7	D9	D11	D13	D15
Wild-type	40	40	40	36	33	15	13	4
ptl-1(ok621)	40	40	34	32	27	11	8	2
htau Tg; *ptl-1(ok621)*	40	40	35	24	22	4	5	1
htau Tg; wild-type	40	40	40	31	23	13	3	1

Figure 5.7: Expression of human Tau does not robustly rescue age-related abnormal neuron morphology in the *ptl-1(ok621)* mutant. Neuron imaging time course of hTau transgenic worms showing data for anterior touch receptor neurons visualised using the P*mec-4*::*gfp (zdIs5)* reporter. **A)** shows control strains together with the hTau

Tg; *ptl-1(ok621)* rescue strain. **B)** shows the effect of the hTau Tg alone, compared with wild-type controls. **C)** compares the hTau Tg lines in wild-type or *ptl-1(ok621)* backgrounds. Sample sizes are indicated below the graph. Control strains (wild-type and *ptl-1(ok621)*) are the same as those shown for the PTL-1 transgenics (**Figure 5.6**). The χ^2 test for independence was used to analyse differences between genotypes. p value is indicated by * < 0.05, ns = not significant. For statistical analysis in **C)**, the expected value is that observed for "hTau Tg; wild-type". For all other graphs the expected value was that observed for wild-type.

Curiously, comparing human Tau transgenic lines that are either wild-type or null for endogenous PTL-1 indicates that the presence of the *ptl-1(ok621)* null mutation improved some of the detrimental effects of human Tau expression. For example, we found that "hTau Tg; wild-type" animals showed a higher incidence of abnormal neuronal structures compared with the hTau Tg line in a *ptl-1* null mutant background at days 1, 3, 5 and 9 of the assay (**Figure 5.7C**). In particular, on day 5, the percentage of "hTau Tg; wild-type" worms displaying branching or blebbing was 60% (n=40), compared with 40% in "hTau Tg; *ptl-1(ok621)*" worms (n=35) and 32% in non-transgenic wild-type worms (n=40). These data suggest some degree of functional conservation between hTau and PTL-1.

We next investigated whether PTL-1 or human Tau re-expression could rescue the functional defects in touch sensitivity observed in *ptl-1(ok621)* mutant animals. We observed that PTL-1 transgenic animals are touch sensitive both in a wild-type and *ptl-1(ok621)* null mutant genetic background (**Figure 5.8A)**. In contrast, the expression of human Tau in the wild-type background resulted in reduced touch sensitivity but rescued touch responsiveness in the null mutant (**Figure 5.8B**). This finding indicates that human Tau cannot compensate for loss of PTL-1 in terms of protecting animals from premature neuronal ageing, but is able to rescue the

functional defect in touch neurons. Furthermore, expression of human Tau together with endogenous PTL-1 appears to be detrimental.

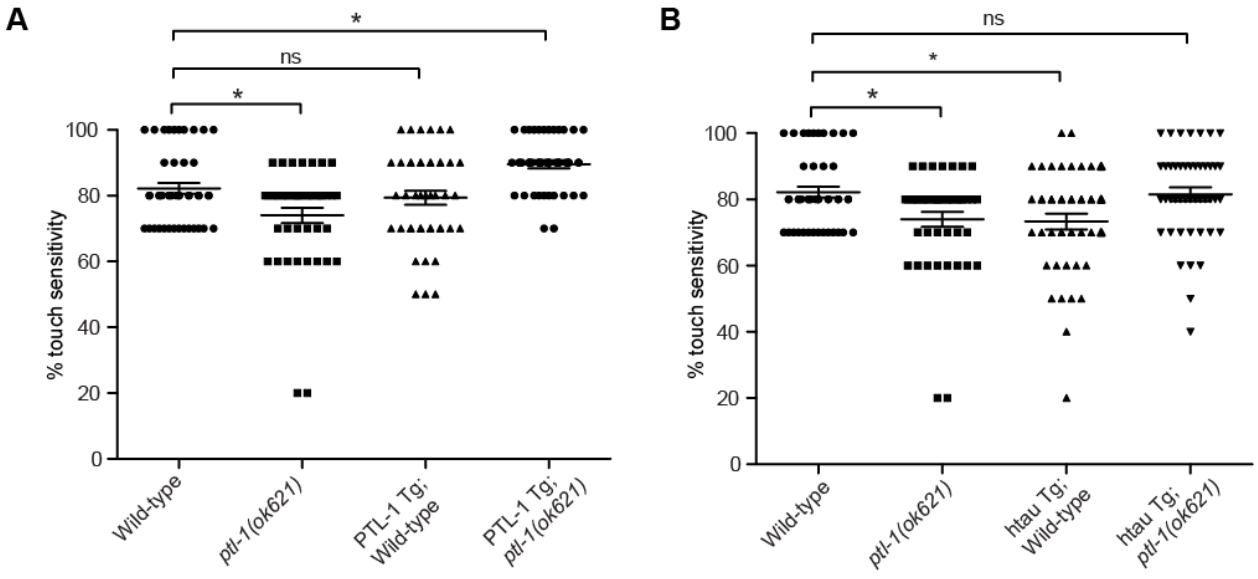

Figure 5.8: Re-expression of PTL-1 but not human Tau rescues touch insensitivity in the *ptl-1(ok621)* mutant. **A,B)** Data for sensitivity to gentle touch, shown for **A)** PTL-1 Tg and **B)** hTau Tg animals (n > 45 total for two biological replicates). Control strains are the same for panel **A** and **B**. Assays were conducted on one day-old adults. Error bars indicate mean ± SEM. One-way ANOVA, Bonferroni post-test, p value is indicated by ns = no significance, * <0.05.

5.6 Discussion

5.6.1. PTL-1 is important for the maintenance of neuronal integrity in C. elegans

In this chapter, we have shown that PTL-1 in *C. elegans* is involved in the age-associated preservation of neuronal structural integrity. Moreover, we observed that the severity of phenotypes observed in human Tau transgenic worms is dependent on the presence or absence of endogenous PTL-1, suggesting some functional conservation between these proteins.

We analysed two *ptl-1* mutant strains in the context of neuronal ageing, the null mutant *ptl-1(ok621)* (Gordon et al., 2008), and *ptl-1(tm543),* which putatively generates a protein product containing only the N-terminal region. Analysis of these mutant strains allowed us not only to investigate the role of PTL-1 in vivo, but also to dissociate functions of PTL-1 that are attributable solely to microtubule-binding from functions of the full-length protein. We found that both mutants of *ptl-1* show a decreased capacity to maintain neuronal integrity with age, as evidenced by a higher frequency of abnormal morphological structures such as branching and blebbing in touch receptor and GABAergic motor neurons in early adulthood compared with wild-type. Interestingly, this effect was also observed when we increased the copy number of full-length PTL-1 by expression of a stable transgene in addition to the endogenous locus. Therefore, correct gene dosage of PTL-1 is critical for the maintenance of neuronal structures with age, as either increasing or decreasing this level is detrimental to the organism. This is consistent with previous investigations showing that transgenic lines generated by microinjection that over-express PTL-1 display a dumpy phenotype and show morphological abnormalities in neurons (Tien et al., 2011). In addition when we assayed touch sensitivity, a response that requires functional touch receptor neurons, we found that the *ptl-1(ok621)* null mutant is less

responsive to gentle touch compared with wild-type, but that there was no difference in touch sensitivity from wild-type in the *ptl-1(tm543)* mutant lacking the MBR domain, suggesting that this allele may be hypomorphic, or that the N-terminal region may have functions that are sufficient to maintain touch sensitivity (**Figure 3.3**). Interestingly, we observed the opposite effect when assaying for defects in cholinergic/GABAergic transmission, with *ptl-1(tm543)* animals displaying a more severe phenotype compared with *ptl-1(ok621).* Importantly, our data indicate that although the microtubule-binding functions of PTL-1 are not necessary for wild-type touch sensitivity, the maintenance of touch neuron structural integrity with age requires full length PTL-1. Our findings also demonstrate that wild-type functioning of neurons may not be sufficient to preserve neuronal health with age. Another *C. elegans* MAP that is expressed in touch receptor neurons is the EMAP-like protein or ELP-1, which does not display high sequence similarity to PTL-1 but also regulates touch sensitivity (Hueston et al., 2008). In light of this, allelic differences in touch sensitivity observed between *ptl-1* mutants could be due to a requirement for both ELP-1 and the N-terminus of PTL-1 for wild-type touch responsiveness. A role of ELP-1 in neuronal ageing, however, remains to be investigated.

PTL-1 is largely enriched in neurons, particularly five of the six touch receptor neurons (the ALMs, AVM, and the PLMs) (Goedert et al., 1996, Gordon et al., 2008). We demonstrated that in these five neurons, loss or mutation in PTL-1 increased the incidence of structural defects in younger adults compared with wild-type, suggesting an accelerated rate of neuronal ageing. We also tested the rate of ageing in a neuron in which PTL-1 is thought not to be expressed. Within the limits of detection, PTL-1 has not been detected in PVM neurons (Gordon et al., 2008, Goedert et al., 1996). We observed a progressive accumulation of structural defects in PVM with

age in all strains, although there was overall no significant difference between the incidence of branching and/or blebbing between *ptl-1* mutant strains and wild-type, even at advanced age. This may be due to:

1) PTL-1 not being expressed in PVM, therefore this neuron does not display accelerated structural defects with aging in *ptl-1* mutants compared with wild-type controls. We acknowledge that at very late time points i.e. day 13 and 15, it appears that there is significantly more blebbing observed in PVM in *ptl-1* mutants compared with wild-type (**Figure 5.3C**), however, at this time point there are very few mutant animals still alive (n= ~4), making these results less statistically reliable.
2) PVM being inherently less susceptible to the formation of abnormal structures. We and others (Toth et al., 2012) have found that in wild-type animals the incidence of abnormal structures in PVM is much lower than observed in the other touch neurons, meaning that it is more difficult to resolve differences (if any) between strains.

Our data indicate that PTL-1 has biological functions in regulating both ageing in neurons and ageing in the whole organism (**Chapter 4**, **Section 4.1**). Does PTL-1 exert these effects from the nervous system alone, or from non-neuronal tissues? In adult worms, it appears that PTL-1 is enriched in neurons (Goedert et al., 1996, Gordon et al., 2008) (**Figure 4.6**). Previous studies have also established a role for PTL-1 specifically in touch neurons, in particular with respect to mechanosensation (Gordon et al., 2008) and microtubule-based transport (Tien et al., 2011). With regards to the role of PTL-1 in regulating organismal lifespan, previous studies have suggested that signalling events in neurons alone are sufficient to alter lifespan (Apfeld and Kenyon, 1999, Alcedo and Kenyon, 2004). If neuronal functions of PTL-1 regulate whole

organism lifespan, it remains to be determined whether this refers to a role in all neurons or in a particular subset of neurons. Ablation of sensory neurons such as thermosensory neurons (Lee and Kenyon, 2009) or gustatory and olfactory neurons (Alcedo and Kenyon, 2004) in *C. elegans* results in a shortening or extension of lifespan, respectively. In addition, *C. elegans* mutants defective in sensory cilia in some neurons have been shown to be long-lived (Apfeld and Kenyon, 1999). Studies performed using several mechanosensory defective (*mec*) mutants predominantly affecting touch receptor neurons, such as *mec-1, mec-8* and *mec-12*, have also demonstrated differences in lifespan compared with wild-type (Apfeld and Kenyon, 1999, Pan et al., 2011). As PTL-1 is expressed in most, if not all, neurons in the worm, the reduced lifespan of *ptl-1* mutants may be due to the loss of PTL-1 function in one or more of these neuronal subsets.

5.6.2 Tau and PTL-1 display some functional conservation in the regulation of neuronal ageing and longevity

We observed in terms of longevity and neuronal ageing, that (1) human Tau expression is detrimental to worms, (2) human Tau does not robustly rescue for loss of PTL-1, and (3) touch sensitivity, neuronal structural health and lifespan phenotypes of human Tau transgenic lines are dependent on PTL-1. The negative effect of expressing human Tau in *C. elegans*, as also observed in (Kraemer et al., 2003, Brandt et al., 2009, Miyasaka et al., 2005), may be due to over-expression of any MAP having a detrimental effect. Or, this could be due to a specific axonal role of Tau that evolved with the diversification of neuronal MAPs into mainly axon-localised Tau and mainly dendrite-localised MAP2. In addition to some shared functions (Sontag et al., 2012), Tau and MAP2 play specific roles in their distinct subcellular compartments (Kosik and Finch, 1987, Hirokawa et al., 1996, Chen et al., 1992, Harada et al., 1994). In *C. elegans*, no

such diversification of neuronal MAPs exists, and as PTL-1 is a homolog of both MAP2 and Tau, it presumably has both axon- and dendrite-specific functions. Therefore, the axon-specific effects of human Tau could negatively affect the worm when Tau is present in addition to endogenous PTL-1, and could also be insufficient to rescue for the loss of PTL-1 in a null mutant with regards to neuronal and whole organismal ageing.

Our observation that human Tau rescues touch insensitivity in a *ptl-1* null mutant, together with the finding that the detrimental effects of expressing Tau are ameliorated in the absence of endogenous PTL-1, suggests some functional conservation between Tau and PTL-1. Although these proteins do not have high similarity over the entire sequence, the imperfect tandem repeats in the C-terminal microtubule-binding domain that constitute the only region of homology between these proteins show high amino acid identity. Therefore, these conserved functions may be those attributable to the microtubule-binding capacity of Tau and PTL-1.

Chapter 6:
Regulation of neuronal ageing by PTL-1 is cell autonomous

6.1 Introduction

In previous chapters, we demonstrated that PTL-1 is involved in the regulation of neuronal ageing and longevity. Here, we extended our investigation into the role of PTL-1 in maintaining the structural integrity of neurons with age by conducting neuron-specific re-expression and knockdown experiments. By investigating neuronal ageing in animals where PTL-1 is either present or knocked down in only one neuronal cell-type, we can test if the regulation of neuronal integrity by PTL-1 is cell autonomous. We chose the touch neurons as our model for this purpose, as (i) PTL-1 is most highly expressed in these neurons, implying that it has a particular physiological role in these cells, (ii) we have developed a robust and comprehensive scoring protocol for age-related structural abnormalities in the touch neurons, and (iii) we have shown that abnormal neuronal structures become apparent in early to mid-adulthood in *ptl-1* mutant animals, making it easier to resolve differences between strains.

6.2 PTL-1 is expressed in neuronal and non-neuronal tissues

Previously, we demonstrated that re-expressing PTL-1 under the regulation of its endogenous promoter is sufficient to rescue both neuronal ageing and lifespan phenotypes observed in *ptl-1* null mutant animals (**Chapter 4 and 5**)(Chew et al., 2013). Immunohistochemistry experiments using a PTL-1-specific antibody detected expression only in touch neurons (Goedert et al., 1996), however a transcriptional reporter expressing GFP under the control of a *ptl-1* promoter showed expression in touch neurons as well as in many other neuronal subtypes including in the nerve ring and ventral cord, suggesting a more widespread expression of PTL-1 (Gordon et al., 2008, McKay et al., 2003). Further analysis using this transcriptional reporter showed that PTL-1 expression is indeed not restricted to neurons (Gordon et al., 2008, Goedert et al., 1996); it is also

expressed in non-neuronal tissues including vulval cells and stomatointestinal muscle (Gordon et al., 2008). As described in **Chapter 4 (Figure 4.6)**, we generated a translational fusion reporter line that expresses PTL-1 fused to GFP at the C-terminus under the control of the *ptl-1* promoter together with an *unc-54* 3′ UTR element for transcript stability. Although our fusion construct is transcribed using the same regulatory elements as the aforementioned transcriptional reporter (McKay et al., 2003), the PTL-1::GFP fusion would localise to particular subcellular sites where PTL-1 protein would be found, in contrast to the transcriptional reporter where GFP is distributed throughout the entire cells of those tissues where the *ptl-1* promoter drives expression. By using this PTL-1::GFP translational fusion reporter, we confirmed the expression pattern detailed previously (**Figure 4.6**) and showed that in neurons, PTL-1 localisation is largely cytoplasmic and not nuclear (**Figure 4.6v,vii**). Given that PTL-1 appears to regulate both neuronal ageing and whole organismal ageing, we aimed to identify if these processes required PTL-1 in the nervous system and/or in non-neuronal tissues.

6.3 Premature ageing of touch neurons in **ptl-1** *null mutant animals can be rescued by pan-neuronal re-expression of PTL-1*

In **Chapter 4**, we described the generation of the pan-neuronal transgenic line ("Pan-neuronal Tg"), which contains a transgene expressing PTL-1::V5 under the regulation of an *aex-3* promoter together with a *ptl-1* 3′ UTR. We tested whether this transgene would be able to rescue neuronal ageing in a *ptl-1* null mutant strain. As previously described (Chew et al., 2013, Tank et al., 2011, Pan et al., 2011, Toth et al., 2012), young touch neurons have straight axons and a round, unbranched cell body, whilst older neurons display cell body branching, axon blebbing and axon branching. We scored for these ageing phenotypes in anterior touch neurons at 20 °C

using the P*mec-4*::*gfp (zdIs5)* reporter. In our previous experiments (**Chapter 5**), we had assayed animals until day 15. In general, we observed differences between wild-type and mutant strains only up to day 9, as after this time point a high proportion of wild-type animals also accumulated structural abnormalities in ageing neurons. Additionally, the short lifespan of *ptl-1* mutant animals meant that at and after day 11, the sample size of these mutant strains was low (n<10 at day 15), making it more difficult to generate statistically meaningful data. For these reasons, for the remaining neuronal imaging experiments at 20 °C, we elected to assay animals on days 1, 5, 7 and 9 of adulthood.

Re-expression of PTL-1 in all neurons in the *ptl-1* null mutant background ("Pan-neuronal Tg; *ptl-1(ok621)*") was able to fully rescue the premature incidence of neuronal branching and blebbing seen in *ptl-1(ok621)* animals at 20 °C (**Figure 6.1A**). Specifically, 14% of wild-type worms on day 5 of adulthood displayed cell body branching in the anterior touch neurons compared with 29% of *ptl-1(ok621)* animals and 8% of "Pan-neuronal Tg; *ptl-1(ok621)*" animals (**Figure 6.1Ai**). In addition, we observed the same trends when the experiment was repeated at 25 °C on days 1, 3, and 5 of adulthood (**Figure 6.1B**). We tested for neuronal ageing at the higher temperature because lifespan experiments shown in **Chapter 4 (Section 4.2)** were conducted at 25 °C, and given the substantial effect that temperature can have on ageing in *C. elegans*, a direct comparison between these phenotypes can only be made if the experiments were conducted at the same temperature. Our results using the pan-neuronal transgenic line indicate that PTL-1 acts within neurons to regulate neuronal ageing.

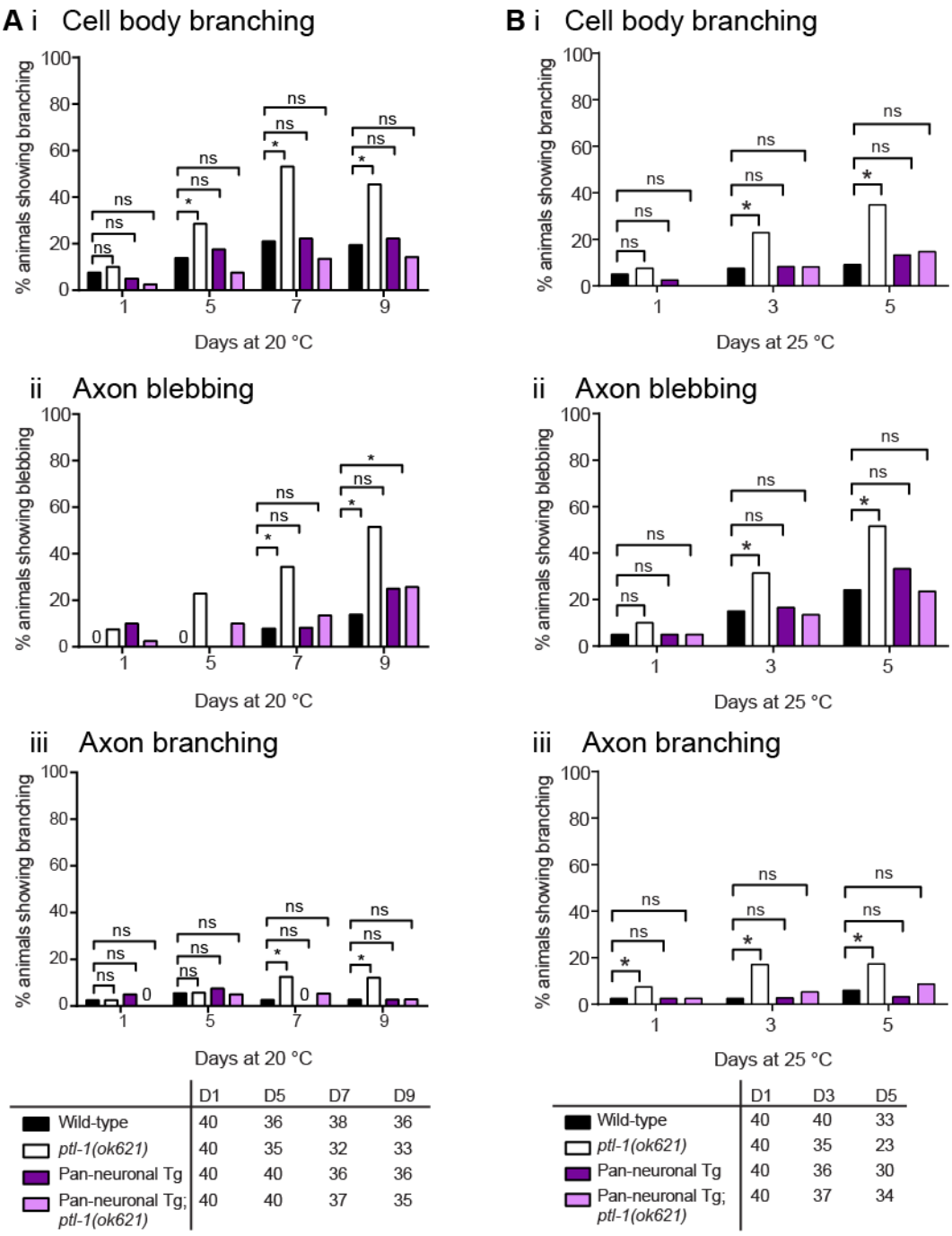

	D1	D5	D7	D9
Wild-type	40	36	38	36
ptl-1(ok621)	40	35	32	33
Pan-neuronal Tg	40	40	36	36
Pan-neuronal Tg; *ptl-1(ok621)*	40	40	37	35

	D1	D3	D5
Wild-type	40	40	33
ptl-1(ok621)	40	35	23
Pan-neuronal Tg	40	36	30
Pan-neuronal Tg; *ptl-1(ok621)*	40	37	34

Figure 6.1: Pan-neuronal re-expression of PTL-1 rescues the neuronal ageing phenotype in touch neurons that is observed in the *ptl-1(ok621)* null mutant. The touch neurons were visualised using the P*mec-4*::*gfp (zdIs5)* reporter construct. The presence of the *ptl-1(ok621)* null mutation in the genetic background of each transgenic line is indicated by the addition of "*ptl-1(ok621)"* in the strain name. Neuron imaging assay conducted at **A)** 20 °C or **B)** 25 °C for pan-neuronal transgenic worms ("Pan-neuronal Tg") showing (i) cell body branching, (ii) axon blebbing,

and (iii) axon branching. The sample size for each strain at each time point is given in the table underneath the graphs. The χ-squared statistical test was used to determine statistical significance. P-value is indicated by ns = not significant, *<0.05. Experiments were conducted twice independently, and the representative data shown are from one experiment. Data from the second independent experiment are shown in **Appendix 7.**

6.4 Premature ageing of GABAergic neurons in **ptl-1** *null mutant animals can be rescued by pan-neuronal re-expression of PTL-1*

We tested if rescue of the neuronal ageing phenotype in the touch neurons with pan-neuronal re-expression of PTL-1 could be observed in another neuronal subset, the GABAergic neurons. We visualised GABAergic neuron branching at 20 °C on days 1, 5, 7 and 9 of adulthood using the P*unc-47*::*gfp (oxIs12)* reporter. As noted previously (Toth et al., 2012, Pan et al., 2011, Tank et al., 2011, Chew et al., 2013), GABAergic neurons in young animals show only a low incidence of branching in the dorsally-projecting commissures, which are often branched in older adults. We found that re-expressing PTL-1 in all neurons in the *ptl-1* null mutant background completely rescued premature neuronal ageing observed in *ptl-1(ok621)* mutant animals (**Figure 6.2A**). For example, at day 5 of adulthood, 10% of wild-type animals displayed branching along the commissures of GABAergic neurons, compared with 36% of *ptl-1(ok621)* animals and 15% of "Pan-neuronal Tg; *ptl-1(ok621)*" animals (**Figure 6.2A**). We also observed the same rescue phenotypes when the experiment was repeated at 25 °C and animals were scored on days 1, 3 and 5 of adulthood (**Figure 6.2B**). These results demonstrate that pan-neuronal re-expression of PTL-1 is able to rescue neuronal ageing in a *ptl-1* null mutant in two subsets of neurons.

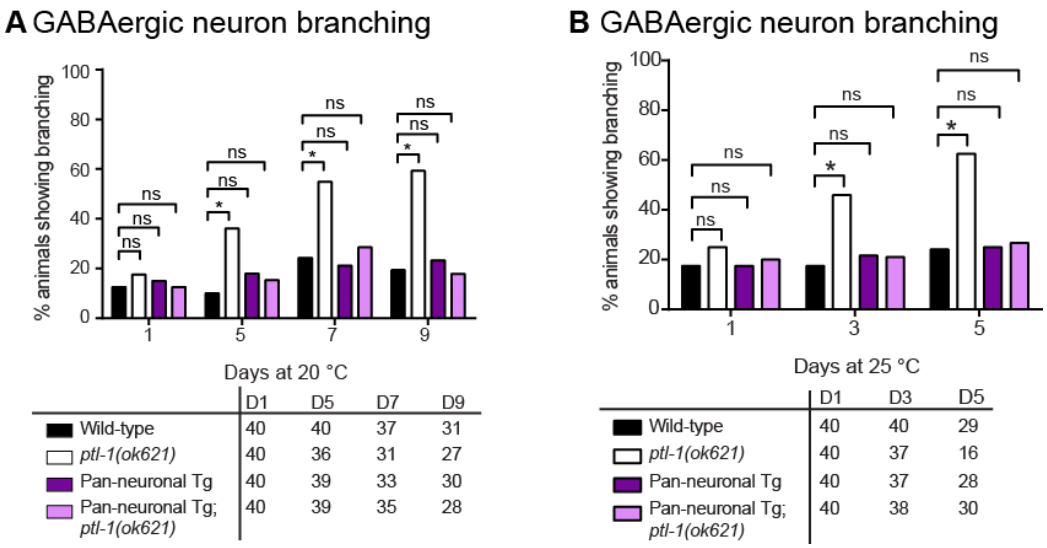

Days at 20 °C	D1	D5	D7	D9
Wild-type	40	40	37	31
ptl-1(ok621)	40	36	31	27
Pan-neuronal Tg	40	39	33	30
Pan-neuronal Tg; *ptl-1(ok621)*	40	39	35	28

Days at 25 °C	D1	D3	D5
Wild-type	40	40	29
ptl-1(ok621)	40	37	16
Pan-neuronal Tg	40	37	28
Pan-neuronal Tg; *ptl-1(ok621)*	40	38	30

Figure 6.2: Pan-neuronal re-expression of PTL-1 rescues the neuronal ageing phenotype in GABAergic neurons that is observed in the *ptl-1(ok621)* null mutant. GABAergic neurons were visualised using the P*unc-47*::*gfp (oxIs12)* reporter. The presence of the *ptl-1(ok621)* mutation in the genetic background of each transgenic line is indicated by the addition of "*ptl-1(ok621)"* in the strain name. Neuron imaging assay conducted at **A)** 20 °C or **B)** 25 °C for "Pan-neuronal Tg" worms. The χ-squared statistical test was used to determine statistical significance. P-value is indicated by ns = not significant, *<0.05. The sample size for each strain at each time point is given in the table underneath the graphs. Experiments were conducted twice independently, and the representative data shown are from one experiment. Data from the second independent experiment are shown in **Appendix 8.**

6.5 The shortened lifespan observed in **ptl-1** *null mutant animals can be rescued by pan-neuronal expression of PTL-1*

We performed lifespan assays to determine if expression of PTL-1 in all neurons would rescue the shortened lifespan of *ptl-1(ok621)* null mutants (Chew et al., 2013). We found that pan-neuronal expression of PTL-1 in a wild-type background ("Pan-neuronal Tg") (median lifespan 10 days) or re-expression in a *ptl-1* null mutant background ("Pan-neuronal Tg; *ptl-1(ok621)*") (median lifespan 11 days) restored the wild-type lifespan (median lifespan 10 days), and these

were all significantly higher than the lifespan of *ptl-1(ok621)* mutant animals (median lifespan 9 days) (**Figure 6.3**). This indicates that PTL-1 regulates lifespan via the nervous system.

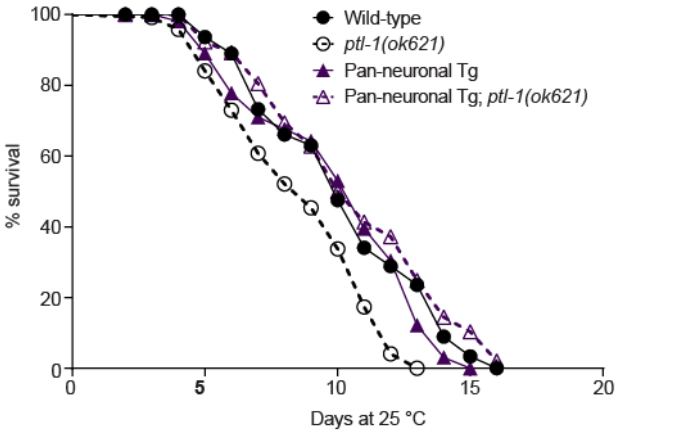

	Log rank test	Gehan-Breslow-Wilcoxon test
Wild-type vs. *ptl-1(ok621)*	<0.05	<0.05
Wild-type vs. "Pan-neuronal Tg"	Not significant	Not significant
Wild-type vs. "Pan-neuronal Tg; *ptl-1(ok621)*"	Not significant	Not significant

Figure 6.3: The short-lived phenotype of *ptl-1* null mutant animals can be rescued by pan-neuronal re-expression of PTL-1. Lifespan assay for pan-neuronal transgenic worms. Survival curves for wild-type and *ptl-1(ok621)* animals in both graphs were obtained in the same experiment. n = 120 at day 0. Results of statistical analysis are indicated by p-values underneath each graph. Lifespan experiments were conducted twice independently, and the representative data shown are from one experiment. Data from the second independent experiment are shown in **Appendix 9.**

6.6 Premature ageing of touch neurons in ptl-1 *null mutant animals can be rescued by touch neuron-specific re-expression of PTL-1*

Our results have shown that pan-neuronal re-expression of PTL-1 is sufficient to rescue neuronal ageing and lifespan phenotypes observed in a *ptl-1* null mutant strain. We next tested if re-expressing PTL-1 in touch neurons alone, the neuronal subset in which PTL-1 is most highly expressed, would also rescue these phenotypes. To this end, we additionally generated a

transgenic line expressing *ptl-1*::V5 cDNA under the regulation of the *mec-7* touch neuron-specific promoter. For clarity, we describe the touch neuron transgenic line as "TRN Tg", followed by "*ptl-1(ok621)*" if it is in the *ptl-1* null mutant background. We immunostained for the V5 epitope tag present at the C-terminus of PTL-1 in the TRN Tg line and confirmed that PTL-1 displayed expression in touch neurons only (**Figure 6.4**).

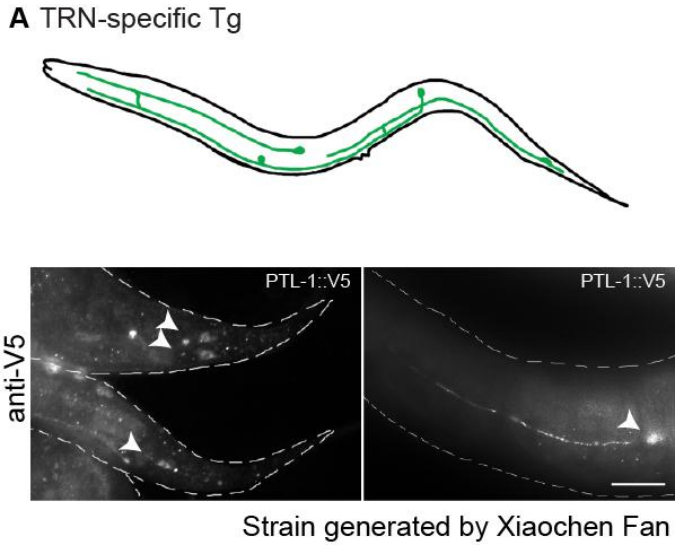

Figure 6.4: Touch neuron-specific expression of PTL-1 can be achieved using a P*mec-7::ptl-1-v5* transgene. A) Staining for PTL-1::V5 in touch neuron-specific transgenic line. The left panel indicates the tail, with PLM neurons indicated by white arrowheads. The right panel indicates the mid-body of the worm, showing an ALM neuron. The white arrowhead here indicates the cell body.

We then investigated if touch neuron-specific expression would affect neuronal ageing in these neurons by scoring for cell body branching, axon blebbing and axon branching in these transgenic lines at both 20 °C and 25 °C. When we assayed for the premature ageing phenotypes in the touch neurons of *ptl-1* mutant animals, we found that these phenotypes were rescued when PTL-1 is re-expressed only in touch neurons ("TRN Tg;*ptl-1(ok621)*") (**Figure 6.5**). For

example, at day 7 of adulthood, 8% of wild-type animals displayed axon blebbing, compared with 35% in *ptl-1(ok621)* mutants and 20% in "TRN Tg;*ptl-1(ok621)*" animals (**Figure 6.5Aii**). There was no observable detrimental effect of over-expressing PTL-1 in the touch neurons in this experiment; at the same time point, 11% of TRN Tg animals displayed axon blebbing, which is not significantly different from wild-type. We observed the same trends for all phenotypes at 25 °C as at 20 °C (**Figure 6.5B**).

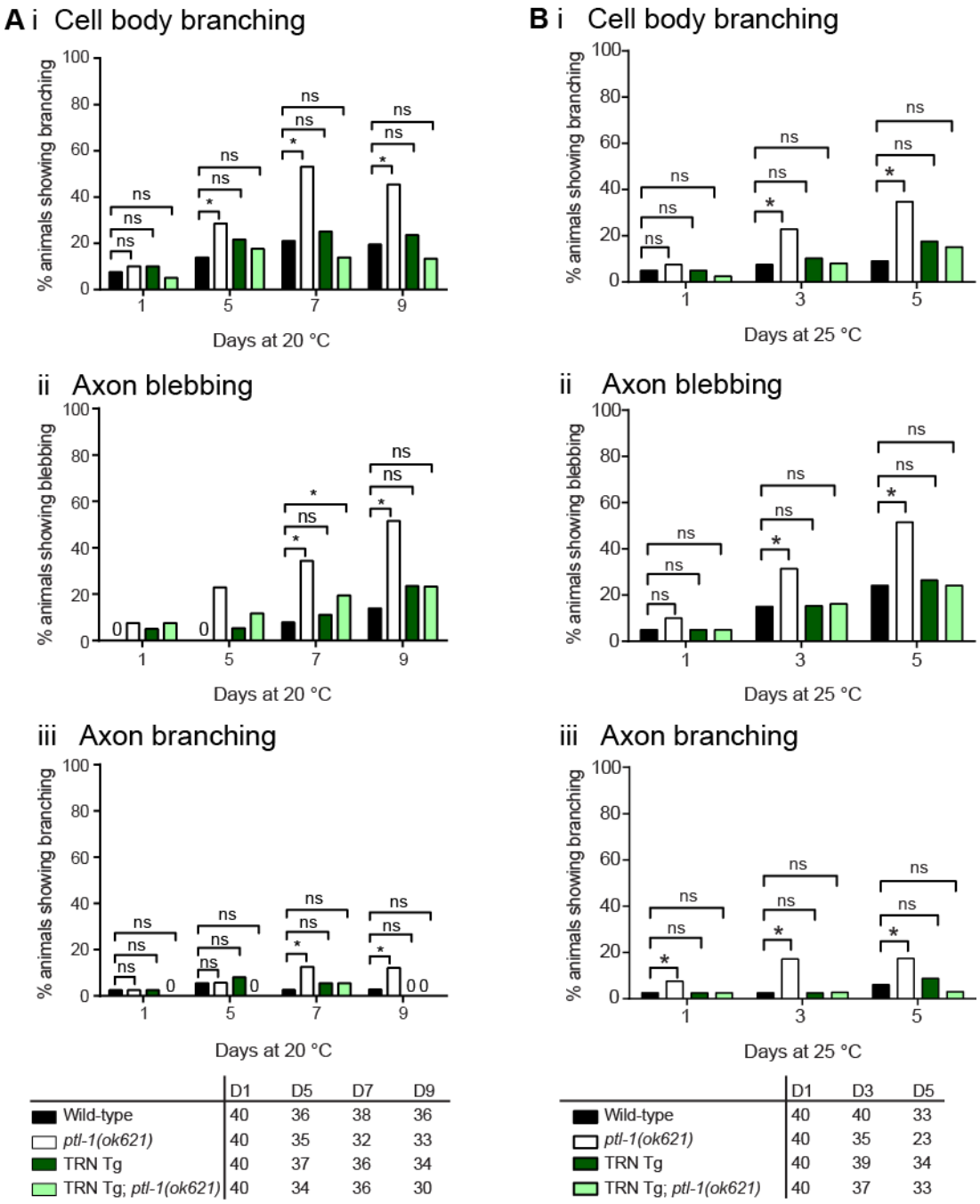

	D1	D5	D7	D9
Wild-type	40	36	38	36
ptl-1(ok621)	40	35	32	33
TRN Tg	40	37	36	34
TRN Tg; *ptl-1(ok621)*	40	34	36	30

	D1	D3	D5
Wild-type	40	40	33
ptl-1(ok621)	40	35	23
TRN Tg	40	39	34
TRN Tg; *ptl-1(ok621)*	40	37	33

Figure 6.5: Touch neuron-specific re-expression of PTL-1 rescues the neuronal ageing phenotype in touch neurons that is observed in the *ptl-1(ok621)* null mutant. The touch neurons were visualised using the P*mec-4*::*gfp* (*zdIs5*) reporter. The presence of the *ptl-1(ok621)* null mutation in the genetic background of each transgenic line is indicated by the addition of "*ptl-1(ok621)"* in the strain name. Neuron imaging assay conducted at **A)** 20 °C or **B)** 25 °C for touch neuron-specific transgenic worms ("TRN Tg"). Data for wild-type and *ptl-1(ok621)* animals in both graphs were obtained in the same experiment as pan-neuronal transgenic lines at the same temperature (**Figure**

6.1). The chi-squared statistical test was used to determine statistical significance. P-value is indicated by ns = not significant, *<0.05. The sample size for each strain at each time point is given in the table underneath the graphs. Experiments were conducted twice independently, and the representative data shown are from one experiment. Data from the second independent experiment are shown in **Appendix 10.**

6.7 Premature ageing of GABAergic neurons in **ptl-1** *null mutant animals is not rescued by touch neuron-specific re-expression of PTL-1*

We next investigated if PTL-1 expression specifically in one neuronal subset, the touch neurons, is able to regulate neuronal ageing in other neurons, such as the GABAergic neurons. To do this, we assayed for GABAergic neuron branching with age in animals expressing the TRN-specific transgene expressing PTL-1. We did not observe a substantial difference in the incidence of abnormal structures between "TRN Tg; *ptl-1(ok621)*" animals (53%) at day 7 of adulthood compared with *ptl-1(ok621)* mutants at the same time point (55%), which are both significantly higher than wild-type (24%) (**Figure 6.6A**). This demonstrates that expression of PTL-1 in one neuronal subset does not impact neuronal ageing in a second subset. Additionally, over-expression of PTL-1 in touch neurons alone does not negatively impact on ageing in GABAergic neurons, as the incidence of branching in "TRN Tg" animals at this time point was 25%, and therefore not significantly different from wild-type. As for the neuronal ageing experiments in touch neurons, we observed the same trends at 25 °C as at 20 °C (**Figure 6.6B**).

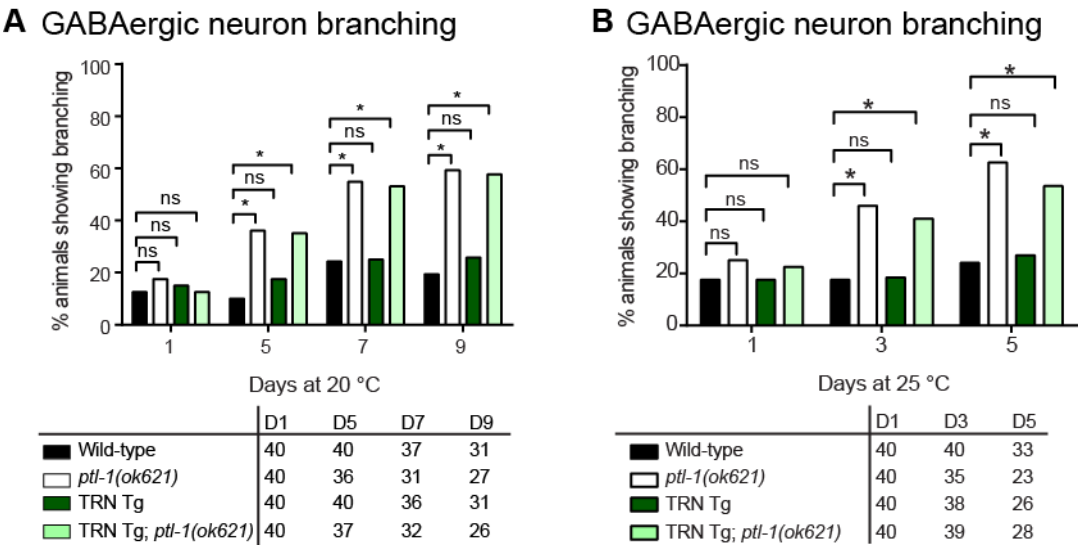

	D1	D5	D7	D9
Wild-type	40	40	37	31
ptl-1(ok621)	40	36	31	27
TRN Tg	40	40	36	31
TRN Tg; *ptl-1(ok621)*	40	37	32	26

	D1	D3	D5
Wild-type	40	40	33
ptl-1(ok621)	40	35	23
TRN Tg	40	38	26
TRN Tg; *ptl-1(ok621)*	40	39	28

Figure 6.6: Touch neuron-specific re-expression of PTL-1 does not rescue the neuronal ageing phenotype in GABAergic neurons that is observed in the *ptl-1(ok621)* null mutant. The GABAergic neurons were visualised using the P*unc-47*::*gfp* (*oxIs12*) reporter. The presence of the *ptl-1(ok621)* mutation in the genetic background of each transgenic line is indicated by the addition of "*ptl-1(ok621)"* in the strain name. Neuron imaging assay conducted at **A)** 20 °C or **B)** 25 °C for "TRN Tg" worms. Data for wild-type and *ptl-1(ok621)* animals were obtained in the same experiment as for pan-neuronal Tg animals at the same temperature (**Figure 6.2**). The chi-squared statistical test was used to determine statistical significance. P-value is indicated by ns = not significant, *<0.05. The sample size for each strain at each time point is given in the table underneath the graphs. Experiments were conducted twice independently, and the representative data shown are from one experiment. Data from the second independent experiment are shown in **Appendix 11.**

6.8 The shortened lifespan observed in ptl-1 *null mutant animals is not rescued by touch neuron-specific re-expression of PTL-1*

We have shown that re-expressing PTL-1 in all neurons or under the regulation of the *ptl-1* promoter rescues the lifespan phenotype of *ptl-1(ok621)* null mutant animals. As we and others have observed that PTL-1 is highly expressed in the touch neurons (Chew et al., 2014b, Goedert et al., 1996, Gordon et al., 2008), we aimed to investigate if PTL-1 expression in these neurons

contributes to its effect on lifespan modulation. We found that expressing PTL-1 in touch neurons alone in the "TRN Tg; *ptl-1(ok621)*" (median lifespan 9 days) strain did not rescue the lifespan phenotype of the *ptl-1(ok621)* null mutant (median lifespan 9 days), as the survival curve of this transgenic line was not significantly different from that of the *ptl-1(ok621)* control (**Figure 6.7**). We also observed a small detrimental effect when PTL-1 was over-expressed in touch neurons: the "TRN Tg" line in a wild-type background displayed a significantly shorter lifespan (median lifespan 9 days) compared with wild-type controls (median lifespan 10 days) according to the log-rank statistical test (**Figure 6.7**). This difference was not significant using the Wilcoxon test, which places more weight on earlier deaths when comparing survival curves (GraphPad Prism 6).

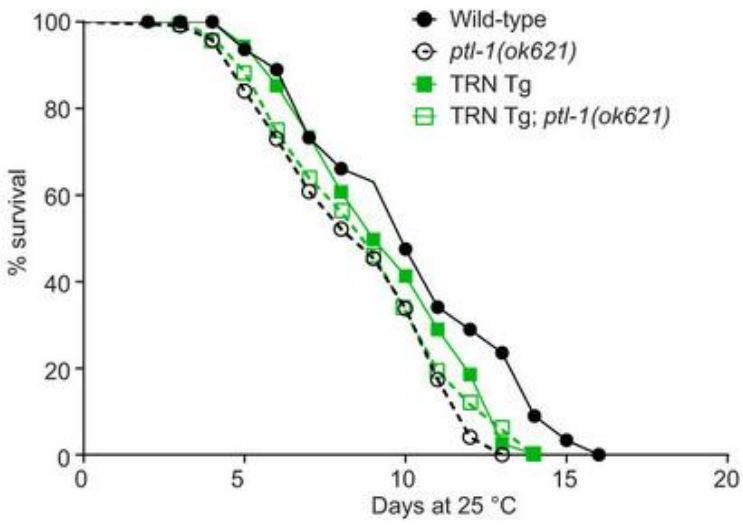

	Log rank test	Gehan-Breslow-Wilcoxon test
Wild-type vs. *ptl-1(ok621)*	<0.05	<0.05
Wild-type vs. "TRN Tg"	<0.05	Not significant
Wild-type vs. "TRN Tg; *ptl-1(ok621)*"	<0.05	<0.05

Figure 6.7: The short-lived phenotype of *ptl-1* null mutant animals cannot be rescued by touch neuron-specific re-expression of PTL-1. Lifespan assay for touch neuron-specific transgenic worms. Survival curves for control wild-type and *ptl-1(ok621)* animals in both graphs were obtained in the same experiment. n = 120 at day 0.

Results of statistical analysis are indicated by p-values underneath each graph. Lifespan experiments were conducted twice independently, and the representative data shown are from one experiment. Data from the second independent replicate are shown in **Appendix 12**.

6.9 Knockdown of PTL-1 in touch neurons only has a cell autonomous effect on neuronal ageing

We next complemented the assays involving tissue-specific re-expression of PTL-1 by conducting knockdown experiments in the touch neurons. We investigated the effect of PTL-1 knockdown in the neuronal subset of touch neurons on the age-associated loss of structural integrity. To do this, we required a strain where the touch neurons are sensitised to RNAi by feeding, but other neurons are refractory. Our methods are summarised in **Figure 6.8**. SID-1 is a transmembrane protein that allows the passive uptake of dsRNA and is required for systemic RNAi knockdown. Wild-type neurons are refractory to RNAi as they do not express SID-1(Feinberg and Hunter, 2003, Winston et al., 2002); however, Calixto *et al.* showed that neuronal re-expression of SID-1 in a *sid-1* null mutant, such as in touch neurons, allowed RNAi knockdown to occur in these neurons (Calixto et al., 2010). The authors demonstrated that feeding *mec-4* RNAi bacteria to these animals resulted in an expected loss of touch sensitivity, indicating that SID-1 expression in touch neurons efficiently sensitized these neurons to knockdown by RNAi treatment (Calixto et al., 2010). These animals that are henceforth referred to as the "TRN SID-1" strain carry a *sid-1(qt2)* mutation and a TRN-specific SID-1 rescue transgene (parent strain TU3403 (Calixto et al., 2010)). We used knockdown of *unc-22* to test for the RNAi sensitivity of these strains. UNC-22 in muscle is required for motility, so feeding wild-type animals (where muscle is sensitive to RNAi) *unc-22* RNAi bacteria results in results in *unc-22* knockdown in muscle that can be observed as paralysis or twitching. However, the TRN SID-

1 strain does not have SID-1 in muscle tissue, so feeding these animals *unc-22* RNAi bacteria does not result in dsRNA being accessible to muscle and thus has no effect on motility (**Figure 6.8**). We used *unc-22* as a control for the RNAi experiment as well as to check strain integrity (see **Methods section 2.2.13**).

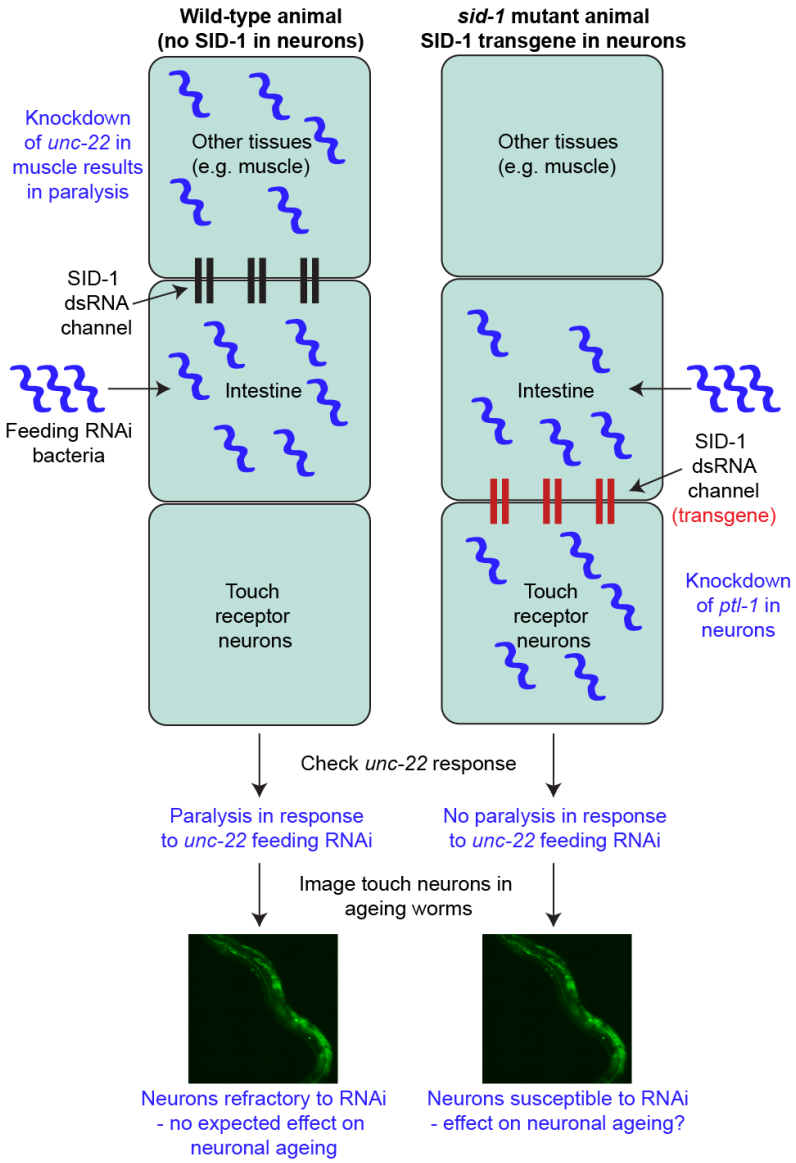

Figure 6.8: Schematic of the protocol for RNAi knockdown experiments. Neurons in wild-type animals are refractory to knockdown by feeding RNAi as they lack the dsRNA transporter SID-1. SID-1 is expressed in other tissues such as the muscle, therefore if dsRNA fed to the animals enters via the intestine it can be passively

transported to non-neuronal tissues. *unc-22* knockdown is able to occur in muscle in wild-type animals, which results in paralysis. When these animals are assayed for neuronal ageing, knockdown by RNAi should not affect transcript levels in neurons. If regulation of neuronal ageing is cell autonomous, there should be no expected effect on neuronal ageing. In contrast, TRN SID-1 animals are mutant for *sid-1* and express a SID-1 transgene in touch neurons only. Therefore, *unc-22* dsRNA fed to TRN SID-1 animals cannot access the muscle via the intestine and these animals are not paralysed. As the touch neurons in this strain are sensitised to RNAi knockdown, feeding RNAi is expected to affect transcript levels in these neurons, which may have an effect on touch neuron ageing if the regulation of neuronal ageing by PTL-1 is cell autonomous.

We first tested whether PTL-1 in touch neurons could be effectively knocked down using this system. We fed either empty vector (EV) and *ptl-1* RNAi bacteria to animals that express both SID-1 only in the touch neurons and a PTL-1::GFP fusion protein. These animals showed a loss of GFP signal in the touch neurons in the *ptl-1* RNAi treated cohort different from those fed EV control RNAi bacteria (**Figure 6.9**), demonstrating the effectiveness of the *ptl-1* RNAi treatment.

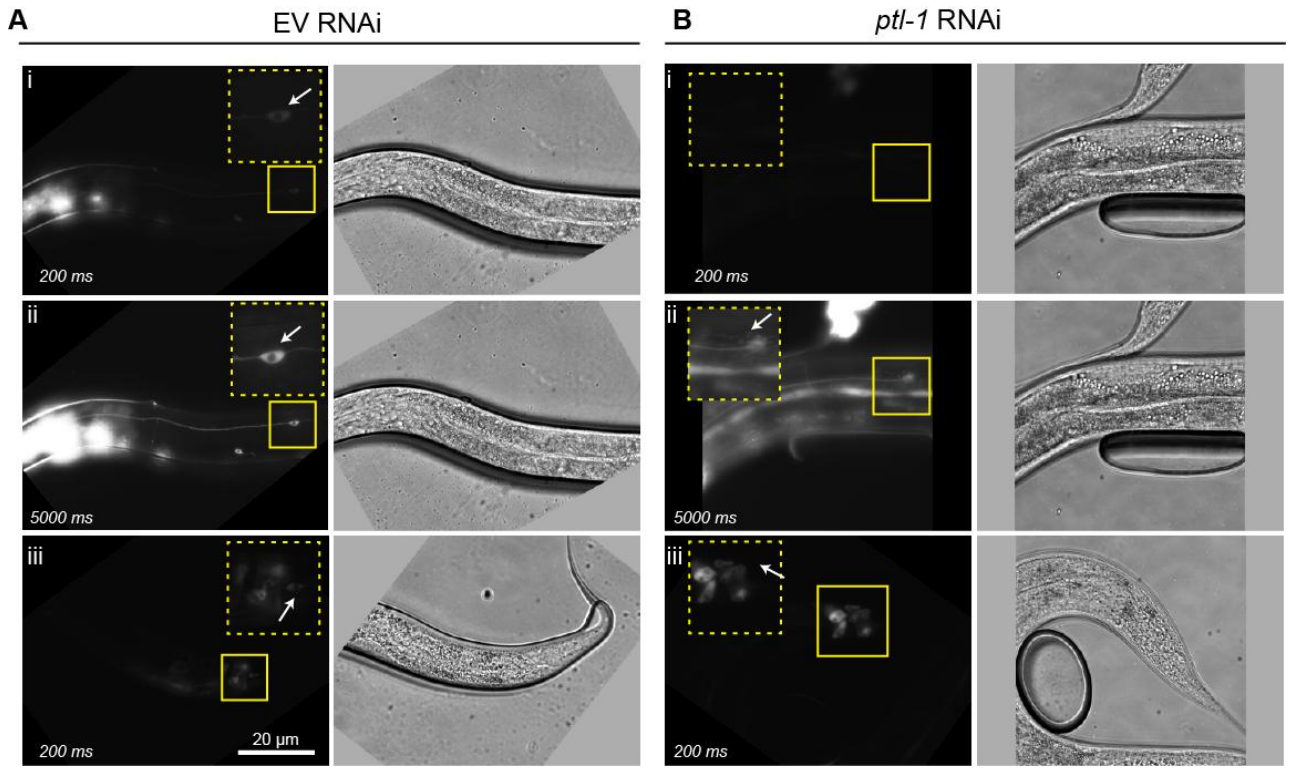

Figure 6.9: Knockdown of PTL-1 in touch neuron RNAi sensitised strains expressing PTL-1::GFP results in loss of fluorescence in touch neurons.

Knockdown of *ptl-1* in a TRN SID-1 transgenic animal results in loss of fluorescence in touch neurons only**.** The strain used for imaging expresses a PTL-1::GFP fusion protein and touch neuron-specific SID-1 in a *sid-1* mutant background. Micrographs are shown for **A)** empty vector (EV) RNAi controls and for **B)** *ptl-1* RNAi treatment with PTL-1::GFP shown on the left and phase images shown on the right. For all micrographs showing fluorescence, boxed regions (solid lines) are shown as a magnified inset that is bordered by dashed lines. **A**(i) The ALM neuron in the EV control is clearly visible at a 200 ms exposure time, indicated by the white arrow. **B**(i). The approximate location of the ALM neuron in an animal exposed to *ptl-1* RNAi treatment shows no fluorescence visible at 200 ms. **A,B**(ii). At a longer exposure time (5000 ms), the ALM neuron is clearly seen in the EV control, indicated by the white arrow (**A**ii) and as a faint signal in the *ptl-1* RNAi-treated animal (**B**ii). (legend continued next page)

Figure 6.9 (continued from previous page) A,B(iii)The PLM neuron cell body is clearly visible in the EV control (**A**iii), indicated by the white arrow but not with *ptl-1* RNAi treatment (**B**iii) at a 200 ms exposure time. Fourth larval stage/first day adult animals were imaged after being fed RNAi bacteria for two generations at 20 °C.

We next crossed TRN SID-1 animals carrying neuronal GFP reporters with those that express SID-1 only in touch neurons. These animals were fed empty vector (EV) or *ptl-1* RNAi feeding clones for two generations and were imaged on days 1, 3, 5 and 7 of adulthood to observe neuronal ageing. As an additional control, we carried out an experiment using animals containing only the neuronal GFP reporters that are wild-type at the *sid-1* locus and do not have the TRN SID-1 transgene. Here, we would expect that no RNAi knockdown would occur within neurons in these animals as the neurons do not express SID-1. These animals did not show a substantial difference in the incidence of abnormal neuronal structures between RNAi treatments, further supporting our conclusion that PTL-1 acts within neurons to regulate neuronal ageing (**Figure 6.10**).

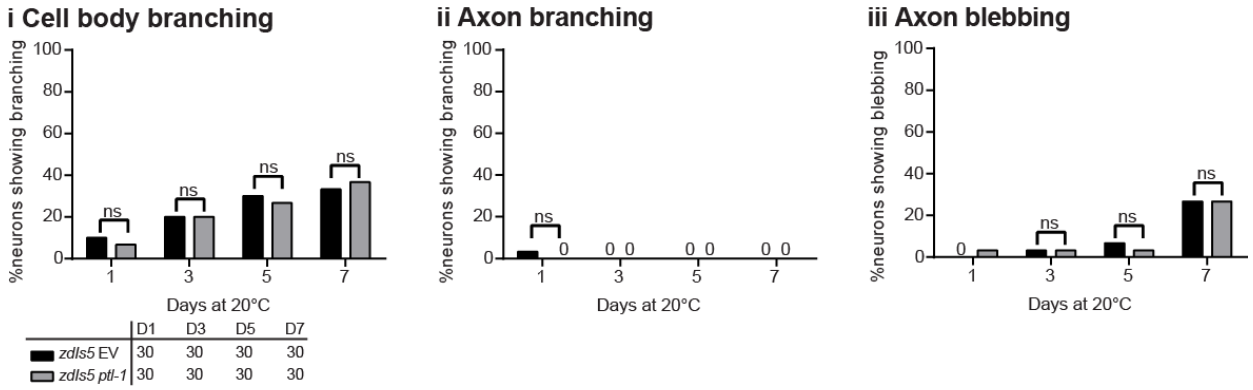

Figure 6.10: Non-neuronal knockdown of PTL-1 has no effect on neuronal ageing. Strains labelled as *zdIs5* indicate the allele name of the *gfp* reporter, are wild-type at the SID-1 locus and do not contain a SID-1 transgene. The RNAi treatment is either empty vector (EV) or *ptl-1* and is indicated after the strain name. Touch neuron imaging assay for animals carrying the *zdIs5* reporter only, indicating data for (i) cell body branching, (ii) axon branching and (iii) axon blebbing. n for each sample is indicated in the table. Statistical analysis: chi-squared test, p-

value is indicated by ns = not significant, *<0.05. Experiments were conducted twice independently, and the representative data shown are from one experiment. Data from the second experiment are shown in **Appendix 13.**

In contrast, when observing the anterior touch neurons in TRN SID-1 transgenic animals, we saw that worms fed with *ptl-1* RNAi bacteria had a higher incidence of cell body branching and axon blebbing compared with those fed EV RNAi bacteria. Specifically, 70% of TRN SID-1 animals fed *ptl-1* RNAi bacteria displayed cell body branching at day 7 compared with 47% in the EV RNAi control, and 53% of *ptl-1* RNAi-fed animals displayed axon blebbing compared with 30% of the control population (**Figure 6.11**). In addition, we observed that TRN SID-1 animals displayed a relatively high frequency of axon branching, which is normally only present in late stage (day 10) adult animals (Chew et al., 2013, Toth et al., 2012) (**Figure 5.3**). TRN SID-1 animals showed considerably higher levels of axon branching in the anterior touch neurons compared with controls that are wild-type at the *sid-1* locus (**Figure 6.10**), although transgenic animals fed *ptl-1* bacteria displayed a higher incidence of this phenotype compared with EV treatments (**Figure 6.11ii**). The high incidence of branching in TRN SID-1 animals could be due to the expression of multiple touch neuron-specific transgenes (both P*mec-18*::*sid-1* and P*mec-4*::*gfp*) that may alter the development or ageing process of the neuron.

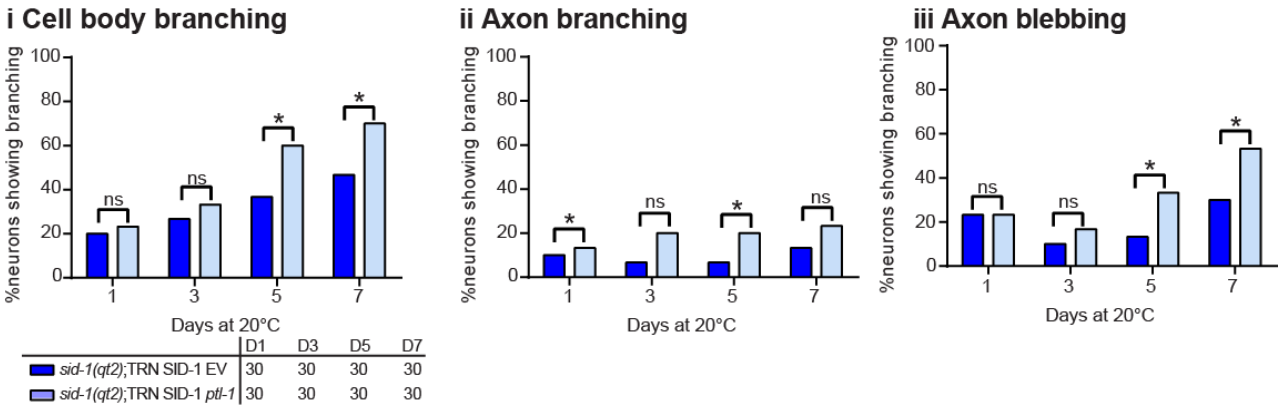

Figure 6.11: Knockdown of PTL-1 in touch neurons results in a loss of structural integrity. SID-1 transgenic worms are labelled as "*sid-1(qt2);*TRN SID-1" to indicate the presence of the *sid-1* mutation and P*mec-18*::*sid-1* transgene. The RNAi treatment is either empty vector (EV) or *ptl-1* and is indicated after the strain name. Touch neuron imaging assay for animals carrying the P*mec-4::gfp (zdIs5)* reporter and the "TRN SID-1" Tg in a *sid-1(qt2)* background, indicating data for (i) cell body branching, (ii) axon branching and (iii) axon blebbing. n for each sample is indicated in the table. Statistical analysis: chi-squared test, p-value is indicated by ns = not significant, *<0.05. Experiments were conducted twice independently, and the representative data shown are from one experiment. Data from the second experiment are shown in **Appendix 13.**

We then further tested the effect of the loss of PTL-1 in touch neurons by examining neuronal ageing in a different set of neurons. For this, we generated a strain expressing a GABAergic neuron GFP reporter in a TRN SID-1 background. As SID-1 is only expressed in touch neurons, we would not expect PTL-1 levels in the GABAergic neurons to be affected by feeding RNAi bacteria in this strain. Therefore, although PTL-1 levels in the touch neurons of TRN SID-1 animals should decrease with *ptl-1* feeding RNAi, PTL-1 expression in the GABAergic neurons of these animals should remain at endogenous levels. As above, we also performed a control RNAi experiment using animals containing only the GABAergic neuron GFP reporter and not the TRN SID-1 transgene, and no differences were observed between RNAi treatments (**Figure 6.12A**). When GABAergic neuron ageing in TRN SID-1 transgenic worms was monitored, we

observed no difference between *ptl-1* RNAi treatment and EV treatment (**Figure 6.12B**). This demonstrates that loss of PTL-1 in the touch neurons appears not to affect neuronal ageing in the GABAergic neurons.

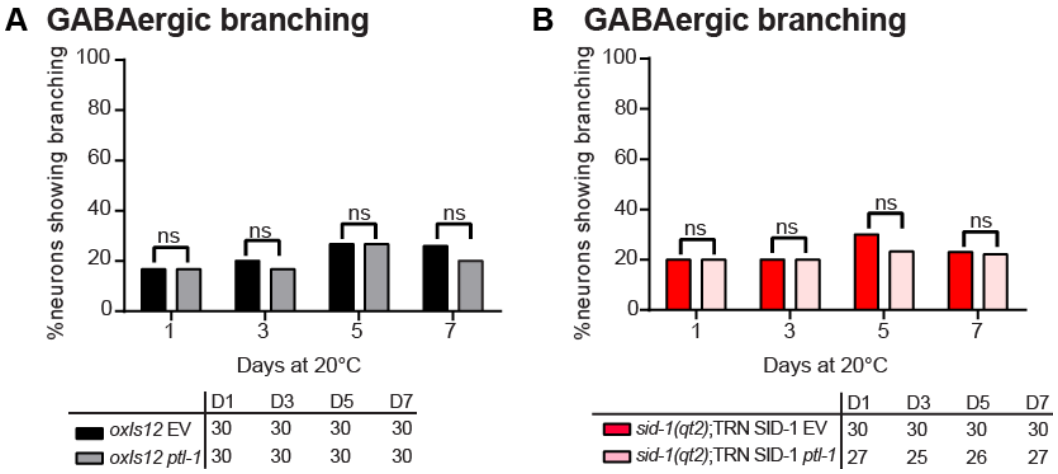

Figure 6.12: Knockdown of PTL-1 in touch neurons does not affect GABAergic neuron integrity during ageing. Strains labelled as *oxIs12* indicate the allele name of the *gfp* reporter, are wild-type at the SID-1 locus and do not contain a SID-1 transgene. SID-1 transgenic worms are labelled as "*sid-1(qt2);*TRN SID-1" to indicate the presence of the *sid-1* mutation and P*mec-18*::*sid-1* transgene. The RNAi treatment is either empty vector (EV) or *ptl-1* and is indicated after the strain name. GABAergic imaging assay **A)** for animals carrying the *oxIs12* reporter only, and **B)** for animals carrying the P*unc-47::gfp (oxIs12)* reporter together with the "TRN SID-1" Tg in a *sid-1(qt2)* mutant background. n for each sample is indicated in the table. Statistical analysis: chi-squared test, p-value is indicated by ns = not significant, *<0.05. Experiments were conducted twice independently, and the representative data shown are from one experiment. Data from the second experiment are shown in **Appendix 13.**

Taken together, these data from tissue-specific re-expression and RNAi knockdown experiments indicate that the effect of *ptl-1* on neuronal ageing is cell autonomous.

6.10 Discussion

The key findings in this chapter are: (i) PTL-1 functions through neurons to regulate organismal ageing, (ii) PTL-1 regulates neuronal ageing in a cell-autonomous manner, and (iii) the processes that regulate organismal ageing and tissue-specific ageing can be separable.

6.10.1 The regulation of neuronal ageing by PTL-1 is cell autonomous

Using a combination of tissue-specific transgene expression and RNAi knockdown, we showed that PTL-1 regulates neuronal structural integrity in a cell autonomous manner. Re-expression or knockdown of PTL-1 in touch neurons alone contributed to the structural stability in those neurons but failed to affect ageing in another neuronal subset, the GABAergic neurons. There is evidence in other pathways that age-associated structural abnormalities in neurons are due to cell-autonomous effects (Toth et al., 2012, Tank et al., 2011). For example, the FOXO transcription factor DAF-16 is required for the longevity effects of the DAF-2 insulin receptor (Kenyon et al., 1993). Expression of DAF-16 only in neurons of a *daf-2;daf-16* mutant delays the formation of abnormal neuron structures compared with a non-transgenic *daf-2;daf-16* control (Tank et al., 2011). In addition, reduced activity of the heat shock factor-1 transcription factor (*hsf-1*) in the whole organism resulted in early onset branching and blebbing in touch receptor neurons, and re-expressing *hsf-1* only in this subset of neurons was able to rescue this effect (Toth et al., 2012).

PTL-1 binds to and stabilizes microtubules (Goedert et al., 1996, McDermott et al., 1996, Tien et al., 2011), and this function may contribute to cell autonomous regulation of structural integrity. Consistent with this, we have shown in the previous chapter that a microtubule-binding domain-

deficient mutant of PTL-1 (*tm543* allele) also displays the same neuronal ageing phenotype as *ptl-1* null mutants (**Figure 5.3**) (Chew et al., 2013).

6.10.2 PTL-1 does not regulate longevity via the touch neurons

Previous research has highlighted the importance of neurons, and sensory neurons in particular, in the modulation of lifespan. Examples include the role of olfactory neurons and ciliated sensory neurons in inhibiting longevity (Alcedo and Kenyon, 2004, Apfeld and Kenyon, 1999), and that of thermosensory neurons in regulating lifespan at high temperatures (Lee and Kenyon, 2009). Our data using a pan-neuronal transgenic line indicate that although PTL-1 is also expressed in non-neuronal tissues (Gordon et al., 2008)(**Figure 4.6**), its neuronal effects are sufficient to regulate whole organismal lifespan. In addition, we also demonstrate that expression of PTL-1 in mechanosensory touch neurons alone, the neuronal subset in which PTL-1 is most highly expressed (Goedert et al., 1996, Gordon et al., 2008), does not rescue the shortened lifespan of *ptl-1* null mutants. Interestingly, *mec* genes that are expressed predominantly in touch neurons have also been implicated in lifespan modulation. Mutations in the mechanosensory channel components MEC-2, MEC-4, MEC-6, MEC-10 and extracellular matrix (ECM) proteins MEC-5 and MEC-9 also result in a shortened lifespan, whereas mutations in the ECM protein MEC-1 and α-tubulin MEC-12 do not (Pan et al., 2011). It is likely that PTL-1 regulates organismal ageing through a combination of neuronal subsets, possibly including the touch neurons.

6.10.3 Regulation of neuronal ageing and lifespan by PTL-1 can be separable

Work detailed in **Chapters 4 and 5** has demonstrated that *ptl-1(ok621)* null mutants display both accelerated organismal ageing and premature neuronal ageing (Chew et al., 2013). We have now shown that animals that express PTL-1 in touch neurons alone have a shortened lifespan compared with wild-type as have *ptl-1(ok621)* null mutants (**Figure 6.7B**), but that their touch neurons age at the same rate as wild-type animals (**Figure 6.5B**). This demonstrates that PTL-1-mediated processes that influence lifespan or neuronal ageing can be decoupled from each other. We also acknowledge the possibility that there may simply be a threshold number of neurons required, such that restoration of *ptl-1* function in only 6 touch neurons out of 302 total neurons may be insufficient to restore normal lifespan. However, our observation that over-expression of PTL-1 in touch neurons on a wild-type background has a small negative impact on lifespan highlights a role for touch neurons compared with other neuronal populations.

A similar segregation of organismal and neuronal ageing has been observed for components of the insulin-like/IGF-1 signalling pathway. Long-lived *daf-2*/insulin receptor mutants show less neuronal branching in early adulthood compared with wild-type, and this effect is ameliorated in *daf-2;daf-16*/FOXO transcription factor double mutants, which have a wild-type lifespan (Tank et al., 2011, Kenyon et al., 1993). However, RNAi-mediated knockdown of *daf-16* in non-neuronal tissues in a *daf-2* mutant results in an animal with wild-type lifespan, but has no effect on the *daf-2*-mediated delay of neuronal ageing (Tank et al., 2011). Therefore, although neuronal cell body branching and axon blebbing increase with age, tissue-specific ageing and whole organism ageing appear to be separable. This suggests that the mechanisms that define these ageing processes contain both distinct and overlapping processes. It is of considerable interest in

the fields of ageing and neurodegeneration to identify the genetic players involved in these processes.

Chapter 7:
General discussion

7.1 Summary

Mammalian Tau has been extensively studied with regards to its role in neurodegenerative diseases, termed Tauopathies, such as Alzheimer's disease (Buee et al., 2000, Iqbal et al., 2010, Ittner et al., 2011, Ittner and Gotz, 2011). Tauopathies are thought to be caused, at least in part, due to a toxic gain-of-function of aggregated and hyperphosphorylated Tau, the loss of an important physiological role played by normally functioning Tau, or a combination of these factors. Despite the large number of advances that have been made using mammalian models to investigate Tau (Gotz et al., 2010), attempts to test the physiological functions of Tau have been made more challenging by the presence of multiple neuronal MAPs that are thought to be functionally redundant *in vivo* (Dehmelt and Halpain, 2005, Kosik and Finch, 1987, Chen et al., 1992). PTL-1 is the sole homolog of Tau/MAP2/MAP4 in *C. elegans,* and contains highly similar C-terminal MBRs to those of the mammalian MAPs (Goedert et al., 1996, McDermott et al., 1996). We have used *C. elegans* as a model to study the physiological roles of a Tau-like protein without the complication of functional redundancy (Chew et al., 2013, Chew et al., 2014a). The overall aim of this work was to investigate the involvement of PTL-1 in the regulation of ageing and stress tolerance, two closely-related processes that are also associated with neurodegenerative disease incidence in humans (Guglielmotto et al., 2009, Zhao and Zhao, 2013, WHO, 2012, Blennow et al., 2006, Bishop et al., 2010). The convenience of the nematode model, particularly its short lifespan of two to three weeks and its ease of maintenance, facilitated our investigation into the role of PTL-1 in both neuronal ageing and whole organism lifespan. In addition, we explored the related functions of PTL-1 in modulating the response to oxidative stress via the Nrf2 transcription factor homolog, SKN-1.

7.2 PTL-1 in the nervous system regulates the oxidative stress response in a pathway that may involve SKN-1

Increased oxidative stress characterizes many pathological conditions and has also been observed in the brains of AD patients and animal models of AD (Butterfield et al., 2007, Filipcik et al., 2006, Guglielmotto et al., 2009, Zhao and Zhao, 2013). The Nrf2 transcription factor is an important mediator of the oxidative stress response in mammals (Leiser and Miller, 2010). Increased Nrf2 activity has been linked to reductions in Tau-mediated neurotoxicity in Tau transgenic mice treated with the aggregation blocker methylene blue (Stack et al., 2014) and in primary neuron culture from a mouse model of AD (Jo et al., 2014). We have shown that PTL-1 regulates the function of the Nrf2 homolog SKN-1 in *C. elegans* possibly by regulating its re-localisation from the cytoplasm into the nucleus of intestinal tissue. We also demonstrated that expression of PTL-1 in the nervous system alone is sufficient to rescue the defects in SKN-1 nuclear accumulation observed in *ptl-1* mutant strains. This process could involve the SV fusion protein UNC-13, which is required to prime SVs for exocytosis (Madison et al., 2005).

The movement of SKN-1 from the intestinal cytoplasm into the nucleus requires p38 MAPK (Inoue et al., 2005), which becomes activated in response to various stressors in both vertebrate and *C. elegans* models (Kyriakis and Avruch, 2001, Johnson and Lapadat, 2002, Lim et al., 2012). PTL-1 in neurons has previously been shown to be involved in microtubule-based motility via kinesin-3 (UNC-104/KIF1A) (Tien et al., 2011). Therefore, the role of PTL-1 in mediating communication between tissues may involve signalling molecules such as neurotransmitters that are transported along microtubules in SVs and are eventually exocytosed. This mode of communication may be required to promote signalling processes such as the p38

MAPK pathway that induces SKN-1 re-localisation. In fact, neurotransmitter release from dopaminergic neurons was previously shown to "condition" the *C. elegans* innate immune response to pathogenic *E. coli*, a process that involves MAPK signalling (Anyanful et al., 2009). This suggests that neurotransmitters that are carried by SVs in neurons are able to activate the p38 MAPK pathway in non-neuronal tissue. However, it is also conceivable that PTL-1 mediates a developmental process within the nervous system that is required for neurons to signal to intestinal SKN-1 and thus trigger nuclear re-localisation during stress. As we could not observe detectable knockdown of *ptl-1* in young adulthood when animals were fed RNAi bacteria at the fourth larval stage, we were unable to determine if the SKN-1 defect in *ptl-1* mutant animals arose post-developmentally or as a result of a developmental defect. However, our observations of the nervous system in young adult *ptl-1* mutant animals indicate that the overall neuronal architecture appears overtly normal (**Chapters 5 and 6**), suggesting that any developmental effects of loss of PTL-1 are subtle or do not affect the gross anatomy of the nervous system. Alternatively, it is possible that the lack of PTL-1 compromises the health of animals to the extent that they are unable to properly respond to environmental insults. However, as *ptl-1* mutant animals are still at least partially able to response to stress (~20% SKN-1 nuclear accumulation in *ptl-1(ok621)* azide-stressed animals), this indicates that lack of functional PTL-1 does not result in an overall inability to detect stress.

Another possibility is that PTL-1 and SKN-1 interact with each other in the nervous system, and that this cross-talk "activates" neuronal SKN-1 to promote its re-localisation in the intestine. Such a mechanism has been postulated for the FOXO transcription factor DAF-16, in that intestinal DAF-16 activation leads to increased DAF-16 activity in other tissues. This "FOXO-

to-FOXO" communication requires the insulin-like gene *ins-7* that is positively regulated by DAF-16 (Murphy et al., 2007). Although the expression pattern of SKN-1 appears restricted to the ASI neurons in the head and the intestine for SKN-1b and SKN-1c, respectively (An and Blackwell, 2003, Bishop and Guarente, 2007), the localisation of SKN-1a remains largely uncharacterised. A transgenic line expressing GFP-tagged SKN-1a under the regulation of a 7.3 kb upstream region, including the coding sequence of a widely-expressed upstream gene *bec-1*, shows GFP localised to many tissues including the ventral nerve cord (Staab et al., 2014). PTL-1 is broadly expressed in the nervous system, including in the ventral cord and in many of the head neurons likely including the ASI neurons (Gordon et al., 2008, Chew et al., 2014a). We showed that, unlike re-expression in all neurons, PTL-1 expression in the ASI neurons where SKN-1b is constitutively localised to the nucleus (An and Blackwell, 2003), is not sufficient to rescue the defect in SKN-1 re-localisation observed in *ptl-1* mutant animals. However, although the *gpa-4* promoter that we used to generate the ASI Tg line had been previously used to express transgenes specifically in the ASI neurons (Bishop and Guarente, 2007), technical difficulties prevented us from confirming that the head neurons in which we observed transgene expression were definitively the ASI neurons. It is possible that a direct interaction between PTL-1 and SKN-1 in other neurons, such as the ventral cord neurons, could modulate SKN-1 in the intestine in response to stress.

7.3 PTL-1 modulates longevity from the nervous system

We showed that *ptl-1* null mutant or MBR-deficient strains are short-lived and that this can be rescued by either re-expression of PTL-1 in the null mutant strain under the regulation of the endogenous promoter or by a pan-neuronal-specific promoter. We also showed that PTL-1

expressed solely in the touch neurons was not sufficient to rescue the premature lifespan observed in *ptl-1* mutant animals. Additionally, over-expression of PTL-1 in touch neurons alone was detrimental to the animal. We noted that the negative effect of touch neuron over-expression (TRN Tg) appears to be subtly less than that of over-expressing PTL-1 under the regulation of its endogenous promoter (PTL-1 Tg), which would express PTL-1 in neuronal and non-neuronal tissues. Although these strains were never assayed in the same experiment, the TRN Tg over-expression strain is not significantly short-lived compared with wild-type using the Wilcoxon statistical test, whereas the PTL-1 Tg over-expression strain (regulated by the *ptl-1* endogenous promoter) is short-lived using the same statistical analysis. Unlike the log-rank test, the Wilcoxon test places more weight on earlier deaths (Machin et al., 2006), suggesting that in terms of survival, the TRN Tg strain, but not the PTL-1 Tg strain, behaves like wild-type in young adulthood. Interestingly, there was no observable adverse effect of over-expressing PTL-1 only in the nervous system (Pan-neuronal Tg). It should be noted that transcript levels of the transgene in each of these transgenic lines are likely to vary to a considerable degree, which according to our data using PTL-1 Tg lines that express PTL-1 under the control of the *ptl-1* promoter, may have an effect on whole organismal ageing. Nonetheless, our observations suggest that the touch neurons play a particular role in lifespan modulation by PTL-1, and that the levels of PTL-1 in non-neuronal tissues may also contribute to this function. It is likely that functional PTL-1 in a combination of neuronal subsets, possibly including the touch neurons, is required to maintain wild-type lifespan.

In addition, we found that human Tau does not rescue the shortened lifespan observed in *ptl-1* mutant strains. This could be because the detrimental effect of expressing the human Tau

transgene in *C. elegans,* which was also observed in other transgenic lines (Brandt et al., 2009, Kraemer et al., 2003, Miyasaka et al., 2005), masks any positive effects that could potentially rescue the longevity phenotype. Or, it could be that unlike PTL-1, human Tau lacks the ability to interact with other *C. elegans* proteins that may be required to maintain wild-type lifespan. The N-termini of PTL-1 and human Tau display limited sequence homology and this region could contain the sequences that are required for protein–protein interactions that mediate longevity in *C. elegans*. For mammalian Tau, the N-terminus is required for several important interactions, such as those required to mediate axonal transport (Kanaan et al., 2012) and post-synaptic targeting of signalling molecules (Ittner et al., 2010).

When we performed lifespan assays with short-lived *ptl-1(ok621)* and *skn-1(zu67)* mutant strains, we found that double mutant *ptl-1;skn-1* animals were not significantly more or less short-lived than the single mutant animals. This suggests that PTL-1 and SKN-1 may regulate lifespan via similar pathways. It is unclear how SKN-1 affects lifespan, although several lines of evidence suggest that this involves components of the insulin-like signalling pathway, which is the most well-characterised lifespan regulator in *C. elegans* (Paek et al., 2012, Tullet et al., 2008, Inoue et al., 2005). The p38 MAPK pathway, which is required for SKN-1 re-localisation to the intestinal nucleus in response to stress, appears to regulate lifespan via SKN-1 and the IIS pathway (Inoue et al., 2005). Mammalian Tau is phosphorylated by p38 MAPKs and glycogen synthase kinase-3β (GSK-3β) (Goedert et al., 1997, Anderton et al., 2001). GSK-3β is modulated by several pathways including insulin signalling (Wada, 2009), and in *C. elegans* it inhibits intestinal SKN-1 from localising to the nucleus in the absence of stress (An et al., 2005). Excessive phosphorylation of Tau by these and other factors is understood to be a major

contributor to neurodegenerative pathology (Goedert et al., 1997, Anderton et al., 2001, Mandelkow et al., 1993, Zheng-Fischhofer et al., 1998, Lovestone et al., 1994). Given the relationship between mammalian Tau and p38 MAPK and GSK-3 β signalling, it is possible that PTL-1 requires these kinases for its roles in neuronal ageing and lifespan in *C. elegans*. We have not tested whether PTL-1 interacts with members of the IIS, p38 MAPK or GSK-3β pathway in its modulation of lifespan.

On a related note, expression of SKN-1b in the ASI neurons has been shown to be critical in the regulation of dietary-restriction-mediated lifespan extension (Bishop and Guarente, 2007). A role for PTL-1 in dietary-restriction-dependent longevity has not been described, although it would be interesting to test if such a phenotype exists and if so, whether it is able to be rescued by ASI-specific PTL-1 re-expression. We also did not test if PTL-1 re-expression in the ASI neurons is sufficient to rescue the shortened lifespan of *ptl-1* null mutant animals observed under *ad libitum* feeding conditions. Curiously, the *skn-1(zu67)* allele, which confers a short-lived phenotype, affects SKN-1a and SKN-1c isoforms only, suggesting that SKN-1b in the ASI neurons does not affect lifespan under non-restricted feeding conditions (Bishop and Guarente, 2007). SKN-1a is potentially expressed in several parts of the nervous system (Staab et al., 2014), whereas SKN-1c appears restricted to the intestine (An and Blackwell, 2003). It is likely that there is some overlap between the expression of PTL-1 and SKN-1 in these tissues, and as noted above, it is possible that PTL-1 and SKN-1 interact within the nervous system. Therefore, to regulate lifespan, PTL-1 and SKN-1 may act within the same tissues, or across tissues.

7.4 PTL-1 maintains age-related structural integrity in neurons potentially by stabilising microtubules

We have shown that PTL-1 is not only involved in mediating whole organism lifespan, but that it also regulates neuronal ageing in two subsets of neurons, the touch neurons and the GABAergic neurons of the ventral cord. We tested only these neuronal subsets because they are the most well-defined in terms of the subtle parameters that characterise neuronal ageing in *C. elegans* (Pan et al., 2011, Tank et al., 2011, Toth et al., 2012). However, our results suggest that PTL-1 is likely to also regulate tissue ageing throughout the nervous system. Using a combination of tissue-specific transgenic re-expression and RNAi knockdown, we have shown that PTL-1 regulates neuronal ageing in a cell autonomous manner. This is perhaps unsurprising, as PTL-1 is a microtubule-binding protein and is likely to maintain structural integrity in neurons by its ability to stabilise the components of the cytoskeleton formed form from microtubules (Goedert et al., 1996, McDermott et al., 1996). Consistent with this theory, we showed that both loss of PTL-1 or expression of a truncated form lacking the MBRs in the *ptl-1(tm543)* mutant strain, results in an age-related loss of neuronal structural integrity. Furthermore, the neurons in which PTL-1 is most highly expressed are the touch receptor neurons, which have specialised 15-protofilament microtubule structures (as opposed to the 'normal' 11-protofilament structures) that are believed to play an essential role in mechanosensation (Chalfie and Sulston, 1981, Savage et al., 1994). This and our observations suggest that PTL-1 plays an important role in stabilising microtubule structures in *C. elegans.* It would be interesting to investigate if these 15-protofilament microtubule structures, which are disrupted in mutations in genes such as the β-tubulin gene *mec-7,* can still be formed in a *ptl-1* mutant strain.

An established function of mammalian Tau/MAP2/MAP4 is the ability to interact with tubulin monomers and to promote microtubule assembly and stability (Witman et al., 1976, Weingarten et al., 1975). The ability to bind microtubules is predominantly conferred by the MBRs, so Tau isoforms that have more MBRs (4 repeat/R Tau versus 3R Tau) bind more strongly (Lee and Rook, 1992), in a similar manner as PTL-1 (Goedert et al., 1996). Interestingly, some mutations in the familial Tauopathy FTDP-17 alter the normal ~50:50 ratio of 4R:3R Tau isoform ratio to one that results in an excess of 4R Tau (Ingram and Spillantini, 2002, Hong et al., 1998). Furthermore, hyperphosphorylation of Tau reduces its ability to bind to microtubules (Iqbal et al., 2010, Alonso et al., 2008). These observations suggest that modulations in the ability of MAPs to bind microtubules can contribute to increased neurodegeneration. In this work, we generated transgenic lines solely using one PTL-1 isoform. Although the functional differences between PTL-1 isoforms have not been extensively studied, given the importance of isoform ratios for mammalian Tau, it is possible that re-expressing different isoforms of PTL-1 could produce varying phenotypes. It is also not known if different *ptl-1* transcripts are expressed in different tissues or subcellular localisations. Future work could expand on our investigations by testing for potential functional differences in PTL-1 isoforms.

7.5 Conclusions

We have shown that levels of PTL-1 need to be tightly controlled in the regulation of neuronal ageing, longevity, and stress tolerance (summarised in **Figure 7.1**). Loss of PTL-1, the expression of a truncated form lacking the MBRs, or expression levels that are too high, all lead to detrimental effects. This has implications for the development of therapeutics for AD and other Tauopathies that rely on the reduction of Tau levels. As aggregated Tau is an important

pathological hallmark for several neurodegenerative diseases, some therapeutic strategies focus on reducing Tau levels. Our data indicate that it may not be ideal to reduce Tau to too low levels in AD patients, as the loss of PTL-1 in *C. elegans* has several negative effects on the organism. Although differences between *C. elegans* and higher organisms may be due to the lack of other Tau/MAP2/MAP4 homologs in the worm that can compensate for loss of PTL-1, our findings nonetheless demonstrate the importance of Tau-like proteins in regulating not only neuronal physiology, but also important biological processes within the whole organism. Further investigations are needed to understand the mechanisms involved in these processes, which would be interesting not solely to the fields of ageing and neurodegeneration, but also to our understanding of how various tissues regulate whole animal physiology.

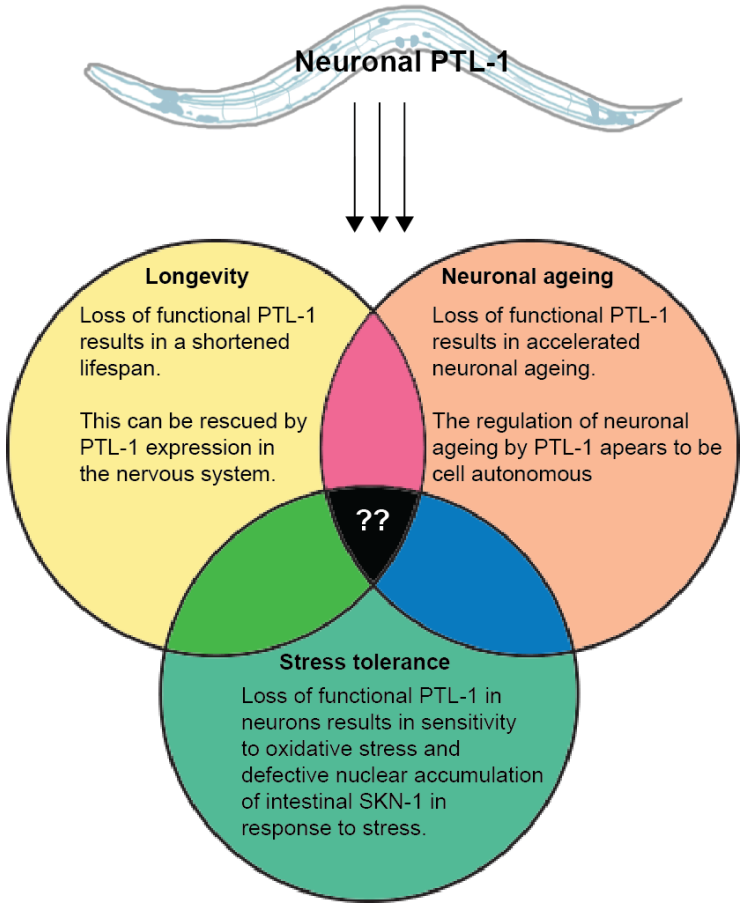

Figure 7.1: Summary of the functions of PTL-1 determined in this investigation. PTL-1 appears to modulate longevity, neuronal ageing, and stress tolerance. Although these phenotypes have been linked to one another, for example increased stress tolerance is correlated with lifespan extension, and *ptl-1* mutant animals that are short-lived have accelerated neuronal ageing (whereas *daf-2* mutant animals are long-lived and show delayed neuronal ageing) (Tank et al., 2011), it is unclear if PTL-1 drives these processes separately or if it is involved in a general pathway that is upstream of these phenotypes.

References

ALCEDO, J. & KENYON, C. 2004. Regulation of C. elegans longevity by specific gustatory and olfactory neurons. *Neuron,* 41**,** 45-55.

ALONSO, A. C., LI, B., GRUNDKE-IQBAL, I. & IQBAL, K. 2008. Mechanism of tau-induced neurodegeneration in Alzheimer disease and related tauopathies. *Curr Alzheimer Res,* 5**,** 375-84.

ALPER, S., MCELWEE, M. K., APFELD, J., LACKFORD, B., FREEDMAN, J. H. & SCHWARTZ, D. A. 2010. The Caenorhabditis elegans germ line regulates distinct signaling pathways to control lifespan and innate immunity. *J Biol Chem,* 285**,** 1822-8.

ALTUN, Z. F. & HALL, D. H. 2005. Introduction to *C. elegans* anatomy. *WormAtlas.*

AMOUTZIAS, G. D., VERON, A. S., WEINER, J., 3RD, ROBINSON-RECHAVI, M., BORNBERG-BAUER, E., OLIVER, S. G. & ROBERTSON, D. L. 2007. One billion years of bZIP transcription factor evolution: conservation and change in dimerization and DNA-binding site specificity. *Mol Biol Evol,* 24**,** 827-35.

AN, J. H. & BLACKWELL, T. K. 2003. SKN-1 links C. elegans mesendodermal specification to a conserved oxidative stress response. *Genes Dev,* 17**,** 1882-93.

AN, J. H., VRANAS, K., LUCKE, M., INOUE, H., HISAMOTO, N., MATSUMOTO, K. & BLACKWELL, T. K. 2005. Regulation of the Caenorhabditis elegans oxidative stress defense protein SKN-1 by glycogen synthase kinase-3. *Proc Natl Acad Sci U S A,* 102**,** 16275-80.

ANDERTON, B. H., BETTS, J., BLACKSTOCK, W. P., BRION, J. P., CHAPMAN, S., CONNELL, J., DAYANANDAN, R., GALLO, J. M., GIBB, G., HANGER, D. P., HUTTON, M., KARDALINOU, E., LEROY, K., LOVESTONE, S., MACK, T., REYNOLDS, C. H. & VAN SLEGTENHORST, M. 2001. Sites of phosphorylation in tau and factors affecting their regulation. *Biochem Soc Symp***,** 73-80.

ANYANFUL, A., EASLEY, K. A., BENIAN, G. M. & KALMAN, D. 2009. Conditioning protects C. elegans from lethal effects of enteropathogenic E. coli by activating genes that regulate lifespan and innate immunity. *Cell Host Microbe,* 5**,** 450-62.

APFELD, J. & KENYON, C. 1998. Cell nonautonomy of C-elegans daf-2 function in the regulation of diapause and life span. *Cell,* 95**,** 199-210.

APFELD, J. & KENYON, C. 1999. Regulation of lifespan by sensory perception in Caenorhabditis elegans. *Nature,* 402**,** 804-9.

AVILA, J., LUCAS, J. J., PEREZ, M. & HERNANDEZ, F. 2004. Role of tau protein in both physiological and pathological conditions. *Physiol Rev,* 84**,** 361-84.

AVRAMOPOULOS, D. 2009. Genetics of Alzheimer's disease: recent advances. *Genome Med,* 1**,** 34.

BERTONIFREDDARI, C., FATTORETTI, P., PAOLONI, R., CASELLI, U., GALEAZZI, L. & MEIERRUGE, W. 1996. Synaptic structural dynamics and aging. *Gerontologia,* 42**,** 170-180.

BISHOP, N. A. & GUARENTE, L. 2007. Two neurons mediate diet-restriction-induced longevity in C. elegans. *Nature,* 447**,** 545-9.

BISHOP, N. A., LU, T. & YANKNER, B. A. 2010. Neural mechanisms of ageing and cognitive decline. *Nature,* 464**,** 529-35.

BLENNOW, K., DE LEON, M. J. & ZETTERBERG, H. 2006. Alzheimer's disease. *Lancet,* 368**,** 387-403.

BOWERMAN, B., EATON, B. A. & PRIESS, J. R. 1992. skn-1, a maternally expressed gene required to specify the fate of ventral blastomeres in the early C. elegans embryo. *Cell,* 68**,** 1061-75.

BRANDT, R., GERGOU, A., WACKER, I., FATH, T. & HUTTER, H. 2009. A Caenorhabditis elegans model of tau hyperphosphorylation: induction of developmental defects by transgenic overexpression of Alzheimer's disease-like modified tau. *Neurobiol Aging,* 30**,** 22-33.

BRENNER, S. 1974. The genetics of Caenorhabditis elegans. *Genetics,* 77**,** 71-94.

BUEE-SCHERRER, V. & GOEDERT, M. 2002. Phosphorylation of microtubule-associated protein tau by stress-activated protein kinases in intact cells. *FEBS Lett,* 515**,** 151-4.

BUEE, L., BUSSIERE, T., BUEE-SCHERRER, V., DELACOURTE, A. & HOF, P. R. 2000. Tau protein isoforms, phosphorylation and role in neurodegenerative disorders. *Brain Res Brain Res Rev,* 33**,** 95-130.

BUFFENSTEIN, R., EDREY, Y. H., YANG, T. & MELE, J. 2008. The oxidative stress theory of aging: embattled or invincible? Insights from non-traditional model organisms. *Age (Dordr),* 30**,** 99-109.

BUTTERFIELD, D. A., REED, T., NEWMAN, S. F. & SULTANA, R. 2007. Roles of amyloid beta-peptide-associated oxidative stress and brain protein modifications in the pathogenesis of Alzheimer's disease and mild cognitive impairment. *Free Radic Biol Med,* 43**,** 658-77.

CALIXTO, A., CHELUR, D., TOPALIDOU, I., CHEN, X. & CHALFIE, M. 2010. Enhanced neuronal RNAi in C. elegans using SID-1. *Nat Methods,* 7**,** 554-9.

CHALFIE, M. & SULSTON, J. 1981. Developmental genetics of the mechanosensory neurons of Caenorhabditis elegans. *Dev Biol,* 82**,** 358-70.

CHALFIE, M., SULSTON, J. E., WHITE, J. G., SOUTHGATE, E., THOMSON, J. N. & BRENNER, S. 1985. The neural circuit for touch sensitivity in Caenorhabditis elegans. *J Neurosci,* 5**,** 956-64.

CHEN, J., KANAI, Y., COWAN, N. J. & HIROKAWA, N. 1992. Projection domains of MAP2 and tau determine spacings between microtubules in dendrites and axons. *Nature,* 360**,** 674-7.

CHEW, Y. L., FAN, X., GOTZ, J. & NICHOLAS, H. R. 2013. PTL-1 regulates neuronal integrity and lifespan in C. elegans. *J Cell Sci,* 126**,** 2079-91.

CHEW, Y. L., FAN, X., GOTZ, J. & NICHOLAS, H. R. 2014a. Regulation of age-related structural integrity in neurons by protein with tau-like repeats (PTL-1) is cell autonomous. *Sci. Rep.,* 4.

CHEW, Y. L., FAN, X., GOTZ, J. & NICHOLAS, H. R. 2014b. Regulation of age-related structural integrity in neurons by protein with tau-like repeats (PTL-1) is cell autonomous. *Sci Rep,* 4**,** 5185.

CHOE, K. P., PRZYBYSZ, A. J. & STRANGE, K. 2009. The WD40 repeat protein WDR-23 functions with the CUL4/DDB1 ubiquitin ligase to regulate nuclear abundance and activity of SKN-1 in Caenorhabditis elegans. *Mol Cell Biol,* 29**,** 2704-15.

CLARK, S. G. & CHIU, C. 2003. C. elegans ZAG-1, a Zn-finger-homeodomain protein, regulates axonal development and neuronal differentiation. *Development,* 130**,** 3781-94.

CLEVELAND, D. W., HWO, S. Y. & KIRSCHNER, M. W. 1977. Purification of tau, a microtubule-associated protein that induces assembly of microtubules from purified tubulin. *J Mol Biol,* 116**,** 207-25.

COPELAND, J. M., CHO, J., LO, T., JR., HUR, J. H., BAHADORANI, S., ARABYAN, T., RABIE, J., SOH, J. & WALKER, D. W. 2009. Extension of Drosophila life span by RNAi of the mitochondrial respiratory chain. *Curr Biol,* 19**,** 1591-8.

CRITTENDEN, S. L. & KIMBLE, J. 1999. Confocal methods for Caenorhabditis elegans. *Methods Mol Biol,* 122**,** 141-51.

D'ANGELO, M. A., RAICES, M., PANOWSKI, S. H. & HETZER, M. W. 2009. Age-dependent deterioration of nuclear pore complexes causes a loss of nuclear integrity in postmitotic cells. *Cell,* 136**,** 284-95.

DAVID, D. C., HAUPTMANN, S., SCHERPING, I., SCHUESSEL, K., KEIL, U., RIZZU, P., RAVID, R., DROSE, S., BRANDT, U., MULLER, W. E., ECKERT, A. & GOTZ, J. 2005. Proteomic and functional analyses reveal a mitochondrial dysfunction in P301L tau transgenic mice. *J Biol Chem,* 280**,** 23802-14.

DAWSON, H. N., FERREIRA, A., EYSTER, M. V., GHOSHAL, N., BINDER, L. I. & VITEK, M. P. 2001. Inhibition of neuronal maturation in primary hippocampal neurons from tau deficient mice. *J Cell Sci,* 114**,** 1179-87.

DEHMELT, L. & HALPAIN, S. 2005. The MAP2/Tau family of microtubule-associated proteins. *Genome Biol,* 6**,** 204.

DELL'AGNELLO, C., LEO, S., AGOSTINO, A., SZABADKAI, G., TIVERON, C., ZULIAN, A., PRELLE, A., ROUBERTOUX, P., RIZZUTO, R. & ZEVIANI, M. 2007. Increased longevity and refractoriness to Ca(2+)-dependent neurodegeneration in Surf1 knockout mice. *Hum Mol Genet,* 16**,** 431-44.

DI TOMMASO, P., MORETTI, S., XENARIOS, I., OROBITG, M., MONTANYOLA, A., CHANG, J. M., TALY, J. F. & NOTREDAME, C. 2011. T-Coffee: a web server for the multiple sequence alignment of protein and RNA sequences using structural information and homology extension. *Nucleic Acids Res,* 39**,** W13-7.

DIAS-SANTAGATA, D., FULGA, T. A., DUTTAROY, A. & FEANY, M. B. 2007. Oxidative stress mediates tau-induced neurodegeneration in Drosophila. *J Clin Invest,* 117**,** 236-45.

DRUBIN, D. G. & KIRSCHNER, M. W. 1986. Tau protein function in living cells. *J Cell Biol,* 103**,** 2739-46.

ECKERT, A., HAUPTMANN, S., SCHERPING, I., MEINHARDT, J., RHEIN, V., DROSE, S., BRANDT, U., FANDRICH, M., MULLER, W. E. & GOTZ, J. 2008. Oligomeric and fibrillar species of beta-amyloid (A beta 42) both impair mitochondrial function in P301L tau transgenic mice. *J Mol Med (Berl),* 86**,** 1255-67.

FATOUROS, C., PIR, G. J., BIERNAT, J., KOUSHIKA, S. P., MANDELKOW, E., MANDELKOW, E. M., SCHMIDT, E. & BAUMEISTER, R. 2012. Inhibition of tau aggregation in a novel Caenorhabditis elegans model of tauopathy mitigates proteotoxicity. *Hum Mol Genet,* 21**,** 3587-603.

FEINBERG, E. H. & HUNTER, C. P. 2003. Transport of dsRNA into cells by the transmembrane protein SID-1. *Science,* 301**,** 1545-7.

FILIPCIK, P., CENTE, M., FERENCIK, M., HULIN, I. & NOVAK, M. 2006. The role of oxidative stress in the pathogenesis of Alzheimer's disease. *Bratisl Lek Listy,* 107**,** 384-94.

FIRE, A., ALBERTSON, D., HARRISON, S. W. & MOERMAN, D. G. 1991. Production of antisense RNA leads to effective and specific inhibition of gene expression in C. elegans muscle. *Development,* 113**,** 503-14.

FONTANA, L., PARTRIDGE, L. & LONGO, V. D. 2010. Extending healthy life span--from yeast to humans. *Science,* 328**,** 321-6.

FRASER, A. G., KAMATH, R. S., ZIPPERLEN, P., MARTINEZ-CAMPOS, M., SOHRMANN, M. & AHRINGER, J. 2000. Functional genomic analysis of C. elegans chromosome I by systematic RNA interference. *Nature,* 408**,** 325-30.

FUKUSHIGE, T., SIDDIQUI, Z. K., CHOU, M., CULOTTI, J. G., GOGONEA, C. B., SIDDIQUI, S. S. & HAMELIN, M. 1999. MEC-12, an alpha-tubulin required for touch sensitivity in C. elegans. *J Cell Sci,* 112 (Pt 3)**,** 395-403.

GAGLIA, M. M., JEONG, D. E., RYU, E. A., LEE, D., KENYON, C. & LEE, S. J. 2012. Genes That Act Downstream of Sensory Neurons to Influence Longevity, Dauer Formation, and Pathogen Responses in Caenorhabditis elegans. *PLoS Genet,* 8**,** e1003133.

GAMBLIN, T. C., KING, M. E., KURET, J., BERRY, R. W. & BINDER, L. I. 2000. Oxidative regulation of fatty acid-induced tau polymerization. *Biochemistry,* 39**,** 14203-10.

GARIGAN, D., HSU, A. L., FRASER, A. G., KAMATH, R. S., AHRINGER, J. & KENYON, C. 2002. Genetic analysis of tissue aging in Caenorhabditis elegans: a role for heat-shock factor and bacterial proliferation. *Genetics,* 161**,** 1101-12.

GEINISMAN, Y., DE TOLEDO-MORRELL, L. & MORRELL, F. 1986. Loss of perforated synapses in the dentate gyrus: morphological substrate of memory deficit in aged rats. *Proc Natl Acad Sci U S A,* 83**,** 3027-31.

GEINISMAN, Y., DETOLEDO-MORRELL, L., MORRELL, F. & HELLER, R. E. 1995. Hippocampal markers of age-related memory dysfunction: behavioral, electrophysiological and morphological perspectives. *Prog Neurobiol,* 45**,** 223-52.

GEMMA, C., VILA, J., BACHSTETTER, A. & BICKFORD, P. C. 2007. Oxidative Stress and the Aging Brain: From Theory to Prevention. *In:* RIDDLE, D. R. (ed.) *Brain Aging: Models, Methods, and Mechanisms.* Boca Raton (FL).

GEMS, D., SUTTON, A. J., SUNDERMEYER, M. L., ALBERT, P. S., KING, K. V., EDGLEY, M. L., LARSEN, P. L. & RIDDLE, D. L. 1998. Two pleiotropic classes of daf-2 mutation affect larval arrest, adult behavior, reproduction and longevity in Caenorhabditis elegans. *Genetics,* 150**,** 129-55.

GLOVER-CUTTER, K. M., LIN, S. & BLACKWELL, T. K. 2013. Integration of the unfolded protein and oxidative stress responses through SKN-1/Nrf. *PLoS Genet,* 9**,** e1003701.

GOEDERT, M., BAUR, C. P., AHRINGER, J., JAKES, R., HASEGAWA, M., SPILLANTINI, M. G., SMITH, M. J. & HILL, F. 1996. PTL-1, a microtubule-associated protein with tau-like repeats from the nematode Caenorhabditis elegans. *J Cell Sci,* 109 (Pt 11)**,** 2661-72.

GOEDERT, M., HASEGAWA, M., JAKES, R., LAWLER, S., CUENDA, A. & COHEN, P. 1997. Phosphorylation of microtubule-associated protein tau by stress-activated protein kinases. *FEBS Lett,* 409**,** 57-62.

GOMEZ-ISLA, T., HOLLISTER, R., WEST, H., MUI, S., GROWDON, J. H., PETERSEN, R. C., PARISI, J. E. & HYMAN, B. T. 1997. Neuronal loss correlates with but exceeds neurofibrillary tangles in Alzheimer's disease. *Ann Neurol,* 41**,** 17-24.

GORDON, P., HINGULA, L., KRASNY, M. L., SWIENCKOWSKI, J. L., POKRYWKA, N. J. & RALEY-SUSMAN, K. M. 2008. The invertebrate microtubule-associated protein PTL-1 functions in mechanosensation and development in Caenorhabditis elegans. *Dev Genes Evol,* 218**,** 541-51.

GOTZ, J., GLADBACH, A., PENNANEN, L., VAN EERSEL, J., SCHILD, A., DAVID, D. & ITTNER, L. M. 2010. Animal models reveal role for tau phosphorylation in human disease. *Biochim Biophys Acta,* 1802**,** 860-71.

GOTZ, J. & ITTNER, L. M. 2008. Animal models of Alzheimer's disease and frontotemporal dementia. *Nat Rev Neurosci,* 9**,** 532-44.

GOTZ, J., XIA, D., LEINENGA, G., CHEW, Y. L. & NICHOLAS, H. 2013. What Renders TAU Toxic. *Front Neurol,* 4**,** 72.

GUGLIELMOTTO, M., TAMAGNO, E. & DANNI, O. 2009. Oxidative stress and hypoxia contribute to Alzheimer's disease pathogenesis: two sides of the same coin. *ScientificWorldJournal,* 9**,** 781-91.

GUTHRIE, C. R., SCHELLENBERG, G. D. & KRAEMER, B. C. 2009. SUT-2 potentiates tau-induced neurotoxicity in Caenorhabditis elegans. *Hum Mol Genet,* 18**,** 1825-38.

GUZMAN-MARTINEZ, L., FARIAS, G. A. & MACCIONI, R. B. 2013. Tau Oligomers as Potential Targets for Alzheimer's Diagnosis and Novel Drugs. *Front Neurol,* 4**,** 167.

HAITHCOCK, E., DAYANI, Y., NEUFELD, E., ZAHAND, A. J., FEINSTEIN, N., MATTOUT, A., GRUENBAUM, Y. & LIU, J. 2005. Age-related changes of nuclear architecture in Caenorhabditis elegans. *Proc Natl Acad Sci U S A,* 102**,** 16690-5.

HALL, D. H. & RUSSELL, R. L. 1991. The posterior nervous system of the nematode Caenorhabditis elegans: serial reconstruction of identified neurons and complete pattern of synaptic interactions. *J Neurosci,* 11**,** 1-22.

HAMMARLUND, M., NIX, P., HAUTH, L., JORGENSEN, E. M. & BASTIANI, M. 2009. Axon regeneration requires a conserved MAP kinase pathway. *Science,* 323**,** 802-6.

HARADA, A., OGUCHI, K., OKABE, S., KUNO, J., TERADA, S., OHSHIMA, T., SATO-YOSHITAKE, R., TAKEI, Y., NODA, T. & HIROKAWA, N. 1994. Altered microtubule organization in small-calibre axons of mice lacking tau protein. *Nature,* 369**,** 488-91.

HEDDEN, T. & GABRIELI, J. D. 2004. Insights into the ageing mind: a view from cognitive neuroscience. *Nat Rev Neurosci,* 5**,** 87-96.

HERNDON, L. A., SCHMEISSNER, P. J., DUDARONEK, J. M., BROWN, P. A., LISTNER, K. M., SAKANO, Y., PAUPARD, M. C., HALL, D. H. & DRISCOLL, M. 2002. Stochastic and genetic factors influence tissue-specific decline in ageing C. elegans. *Nature,* 419**,** 808-14.

HIROKAWA, N., FUNAKOSHI, T., SATO-HARADA, R. & KANAI, Y. 1996. Selective stabilization of tau in axons and microtubule-associated protein 2C in cell bodies and dendrites contributes to polarized localization of cytoskeletal proteins in mature neurons. *J Cell Biol,* 132**,** 667-79.

HONDA, Y. & HONDA, S. 1999. The daf-2 gene network for longevity regulates oxidative stress resistance and Mn-superoxide dismutase gene expression in Caenorhabditis elegans. *FASEB J,* 13**,** 1385-93.

HONG, M., ZHUKAREVA, V., VOGELSBERG-RAGAGLIA, V., WSZOLEK, Z., REED, L., MILLER, B. I., GESCHWIND, D. H., BIRD, T. D., MCKEEL, D., GOATE, A., MORRIS, J. C., WILHELMSEN, K. C., SCHELLENBERG, G. D., TROJANOWSKI, J. Q. & LEE, V. M. 1998. Mutation-specific functional impairments in distinct tau isoforms of hereditary FTDP-17. *Science,* 282**,** 1914-7.

HUANG, C., XIONG, C. & KORNFELD, K. 2004. Measurements of age-related changes of physiological processes that predict lifespan of Caenorhabditis elegans. *Proc Natl Acad Sci U S A,* 101**,** 8084-9.

HUESTON, J. L., HERREN, G. P., CUEVA, J. G., BUECHNER, M., LUNDQUIST, E. A., GOODMAN, M. B. & SUPRENANT, K. A. 2008. The C. elegans EMAP-like protein, ELP-1 is required for touch sensation and associates with microtubules and adhesion complexes. *BMC Dev Biol,* 8**,** 110.

INGRAM, E. M. & SPILLANTINI, M. G. 2002. Tau gene mutations: dissecting the pathogenesis of FTDP-17. *Trends Mol Med,* 8**,** 555-62.

INOUE, H., HISAMOTO, N., AN, J. H., OLIVEIRA, R. P., NISHIDA, E., BLACKWELL, T. K. & MATSUMOTO, K. 2005. The C. elegans p38 MAPK pathway regulates nuclear localization of the transcription factor SKN-1 in oxidative stress response. *Genes Dev,* 19**,** 2278-83.

IQBAL, K., LIU, F., GONG, C. X. & GRUNDKE-IQBAL, I. 2010. Tau in Alzheimer disease and related tauopathies. *Curr Alzheimer Res,* 7**,** 656-64.

ISHII, N., TAKAHASHI, K., TOMITA, S., KEINO, T., HONDA, S., YOSHINO, K. & SUZUKI, K. 1990. A methyl viologen-sensitive mutant of the nematode Caenorhabditis elegans. *Mutat Res,* 237**,** 165-71.

ITTNER, A., KE, Y. D., VAN EERSEL, J., GLADBACH, A., GOTZ, J. & ITTNER, L. M. 2011. Brief update on different roles of tau in neurodegeneration. *IUBMB Life,* 63**,** 495-502.

ITTNER, L. M., FATH, T., KE, Y. D., BI, M., VAN EERSEL, J., LI, K. M., GUNNING, P. & GOTZ, J. 2008. Parkinsonism and impaired axonal transport in a mouse model of frontotemporal dementia. *Proc Natl Acad Sci U S A,* 105**,** 15997-6002.

ITTNER, L. M. & GOTZ, J. 2011. Amyloid-beta and tau--a toxic pas de deux in Alzheimer's disease. *Nat Rev Neurosci,* 12**,** 65-72.

ITTNER, L. M., KE, Y. D., DELERUE, F., BI, M., GLADBACH, A., VAN EERSEL, J., WOLFING, H., CHIENG, B. C., CHRISTIE, M. J., NAPIER, I. A., ECKERT, A., STAUFENBIEL, M., HARDEMAN, E. & GOTZ, J. 2010. Dendritic function of tau mediates amyloid-beta toxicity in Alzheimer's disease mouse models. *Cell,* 142**,** 387-97.

JO, C., GUNDEMIR, S., PRITCHARD, S., JIN, Y. N., RAHMAN, I. & JOHNSON, G. V. 2014. Nrf2 reduces levels of phosphorylated tau protein by inducing autophagy adaptor protein NDP52. *Nat Commun,* 5**,** 3496.

JOHNSON, G. L. & LAPADAT, R. 2002. Mitogen-activated protein kinase pathways mediated by ERK, JNK, and p38 protein kinases. *Science,* 298**,** 1911-2.

KAHN, N. W., REA, S. L., MOYLE, S., KELL, A. & JOHNSON, T. E. 2008. Proteasomal dysfunction activates the transcription factor SKN-1 and produces a selective oxidative-stress response in Caenorhabditis elegans. *Biochem J,* 409**,** 205-13.

KALETSKY, R. & MURPHY, C. T. 2010. The role of insulin/IGF-like signaling in C. elegans longevity and aging. *Dis Model Mech,* 3**,** 415-9.

KANAAN, N. M., MORFINI, G., PIGINO, G., LAPOINTE, N. E., ANDREADIS, A., SONG, Y., LEITMAN, E., BINDER, L. I. & BRADY, S. T. 2012. Phosphorylation in the amino terminus of tau prevents inhibition of anterograde axonal transport. *Neurobiol Aging,* 33**,** 826 e15-30.

KANG, J. H., COOK, N., MANSON, J., BURING, J. E. & GRODSTEIN, F. 2006. A randomized trial of vitamin E supplementation and cognitive function in women. *Arch Intern Med,* 166**,** 2462-8.

KAYSER, E. B., SEDENSKY, M. M., MORGAN, P. G. & HOPPEL, C. L. 2004. Mitochondrial oxidative phosphorylation is defective in the long-lived mutant clk-1. *J Biol Chem,* 279**,** 54479-86.

KE, Y. D., SUCHOWERSKA, A. K., VAN DER HOVEN, J., DE SILVA, D. M., WU, C. W., VAN EERSEL, J., ITTNER, A. & ITTNER, L. M. 2012. Lessons from tau-deficient mice. *Int J Alzheimers Dis,* 2012**,** 873270.

KENYON, C., CHANG, J., GENSCH, E., RUDNER, A. & TABTIANG, R. 1993. A C. elegans mutant that lives twice as long as wild type. *Nature,* 366**,** 461-4.

KHACHATURIAN, Z. S. 1994. Calcium hypothesis of Alzheimer's disease and brain aging. *Ann N Y Acad Sci,* 747**,** 1-11.

KIM, J., BASAK, J. M. & HOLTZMAN, D. M. 2009. The role of apolipoprotein E in Alzheimer's disease. *Neuron,* 63**,** 287-303.

KIMURA, K. D., RIDDLE, D. L. & RUVKUN, G. 2011. The C. elegans DAF-2 insulin-like receptor is abundantly expressed in the nervous system and regulated by nutritional status. *Cold Spring Harb Symp Quant Biol,* 76**,** 113-20.

KOSIK, K. S. & FINCH, E. A. 1987. MAP2 and tau segregate into dendritic and axonal domains after the elaboration of morphologically distinct neurites: an immunocytochemical study of cultured rat cerebrum. *J Neurosci,* 7**,** 3142-53.

KRAEMER, B. C. & SCHELLENBERG, G. D. 2007. SUT-1 enables tau-induced neurotoxicity in C. elegans. *Hum Mol Genet,* 16**,** 1959-71.

KRAEMER, B. C., ZHANG, B., LEVERENZ, J. B., THOMAS, J. H., TROJANOWSKI, J. Q. & SCHELLENBERG, G. D. 2003. Neurodegeneration and defective neurotransmission in a Caenorhabditis elegans model of tauopathy. *Proc Natl Acad Sci U S A,* 100**,** 9980-5.

KUBOTA, Y., NAGATA, K., SUGIMOTO, A. & NISHIWAKI, K. 2012. Tissue architecture in the Caenorhabditis elegans gonad depends on interactions among fibulin-1, type IV collagen and the ADAMTS extracellular protease. *Genetics,* 190**,** 1379-88.

KYRIAKIS, J. M. & AVRUCH, J. 2001. Mammalian mitogen-activated protein kinase signal transduction pathways activated by stress and inflammation. *Physiol Rev,* 81**,** 807-69.

LAPOINTE, J. & HEKIMI, S. 2008. Early mitochondrial dysfunction in long-lived Mclk1+/- mice. *J Biol Chem,* 283**,** 26217-27.

LARSEN, P. L., ALBERT, P. S. & RIDDLE, D. L. 1995. Genes that regulate both development and longevity in Caenorhabditis elegans. *Genetics,* 139**,** 1567-83.

LEE, G. & LEUGERS, C. J. 2012. Tau and tauopathies. *Prog Mol Biol Transl Sci,* 107**,** 263-93.

LEE, G. & ROOK, S. L. 1992. Expression of tau protein in non-neuronal cells: microtubule binding and stabilization. *J Cell Sci,* 102 (Pt 2)**,** 227-37.

LEE, R. Y., HENCH, J. & RUVKUN, G. 2001a. Regulation of C. elegans DAF-16 and its human ortholog FKHRL1 by the daf-2 insulin-like signaling pathway. *Curr Biol,* 11**,** 1950-7.

LEE, S. J. & KENYON, C. 2009. Regulation of the longevity response to temperature by thermosensory neurons in Caenorhabditis elegans. *Curr Biol,* 19**,** 715-22.

LEE, V. M., GOEDERT, M. & TROJANOWSKI, J. Q. 2001b. Neurodegenerative tauopathies. *Annu Rev Neurosci,* 24**,** 1121-59.

LEISER, S. F. & MILLER, R. A. 2010. Nrf2 signaling, a mechanism for cellular stress resistance in long-lived mice. *Mol Cell Biol,* 30**,** 871-84.

LEWIS, J. A., WU, C. H., LEVINE, J. H. & BERG, H. 1980. Levamisole-resistant mutants of the nematode Caenorhabditis elegans appear to lack pharmacological acetylcholine receptors. *Neuroscience,* 5**,** 967-89.

LEWIS, K. N., MELE, J., HAYES, J. D. & BUFFENSTEIN, R. 2010. Nrf2, a guardian of healthspan and gatekeeper of species longevity. *Integr Comp Biol,* 50**,** 829-43.

LI, W. H., SHI, Y. C., CHANG, C. H., HUANG, C. W. & HSIU-CHUAN LIAO, V. 2014. Selenite protects Caenorhabditis elegans from oxidative stress via DAF-16 and TRXR-1. *Mol Nutr Food Res,* 58**,** 863-74.

LIAO, V. H. & YU, C. W. 2005. Caenorhabditis elegans gcs-1 confers resistance to arsenic-induced oxidative stress. *Biometals,* 18**,** 519-28.

LIBINA, N., BERMAN, J. R. & KENYON, C. 2003. Tissue-specific activities of C. elegans DAF-16 in the regulation of lifespan. *Cell,* 115**,** 489-502.

LIM, D., ROH, J. Y., EOM, H. J., CHOI, J. Y., HYUN, J. & CHOI, J. 2012. Oxidative stress-related PMK-1 P38 MAPK activation as a mechanism for toxicity of silver nanoparticles to reproduction in the nematode Caenorhabditis elegans. *Environ Toxicol Chem,* 31**,** 585-92.

LIN, X. G., MING, M., CHEN, M. R., NIU, W. P., ZHANG, Y. D., LIU, B., JIU, Y. M., YU, J. W., XU, T. & WU, Z. X. 2010. UNC-31/CAPS docks and primes dense core vesicles in C. elegans neurons. *Biochem Biophys Res Commun,* 397**,** 526-31.

LOVESTONE, S., REYNOLDS, C. H., LATIMER, D., DAVIS, D. R., ANDERTON, B. H., GALLO, J. M., HANGER, D., MULOT, S., MARQUARDT, B., STABEL, S. & ET AL. 1994. Alzheimer's disease-like phosphorylation of the microtubule-associated protein tau by glycogen synthase kinase-3 in transfected mammalian cells. *Curr Biol,* 4**,** 1077-86.

MACHIN, D., CHEUNG, Y. & PARMAR, M. 2006. *Survival Analysis: A Practical Approach*, Wiley, NJ.

MADISON, J. M., NURRISH, S. & KAPLAN, J. M. 2005. UNC-13 interaction with syntaxin is required for synaptic transmission. *Curr Biol,* 15**,** 2236-42.

MAHONEY, T. R., LIU, Q., ITOH, T., LUO, S., HADWIGER, G., VINCENT, R., WANG, Z. W., FUKUDA, M. & NONET, M. L. 2006. Regulation of synaptic transmission by RAB-3 and RAB-27 in Caenorhabditis elegans. *Mol Biol Cell,* 17**,** 2617-25.

MANDELKOW, E. M., BIERNAT, J., DREWES, G., STEINER, B., LICHTENBERG-KRAAG, B., WILLE, H., GUSTKE, N. & MANDELKOW, E. 1993. Microtubule-associated protein tau, paired helical filaments, and phosphorylation. *Ann N Y Acad Sci,* 695**,** 209-16.

MARGETA, M. A., WANG, G. J. & SHEN, K. 2009. Clathrin adaptor AP-1 complex excludes multiple postsynaptic receptors from axons in C. elegans. *Proc Natl Acad Sci U S A,* 106**,** 1632-7.

MATSUMOTO, A. 1998. Synaptic changes in the perineal motoneurons of aged male rats. *Journal of Comparative Neurology,* 400**,** 103-109.

MCCORMICK, A. V., WHEELER, J. M., GUTHRIE, C. R., LIACHKO, N. F. & KRAEMER, B. C. 2013. Dopamine D2 receptor antagonism suppresses tau aggregation and neurotoxicity. *Biol Psychiatry,* 73**,** 464-71.

MCDERMOTT, J. B., AAMODT, S. & AAMODT, E. 1996. ptl-1, a Caenorhabditis elegans gene whose products are homologous to the tau microtubule-associated proteins. *Biochemistry,* 35**,** 9415-23.

MCINTIRE, S. L., REIMER, R. J., SCHUSKE, K., EDWARDS, R. H. & JORGENSEN, E. M. 1997. Identification and characterization of the vesicular GABA transporter. *Nature,* 389**,** 870-6.

MCKAY, S. J., JOHNSEN, R., KHATTRA, J., ASANO, J., BAILLIE, D. L., CHAN, S., DUBE, N., FANG, L., GOSZCZYNSKI, B., HA, E., HALFNIGHT, E., HOLLEBAKKEN, R., HUANG, P., HUNG, K., JENSEN, V., JONES, S. J., KAI, H., LI, D., MAH, A., MARRA, M., MCGHEE, J., NEWBURY, R., POUZYREV, A., RIDDLE, D. L., SONNHAMMER, E., TIAN, H., TU, D., TYSON, J. R., VATCHER, G., WARNER, A., WONG, K., ZHAO, Z. & MOERMAN, D. G. 2003. Gene expression profiling of cells, tissues, and developmental stages of the nematode C. elegans. *Cold Spring Harb Symp Quant Biol,* 68**,** 159-69.

MIYASAKA, T., DING, Z., GENGYO-ANDO, K., OUE, M., YAMAGUCHI, H., MITANI, S. & IHARA, Y. 2005. Progressive neurodegeneration in C. elegans model of tauopathy. *Neurobiol Dis,* 20**,** 372-83.

MORLEY, J. F. & MORIMOTO, R. I. 2004. Regulation of longevity in Caenorhabditis elegans by heat shock factor and molecular chaperones. *Mol Biol Cell,* 15**,** 657-64.

MURPHY, C. T., LEE, S. J. & KENYON, C. 2007. Tissue entrainment by feedback regulation of insulin gene expression in the endoderm of Caenorhabditis elegans. *Proc Natl Acad Sci U S A,* 104**,** 19046-50.

NAIDOO, N., FERBER, M., MASTER, M., ZHU, Y. & PACK, A. I. 2008. Aging impairs the unfolded protein response to sleep deprivation and leads to proapoptotic signaling. *J Neurosci,* 28**,** 6539-48.

O'BRIEN, R. J. & WONG, P. C. 2011. Amyloid precursor protein processing and Alzheimer's disease. *Annu Rev Neurosci,* 34**,** 185-204.

O'LEARY, J. C., 3RD, LI, Q., MARINEC, P., BLAIR, L. J., CONGDON, E. E., JOHNSON, A. G., JINWAL, U. K., KOREN, J., 3RD, JONES, J. R., KRAFT, C., PETERS, M., ABISAMBRA, J. F., DUFF, K. E., WEEBER, E. J., GESTWICKI, J. E. & DICKEY, C. A. 2010. Phenothiazine-mediated rescue of cognition in tau transgenic mice requires neuroprotection and reduced soluble tau burden. *Mol Neurodegener,* 5**,** 45.

OGG, S., PARADIS, S., GOTTLIEB, S., PATTERSON, G. I., LEE, L., TISSENBAUM, H. A. & RUVKUN, G. 1997. The Fork head transcription factor DAF-16 transduces insulin-like metabolic and longevity signals in C. elegans. *Nature,* 389**,** 994-9.

OH, S. W., MUKHOPADHYAY, A., SVRZIKAPA, N., JIANG, F., DAVIS, R. J. & TISSENBAUM, H. A. 2005. JNK regulates lifespan in Caenorhabditis elegans by modulating nuclear translocation of forkhead transcription factor/DAF-16. *Proc Natl Acad Sci U S A,* 102**,** 4494-9.

OKUYAMA, T., INOUE, H., OOKUMA, S., SATOH, T., KANO, K., HONJOH, S., HISAMOTO, N., MATSUMOTO, K. & NISHIDA, E. 2010. The ERK-MAPK pathway regulates longevity through SKN-1 and insulin-like signaling in Caenorhabditis elegans. *J Biol Chem,* 285**,** 30274-81.

OLIVEIRA, R. P., PORTER ABATE, J., DILKS, K., LANDIS, J., ASHRAF, J., MURPHY, C. T. & BLACKWELL, T. K. 2009. Condition-adapted stress and longevity gene regulation by Caenorhabditis elegans SKN-1/Nrf. *Aging Cell,* 8**,** 524-41.

PAEK, J., LO, J. Y., NARASIMHAN, S. D., NGUYEN, T. N., GLOVER-CUTTER, K., ROBIDA-STUBBS, S., SUZUKI, T., YAMAMOTO, M., BLACKWELL, T. K. &

CURRAN, S. P. 2012. Mitochondrial SKN-1/Nrf mediates a conserved starvation response. *Cell Metab,* 16**,** 526-37.

PAN, C. L., PENG, C. Y., CHEN, C. H. & MCINTIRE, S. 2011. Genetic analysis of age-dependent defects of the Caenorhabditis elegans touch receptor neurons. *Proc Natl Acad Sci U S A,* 108**,** 9274-9.

PAPP, D., CSERMELY, P. & SOTI, C. 2012. A role for SKN-1/Nrf in pathogen resistance and immunosenescence in Caenorhabditis elegans. *PLoS Pathog,* 8**,** e1002673.

PARK, S. K., TEDESCO, P. M. & JOHNSON, T. E. 2009. Oxidative stress and longevity in Caenorhabditis elegans as mediated by SKN-1. *Aging Cell,* 8**,** 258-69.

PETERSEN, R. C., THOMAS, R. G., GRUNDMAN, M., BENNETT, D., DOODY, R., FERRIS, S., GALASKO, D., JIN, S., KAYE, J., LEVEY, A., PFEIFFER, E., SANO, M., VAN DYCK, C. H., THAL, L. J. & ALZHEIMER'S DISEASE COOPERATIVE STUDY, G. 2005. Vitamin E and donepezil for the treatment of mild cognitive impairment. *N Engl J Med,* 352**,** 2379-88.

POLLEY, S. R., KUZMANOV, A., KUANG, J., KARPEL, J., LAZETIC, V., KARINA, E. I., VEO, B. L. & FAY, D. S. 2014. Implicating SCF complexes in organogenesis in Caenorhabditis elegans. *Genetics,* 196**,** 211-23.

PRAITIS, V., CASEY, E., COLLAR, D. & AUSTIN, J. 2001. Creation of low-copy integrated transgenic lines in Caenorhabditis elegans. *Genetics,* 157**,** 1217-26.

PROKOCIMER, M., BARKAN, R. & GRUENBAUM, Y. 2013. Hutchinson-Gilford progeria syndrome through the lens of transcription. *Aging Cell*.

PRZYBYSZ, A. J., CHOE, K. P., ROBERTS, L. J. & STRANGE, K. 2009. Increased age reduces DAF-16 and SKN-1 signaling and the hormetic response of Caenorhabditis elegans to the xenobiotic juglone. *Mech Ageing Dev,* 130**,** 357-69.

RAIZEN, D. M., LEE, R. Y. & AVERY, L. 1995. Interacting genes required for pharyngeal excitation by motor neuron MC in Caenorhabditis elegans. *Genetics,* 141**,** 1365-82.

RAND, J. B. 2007. Acetylcholine. *WormBook.*

RAPOPORT, M., DAWSON, H. N., BINDER, L. I., VITEK, M. P. & FERREIRA, A. 2002. Tau is essential to beta -amyloid-induced neurotoxicity. *Proc Natl Acad Sci U S A,* 99**,** 6364-9.

REA, S. L., VENTURA, N. & JOHNSON, T. E. 2007. Relationship between mitochondrial electron transport chain dysfunction, development, and life extension in Caenorhabditis elegans. *PLoS Biol,* 5**,** e259.

REYNOLDS, C. H., NEBREDA, A. R., GIBB, G. M., UTTON, M. A. & ANDERTON, B. H. 1997. Reactivating kinase/p38 phosphorylates tau protein in vitro. *J Neurochem,* 69**,** 191-8.

RICHMOND, J. E., DAVIS, W. S. & JORGENSEN, E. M. 1999. UNC-13 is required for synaptic vesicle fusion in C. elegans. *Nat Neurosci,* 2**,** 959-64.

RICHMOND, J. E. & JORGENSEN, E. M. 1999. One GABA and two acetylcholine receptors function at the C. elegans neuromuscular junction. *Nat Neurosci,* 2**,** 791-7.

RIDDLE, D. L., SWANSON, M. M. & ALBERT, P. S. 1981. Interacting genes in nematode dauer larva formation. *Nature,* 290**,** 668-71.

ROBERSON, E. D., SCEARCE-LEVIE, K., PALOP, J. J., YAN, F., CHENG, I. H., WU, T., GERSTEIN, H., YU, G. Q. & MUCKE, L. 2007. Reducing endogenous tau ameliorates amyloid beta-induced deficits in an Alzheimer's disease mouse model. *Science,* 316**,** 750-4.

ROBIDA-STUBBS, S., GLOVER-CUTTER, K., LAMMING, D. W., MIZUNUMA, M., NARASIMHAN, S. D., NEUMANN-HAEFELIN, E., SABATINI, D. M. & BLACKWELL, T. K. 2012. TOR signaling and rapamycin influence longevity by regulating SKN-1/Nrf and DAF-16/FoxO. *Cell Metab,* 15**,** 713-24.

SANZ, A. & STEFANATOS, R. K. 2008. The mitochondrial free radical theory of aging: a critical view. *Curr Aging Sci,* 1**,** 10-21.

SAVAGE, C., XUE, Y., MITANI, S., HALL, D., ZAKHARY, R. & CHALFIE, M. 1994. Mutations in the Caenorhabditis elegans beta-tubulin gene mec-7: effects on microtubule assembly and stability and on tubulin autoregulation. *J Cell Sci,* 107 (Pt 8)**,** 2165-75.

SCHAFER, J. C., WINKELBAUER, M. E., WILLIAMS, C. L., HAYCRAFT, C. J., DESMOND, R. A. & YODER, B. K. 2006. IFTA-2 is a conserved cilia protein involved in pathways regulating longevity and dauer formation in Caenorhabditis elegans. *J Cell Sci,* 119**,** 4088-100.

SCHNEIDER, C. A., RASBAND, W. S. & ELICEIRI, K. W. 2012. NIH Image to ImageJ: 25 years of image analysis. *Nat Methods,* 9**,** 671-5.

SEMPLE, J. I., BIONDINI, L. & LEHNER, B. 2012. Generating transgenic nematodes by bombardment and antibiotic selection. *Nat Methods,* 9**,** 118-9.

SHEN, J. & KELLEHER, R. J., 3RD 2007. The presenilin hypothesis of Alzheimer's disease: evidence for a loss-of-function pathogenic mechanism. *Proc Natl Acad Sci U S A,* 104**,** 403-9.

SINGH, P. P., SINGH, M. & MASTANA, S. S. 2006. APOE distribution in world populations with new data from India and the UK. *Ann Hum Biol,* 33**,** 279-308.

SONTAG, J. M., NUNBHAKDI-CRAIG, V., WHITE, C. L., 3RD, HALPAIN, S. & SONTAG, E. 2012. The protein phosphatase PP2A/Balpha binds to the microtubule-associated proteins Tau and MAP2 at a motif also recognized by the kinase Fyn: implications for tauopathies. *J Biol Chem,* 287**,** 14984-93.

STAAB, T. A., EGRAFOV, O., KNOWLES, J. A. & SIEBURTH, D. 2014. Regulation of Synaptic nlg-1/Neuroligin Abundance by the skn-1/Nrf Stress Response Pathway Protects against Oxidative Stress. *PLoS Genet,* 10**,** e1004100.

STAAB, T. A., GRIFFEN, T. C., CORCORAN, C., EVGRAFOV, O., KNOWLES, J. A. & SIEBURTH, D. 2013. The conserved SKN-1/Nrf2 stress response pathway regulates synaptic function in Caenorhabditis elegans. *PLoS Genet,* 9**,** e1003354.

STACK, C., JAINUDDIN, S., ELIPENAHLI, C., GERGES, M., STARKOVA, N., STARKOV, A. A., JOVE, M., PORTERO-OTIN, M., LAUNAY, N., PUJOL, A., KAIDERY, N. A., THOMAS, B., TAMPELLINI, D., BEAL, M. F. & DUMONT, M. 2014. Methylene blue upregulates Nrf2/ARE genes and prevents tau-related neurotoxicity. *Hum Mol Genet*.

SU, B., WANG, X., LEE, H. G., TABATON, M., PERRY, G., SMITH, M. A. & ZHU, X. 2010. Chronic oxidative stress causes increased tau phosphorylation in M17 neuroblastoma cells. *Neurosci Lett,* 468**,** 267-71.

TANAKA-HINO, M., SAGASTI, A., HISAMOTO, N., KAWASAKI, M., NAKANO, S., NINOMIYA-TSUJI, J., BARGMANN, C. I. & MATSUMOTO, K. 2002. SEK-1 MAPKK mediates Ca2+ signaling to determine neuronal asymmetric development in Caenorhabditis elegans. *EMBO Rep,* 3**,** 56-62.

TANK, E. M., RODGERS, K. E. & KENYON, C. 2011. Spontaneous age-related neurite branching in Caenorhabditis elegans. *J Neurosci,* 31**,** 9279-88.

THINAKARAN, G. & KOO, E. H. 2008. Amyloid precursor protein trafficking, processing, and function. *J Biol Chem,* 283**,** 29615-9.

TIEN, N. W., WU, G. H., HSU, C. C., CHANG, C. Y. & WAGNER, O. I. 2011. Tau/PTL-1 associates with kinesin-3 KIF1A/UNC-104 and affects the motor's motility characteristics in C. elegans neurons. *Neurobiol Dis,* 43**,** 495-506.

TIMMONS, L., COURT, D. L. & FIRE, A. 2001. Ingestion of bacterially expressed dsRNAs can produce specific and potent genetic interference in Caenorhabditis elegans. *Gene,* 263**,** 103-12.

TIMMONS, L. & FIRE, A. 1998. Specific interference by ingested dsRNA. *Nature,* 395**,** 854.

TIRABOSCHI, P., HANSEN, L. A., MASLIAH, E., ALFORD, M., THAL, L. J. & COREY-BLOOM, J. 2004. Impact of APOE genotype on neuropathologic and neurochemical markers of Alzheimer disease. *Neurology,* 62**,** 1977-83.

TOKUDA, T., CALERO, M., MATSUBARA, E., VIDAL, R., KUMAR, A., PERMANNE, B., ZLOKOVIC, B., SMITH, J. D., LADU, M. J., ROSTAGNO, A., FRANGIONE, B. & GHISO, J. 2000. Lipidation of apolipoprotein E influences its isoform-specific interaction with Alzheimer's amyloid beta peptides. *Biochem J,* 348 Pt 2**,** 359-65.

TOTH, M. L., MELENTIJEVIC, I., SHAH, L., BHATIA, A., LU, K., TALWAR, A., NAJI, H., IBANEZ-VENTOSO, C., GHOSE, P., JEVINCE, A., XUE, J., HERNDON, L. A., BHANOT, G., RONGO, C., HALL, D. H. & DRISCOLL, M. 2012. Neurite Sprouting and Synapse Deterioration in the Aging Caenorhabditis elegans Nervous System. *J Neurosci,* 32**,** 8778-8790.

TUCKER, K. L., MEYER, M. & BARDE, Y. A. 2001. Neurotrophins are required for nerve growth during development. *Nat Neurosci,* 4**,** 29-37.

TULLET, J. M., HERTWECK, M., AN, J. H., BAKER, J., HWANG, J. Y., LIU, S., OLIVEIRA, R. P., BAUMEISTER, R. & BLACKWELL, T. K. 2008. Direct inhibition of the longevity-promoting factor SKN-1 by insulin-like signaling in C. elegans. *Cell,* 132**,** 1025-38.

VILLANUEVA, A., LOZANO, J., MORALES, A., LIN, X., DENG, X., HENGARTNER, M. O. & KOLESNICK, R. N. 2001. jkk-1 and mek-1 regulate body movement coordination and response to heavy metals through jnk-1 in Caenorhabditis elegans. *EMBO J,* 20**,** 5114-28.

VOGEL, B. E. & HEDGECOCK, E. M. 2001. Hemicentin, a conserved extracellular member of the immunoglobulin superfamily, organizes epithelial and other cell attachments into oriented line-shaped junctions. *Development,* 128**,** 883-94.

VOWELS, J. J. & THOMAS, J. H. 1992. Genetic analysis of chemosensory control of dauer formation in Caenorhabditis elegans. *Genetics,* 130**,** 105-23.

WADA, A. 2009. GSK-3 inhibitors and insulin receptor signaling in health, disease, and therapeutics. *Front Biosci (Landmark Ed),* 14**,** 1558-70.

WADE-MARTINS, R. 2012. Genetics: The MAPT locus-a genetic paradigm in disease susceptibility. *Nat Rev Neurol,* 8**,** 477-8.

WANG, J., ROBIDA-STUBBS, S., TULLET, J. M., RUAL, J. F., VIDAL, M. & BLACKWELL, T. K. 2010. RNAi screening implicates a SKN-1-dependent transcriptional response in stress resistance and longevity deriving from translation inhibition. *PLoS Genet,* 6.

WEINGARTEN, M. D., LOCKWOOD, A. H., HWO, S. Y. & KIRSCHNER, M. W. 1975. A protein factor essential for microtubule assembly. *Proc Natl Acad Sci U S A,* 72**,** 1858-62.

WES, P. D. & BARGMANN, C. I. 2001. C. elegans odour discrimination requires asymmetric diversity in olfactory neurons. *Nature,* 410**,** 698-701.

WHITE, J. G., SOUTHGATE, E., THOMSON, J. N. & BRENNER, S. 1986. The structure of the nervous system of the nematode Caenorhabditis elegans. *Philos Trans R Soc Lond B Biol Sci,* 314**,** 1-340.

WHO 2012. Dementia: a public health priority.

WINSTON, W. M., MOLODOWITCH, C. & HUNTER, C. P. 2002. Systemic RNAi in C. elegans requires the putative transmembrane protein SID-1. *Science,* 295**,** 2456-9.

WITMAN, G. B., CLEVELAND, D. W., WEINGARTEN, M. D. & KIRSCHNER, M. W. 1976. Tubulin requires tau for growth onto microtubule initiating sites. *Proc Natl Acad Sci U S A,* 73**,** 4070-4.

WOLKOW, C. A., KIMURA, K. D., LEE, M. S. & RUVKUN, G. 2000. Regulation of C. elegans life-span by insulinlike signaling in the nervous system. *Science,* 290**,** 147-50.

YAFFE, K., CLEMONS, T. E., MCBEE, W. L., LINDBLAD, A. S. & AGE-RELATED EYE DISEASE STUDY RESEARCH, G. 2004. Impact of antioxidants, zinc, and copper on cognition in the elderly: a randomized, controlled trial. *Neurology,* 63**,** 1705-7.

YANKNER, B. A., LU, T. & LOERCH, P. 2008. The aging brain. *Annu Rev Pathol,* 3**,** 41-66.

YOUNGMAN, M. J., ROGERS, Z. N. & KIM, D. H. 2011. A decline in p38 MAPK signaling underlies immunosenescence in Caenorhabditis elegans. *PLoS Genet,* 7**,** e1002082.

ZHAO, Y. & ZHAO, B. 2013. Oxidative stress and the pathogenesis of Alzheimer's disease. *Oxid Med Cell Longev,* 2013**,** 316523.

ZHENG-FISCHHOFER, Q., BIERNAT, J., MANDELKOW, E. M., ILLENBERGER, S., GODEMANN, R. & MANDELKOW, E. 1998. Sequential phosphorylation of Tau by glycogen synthase kinase-3beta and protein kinase A at Thr212 and Ser214 generates the Alzheimer-specific epitope of antibody AT100 and requires a paired-helical-filament-like conformation. *Eur J Biochem,* 252**,** 542-52.

ZHOU, K. I., PINCUS, Z. & SLACK, F. J. 2011. Longevity and stress in Caenorhabditis elegans. *Aging (Albany NY),* 3**,** 733-53.

ZHU, X., ROTTKAMP, C. A., BOUX, H., TAKEDA, A., PERRY, G. & SMITH, M. A. 2000. Activation of p38 kinase links tau phosphorylation, oxidative stress, and cell cycle-related events in Alzheimer disease. *J Neuropathol Exp Neurol,* 59**,** 880-8.

Appendices

Appendix 1

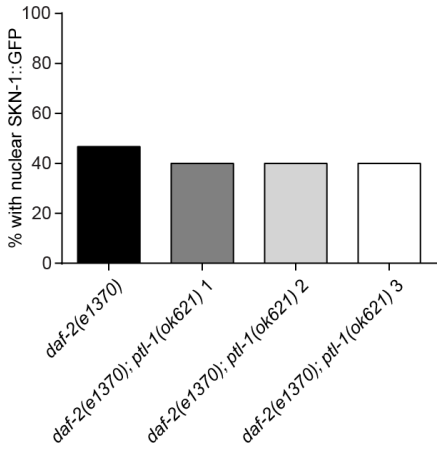

Appendix 1: Three distinct *daf-2(e1370)ptl-1(ok621)* recombinant lines are not substantially different from *daf-2(e1370)* single mutant animals in regulating the re-localisation of SKN-1::GFP to the intestinal nucleus in response to stress. Recombinant lines were generating by crossing *ptl-1(ok621) III* males with *daf-2(e1370)* hermaphrodites and genotyping >100 animals to isolate rare recombinants. No nuclear SKN-1::GFP was observed in untreated animals. n=15 per genotype.

Appendix 2

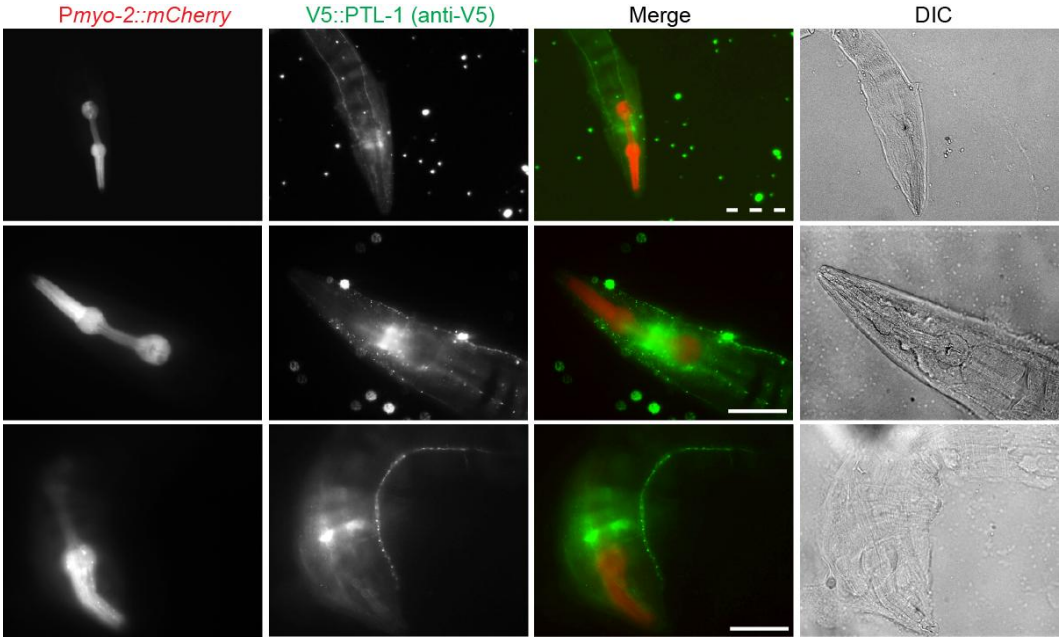

Appendix 2: The V5::PTL-1 transgene expressed from the *ptl-1* promoter is widely expressed in neurons. Immunofluorescence micrographs showing the expression of the V5::PTL-1 transgene (anti-V5 antibody). The

P*myo-2::mCherry* co-transformation marker is also shown. All images show clear anti-V5 immunostaining in the nerve ring in the head and in axons. Scale, dotted line 50 µm, solid line 20 µm.

Appendix 3

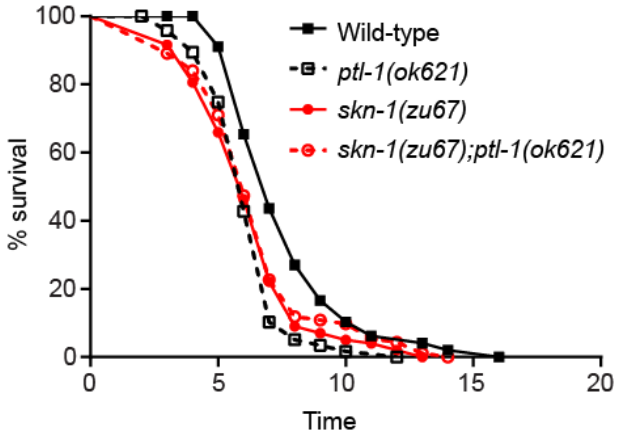

Comparison	Log rank test	Gehan-Breslow-Wilcoxon test
Wild-type vs. *ptl-1(ok621)*	<0.05	<0.05
Wild-type vs. *skn-1(zu67)*	<0.05	<0.05
Wild-type vs. *ptl-1(ok621);skn-1(zu67)*	<0.05	<0.05
skn-1(zu67) vs. *ptl-1(ok621)*	n.s.	n.s.
ptl-1(ok621);skn-1(zu67) vs. *ptl-1(ok621)*	n.s.	n.s.
skn-1(zu67) vs. *ptl-1(ok621);skn-1(zu67)*	n.s.	n.s.

Appendix 3: *ptl-1(ok621);skn-1(zu67)* double mutant animals are not significantly shorter or longer lived compared to *ptl-1(ok621)* or *skn-1(zu67)* single mutant animals. Survival curves for *skn-1(zu67)* and *ptl-1(ok621)* single mutants together with the *skn-1(zu67);ptl-1(ok621)* double mutant strain. n = 120 at day 0. Results of statistical analysis are indicated by p-values underneath each graph. Lifespan experiments were conducted twice independently and the results of one lifespan experiment are shown. Data from the first experiment are shown in **Figure 4.15**. Median lifespans are 7 days (wild-type), 7 days (*ptl-1(ok621)*), 6 days (*skn-1(zu67)*), and 6 days (*skn-1(zu67);ptl-1(ok621)*).

Appendix 4

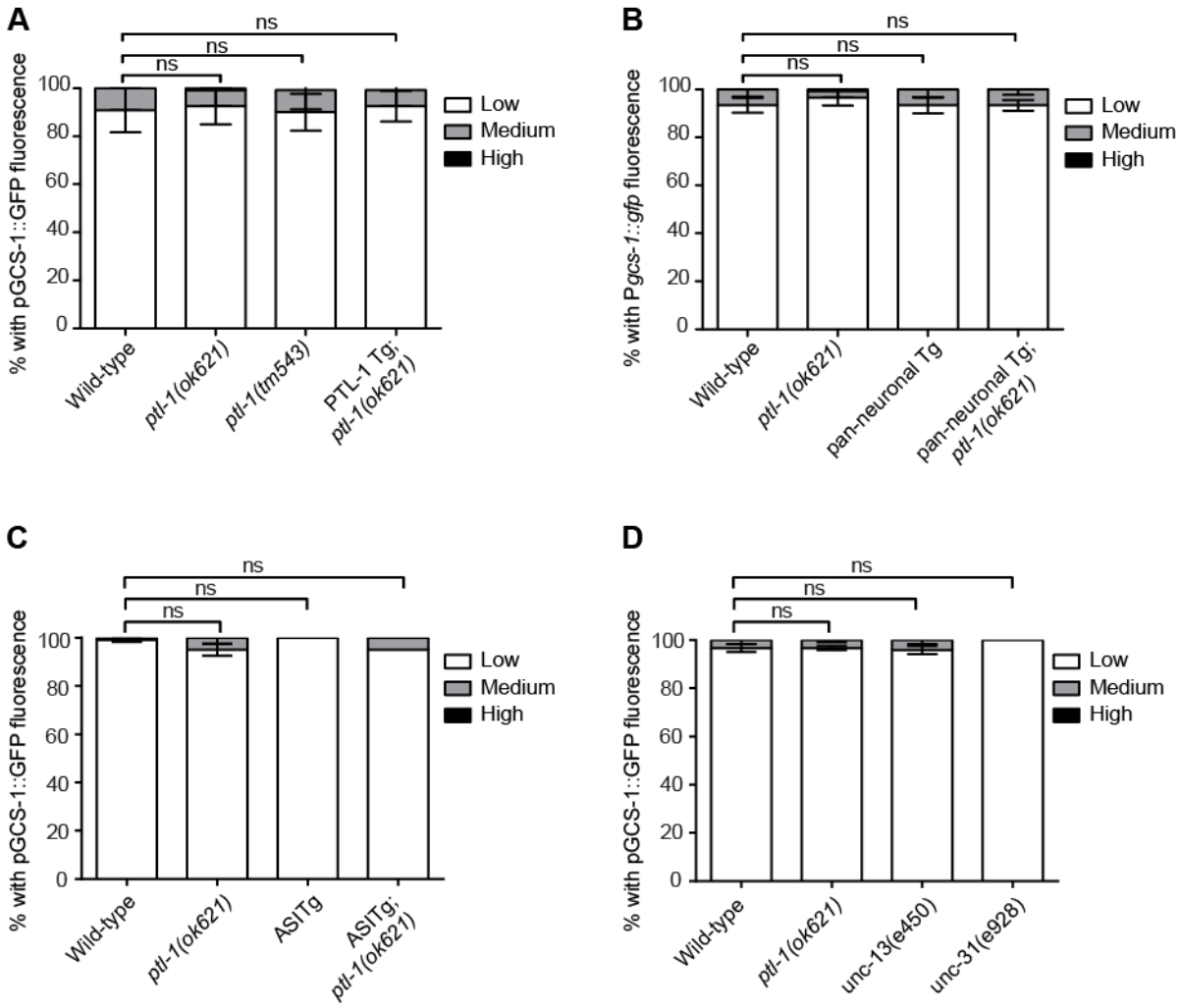

Appendix 4: Non-stressed animals display a low basal induction of P*gcs-1::gfp*. Day one adult animals were assayed at the same time as the relevant strains incubated with sodium azide (**Chapter 4, section 4.1**). If the transgenic line has been crossed into the *ptl-1(ok621)* mutant background this is indicated by "*ptl-1(ok621)"* stated following the transgene name. P*gcs-1::gfp* fluorescence is shown in non-stressed animals for **A)** transgenic lines expressing PTL-1 under the regulation of the *ptl-1* promoter ("PTL-1 Tg"), **B)** transgenic lines expressing PTL-1 in neurons using the *aex-3* promoter ("pan-neuronal Tg"), **C)** transgenic lines expressing PTL-1 in ASI neurons using the *gpa-4* promoter, and **D)** *unc-13(e450)* and *unc-31(e928)* mutant animals. The graphs show averaged data from 3 independent experiments. Scoring was conducted as in (Wang et al., 2010). p-value: ns=not significant.

Appendix 5

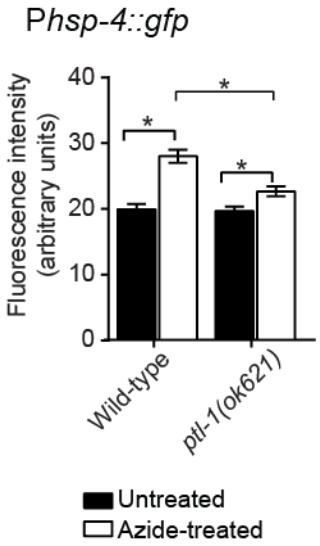

Appendix 5: *ptl-1(ok621)* mutant animals display a lower induction of P*hsp-4::gfp (zcIs4)* compared with wild-type in response to azide stress. 20 young adult animals of each genotype were assayed per replicate. GFP signal from the posterior end of the worm to the anterior-most portion of the intestine was quantified using ImageJ software. The graphs show averaged data from 2 independent experiments. Error bars indicate mean ±SEM. Statistical analysis: one-way ANOVA (GraphPad Prism). p-value: ns=not significant, *<0.05.

Appendix 6

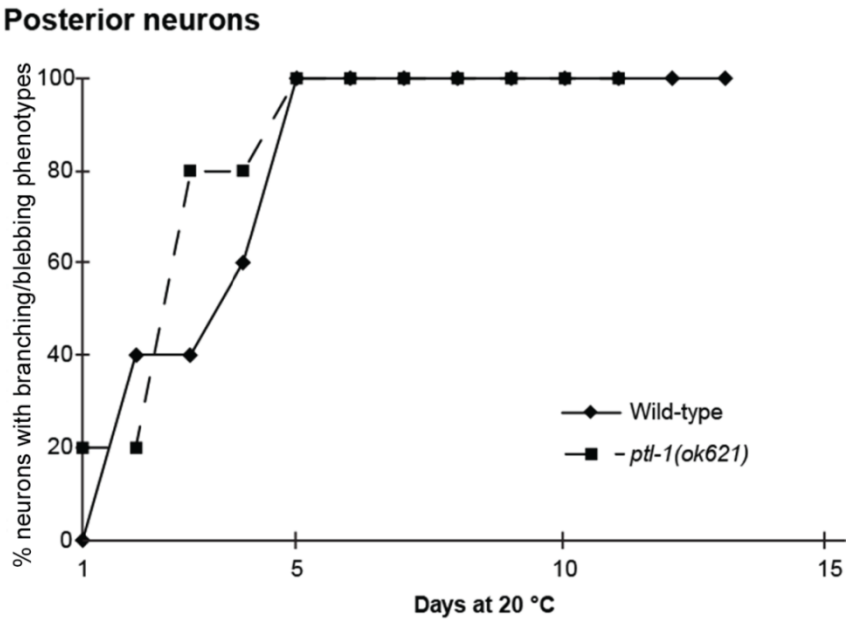

Appendix 6: Percentage of branching/blebbing observed in the posterior touch receptor neurons of wild-type and *ptl-1(ok621)* animals (n =5) assayed in a longitudinal experiment. Compared with anterior touch neurons assayed at the same stages of adulthood (**Figure 4.2**), the incidence of branching/blebbing structures appears to be higher in the posterior neurons.

Appendix 7

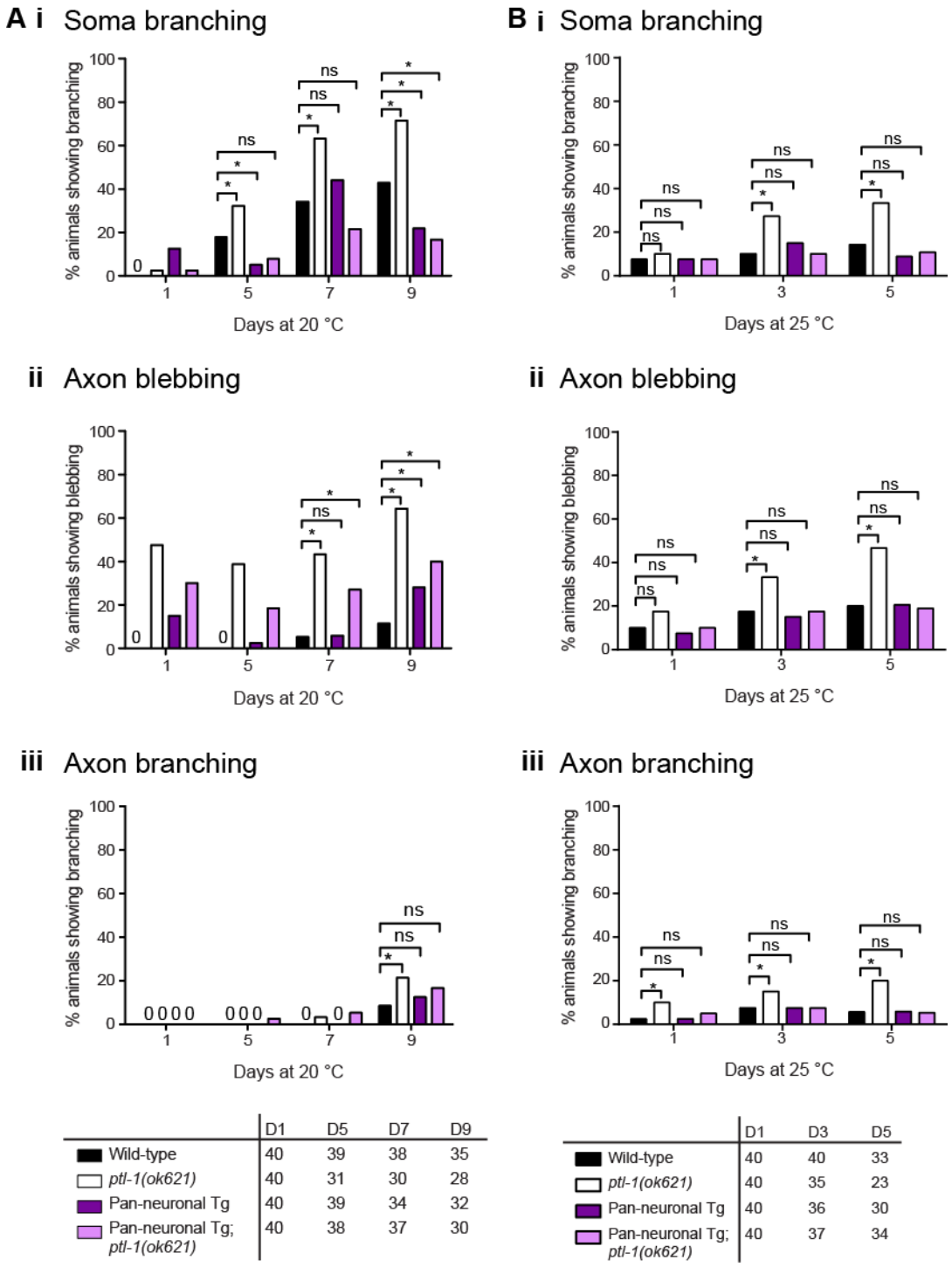

	D1	D5	D7	D9
Wild-type	40	39	38	35
ptl-1(ok621)	40	31	30	28
Pan-neuronal Tg	40	39	34	32
Pan-neuronal Tg; *ptl-1(ok621)*	40	38	37	30

	D1	D3	D5
Wild-type	40	40	33
ptl-1(ok621)	40	35	23
Pan-neuronal Tg	40	36	30
Pan-neuronal Tg; *ptl-1(ok621)*	40	37	34

Appendix 7: Pan-neuronal re-expression of PTL-1 rescues the neuronal ageing phenotype in TRNs that is observed in the *ptl-1(ok621)* null mutant. The TRNs were visualised using the P*mec-4*::*gfp (zdIs5)* reporter. The presence of the *ptl-1(ok621)* mutation in the genetic background of each transgenic line is indicated by the addition

of "*ptl-1(ok621)"* in the strain name. Neuron imaging assay conducted at **A)** 20 °C or **B)** 25 °C for pan-neuronal transgenic worms ("Pan-neuronal Tg") showing (i) cell body branching, (ii) axon blebbing, and (iii) axon branching. The chi-squared statistical test was used to determine statistical significance. P-value is indicated by ns = not significant, *<0.05. The sample size for each strain at each time point is given in the table underneath the graphs. Experiments were conducted twice independently, and the representative data shown are from one experiment. Data from the first experiment are shown in **Figure 6.1.**

Appendix 8

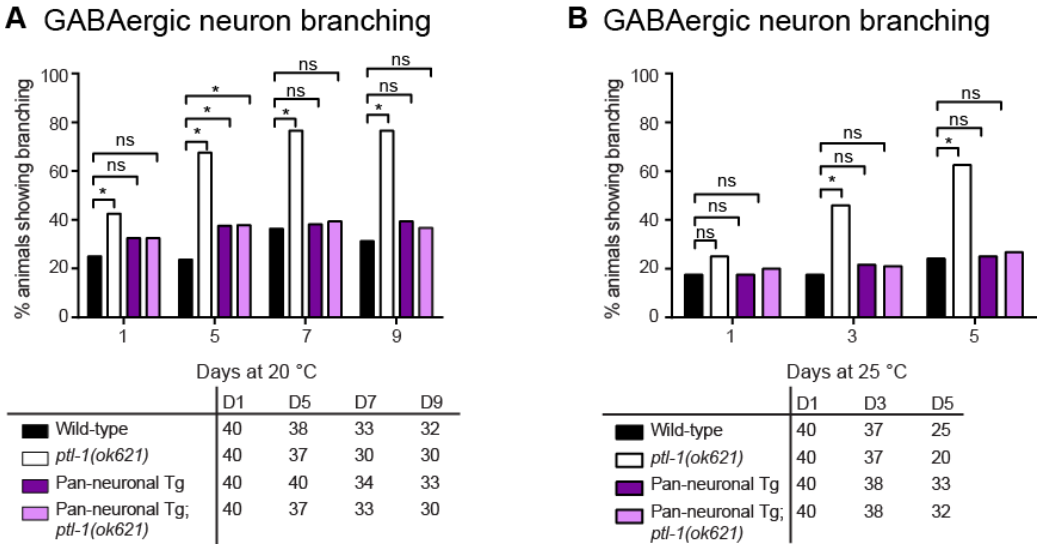

Days at 20 °C	D1	D5	D7	D9
Wild-type	40	38	33	32
ptl-1(ok621)	40	37	30	30
Pan-neuronal Tg	40	40	34	33
Pan-neuronal Tg; *ptl-1(ok621)*	40	37	33	30

Days at 25 °C	D1	D3	D5
Wild-type	40	37	25
ptl-1(ok621)	40	37	20
Pan-neuronal Tg	40	38	33
Pan-neuronal Tg; *ptl-1(ok621)*	40	38	32

Appendix 8: Pan-neuronal re-expression of PTL-1 rescues the neuronal ageing phenotype in GABAergic neurons that is observed in the *ptl-1(ok621)* null mutant. The GABAergic neurons were visualised using the P*unc-47*::*gfp (oxIs12)* reporter. The presence of the *ptl-1(ok621)* mutation in the genetic background of each transgenic line is indicated by the addition of "*ptl-1(ok621)"* in the strain name. Neuron imaging assay conducted at **A)** 20 °C or **B)** 25 °C for "Pan-neuronal Tg" worms. The chi-squared statistical test was used to determine statistical significance. P-value is indicated by ns = not significant, *<0.05. The sample size for each strain at each time point is given in the table underneath the graphs. Experiments were conducted twice independently, and the representative data shown are from one experiment. Data from the first experiment are shown in **Figure 6.2.**

Appendix 9

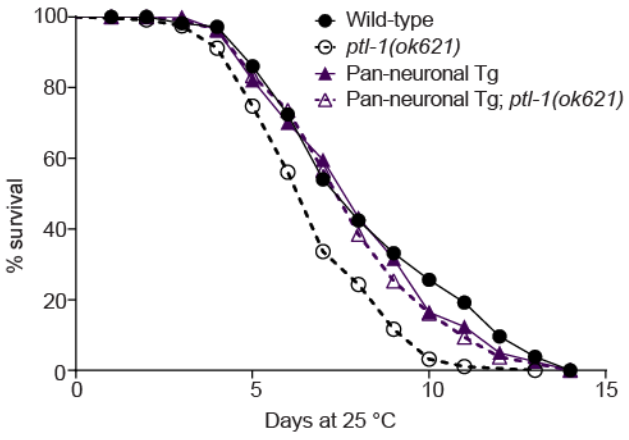

	Log rank test	Gehan-Breslow-Wilcoxon test
Wild-type vs. *ptl-1(ok621)*	<0.05	<0.05
Wild-type vs. "Pan-neuronal Tg"	Not significant	Not significant
Wild-type vs. "Pan-neuronal Tg; *ptl-1(ok621)*"	Not significant	Not significant

Appendix 9: The short-lived phenotype of *ptl-1* null mutants can be rescued by pan-neuronal re-expression of PTL-1. Lifespan assay for pan-neuronal transgenic worms. n = 120 at day 0. Results of statistical analysis are indicated by p-values underneath each graph. Lifespan experiments were conducted twice independently, and the representative data shown are from one experiment. Data from the first experiment are shown in **Figure 6.3.** Median lifespans are 8 days (wild-type), 7 days (*ptl-1(ok621)*, 8 days (Pan-neuronal Tg; wild-type), and 8 days (Pan-neuronal Tg*; ptl-1(ok621)*).

Appendix 10

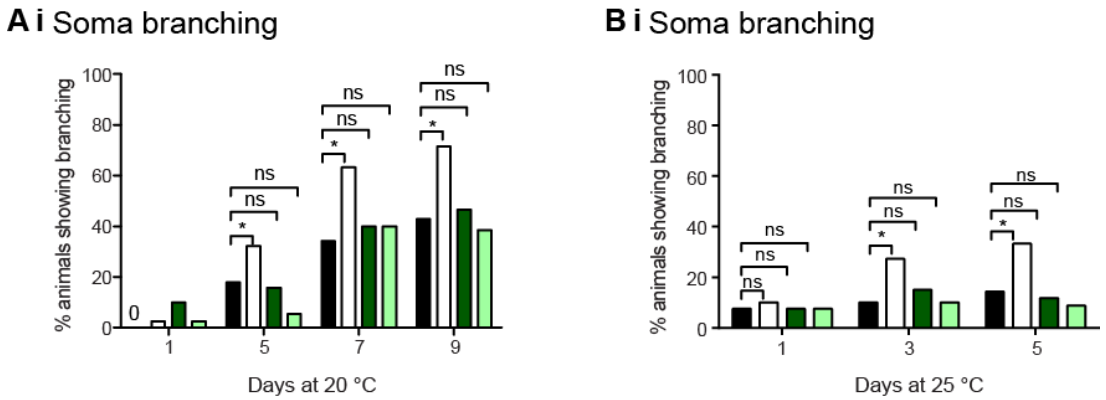

	D1	D5	D7	D9
Wild-type	40	39	38	35
ptl-1(ok621)	40	31	30	28
TRN Tg	40	38	35	28
TRN Tg; *ptl-1(ok621)*	40	37	35	26

	D1	D3	D5
Wild-type	40	40	33
ptl-1(ok621)	40	35	23
TRN Tg	40	36	30
TRN Tg; *ptl-1(ok621)*	40	37	34

Appendix 10: TRN-specific re-expression of PTL-1 rescues the neuronal ageing phenotype in TRNs that is observed in the *ptl-1(ok621)* null mutant. The TRNs were visualised using the P*mec-4*::*gfp (zdIs5)* reporter. The presence of the *ptl-1(ok621)* mutation in the genetic background of each transgenic line is indicated by the addition of "*ptl-1(ok621)"* in the strain name. Neuron imaging assay conducted at **A)** 20 °C or **B)** 25 °C for TRN-specific

transgenic worms ("TRN Tg"). Data for wild-type and *ptl-1(ok621)* animals in both graphs were obtained in the same experiment as pan-neuronal transgenic lines at the same temperature (**Appendix 7**). The chi-squared statistical test was used to determine statistical significance. P-value is indicated by ns = not significant, *<0.05. The sample size for each strain at each time point is given in the table underneath the graphs. Experiments were conducted twice independently, and the representative data shown are from one experiment. Data from the first experiment are shown in **Figure 6.5.**

Appendix 11

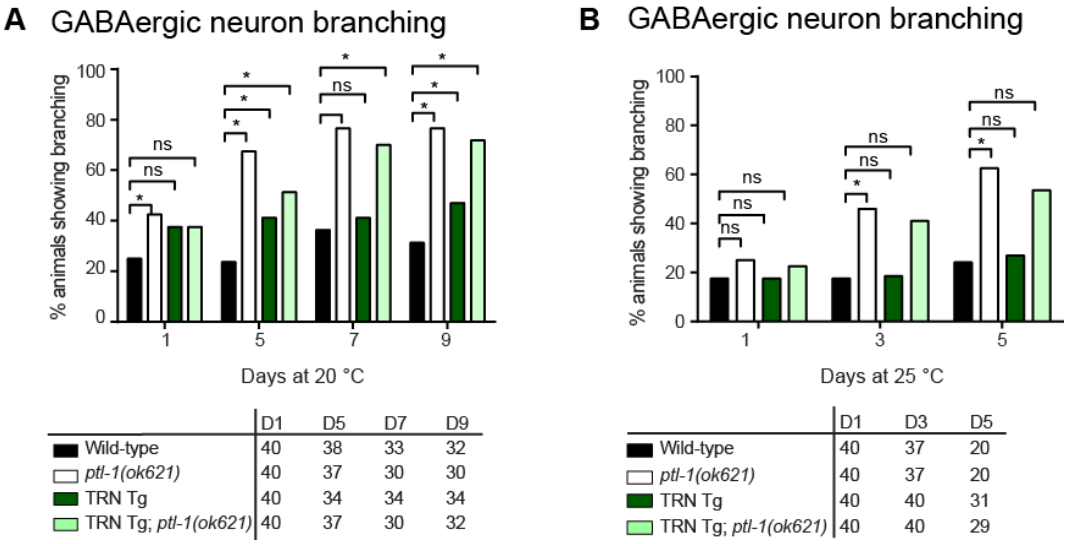

	D1	D5	D7	D9
Wild-type	40	38	33	32
ptl-1(ok621)	40	37	30	30
TRN Tg	40	34	34	34
TRN Tg; *ptl-1(ok621)*	40	37	30	32

	D1	D3	D5
Wild-type	40	37	20
ptl-1(ok621)	40	37	20
TRN Tg	40	40	31
TRN Tg; *ptl-1(ok621)*	40	40	29

Appendix 11: TRN-specific re-expression of PTL-1 does not rescue the neuronal ageing phenotype in GABAergic neurons that is observed in the *ptl-1(ok621)* null mutant. The GABAergic neurons were visualised using the P*unc-47*::*gfp (oxIs12)* reporter. The presence of the *ptl-1(ok621)* mutation in the genetic background of each transgenic line is indicated by the addition of "*ptl-1(ok621)"* in the strain name. Neuron imaging assay conducted at **A)** 20 °C or **B)** 25 °C for "TRN Tg" worms. Data for wild-type and *ptl-1(ok621)* animals were obtained in the same experiment as for pan-neuronal Tg animals at the same temperature (**Appendix 8)**. The chi-squared statistical test was used to determine statistical significance. P-value is indicated by ns = not significant, *<0.05. The sample size for each strain at each time point is given in the table underneath the graphs. Experiments were conducted twice independently, and the representative data shown are from one experiment. Data from the first experiment are shown in **Figure 6.6.**

Appendix 12

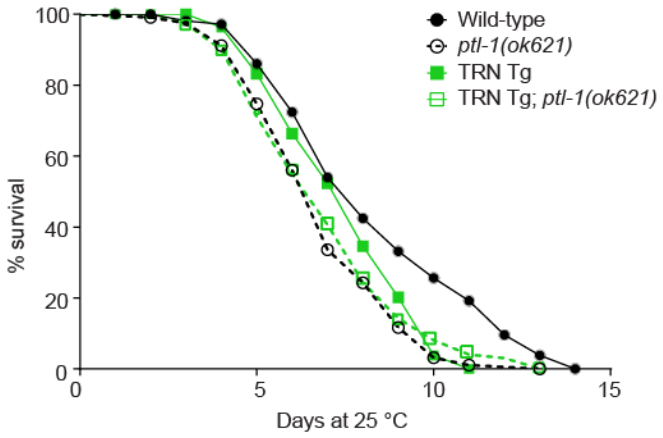

	Log rank test	Gehan-Breslow-Wilcoxon test
Wild-type vs. *ptl-1(ok621)*	<0.05	<0.05
Wild-type vs. "TRN Tg"	<0.05	Not significant
Wild-type vs. "TRN Tg; *ptl-1(ok621)*"	<0.05	<0.05

Appendix 12: The short-lived phenotype of *ptl-1* null mutants cannot be rescued by TRN-specific re-expression of PTL-1. Lifespan assay for TRN-specific transgenic worms. Survival curves for control wild-type and *ptl-1(ok621)* animals were obtained in the same experiment as shown in **Appendix 9**. n = 120 at day 0. Results of statistical analysis are indicated by p-values underneath each graph. Lifespan experiments were conducted twice independently, and the representative data shown are from one experiment. Data from the first experiment are shown in **Figure 6.7.** Median lifespans are 8 days (wild-type), 7 days (*ptl-1(ok621)*, 8 days (TRN Tg; wild-type), and 7 days (TRN Tg*; ptl-1(ok621)*).

Appendix 13

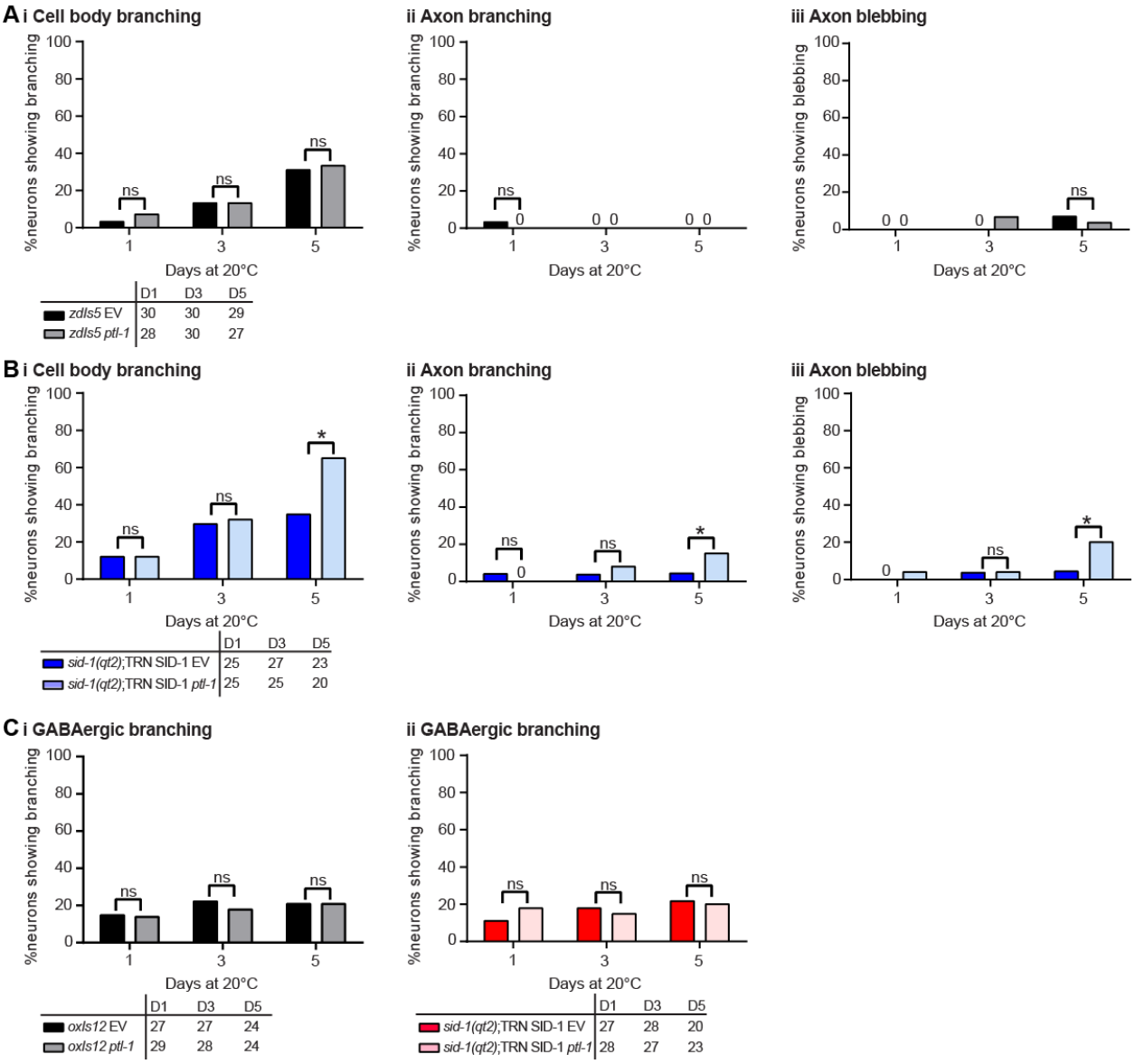

Appendix 13: Knockdown of PTL-1 in touch neurons has a cell autonomous effect on neuronal ageing. Strains labelled as *zdIs5* or *oxIs12* indicate the allele name of the *gfp* reporter, are wild-type at the SID-1 locus and do not contain a SID-1 transgene. SID-1 transgenic worms are labelled as "*sid-1(qt2);*TRN SID-1" to indicate the presence of the *sid-1* mutation and P*mec-18*::*sid-1* transgene. The RNAi treatment is either empty vector (EV) or *ptl-1* and is indicated after the strain name. **A)** TRN imaging assay for animals carrying the *zdIs5* reporter only, indicating data for (i) cell body branching, (ii) axon branching and (iii) axon blebbing. **B)** TRN imaging assay for animals carrying the *zdIs5* reporter together with the "TRN SID-1" Tg in a *sid-1(qt2)* mutant background, indicating data for (i) cell

body branching, (ii) axon blebbing and (iii) axon branching. **C)** GABAergic imaging assay for animals carrying the *oxIs12* reporter, (i) strains assayed carry the *oxIs12* reporter alone, (ii) strains assayed also carry the "*sid-1(qt2);* TRN SID-1" transgene. Statistical analysis: chi-squared test, p-value is indicated by ns = not significant, *<0.05. The sample size for each strain at each time point is given in the table underneath the graphs. Experiments were conducted twice independently, and the representative data shown are from one experiment. Data from the first experiment are shown in **Figures 6.10, 6.11 and 6.12.**